Molecular function of WISP1/CCN4 in the musculoskeletal system with special reference to apoptosis and cell survival

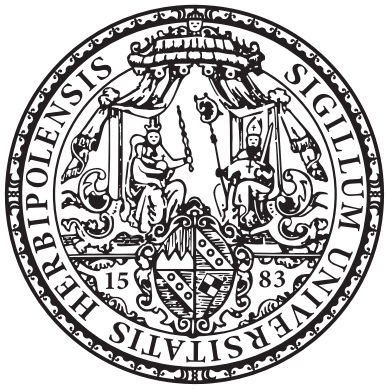

vorgelegt von
Dipl. Biol. Katrin Schlegelmilch
Würzburg, 2012

Dissertation zur Erlangung des
naturwissenschaftlichen Doktorgrades (Dr. rer. nat.)
der Bayerischen Julius-Maximilians-Universität Würzburg

Einreichung: _____ in Würzburg

Mitglieder der Promotionskommission:

Vorsitzender:	Prof. Dr. Wolfgang Rössler
1. Gutachter:	Prof. Dr. Norbert Schütze
2. Gutachter:	Prof. Dr. Georg Krohne

Promotionskolloquium: _____ in Würzburg

Aushändigung Doktorurkunde: _____ in Würzburg

TABLE OF CONTENTS

ACKNOWLEDGEMENTS

This dissertation was conducted in the laboratory of the Orthopaedic Centre for Musculoskeletal Research, which is integrated in the university Orthopaedic Clinic of Würzburg, Bavaria. My research project would not have been possible without the support of many people. Therefore, it is a pleasure to thank all supervisors and colleagues of the research centre for their support in a number of ways.

I am very grateful to my direct supervisor, Prof. Dr. Norbert Schütze, whose encouragement, supervision and support from the preliminary to the concluding level enabled me to develop an understanding and arbitrary handling of the subject. Furthermore, I am very thankful for the opportunities to present important parts of my work at national and international symposia.

I would also thank Prof. Dr. Georg Krohne of the Faculty of Biology (University of Würzburg) for accepting the position of an assessor, thereby enabling this scientific dissertation at the Faculty of Medicine.

I am indebted to many of my colleagues, but especially to Roderich Laug, Viola Zehe and Patrick Prager, for their invaluable assistance with my laboratory tasks and mental support during the last years.

Further I would like to thank the entire working groups of Prof. Dr. Franz Jakob, PD Dr. André Steinert and PD Dr. Ulrich Nöth for their helpfulness and cooperation in many aspects and Monika Hofmann for her patient help with any kind of organizational tasks in the Orthopaedic Clinic.

I also deeply acknowledge the support of my parents. They always assisted me financially and particularly morally during my education and finally the conduction of this thesis. In this context, I also would like to thank my brother Timm. Once, his trust in my abilities encouraged me to keep on finding my own ways. I am very glad that he was right after all. ;)

Lastly, I owe my deepest gratitude to my boyfriend Alex, for his support in performing microarray analyses, for sharing his statistical skills, for reviewing my thesis consistently, for his patient and moderate way to answer all my questions and at least for his comprehension and encouragement during all stages of this dissertation. Thank you so much!

SUMMARY/ZUSAMMENFASSUNG

Summary

Human adult cartilage is an aneural and avascular type of connective tissue, which consequently reflects reduced growth and repair rates. The main cell type of cartilage are chondrocytes, previously derived from human mesenchymal stem cells (hMSCs). They are responsible for the production and maintainance of the cartilaginous extracellular matrix (ECM), which consists mainly of collagen and proteoglycans. Signal transmission to or from chondrocytes, generally occurs via interaction with signalling factors connected to the cartilaginous ECM. In this context, proteins of the CCN family were identified as important matricellular and multifunctional regulators with high significance during skeletal development and fracture repair. In this thesis, main focus lies on WISP1/CCN4, which is known as a general survival factor in a variety of cell types and seems to be crucial during lineage progression of hMSCs into chondrocytes. We intend to counter the lack of knowledge about the general importance of WISP1-signalling within the musculoskeletal system and especially regarding cell death and survival by a variety of molecular and cell biology methods.

First, we established a successful down-regulation of endogenous WISP1 transcripts within different cell types of the human musculoskeletal system through gene-silencing. Interestingly, WISP1 seems to be crucial to the survival of all examined cell lines and primary hMSCs, since a loss of WISP1 resulted in cell death. Bioinformatical analyses of subsequent performed microarrays (WISP1 down-regulated vs. control samples) confirmed this observation in primary hMSCs and the chondrocyte cell line Tc28a2. Distinct clusters of regulated genes, closely related to apoptosis induction, could be identified. In this context, TRAIL induced apoptosis as well as p53 mediated cell death seem to play a crucial role during the absence of WISP1 in hMSCs. By contrast, microarray analysis of WISP1 down-regulated chondrocytes indicated rather apoptosis induction via MAPK-signalling. Despite apoptosis relevant gene regulations, microarray analyses also identified clusters of differentially expressed genes of other important cellular activities, e.g. a huge cluster of interferon-inducible genes in hMSCs or gene regulations affecting cartilage homeostasis in chondrocytes.

Results of this thesis emphasize the importance of regulatory mechanisms that influence cell survival of primary hMSCs and chondrocytes in the enforced absence of WISP1. Moreover, findings intensified the assumed importance for WISP1-signalling in cartilage homeostasis. Thus, this thesis generated an essential fundament for further examinations to investigate the role of WISP1-signalling in cartilage homeostasis and cell death.

Zusammenfassung

Humaner adulter Knorpel besitzt weder Blutgefäße noch Nerven, weswegen diese Knorpelart im Vergleich zu anderen Gewebetypen ein verringertes Wachstum und Regenerierung wiederspiegelt. Den Hauptteil der Zellen im adulten Knorpel stellen die Chondrozyten (Knorpelzellen) dar, welche sich zuvor aus humanen mesenchymalen Stammzellen (hMSCs) entwickelt haben. Sie sind verantwortlich für die Bildung und Aufrechterhaltung der extrazellulären Matrix (ECM) des Knorpelgewebes, welche hauptsächlich aus Kollagen und Proteoglykanen besteht. Signale, die durch Chondrozyten erzeugt oder weitergeleitet werden, finden in der Regel durch Interaktion mit Molekülen der im Knorpel liegenden ECM statt. Mitglieder der CCN-Familie gelten hierbei als bedeutende extrazelluläre Matrixproteine, die bei verschiedenen regulatorischen Prozessen während der Skelettentwicklung und der Frakturheilung eine Rolle spielen. In dieser Doktorarbeit liegt das Hauptaugenmerk auf dem CCN Protein WISP1/CCN4. Dieses Protein gilt bereits in verschiedenen Zellen als ein notwendiger Überlebensfaktor und scheint des Weiteren eine regulatorische Funktion während der Differenzierung von hMSCs in Chondrozyten auszuüben. Die generelle Bedeutung von WISP1 für das muskuloskelettale System ist bislang jedoch weitgehend ungeklärt und soll während dieser Doktorarbeit mittels einer Reihe von molekular- und zellbiologischer Methoden genauer untersucht werden.

Hierfür wurde zu Beginn eine erfolgreiche Herunterregulierung endogen hergestellter WISP1 Transkripte mittels Genexpressionshemmung (gene-silencing) in verschiedenen muskuloskelettalen Zellen erzielt. Interessanterweise scheint WISP1 eine bedeutende Rolle für das Überleben dieser Zellen zu spielen, da ein Verlust bei allen untersuchten Zelllinien und primären hMSCs zum Zelltod führte. Um zu Grunde liegende Mechanismen genauer zu untersuchen, wurden daraufhin Microarray Analysen von hMSCs und Tc28a2 Chondrocyten durchgeführt (jeweils WISP1 herunterreguliert vs Kontrollzellen). In diesem Zusammenhang identifizierten bioinformatische Analysen differentielle Expressionen verschiedener apoptoseresponsiver Gene. So scheint eine Apoptoseinduktion über TRAIL und/oder p53 in hMSCs stattzufinden, wohingegen eine starke Regulation des MAPK-Signalweges in Chondrozyten detektiert wurde. Neben diesen Genregulationen, deckten die Analysen ebenso Gengruppen auf, die bei anderen wichtigen zellulären Abläufen eine Rolle spielen. Hier sind in WISP1 herunterregulierten hMSCs u.a. viele differenziell exprimierte Gene zu nennen, die durch Interferone induzierbar sind. In Chondrozyten dagegen scheint eine verringerte WISP1 Expression Genexpressionen zu beeinflussen, welche die Knorpelhomeostase regulieren.

Die Ergebnisse, die während dieser Doktorarbeit erzielt wurden, verdeutlichen die Wichtigkeit von WISP1 für das Überleben von primären hMSCs und Chondrozyten. Darüberhinaus verstärken die bioinformatischen Analysen die Annahme, das WISP1 regulatorische Funktionen für die Knorpelhomeostase ausübt. Somit bietet diese Doktorarbeit ein essentielles Fundament, um die Rolle von WISP1 bei der Aufrechterhaltung der Knorpelhomeostase und des Zelltodes weiter zu erforschen.

Part I.

Introduction

CHAPTER

ONE

MUSCULOSKELETAL SYSTEM

The human musculoskeletal system comprises over 200 bones as well as cartilage, muscles, ligaments and all associated connective tissues. Main functions of the musculoskeletal system are to stabilize the whole body, protecting organs and facilitate movements. Beside these well known features, it additionally plays important roles in a variety of metabolic and regulatory processes. Bones, for example, serve as a main storage for minerals, thereby controling organs and cellular activities (Martin 1983). Further, bones and their adhesive musculoskeletal tissues regulate important physiological processes through keeping a general stem cell reservoir and initiating development or differentiation of blood cells. Regarding all of these functions together, the musculoskeletal system represents an essential part of the human body, which has often been under-estimated and neglected in fundamental molecular research.

1.1. Cells of the musculoskeletal system

1.1.1. Cells with multilineage differentiation potential: stem cells

The internal cavities of many bones are filled with red marrow containing undifferentiated heamatopoietic stem cells (HSCs) and mesenchymal stem cells (MSCs). Stem cells in general have the capability of replacing or renewing itself to conserve the stem cell pool or developing into specialized cells of a variety of cell types. Thereby, they form new organs during embryonic development or regenerate tissues in adult organisms (Caplan 1991). While totipotent embryonic stem cells can differentiate into all cell types of the organism, multipotent HSCs and MSCs of the adult organism are restricted in their differentiation potential. HSCs are necessary for the constant renewal of blood, thereby producing different types of red blood cells and lymphocytes (Baum et al. 1992; Reya 2003; Till and McCulloch 2011). MSCs in contrast, generate a limited number of cells of mesenchymal tissues like bone (osteoblasts), cartilage (chondrocytes), muscle (myoblasts), and adipose (adipocytes) (Barry and Murphy 2004; Muraglia et al. 2000; Pereira et al. 1995; Pittenger et al. 1999; Prockop 1997; Verfaillie 2002). MSCs are known as quiescent cells, remaining in the stem cell niche until growth factors initiate asymmetric cell division. This results in one identical daughter cell and one cell with a lineage-dependent specific differentiation program (Baksh et al. 2004; Fuchs et al. 2004). In vitro, it is difficult to differ between pure MSC populations and those containing mixtures of lineage-specific progenitor cells. This is because a single cell marker is not completely proven until now. MSCs, as well as HSCs, are positive for the CD34 antigen directly after the isolation from bone marrow. In contrast to the HSCs, which express CD34 permanently, MSCs loose this antigen during *in vitro* culture (Tuan et al. 2003). Immuno-selection via detection of a

variety of MSC surface markers e.g. STRO-1, src homology 2 (SH2), src homology 3 (SH3), CD44, CD90 and CD146 (Bianco et al. 2001; Gronthos and Simmons 1996; Pittenger et al. 1999; Sacchetti et al. 2007; Simmons et al. 1994) are discussed. They are mostly used together with detection of MSC ability to differentiate in osteocytes, chondrocytes and adipocytes (Nöth et al. 2002; Pittenger et al. 1999; Schilling et al. 2008; Schuetze et al. 2005). The differentiation capacity of MSCs *in vivo* and *in vitro* arouse the interest of many researchers in the area of tissue engineering as well as gene therapy application. This is mainly due to the fact that autologous MSCs induce no immuno-reactivity after transplantation and ethical constraints are not to be expected (Baksh et al. 2004; Bianco and Robey 2001; Young et al. 2005).

1.1.2. Bone remodelling: osteoclasts, osteoblasts and osteocytes

At childbirth, the human body is build up with over 270 bones. During ontogenesis, many bones fuse together leaving a total of 206 separate bones in an adult. But even afterwards, the skeleton is a metabolically active organ that undergoes continuous remodelling throughout life. This involves a balance of removing mature bone tissue - a process called bone resorption - and the replacement with new bone matrix, namely ossification or bone formation (Caplan 2005; Martin 1983). Bone resorption is primary accomplished by multinucleated osteoclasts, which derive from monocytes of the heamatopoietic lineage (Suda et al. 1999; Väänänen et al. 2000). Several cytokines, e.g. interleukin 1 (IL1), nuclear factor kappa B (NFκB), receptor activator of nuclear factor kappa B ligand (RANKL), tumour necrosis factor alpha (TNFα) and hormones e.g. parathyroid hormone (PTH), estrogen and leptin, are essential for osteoclast differentiation, activation and recruitment (Nakamura et al. 2011). After being recruited to a specific site, they attach to the bone surface and seal it off from the extracellular environment. Proteolytic enzymes are secreted to remove the bone matrix and expose the bone mineral (Horowitz et al. 2001).

Osteoblasts, in contrast, are cells that are primarily responsible for ossification. They derive from MSC generated osteoprogenitor cells and function by secreting the bone extracellular matrix (osteoid). Insulin-like growth factor 1 (IGF1), fibroblast growth factor 2 (FGF2), transforming growth factor beta 1 (TGFβ1) and different members of the bone morphing protein (BMP) family are released during bone resorption and seem to be essential for the recruitment of MSCs and subsequent osteogenesis (Habisch et al. 2008; Pederson et al. 2008; Ponte et al. 2007; Sims and Gooi 2008). Mature osteoblasts migrate to previously resorbed sites. They are found in clusters along the bone surface on a layer of bone matrix that they are continuously producing. The osteoid consists mainly of collagen type I fibers, which serves as a scaffold for subsequent calcification. After osteoid secreting, 15% of mature osteoblasts are entrapped in the new bone matrix and differentiate into osteocytes. They can be easily identified by their star-shaped appearance, forming a network of thin canaliculi permeating the entire bone matrix (Hadjidakis and Androulakis 2006). Osteocytes can regulate bone formation by secerning sclerostin, which migrates along the canaliculi to the bone surface. Sclerostin inhibits WNT- and BMP-signalling, therefore decreasing osteoprogenitor cell proliferation and bone mineralization (Galli et al. 2010; ten Dijke et al. 2008).

1.1.3. Cartilage: chondroblasts and chondrocytes

Cartilage is a type of elasticity connective tissue, which is not as tight as bone and less flexible than muscles. The main cell types of cartilage are chondrocytes, previously derived from MSC generated chondroblasts. These cells are responsible for the production and maintenance of the cartilagous extracellular matrix (ECM), a matrix composed of collagen type II fibers, elastin and proteoglycans (Buckwalter and Mankin 1998; Palfrey and Davies 1966). The en-

doskeleton of early vertebrates comprised exclusively a composition of cartilaginous tissues. During vertebrate evolution, cartilage seems to have been gradually replaced by bone formation (Kubota and Takigawa 2011). Thus, the authors of the aforementioned studies classified cartilage roughly into two distinct classes: temporary and permanent cartilages. Temporary cartilage is localized in the cartilage growth plate, where endochondral bone formation took place during the skeletal development (Fukunaga et al. 2003). This process is initiated by MSC condensation and subsequent differentiation into chondrocytes (Hill et al. 2005). Chondrocyte proliferation and hypertrophic differentiation generate a calcified cartilage matrix (Shu et al. 2011). Afterwards, hypertrophic chondrocytes undergo apoptosis, leaving cavities within the bone. Osteoblasts differentiate nearby these cavities, using the calcified cartilage as scaffolds. They deposit bone matrix onto the degraded mineralized cartilaginous matrix, thereby generating the basis for new bones (Hojo et al. 2010).

In contrast to temporary cartilage, permanent cartilage is aneural and avascular and can be found in many areas of the human body. Its function is in most cases dependent on its location. Based upon the relative contribution and distribution of fibers within the ECM, permanent cartilage can be divided into three subgroups: hyaline, elastic and fibrous cartilage. Articular cartilage, the main type of hyaline cartilage, covers the end of bones in joints e.g. knee, elbow, and rib cage. This enables bones to slide smoothly and easily past each other. Interestingly, articular cartilage and the cartilage growth plate develop from the same origin, but chondrocytes in articular cartilage do not undergo hypertrophic differentiation to generate a calcified cartilage matrix. Elastic cartilage, generally found in areas of the human face, is histologically similar to hyaline cartilage, but contains fibers of elastin, which confers more elastic flexibility. Fibrocartilage, found in the meniscus, has the greatest tensile strength and is the only cartilage type that contains collagen type I additional to collagen type II, building a dense matrix by compact collagenous bundles.

In the research area comprising tissue engineering and regenerative medicine, investigation of adult cartilage is of main interest. Since it contains no blood vessels or nerves, it is consequently a connective tissue with reduced growth and repair rates compared to other tissues. Signal transmission to or from chondrocytes generally occurs via interaction with signalling factors of the cartilaginous ECM (Chen and Lau 2010). Thus, top priority of this study was the investigation of potential proteins that modify signalling of molecules associated with the ECM.

CHAPTER

TWO

CCN PROTEIN FAMILY

2.1. Nomenclature and development

The CCN family of proteins comprises six distinct members: cysteine-rich 61 (CYR61/CCN1), connective tissue growth factor (CTGF/CCN2), nephroblastoma overexpressed (NOV/CCN3) and WNT-induced secreted proteins-1 (WISP1/CCN4), -2 (WISP2/CCN5) and further -3 (WISP3/CCN6). Each protein is additional numbered by its order of discovery, CCN1-CCN6 (Brigstock 2003) at which the acronym CCN comes from the first three discovered members CYR61, CTGF and NOV (Bradham et al. 1991; Joliot et al. 1992; O'Brien et al. 1990). All members are characterized as matricellular proteins which share up to four structural domains with partial sequence identity to insulin-like growth factor binding proteins (IGFBP domain), von Willebrand factor type C repeat (VWC domain), thrombospondin type 1 repeat (TSP domain) and a C-terminus (CT domain), containing a putative cysteine knot (Fig. 2.1) (Bork 1993; Lau and Lam 1999; Perbal 2001). In addition to the 30-50% amino acid sequence identity, all members contain highly conserved cysteine residues (nearly 10% by mass) spread over the existing domains (Lau and Lam 1999).

Apart from the full-length CCN proteins (including WISP2), also truncated variants, lacking one or more of the four structural domains, have been identified (Perbal 2004). It is well known, that post-translational processing as well as alternative splicing of the corresponding mRNA are the basis of truncated CCN variants. One truncated isoform of WISP1/CCN4 (transcript variant 2; -T2), which lacks the VWC domain has been detected in non-transformed chondrocytes (Yanagita et al. 2007). But mostly, truncated proteins, or proteins missing internal modules, have been shown to be associated with pathological situations (Yanagita et al. 2007).

2.1.1. Multifunctional signalling

In general, CCN proteins are matricellular proteins that modify signalling of molecules associated with the ECM. Induction of expression occurs early in development to facilitate multiple tissue and organ functions. Like many ECM proteins, members of the CCN family comprise multifunctional roles in crucial areas of physiology such as angiogenesis, skeletal development, tumourgenesis, cell proliferation, wound healing, fracture repair and cell survival (Babic et al. 1998; Holloway et al. 2005; Lin et al. 2003, 2005; Nakanishi et al. 2000; Nishida et al. 2000; Schuetze et al. 2005; Zhang et al. 2005). Their functions are on the one hand overlapping, however on the other hand of distinct manner and cell- and tissue-specific (Leask and Abraham 2006; Perbal 2004). Looking at the structural similarities amongst the CCN proteins, it is not easily to understand how functional differences could exist. They comprise a homeostatic

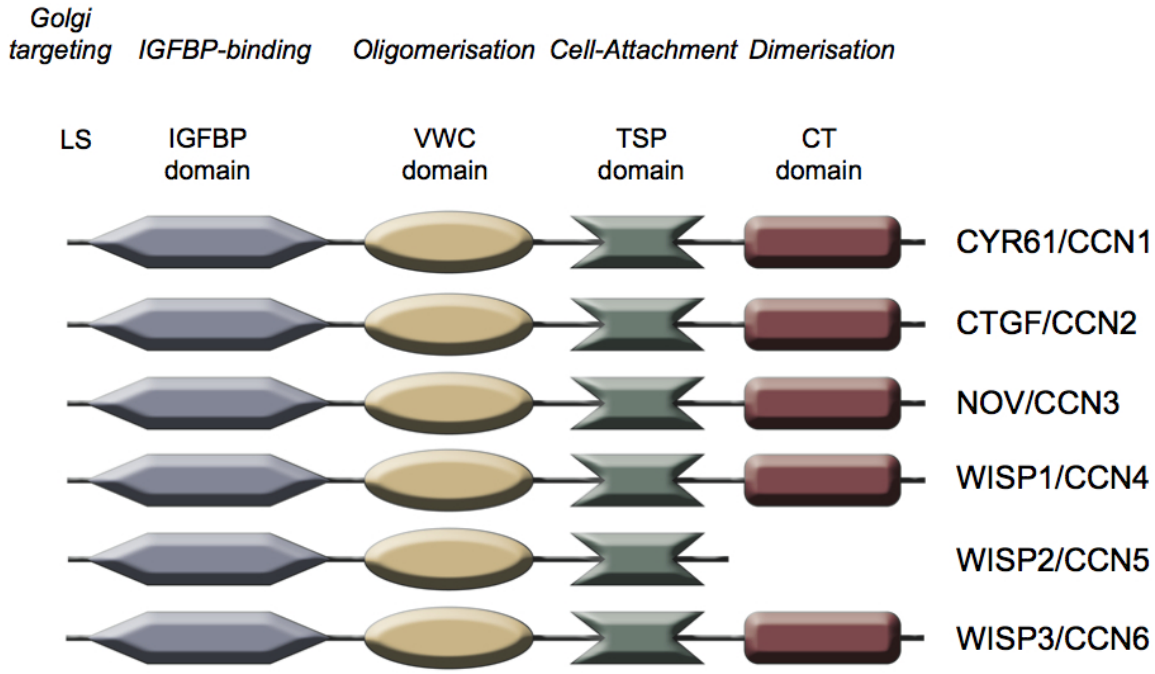

Figure 2.1.: *Modular structure of the CCN protein family. CCN1-CCN6 share up to four structural domains with amino acid sequence identy of 38–98% within individual modules. Full-length WISP2/CCN5 is lacking the fourth module, the CT domain. Bioactive forms of CCN1, -2, -3, -4 and -6, lacking one or more of the structural domains, have also been reported.*

regulatory system, in which one member drives a process while a closely related member can inhibit the same process. Several studies illustrate that the function of an individual CCN protein is also tissue specific and may even be contrary in different target cells. Factors that allow this cell- specificity are based on interactions of these proteins with a variety of components of the ECM, thereby providing a link to the cell surface (Yeger and Perbal 2007). Noticeable, during the last ten years all CCN members received more and more attention in the research field comprising the musculoskeletal system. The main focus is indeed located to the well-studied and first identified CCN members (CCN1-3). But also the WISP proteins (CCN4-6) rouse higher interest concerning regulations during the differentiation of bone marrow derived human mesenchymal stem cells (hMSCs) as well as bone formation and fracture repair (French et al. 2004; Schuetze et al. 2005).

CHAPTER
THREE

SPECIAL VIEW ON THE CCN FAMILY MEMBERS: WISP1-3

3.1. Constitution and homologies

Human WISP proteins (WISP1-3) were all identified by Pennica et al. (1998). WISP1 and -2 were clearly assigned as WNT1-induced genes in the mammary epithelial cell line C57MG. They were allocated to the CCN family in 2003 and renamed in CCN4/WISP1, CCN5/WISP2 and CCN6/WISP3 (Brigstock 2003). Figure 3.1 illustrates the encoded amino acid sequence alignment of the three human WISP proteins. On close examination, it is conspicuous that the four modules show distinct homologies as well as clear differences in their sequence. The N-terminal domain contains a consensus sequence (GCGC-CXXC) conserved in most insulin-like growth factor binding proteins (IGFBP). This sequence is present in WISP2 and -3, whereas WISP1 has a glutamine in the third position instead of a glycine (Pennica et al. 1998). The second module, the VWC domain, which is thought to participate in protein complex formation and oligomerization (Mancuso et al. 1989), contains less conserved cysteine residues in WISP3 than in WISP1 and -2. Between the VWC and TSP domains is a highly variable sequence of amino acids, which acts as a molecular hinge and is susceptible to proteolytic degradation by matrix metalloproteinases (Hashimoto et al. 2002). And in the end, the CT domain, which is involved in dimerization and receptor binding (Voorberg et al. 1991) and is completely absent in WISP2.

3.2. Mode of function in the musculoskeletal system

Within the musculoskeletal system, previous studies showed that WISP2 and -3 are expressed during the chondrogenic, osteogenic and adipogenic differentiation of MSCs (Schuetze et al. 2005), therefore indicating a central role during development and bone formation. French et al. (2004) demonstrated also the role of WISP1 as an osteogenic potentiating factor, promoting MSC proliferation and osteoblastic differentiation as well as repressing chondrocytic differentiation. Additional data regarding osteogenic differentiation indicate a correlation of WISP1 with bone morphogenetic protein-signalling (Ono et al. 2011) and transforming growth factor-signalling (Inkson et al. 2008). Concerning protein interactions, the major binding partners for WISP1 are the ECM-associated proteoglycans decorin and biglycan (Desnoyers et al. 2001). Inkson et al. (2009) described the interaction between WISP1 and biglycan by showing that WISP1 abrogates the repression of proliferation in bone marrow stromal cells, previously induced by biglycan. Furthermore, a prominent role of WISP1 in experimental and human osteoarthritis (OA) has been suggested from gene expression studies (Blom et al. 2009) and the association of a single nucleotide polymorphism with OA (Urano et al. 2007).

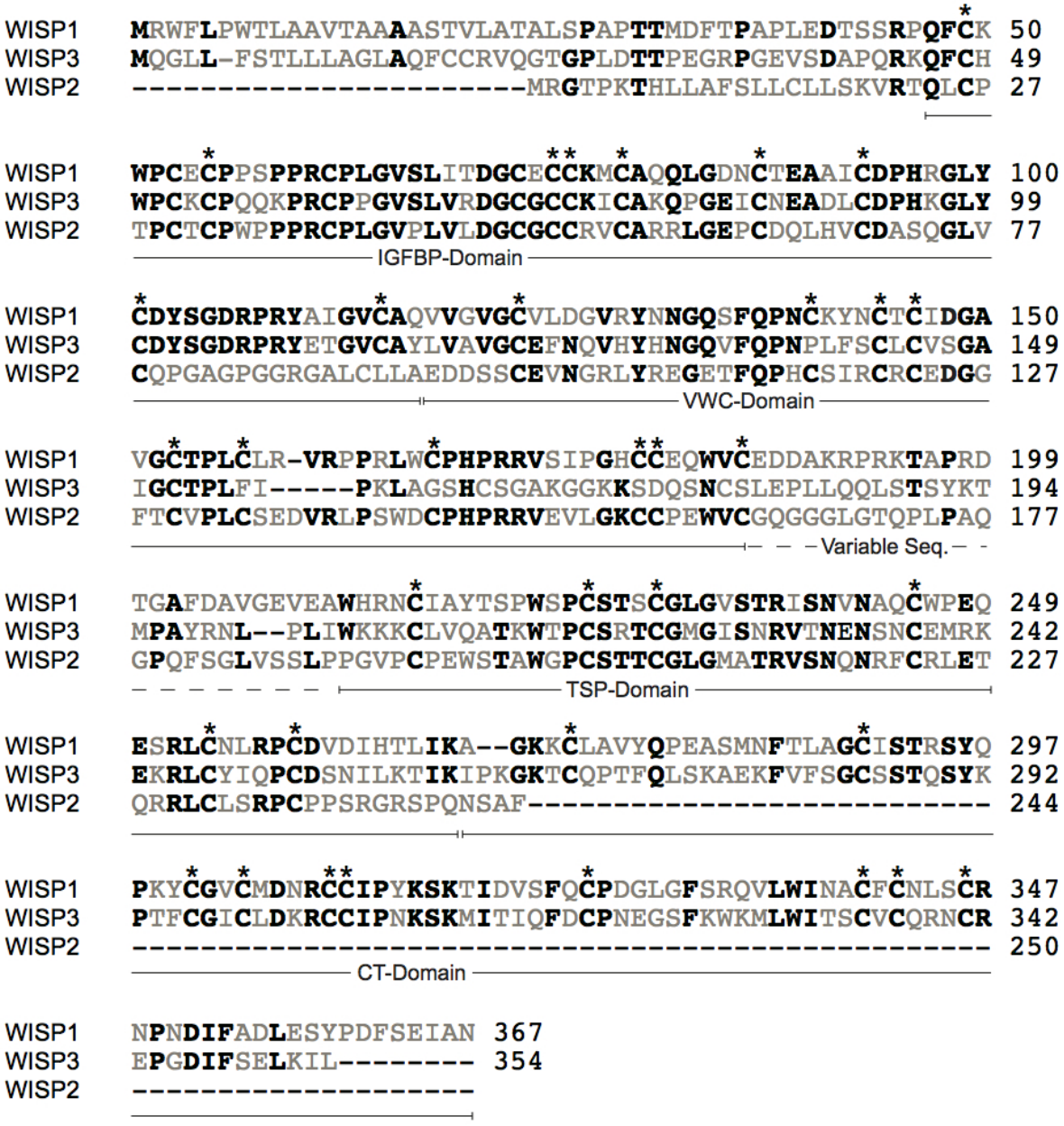

Figure 3.1.: *Encoded amino acid sequence alignment of human WISP1-3. Identities are visualized with bold letters. WISP1 and -3 are most similar (42% identity), whereas WISP2 has 37% identity with WISP1 and 32% identity with WISP3. Conserved cysteine residues are marked with stars. Domains (insulin-like growth factor-binding protein (IGFBP), von Willebrand factor type C (VWC), thrombospondin (TSP), and C-terminal (CT)) are underlined and labelled correspondingly.*

WISP2 is the least studied protein of the CCN family in relation to functional properties within the musculoskeletal system. Its expression seems to be donor dependent in hMSCs and completely depleted in different osteoblast, osteosarcoma and chondrocyte cell lines (Chap. 8). These findings are in line with the observations of Schuetze et al. (2005), who described a decreased expression of WISP2 during the chondrogenic- and adipogenic differentiation of MSCs. The declined expression of WISP2 during adipogenesis could be explained by the negative regulation of adipocyte differentiation through WNT-signalling (Ross et al. 2000). WISP2 is a known down-stream target of the WNT-signalling cascades and its expression is clearly enhanced after WNT1-activation (Longo et al. 2002; Pennica et al. 1998).

WISP3 is exceptional within the CCN family of proteins, since it represents the only CCN protein that is directly linked to a human disease in a causal manner. Inactivating frameshift- and nonsense mutations in exons 1, 2 and 5 of the human WISP3 gene were identified and clearly associated with the hereditary disease Progressive Pseudorheumatoid Dysplasia (PPD) (Hurvitz et al. 1999). This initial finding was confirmed by a number of additional case-studies indicating a potential role of WISP3 for cartilage homeostasis (Delague et al. 2005; Ehl et al. 2004). Recently, studies that investigated gain and loss of function in the zebrafish model revealed that WISP3 appears to be able to modify bone morphogenetic protein and WNT-signalling. With that, it influenced pharyngeal cartilage size and shape in development (Nakamura et al. 2007). A possible role of WISP3 in cartilage is supported from studies using a C28I2 derivative chondrogenic cell line that over-expresses WISP3. The up-regulation of collagen type II and aggrecan expression via the SOX9 pathway indicated a potential role of WISP3 for cartilage differentiation (Sen et al. 2004). Superoxide dismutase expression and activity was promoted both by recombinant WISP3 treatment and WISP3 transduction of C28I2 chondrocytes (Davis et al. 2006).

3.3. WISP1 and its connection to cell survival

Despite these findings, the role of WISP proteins in cartilage and cells of the musculoskeletal system is widely unknown, but several working groups depict WISP1 as an important survival factors in a variety of cells types. In this regard, Su et al. (2002) documented first the importance of WISP1 for the cell survival of rat kidney fibroblasts. WISP1 thereby leads to phosphorylation and activation of the survival factor v-akt murine thymoma viral oncogene homolog (AKT), which is known to promote cell survival by inactivation of BCL2-associated agonist of cell death (BAD) and caspase 9 (CASP9) (Cardone et al. 1998; Datta et al. 1997; Zha et al. 1996). Additional, Su et al. (2002) discovered in human lung carcinoma cells (H460 cells) that WISP1 might affect p53 induced apoptosis after DNA damage. It seems that WISP1 has the ability to block cytochrome c release and thus prevent the assembly of the apoptosome and subsequent cleavage of the effector caspase 3 (CASP3). The importance of WISP1 in p53 dependent cell death by preventing the release of cytochrome c in the cytosol, was also confirmed by recent studies using anthracycline antibiotic doxorubicin (DOX), a potent cancer chemotherapeutic agent. DOX induced cell death in adult mouse cardiomyocytes is attenuated by pretreatment with WISP1 (Venkatesan et al. 2010). WISP1 inhibits DOX mediated p53 activation and furthermore decreases the mitochondrial translocation of BCL2-associated X protein (BAX). Additionally, WISP1 reverses DOX-induced suppression of the survival factors B-cell CLL/lymphoma 2 (BCL2), BCL2-like 1 (BCLXL) and AKT.

CHAPTER
FOUR

AIM OF THE STUDY

Based on their correlation with the WNT-signalling pathway and their known interactions with molecules of the ECM, WISP proteins achieve more and more attention in research areas of tissue engineering and regenerative medicine. These characteristics wakened the interest concerning these proteins in our working group. In this thesis, we focus on molecular backgrounds concerning consequences of WISP-signalling in primary cells (hMSCs) and different cell lines connected to the musculoskeletal system. Hereby, our major goals are to:

1. identify natural expression of WISP1 (two transcript variants) and WISP2 in a variety of musculoskeletal cell types, i.e. hMSCs, osteoblasts and chondrocytes.

2. establish necessary molecular and cell biological tools to measure and analyze whole genome expression in different conditions, like recombinant protein production and knock-down approaches.

3. examine WISP-signalling and associated regulatory processes in detail after gene-silencing within naturally expressing tissues.

4. examine WISP-signalling and associated regulatory processes by treatment of gene-silenced cells with recombinant protein.

To dissect these molecular mechanisms, (1) RT-PCR analyses were performed to confirm a native expression of WISP1 and -2 in different cells of the musculoskeletal system. (2) This study comprised the production of recombinant (r)proteins of WISP1-T1 and -T2 and WISP2. Furthermore, a forced reduction of the endogenous protein expression was achieved by gene-silencing with different shRNA constructs, confirmed by subsequent RT-PCR analyses. (3) Genome-wide microarrays, taken shortly after down-regulation of WISP1 expression, were compared to control chips (cells treated with scrambled constructs) to examine global gene expression patterns. A bioinformatical workflow has been developed for this purpose. Several highly ranked candidates of regulated genes were selected for validation with RT-PCR. (4) Subsequent to a successful down-regulation of a given native WISP1 expression, cells were partially treated with rWISP1-T1 and -T2. Untreated and treated cells were compared by microscopic essays and isolated mRNA was used for microarray analyses. Further, we examined self-regulation of WISP1-T1, -T2 and WISP2 with RT-PCR of treated and untreated cells.

With this thesis we intend to counter the lack of knowledge about the general importance of WISP-signalling within the musculoskeletal system by a variety of molecular and cell biological methods. The project will thereby contribute to a better understanding of the potential of WISP-associated signalling for cartilage homeostasis and could provide new options for maintenance and regeneration of cartilage.

Part II.

Materials and Methods

CHAPTER
FIVE

MATERIALS

5.1. Consumables

Table 5.1.: *Listed are all utilized consumables with their corresponding suppliers.*

Consumables	**Supplier**
Autoradiography films	Fuji, purchased from A. Hartenstein GmbH, Würzburg, Germany
Blotting paper	Schleicher & Schuell, purchased from A. Hartenstein GmbH, Würzburg, Germany
Cell culture flasks (175cm^2)	Greiner Bio-One GmbH, Frickenhausen, Germany
Cell culture flasks (25cm^2, 75cm^2, 150cm^2)	TPP, Biochrom AG, Berlin, Germany
Cell scraper	SPL Lifesciences, purchased from A. Hartenstein GmbH, Würzburg, Germany
Cell strainers	BD Falcon, purchased from A. Hartenstein GmbH, Würzburg, Germany
Centrifugation tubes (15ml, 50ml)	Greiner Bio-One GmbH, Frickenhausen, Germany
Cryo.s^{TM}(2ml)	Greiner Bio-One GmbH, Frickenhausen, Germany
Eppendorf micro test tubes	Greiner Bio-one GmbH, Frickenhausen, Germany
GeneChip HG-U 133 Plus 2.0	Affymetrix UK Ltd., High Wycombe, UK
HiTrap^{TM}Protein G HP columns	GE Healthcare Europe GmbH, München, Germany
Lab-Tek Chamber Slides	Nunc, purchased from A. Hartenstein GmbH, Würzburg, Germany
Multitips	Eppendorf AG, purchased from A. Hartenstein GmbH, Würzburg, Germany

...continues on next page

Table 5.1.: *(...continued)*

Consumables	Supplier
NucleoSEQ columns	Macherey-Nagel GmbH & Co. KG, Düren, Germany
Pasteur pipettes	A. Hartenstein GmbH, Würzburg, Germany
PCR reaction tubes	Greiner Bio-one GmbH, Frickenhausen, Germany
Pipette tips	Brandt, purchased from Laug & Scheller GmbH, Kürnch, Germany
Pipette tips, aseptic	Becton Dickinson, USA, purchased from A. Hartenstein GmbH, Würzburg, Germany
Plastik pipettes (5ml, 10ml, 25ml)	Greiner Bio-One GmbH, Frickenhausen, Germany
Plates (6-, 12-, 24well)	Greiner Bio-One GmbH, Frickenhausen, Germany
Protran nitrocellulose transfer membrane	Whatman Schleicher & Schuell, purchased from A. Hartenstein GmbH, Würzburg, Germany
PVDF blotting membran	Whatman GmbH, purchased from A. Hartenstein GmbH, Würzburg, Germany
Sequencing sample tubes	Applied Biosystems Applera Deutschland GmbH, Darmstadt, Germany
Sterile filters	Carl Roth GmbH & Co. KG, Karlsruhe, Germany
UVettes	Eppendorf AG, purchased from A. Hartenstein GmbH, Würzburg, Germany
Whatman paper	Whatman GmbH, purchased from A. Hartenstein GmbH, Würzburg, Germany

5.2. Chemicals and reagents

Table 5.2.: *Listed are all utilized chemicals and reagents with their corresponding suppliers.*

Chemicals and reagents	Supplier
1,4-Dithiothreitol (DTT)	Roche Diagnostics GmbH, Mannheim, Germany
2-Mercaptoethanol	AppliChem, purchased from A. Hartenstein GmbH, Würzburg, Germany

...continues on next page

Table 5.2.: *(...continued)*

Chemicals and reagents	**Supplier**
2-Propanol	Carl Roth GmbH & Co. KG, Karlsruhe, Germany
Acetic acid	Carl Roth GmbH & Co. KG, Karlsruhe, Germany
Acetone	AppliChem, purchased from A. Hartenstein GmbH, Würzburg, Germany
Agar	AppliChem, purchased from A. Hartenstein GmbH, Würzburg, Germany
Agarose multi-purpose	Bioline GmbH, Luckenwalde, Germany
Albumin from bovine serum (BSA)	Sigma-Aldrich Chemie GmbH, Schnelldorf, Germany
Ammonia solution (25%)	Merck KGaA, Darmstadt, Germany
Ammonium persulfate (APS)	PAA Laboratories GmbH, Pasching, Austria
Ampicillin	Carl Roth GmbH & Co. KG, Karlsruhe, Germany
BacPAK complete Medium	Takara Bio Europe/Clontech, Saint-German-en-Laye, France
BacPAK Grace‘s Basic Medium	Takara Bio Europe/Clontech, Saint-German-en-Laye, France
Biozym LE Agarose	Biozym Scientific GmbH, Hessisch-Oldendorf, Germany
Boric acid	Merck KGaA, Darmstadt, Germany
Bromphenol blue sodium salt	Carl Roth GmbH & Co. KG, Karlsruhe, Germany
Citric acid anhydrous	AppliChem, purchased from A. Hartenstein GmbH, Würzburg, Germany
Colored reaction buffer (5x)	Bioline GmbH, Luckenwalde, Germany
Complete protease inhibitor cocktail	Roche Diagnostics GmbH, Mannheim, Germany
Developer	Kodak, purchased from A. Hartenstein, Würzburg, Germany
Dexamethasone	Sigma-Aldrich Chemie GmbH, Schnelldorf, Germany
Dimethyformamide	Carl Roth GmbH & Co. KG, Karlsruhe, Germany
Dimethylsulfoxide (DMSO)	Carl Roth GmbH & Co. KG, Karlsruhe, Germany
DMEM/HAMs F-12 with L-Glutamine	PAA Laboratories GmbH, Pasching, Austria

...continues on next page

Table 5.2.: *(...continued)*

Chemicals and reagents	**Supplier**
DNA ladder (1kb)	PEQLAB Biotechnology GmbH, Erlangen, Germany
DNA ladder plus (100bp)	PEQLAB Biotechnology GmbH, Erlangen, Germany
Dulbecco's phosphate buffered saline (PBS) powder	Biochrome AG, Berlin, Germany
Ethanol (100%)	AppliChem, purchased from A. Hartenstein GmbH, Würzburg, Germany
Ethanol (98%, denatured)	Carl Roth GmbH & Co. KG, Karlsruhe, Germany
Ethidium bromide	AppliChem, purchased from A. Hartenstein GmbH, Würzburg, Germany
Ethylenediaminetetraacetic acid (EDTA)	AppliChem, purchased from A. Hartenstein GmbH, Würzburg, Germany
Fetal calf serum (FCS)	PAA Laboratories GmbH, Pasching, Austria
Fixer	Kodak, purchased from A. Hartenstein, Würzburg, Germany
Glycerol 2-phosphat disodium salt hydrate	Sigma-Aldrich Chemie GmbH, Schnelldorf, Germany
Glycerol	Merck KGaA, Darmstadt, Germany
Glycine	AppliChem, purchased from A. Hartenstein GmbH, Würzburg, Germany
Heparin sodium salt	Sigma-Aldrich Chemie GmbH, Schnelldorf, Germany
Hexadimethrine bromide (polybrene)	Sigma-Aldrich Chemie GmbH, Schnelldorf, Germany
Horse serum	PAA Laboratories GmbH, Pasching, Austria
HPLC-H_2O	Carl Roth GmbH & Co. KG, Karlsruhe, Germany
Hydrochloric acid (1M)	AppliChem, purchased from A. Hartenstein GmbH, Würzburg, Germany
Insect Express Sf9-S2 Medium	PAA Laboratories GmbH, Pasching, Austria
LE agarose	Biozym Scientific GmbH, Hessisch-Oldendorf, Germany
L-Ascorbic acid 2-phosphate	Sigma-Aldrich Chemie GmbH, Schnelldorf, Germany
Lipofectamine 2000	Invitrogen GmbH, Darmstadt, Germany
Loading dye (6x)	Peqlab Biotechnology GmbH, Erlangen, Germany

...continues on next page

Table 5.2.: *(...continued)*

Chemicals and reagents	**Supplier**
Magnesium chloride	AppliChem, purchased from A. Hartenstein GmbH, Würzburg, Germany
MitoTracker®Red	Invitrogen GmbH, Darmstadt, Germany
Methanol	AppliChem, purchased from A. Hartenstein GmbH, Würzburg, Germany
N,N,N-N-tetramethylethylene-diamine (TEMED)	Merck KGaA, Darmstadt, Germany
NE Buffer (10x)	New England Biolabs GmbH, Frankfurt, Germany
Penicillin/Streptomycin	PAA Laboratories GmbH, Pasching, Austria
Ponceau S solution	Sigma-Aldrich Chemie GmbH, Schnelldorf, Germany
Pyruvate	Sigma-Aldrich Chemie GmbH, Schnelldorf, Germany
Rainbowmarker RPN 800	GE Healthcare Europe GmbH, München, Germany
Random hexamer primers	Invitrogen GmbH, Darmstadt, Germany
Roti-Quant (5x)	Carl Roth GmbH & Co. KG, Karlsruhe, Germany
Rotiphorese gel 40 acrylamide/bisacrylamide mix	Carl Roth GmbH & Co. KG, Karlsruhe, Germany
Skim milk powder	AppliChem, purchased from A. Hartenstein GmbH, Würzburg, Germany
S.O.C medium	Invitrogen GmbH, Darmstadt, Germany
Sodium acetate	AppliChem, purchased from A. Hartenstein GmbH, Würzburg, Germany
Sodium chloride	AppliChem, purchased from A. Hartenstein GmbH, Würzburg, Germany
Sodium dodecyl sulfate (SDS)	Merck KGaA, Darmstadt, Germany
Sodium hydroxide pellets	Merck KGaA, Darmstadt, Germany
Sodium hydroxide solution (1N)	AppliChem, purchased from A. Hartenstein GmbH, Würzburg
Template Suppression Reagent (TSR)	Applied Biosystems Aplera Deutschland GmbH, Darmstadt, Germany
Tris-Hydrochlorid (99%)	Carl Roth GmbH & Co. KG, Karlsruhe, Germany

...continues on next page

Table 5.2.: *(...continued)*

Chemicals and reagents	Supplier
Tris-aminomethane	AppliChem, purchased from A. Hartenstein GmbH, Würzburg, Germany
Triton X-100	Carl Roth GmbH & Co. KG, Karlsruhe, Germany
Trypan blue (0.4%)	Sigma-Aldrich Chemie GmbH, Schnelldorf, Germany
Trypsin (10x)	PAA Laboratories GmbH, Pasching, Austria
Trypsin-EDTA (1x)	PAA Laboratories GmbH, Pasching, Austria
Tryptone	AppliChem, purchased from A. Hartenstein GmbH, Würzburg, Germany
Tween20	Merck KGaA, Darmstadt, Germany
Yeast extract	AppliChem, purchased from A. Hartenstein GmbH, Würzburg, Germany

5.3. Equipment

Table 5.3.: *Listed is the utilized equipment with the corresponding suppliers.*

Equipment	Supplier
Autoclave Systec VX-75	Systec GmbH, Wettenberg, Germany
BioPhotometer	Eppendorf AG, Hamburg, Germany
Camera Canon EOS 1000D	Canon, purchased from A. Hartenstein, Würzburg, Germany
Centrifuge Biofuge Fresco	Thermo Electron LED GmbH, Langenselbold, Germany
Centrifuge Function Line	Thermo Electron LED GmbH, Langenselbold, Germany
Centrifuge Micro FugOne	Thermo Electron LED GmbH, Langenselbold, Germany
Chemical balance	Kern, purchased from A. Hartenstein, Würzburg, Germany

...continues on next page

Table 5.3.: *(...continued)*

Equipment	**Supplier**
CO_2 incubator CB 150	Binder GmbH, Tuttlingen, Germany
CO_2 incubator Kelvitron T	Thermo Electron LED GmbH, Langenselbold, Germany
Dishwasher	Miele &Cie. KG, Gütersloh, Germany
Drier	Thermo Electron LED GmbH, Langenselbold, Germany
Freezer Economic (-20°C)	Bosch GmbH, Gerlingen-Schillerhöhe, Germany
Freezer II Shin (-80°C)	Nunc GmbH & Co. KG, Wiesbaden, Germany
Fridge Freshcenter	Bosch GmbH, Gerlingen-Schillerhöhe, Germany
Gel elektrophoresis Mini Protean 3cell	Bio-Rad Laboratories GmbH, München, Germany
Glas jars	Schott, purchased from A. Hartenstein, Würzburg, Germany
Glas pipettes	A. Hartenstein, Würzburg, Germany
Heater	Medax, purchased from A. Hartenstein, Würzburg, Germany
Heat shaker TH15	Edmund Bühler GmbH, Hechingen, Germany
Laminar air flow box Hera Safe KS12	Thermo Electron LED GmbH, Langenselbold, Germany
Magnetic stirrer	A. Hartenstein, Würzburg, Germany
Microskope Axiovert 25	Carl Zeiss Jena GmbH, Jena, Germany
PerfectBlue semi-dry electroblotter	PEQLAB Biotechnologie GmbH, Erlangen, Germany
PH meter inolab ph level 1	WTW, purchased from A. Hartenstein, Würzburg, Germany
Pipetboy Acu	IBS Integra Biosciences, Fernwald, Germany
Power Pac 300	Bio-Rad Laboratories GmbH, München, Deutschland
Precision balance SPO51	Scaltec Instruments, purchased from A. Hartenstein, Würzburg, Germany
Radiographic hypercassette	Amersham Lifesciences, purchased from A. Hartenstein, Würzburg, Germany

...continues on next page

Table 5.3.: *(...continued)*

Equipment	Supplier
Sequencer ABI PRISM 310	Applied Biosystems Applera Deutschland GmbH, Darmstadt, Germany
Sonificator Sonoplus	Bendelin Electronic GmbH &. Co KG, Berlin, Germany
Single channel pipette	Abimed, Langenfeld, Germany
Speed Vac SC 110	Savant, Thermo Electron LED GmbH, Langenselbold, Germany
Thermal cycler PTC-200	Peltier, MJ Research, purchased from Biozym Scientific GmbH, Hessisch Oldendorf, Germany
Thermal printer Seico	LTF Labortechnik GmbH & Co. KG, Wasserburg, Germany
Vortexer Vortex-Genie 2	Scientific Industries, purchased from A. Hartenstein, Würzburg, Germany
Water bath WB7	Memmert, purchased from A. Hartenstein, Würzburg, Germany

5.4. Kits

Table 5.4.: *Listed are all utilized kits with their corresponding suppliers.*

Kits	Supplier
BacPAK^{TM}Baculovirus Expression System	Takara Bio Europe/Clontech, Saint-German-en-Laye, France
Big Dye Terminator v1.1 Cycle Sequencing	Applied Biosystems Aplera Deutschland GmbH, Darmstadt, Germany
dNTP Set (100mM)	Bioline GmbH, Luckenwalde, Germany
ECL Plus Detection	Amersham, purchased from GE Healthcare Europe GmbH, München, Germany
Fast-Link DNA Ligation	Biozym Scientific GmbH, Hessisch-Oldendorf, Germany

...continues on next page

Table 5.4.: *(...continued)*

Kits	Supplier
Lentiviral Expression System	Open Biosystems, Inc., Fisher Scientific GmbH, Schwerte, Germany
NucleoSpin extract II (PCR clean-up gel extraction)	Macherey-Nagel GmbH & Co. KG, Düren, Germany
NucleoSpin plasmid purification (mini preparation)	Macherey-Nagel GmbH & Co. KG, Düren, Germany
NucleoSpin RNA II (RNA/protein extraction)	Macherey-Nagel GmbH & Co. KG, Düren, Germany
PlusOne™Silver Staining Kit, protein	Amersham, purchased from GE Healthcare Europe GmbH, München, Germany
PureYield plasmid midi preperation	Promega GmbH, Mannheim, Germany
Sulforhodamine FLICA™	Immunochemistry Technologies, Bloomington, USA
TOPO TA cloning	Invitrogen GmbH, Darmstadt, Germany

5.5. shRNA target sets

Table 5.5.: *Listed is a set of five different shRNA constructs and one shRNA scrambled negative control, commercially supplied from the RNAi Consortium (TRC) of Thermo Fisher Scientific (Open Biosystems, Inc., Fisher Scientific GmbH, Schwerte, Germany). The shRNA constructs include a hairpin of 21bp (sense and antisense) linked with a loop of 6bp. Each hairpin was cloned into the lentiviral vector pLKO.1.*

Name	Oligo ID	Homology	Sequence ID
shRNA1	TRCN0000033349	Homo sapiens	NM_003882, NM_080838
shRNA2	TRCN0000033350	Homo sapiens	NM_003882, NM_080838
shRNA3	TRCN0000033351	Homo sapiens	NM_003882, NM_080838
shRNA4	TRCN0000033352	Homo sapiens	NM_003882, NM_080838
shRNA5	TRCN0000033353	Homo sapiens	NM_003882, NM_080838

Hairpin sequences of shRNA constructs:

shRNA1: 5' -CCGGGCATCCATGAACTTCACACTTCTCGAGAAGTGTGAAGTTCATGGATGCTTTTTG- 3'

shRNA2: 5' -CCGGCCACTCGGATCTCCAATGTTACTCGAGTAACATTGGAGATCCGAGTGGTTTTTG- 3'

shRNA3: 5' -CCGGCTGTGGAGTTTGCATGGACAACTCGAGTTGTCCATGCAAACTCCACAGTTTTTG- 3'

shRNA4: 5' -CCGGCCACTCGGATCTCCAATGTTACTCGAGTAACATTGGAGATCCGAGTGGTTTTTG- 3'

shRNA5: 5' -CCGGGCTTCTGTAACCTGAGCTGTACTCGAGTACAGCTCAGGTTACAGAAGCTTTTTG- 3'

Hairpin sequences of shRNA scrambled negative control:

5' -CCGGCCTAAGGTTAAGTCGCCCTCGCTCGAGCGAGGGCGACTTAACCTTAGGTTTTTG- 3'

5.6. Enzymes

Table 5.6.: *Listed are all utilized enzymes with their corresponding suppliers.*

Enzymes	**Supplier**
Bioscript™ reverse transcriptase	Bioline GmbH, Luckenwalde, Germany
Calf intestine alkaline phosphatase (CIAP)	Invitrogen GmbH, Darmstadt, Germany
DNA polymerase Biotaq™	Bioline GmbH, Luckenwalde, Germany
DNA polymerase Mango Taq™	Bioline GmbH, Luckenwalde, Germany
DNA polymerase Pfx50™	Invitrogen GmbH, Darmstadt, Germany
Restriction enzyme AgeI	New England Biolabs GmbH, Frankfurt, Germany
Restriction enzyme BsrGI	New England Biolabs GmbH, Frankfurt, Germany
Restriction enzyme EcoRI	New England Biolabs GmbH, Frankfurt, Germany
Restriction enzyme EcoRV	New England Biolabs GmbH, Frankfurt, Germany
Restriction enzyme NcoI	New England Biolabs GmbH, Frankfurt, Germany
Restriction enzyme NotI	New England Biolabs GmbH, Frankfurt, Germany
Restriction enzyme Xho	New England Biolabs GmbH, Frankfurt, Germany
Trypsin (10x)	PAA Laboratories GmbH, Pasching, Austria
Trypsin-EDTA (1x)	PAA Laboratories GmbH, Pasching, Austria

5.7. Antibodies

Table 5.7.: *Listed are all utilized antibodies with their corresponding suppliers.*

Antibodies	**Supplier**
Goat anti-rabbit IgG-peroxidase sec. antibody, (A4174)	Sigma-Aldrich Chemie GmbH, Steinheim, Germany
Goat anti-rabbit IgG-FITC sec. antibody, (sc-2012)	Santa Cruz Biotechnology Inc., Heidelberg, Germany
Mouse anti-cytochrome c prim. antibody, 6H2.B4 (556432)	BD Biosciences, Heidelberg, Germany
Rabbit anti-Fc-tag prim. antibody, custom made (216)	ImmunoGlobe GmbH, Himmelstadt, Germany
Rabbit anti-mouse IgG-FITC sec. antibody, (F-0261)	DakoCytomation, Copenhagen, Denmark
Rabbit anti-p53 prim. antibody, FL-393 (sc-6243)	Santa Cruz Biotechnology Inc., Heidelberg, Germany

5.8. Competent cells

Table 5.8.: *Listed are all utilized competent cells with their corresponding suppliers.*

Competent cells	**Supplier**
One Shot®Stbl3™	Invitrogen GmbH, Darmstadt, Germany
One Shot®TOP 10 cells (TOPO TA Cloning Kit)	Invitrogen GmbH, Darmstadt, Germany
XL-10 GOLD	Stratagene, Waldbronn, Germany

5.9. cDNA clones

Table 5.9.: *Listed are all utilized cDNA clones with their corresponding suppliers.*

cDNA clones	Supplier
WISP1-T1 (full-length clone IOH42456)	ImaGenes GmbH, Berlin; Germany
WISP1-T2 (full-length clone)	ImaGenes GmbH, Berlin; Germany
WISP2 (full-length clone)	ImaGenes GmbH, Berlin; Germany

5.10. Plasmids

Table 5.10.: *Listed are all utilized plasmids with their corresponding suppliers.*

Name	Size (bp)	Supplier
TOPO pCR2.1 cloning vector	3900	Invitrogen GmbH, Darmstadt, Germany
pLKO.1-puro cloning vector	8901	Sigma-Aldrich Chemie GmbH, Schnelldorf, Germany
pLKO.1-puro control vector	7052	Sigma-Aldrich Chemie GmbH, Schnelldorf, Germany
pLKO.1-puro non-target shRNA	7086	Sigma-Aldrich Chemie GmbH, Schnelldorf, Germany
pLKO.1-puro turbo GFP control plasmid	8347	Sigma-Aldrich Chemie GmbH, Schnelldorf, Germany
psPAX2 packaging plasmid	10703	Addgene Inc., Cambridge, USA
VSV-G/pMD2.G	5824	Addgene Inc., Cambridge, USA

5.11. Primers

Primers were designed using the free online software Primer3Plus (Rozen and Skaletsky 2000) and commercially supplied by Eurofins MWG GmbH, Ebersberg, Germany. Intron spanning primer pairs were chosen (when possible) to obviate genomic DNA impureness within the samples.

Table 5.11.: *Listed are all sequences of primers used for open reading frame amplification of WISP1-T1, WISP1-T2 and WISP2. Columns (from left to right) describe primer sequence, annealing temperature (T_A), PCR product size (S_P) in base pairs (bp) and the sequence ID of the corresponding gene product.*

	Primer sequence	T_A [°C]	S_P (bp)	Sequence ID
WISP1-T1 (WNT1 inducible signalling pathway protein 1)				
for:	5'-ATACTCGAGCGTCCAGGCATGAGGTGGTTCCTGCCCTGGA-3'	60	1103	NM_003882.2
rev:	5'-ATAGAATTCGTTGGCAATTTCTGAGAAGTCAGG'-3'	60		
WISP1-T2 (WNT1 inducible signalling pathway protein 1)				
for:	5'-ATACTCGAGCGTCCAGGCATGAGGTGGTTCCTGCCCTGGA-3'	60	842	NM_003882.2, NM_080838.1
rev:	5'-ATAGAATTCGTTGGCAATTTCTGAGAAGTCAGG-3'	60		
WISP2 (WNT1 inducible signalling pathway protein 2)				
for:	5'-ATACTCGAGGCAGGGGACATGAGAGGCACACCGAAGACCC-3'	60	752	NM_003881.2
rev:	5'-ATAGAATTCGAAGGCACTGTTTTGTGGACTGCG-3'	60		

Table 5.12.: *Listed are all sequences of primers used for reverse transcriptase PCR (RT-PCR) analyses. Columns (from left to right) describe primer sequence, annealing temperature (T_A), PCR product size (S_P) in base pairs (bp) and the sequence ID of the corresponding gene product.*

	Primer sequence	T_A [°C]	S_P (bp)	Sequence ID
APOL1 (apolipoprotein L1) [1]				
for:	5'-GCCAGAGCCAATCTTCAGTC-3'	56	230	NM_001136540.1, NM_003661.3, NM_145343.2
rev:	5'-GACTTTGCCCCCTCATGTAA-3'	56		
DCN (decorin) [1]				
for:	5'-GGACCGTTTCAACAGAGAGG-3'	57	158	NM_133503.2, NM_133504.2
rev:	5'-TCAGAACACTGGACCACTCG-3'	57		

...continues on next page

[1] PCR reaction mix as described in subsection 6.4.5: standard assay

Table 5.12.: *(...continued)*

Primer sequence	T_A [°C]	S_P (bp)	Sequence ID
			NM_133505.2, NM_133506.2
DDX58 (DEAD (Asp-Glu-Ala-Asp) box polypeptide 58) [1]			
for: 5'-AGAGCACTTGTGGACGCTTT-3'	55	213	NM_014314.3
rev: 5'-TGCAATGTCAATGCCTTCAT-3'	55		
EF1α (eucaryotic translation elongation factor 1-alpha) [1]			
for: 5'-AGGTGATTATCCTGAACCATCC-3'	54	235	NM_001402
rev: 5'-AAAGGTGGATAGTCTGAGAAGC-3'	54		
FBN1 (fibrillin) [1]			
for: 5'-GTGACTGCCCACCTGATTTT-3'	53	156	NM_000138.4
rev: 5'-AGCAGGAAGCTTTGGAAACA-3'	53		
HDAC3 (histone deacetylase 3) [1]			
for: 5'-TGCTGGTAGAAGAGGCCATT-3'	54	243	NM_003883.3
rev: 5'-CAGCCTCATCAGTCCTGTCA-3'	54		
IFIH1 (interferon induced with helicase C domain 1) [1]			
for: 5'-TGCAGTGTGCTAGCCTGTTC-3'	55	201	NM_022168.2
rev: 5'-TAAGCCTTTGTGCACCATCA-3'	55		
IFNβ1 (interferon, beta 1, fibroblast) [1]			
for: 5'-AGCACTGGCTGGAATGAGAC-3'	55	185	NM_002176.2
rev: 5'-TCCTTGGCCTTCAGGTAATG-3'	55		
IGF2BP2 (insulin-like growth factor 2 mRNA binding protein 2) [1]			
for: 5'-TGGAAGCGCATATCAGAGTG-3'	54	165	NM_001007225.1, NM_006548.4
rev: 5'-AGTGCCCGATAATTCTGACG-3'	54		

...continues on next page

Table 5.12.: *(...continued)*

Primer sequence	T_A [°C]	S_P (bp)	Sequence ID
IGFBP5 (insulin-like growth factor binding protein 5) [1]			
for: 5'-GAGCTGAAGGCTGAAGCAGT-3'	55	237	NM_000599.3
rev: 5'-GAATCCTTTGCGGTCACAAT-3'	55		
ING1 (inhibitor of growth family, member 1) [1]			
for: 5'-CAACAACGAGAACCGTGAGA-3'	56	195	NM_005537.3, NM_198217.1, NM_198218.1, NM_198219.1
rev: 5'-GAGACCTGGTTGCACAGACA-3'	56		
ISG15 (ubiquitin-like modifier) [1]			
for: 5'-TGTCGGTGTCAGAGCTGAAG-3'	56	206	NM_005101.3
rev: 5'-GCCCTTGTTATTCCTCACCA-3'	56		
LAMA1 (laminin, alpha 1) [2]			
for: 5'-AGCGGATATGCAGCTCTTGT-3'	56	150	NM_005559.2
rev: 5'-GCCGTCCACAAGCTCTAGTC-3'	56		
MAP1B (microtubule-associated protein 1B) [1]			
for: 5'-CCTGAAGTCCCAGGACAAAA-3'	53	197	NM_005909.3
rev: 5'-AAAGAGCCGGACTGGAGAAT-3'	53		
MDM2 (p53 binding protein homolog (mouse)) [1]			
for: 5'-GGTGGGAGTGATCAAAAGGA-3'	54	210	NM_001145336.1, NM_001145337.1, NM_001145339.1, NM_002392.3
rev: 5'-ACACAGAGCCAGGCTTTCAT-3'	54		
NID2 (nidogen 2) [1]			
for: 5'-GTGCCGGAGTGGTTATGAGT-3'	55	233	NM_007361.3

...continues on next page

[2] PCR reaction mix as described in subsection 6.4.5: standard assay including 3μl $MgCl_2$ (50mM)

Table 5.12.: *(...continued)*

	Primer sequence	T_A [°C]	S_P (bp)	Sequence ID
rev:	5'-TAGCTGCAGGGTGACATCTG-3'	55		
PAPPA (pregnancy-associated plasma protein A, pappalysin 1) [1]				
for:	5'-TGGCCTCCATCCTACATCTC-3'	55	155	NM_002581.3
rev:	5'-ATCGCCACAGTACCCACTTC-3'	55		
PMAIP1/NOXA (phorbol-12-myristate-13-acetate-induced protein 1) [1]				
for:	5'-CAGTGCCAACTCAGCACATTG-3'	55	210	NM_021127.2
rev:	5'-GTAACGCCCAACAGGAACAC-3'	55		
PRKA1A (protein kinase, cAMP-dependent, regulatory, type I, alpha) [1]				
for:	5'-GGGAAGCACACTGAGAAAGC-3'	55	198	NM_002734.3, NM_212471.1, NM_212472.1
rev:	5'-ACAGCAGCTGACCCCTCTAA-3'	55		
RAN (RAN, member RAS oncogene family) [1]				
for:	5'-TGTGTGGCAACAAAGTGGAT-3'	53	223	NM_006325.3
rev:	5'-AAAGCTGGGTCCATGACAAC-3'	53		
SDC (syndecan1) [1]				
for:	5'-GGCTGTAGTCCTGCCAGAAG-3'	56	234	NM_001006946.1, NM_002997.4
rev:	5'-TCTGTGTGGGGAGTGTGAAG-3'	56		
TLR3 (Toll-like receptor 3) [1]				
for:	5'-AGCCTTCAACGACTGATGCT-3'	55	201	NM_003265.2
rev:	5'-TTTCCAGAGCCGTGCTAAGT-3'	55		
TNSF10/TRAIL (tumor necrosis factor (ligand) superfamily, member 10) [1]				
for:	5'-TGAGAACCTCTGAGGAAACCA-3'	55	226	NM_001190942.1, NM_001190943.1, NM_003810.3
rev:	5'-CAAGTGCAAGTTGCTCAGGA-3'	55		

...continues on next page

Table 5.12.: *(...continued)*

	Primer sequence	T_A [°C]	S_P (bp)	Sequence ID
WISP1 (WNT1 inducible signalling pathway protein 1) [3]				
for:	5'-ACAGATGGCTGTGAGTGCTG-3'	55	199	NM_003882.2, NM_080838.1
rev:	5'-AGGACTGGCCGTTGTTGTAG-3'	55		
WISP1-T1 (WNT1 inducible signalling pathway protein 1) [3]				
for:	5'-CAGATGGCTGTGAGTGCTGT-3'	56	184	NM_003882.2
rev:	5'-AGGACTGGCCGTTGTTGTAG-3'	56		
WISP1-T1, -T2 (WNT1 inducible signalling pathway protein 1) [3]				
for:	5'-CAGATGGCTGTGAGTGCTGT-3'	56	561,	NM_003882.2,
rev:	5'-ACTGGGCGTTAACATTGGAG-3'	56	265	NM_080838.1
WISP2 (WNT1 inducible signalling pathway protein 2) [3,4]				
for:	GAGTACCCCTGGTGCTGGATG-3'		211	NM_003881.2
rev:	GTCTCCCCTTCCCGATACA-3'			

Table 5.13.: *Listed are all sequences of primers used for sequencing PCR reaction. Columns (from left to right) describe primer sequence, annealing temperature (T_A) and the sequence ID of the corresponding gene product, if possible.*

	Primer sequence	T_A [°C]	Sequence ID
Bac1 (pBacPAK8 vector)			
for:	5'-ACCATCTCGCAAATAAATAAG-3'	50	
Bac2 (pBacPAK8 vector)			
for:	5'-ACAACGCACAGAATCTAGCG-3'	50	

...continues on next page

[3] PCR reaction mix as described in subsection 6.4.5: standard assay including 2μl $MgCl_2$, 6% DMSO
[4] Primer combination detects both WISP1 isoforms: WISP1-T1 (561bp); WISP1-T2 (265bp)

Table 5.13.: *(...continued)*

	Primer sequence	T_A [°C]	Sequence ID
IgG Fc (Fc-tag)			
for:	5'-ATAGAATTCACCATGGGATCCGTCGACAAAACTCACAC-3'	50	
rev:	5'-ATAGCGGCCGCGCGCACTCATTTACCCGGAGA-3'	50	
IgG Fc (Fc-tag) for2			
for:	5'-ATAGAATTCTTAGTACCTCGAGGAAGCGGATCCGTCGACAAAATCAC-3'	50	
M13 (TOPO vector)			
for:	5'-GTAAAACGACGGCCAG-3'	50	
rev:	5'-CAGGAAACAGCTATGAC-3'	50	
T3 Promotor (PCR cloning vector)			
rev:	5'-ATTAACCCTCACTAAAG-3'	50	
T7 Promotor (PCR cloning vector)			
for:	5'-TAATACGACTCACTATAGGG-3'	50	
LKO 1.5 (pLKO.1 vector)			
for:	5'-GACTATCATATGCTTACCGT-3'	50	
WISP1 (WNT1 inducible signalling pathway protein 1) seq1			
for:	5'-CCTACGACCATGGACTTT-3'	50	NM_003882.2, NM_080838.1
WISP1 (WNT1 inducible signalling pathway protein 1) seq2			
for:	5'-CAACTGCACGGAGGCTGC-3'	50	NM_003882.2, NM_080838.1
WISP1 (WNT1 inducible signalling pathway protein 1) seq3			

...continues on next page

Table 5.13.: *(...continued)*

	Primer sequence	T_A [°C]	Sequence ID
for:	5'-GTGAGCATACCTGGCCAC-3'	50	NM_003882.2
WISP1 (WNT1 inducible signalling pathway protein 1) seq4			
for:	5'-GCGATGTGGACATCCATAC-3'	50	NM_003882.2, NM_080838.1
WISP1 (WNT1 inducible signalling pathway protein 1) seq5			
for:	5'-AGACTATCGACGTGTCCT-3'	50	NM_003882.2, NM_080838.1
WISP1_shRNA (WNT1 inducible signalling pathway protein 1) seq1			
rev:	5'-GAATACTGCCATTTGTCTC-3'	50	NM_003882.2
WISP1_shRNA (WNT1 inducible signalling pathway protein 1) seq2			
rev:	5'-TCTGTTGCTATTATGTCTAC-3'	50	NM_003882.2
WISP2 (WNT1 inducible signalling pathway protein 2) seq1			
for:	5'-AGGAGGGTCGAGGTCCTG-3'	50	NM_003881.2
WISP2 (WNT1 inducible signalling pathway protein 2) seq2			
for:	5'-ACTTTAGCTTGGGTCCACCA-3'	50	NM_003881.2
WISP2 (WNT1 inducible signalling pathway protein 2) seq3			
for:	5'-CTCTTGGCAGAGGACGACAG-3'	50	NM_003881.2
WISP2 (WNT1 inducible signalling pathway protein 2) seq4			
for:	5'-ACCATGTACCTGCCCCTGGC-3'	50	NM_003881.2

5.12. Buffers and solutions

5.12.1. Molecular biology

Table 5.14.: *Listed are all established buffers and solutions, used for molecular biology methods.*

0.5M EDTA (autoclaved)	• EDTA tetrasodium salt hydrate • ad distilled water • pH adjusted to 8.0	19.00g 100.00ml
3M Sodium acetate	• sodium acetate • ad distilled water • pH adjusted to 4.3	24.60g 100.00ml
50mM Tris base (autoclaved) for 10mM Tris base diluted 1:5 with distilled water	• tris base • ad distilled water • pH adjusted to 7.2-7.5	3.03g 500.00ml
10x TBE	• tris base • boric acid • EDTA tetrasodium salt hydrate • ad distilled water • pH adjusted to 8.3	108.00g 55.00g 9.05g 1000.00ml
Working solution	• TBE buffer 10x • ad distilled water	50.00ml 1000.00ml

5.12.2. SDS-PAGE

Table 5.15.: *Listed are all established buffers and solutions, used during SDS-PAGE procedures.*

0.5% Bromphenol blue	• bromophenol blue sodium salt • ad distilled water • pH adjusted to 8.0	0.05g 10.00ml
10% APS storage in aliquots at -20°C	• ammonium persulfate • ad distilled water	1.00g 10.00ml
10% SDS	• sodium dodecyl sulfate • ad distilled water	10.00g 100.00ml
Lower buffer *10x stock solution*	• Tris base • glycine • ad distilled water	15.10g 71.40g 500.00ml
Working solution	• 10x stock solution • ad distilled water	100.00ml 1000.00ml
Sample buffer *20x stock solution*	• 0.5M Tris base (pH 6.8) • glycerol • 10% SDS • 0.5% bromophenol blue	1.20ml 1.00ml 2.00ml 0.50ml

...continues on next page

Table 5.15.: *(...continued)*

	• ad distilled water	4.80ml
storage at 4° C		
Working solution	• 20x stock solution	0.95ml
	• 2-mercaptoethanol	0.05ml
Separating gel buffer 0.5M Tris base	• Tris base	60.57g
	• ad distilled water	1000.00ml
	• pH adjusted to 6.8	
Separating gel buffer 3M Tris base	• Tris base	363.42g
	• ad distilled water	1000.00ml
	• pH adjusted to 8.8	
Upper buffer		
	• Tris base	6.80g
	• glycine	28.55g
4x stock solution	• SDS	2.00g
	• ad distilled water	500.00ml
	• 4x stock solution	100.00ml
Working solution	• thioglycolic acid	84 μl
	• ad distilled water	500.00ml

5.12.3. Western blotting

Table 5.16.: *Listed are all established buffers and solutions, used for Western blotting.*

0.25M EDTA	• EDTA tetrasodium salt hydrate • ad distilled water • pH adjusted to 8.0	10.40g 100.00ml
1M sodium chloride	• sodium chloride • ad distilled water	292.20g 1000.00ml
1M Tris/HCL	• Tris base • ad distilled water • pH adjusted to 7.5 by addition of hydrochloric acid	121.14g 1000.00ml
10% Triton X-100	• Triton X-100 • ad distilled water	10.00ml 100.00ml
0.1% Tween 20/PBS	• Tween 20 • ad 1x PBS	1.00ml 100.00ml
Transfer buffer *10x stock solution*	• Tris base • glycine • ad distilled water	30.00g 144.00g 1000.00ml

...continues on next page

Table 5.16.: *(...continued)*

	• pH adjusted to 10.0 by addition of sodium hydroxide pellets	
Working solution	• 10x stock solution	100.00ml
	• methanol	200.00ml
	• ad distilled water	1000.00ml
Washing buffer I	• 1M Tris-HCl (pH 7.5)	10.00ml
	• 5M sodium chloride	30.00ml
	• 0.25M EDTA (pH 8.0)	8.00ml
	• 10% Triton X-100	10.00ml
	• ad distilled water	1000.00ml
Washing buffer II	• 1M Tris-HCl (pH 7.5)	10.00ml
	• 5M sodium chloride	200.00ml
	• 0.25M EDTA (pH 8.0)	8.00ml
	• 10% Triton X-100	10.00ml
	• ad distilled water	1000.00ml
Blocking solution	• BSA	1.25g
	• skim milk powder	1.25g
	• horse serum	1.00ml
	• ad 0.1% Tween 20/PBS	50.00ml
prepared freshly before use		

...continues on next page

Table 5.16.: *(...continued)*

Prim. antibody solution	• BSA	0.25g
	• skim milk powder	0.25g
	• horse serum	0.25ml
	• ad 0.1% Tween 20/PBS	25.00ml
	• plus appropriate dilution of the respective primary antibody	
prepared freshly before use		
Sec. antibody solution	• BSA	0.40g
	• skim milk powder	0.40g
	• horse serum	0.40ml
	• ad 0.1% Tween 20/PBS	40.00ml
	• plus appropriate dilution of the respective secondary antibody	
prepared freshly before use		
Washing solution I	• BSA	2.00g
	• skim milk powder	2.00g
	• horse serum	2.00ml
	• ad washing buffer I	200.00ml
prepared freshly before use		
Washing solution II	• BSA	2.00g
	• skim milk powder	2.00g
	• horse serum	2.00ml

...continues on next page

Table 5.16.: *(...continued)*

	• ad Washing solution II	200.00ml
prepared freshly before use		

5.12.4. Silver staining

Table 5.17.: *Listed are all established buffers and solutions, used during silver staining procedure.*

Fixation	• ethanol (100%)	75.00ml
	• acetic acid (100%)	25.00ml
	• ad distilled water	250.00ml
Sensitization	• ethanol (100%)	100.00ml
	• sodium thiosulfate (5%)	10.00ml
	• sodium acetate	17.00g
	• glutaraldehyde (25%)	1.25ml
	• ad distilled water	250.00ml
Staining solution	• silver nitrate (2.5%)	25.00ml
	• formaldehyde (37%)	0.10ml
	• ad distilled water	250.00ml
Developer	• sodium carbonate	6.25g
	• formaldehyde (37%)	0.05ml

...continues on next page

Table 5.17.: *(...continued)*

	• ad distilled water	250.00ml
Stop solution	• EDTA-Na_2x2H_2O	3.65g
	• ad distilled water	250.00ml

5.12.5. Cell culture media and additives

Table 5.18.: *Listed are all utilized media and additives, used during cell cultivation.*

Standard culture medium[5]	• FCS	50.00ml
	• 1xPen/Strep	5.00ml
	• ad DMEM Ham's F12 with L-Glutamine	500.00ml
Culture medium: hMSCs	• FCS	50.00ml
	• 1xPen/Strep	5.00ml
	• L-ascorbic acid 2-phosphate	0.05ml
	• ad DMEM Ham's F12 with L-Glutamine	500.00ml
1x PBS (autoclaved)	• PBS Dulbecco w/o Ca^{2+}, Mg^{2+}	9.55g
	• ad distilled water	1000.00ml
	• pH adjusted to 7.4	

...continues on next page

[5]Standard culture medium was used for following cell lines: C28I2, HEK-293T, hFOB, hMSC-TERT4, hMSC-TERT20, MG-63, TE-85, Tc28a2, U2

Table 5.18.: *(...continued)*

1x PBS/EDTA (autoclaved)	• PBS Dulbecco w/o Ca^{2+}, Mg^{2+}	9.55g
	• EDTA tetrasodium salt hydrate	0.20g
	• ad distilled water	1000.00ml
	• pH adjusted to 7.4	
Polybrene (sterile filtrated)	• polybrene	0.01g
	• ad distilled water	10.00ml
Application: 8μg/ml medium; storage in aliquots at -20° C		

5.12.6. Bacteria cultivation

Table 5.19.: *Listed are all utilized solutions, used during bacteria cultivation.*

LB (Luria Bertani) medium (autoclaved)	• tryptone	10.00g
	• yeast extract	5.00g
	• sodium chloride	5.00g
	• ad distilled water	1000.00ml
LB-agar/ampicillin plates (autoclaved)	• tryptone	10.00g
	• yeast extract	5.00g
	• sodium chloride	10.00g
	• agar	15.00g

...continues on next page

Table 5.19.: *(...continued)*

• ad distilled water	1000.00ml

Chill autoclaved LB-agar medium to 55°C prior to Ampicillin (100mg/ml) application

5.13. Software and online sources

Table 5.20.: *Listed are all utilized software tools and online sources.*

Software/Database	**Company/URL**
ABI PRISM 310 collection	Applied Biosystems Applera Deutschland GmbH, Darmstadt, Germany
AxioVision Rel.4.8	Carl Zeiss Vision GmbH, Aalen, Germany
Bio-Capt 12.5	LTF Labortechnik GmbH & Co. KG, Wasserburg, Germany
BLAST	(Altschul et al. 1990)
ChemBioDraw	PerkinElmer, Morrisville, NC, USA
ClustalW2	(Thompson et al. 2002)
GelAnalyzer 2010a	http://www.gelanalyzer.com
GenBank	(Benson et al. 1997)
GeneCards V3	http://www.genecards.org
Illustrator 4.0®	Adobe Systems Incorporated, San Jose, CA, USA
KEGG PATHWAY Database	http://www.genome.jp/kegg
Latex	http://www.latex-project.org
LEO Dictionary	http://dict.leo.org
Microsoft Office 2011®	Microsoft Corporation, Redmond, WA, USA
NCBI Pubmed	http://www.ncbi.nlm.nih.gov/pubmed
Papers	http://www.mekentosj.com

...continues on next page

Table 5.20.: *(...continued)*

Software/Database	**Company/URL**
Photoshop 4.0®	Adobe Systems Incorporated, San Jose, CA, USA
Primer3Plus	(Rozen and Skaletsky 2000)
R	(R Development Core Team 2010)
Wikipedia	http://www.wikipedia.org

CHAPTER
SIX

METHODS

6.1. Cell culture

6.1.1. Isolation of primary human mesenchymal stem cells (hMSCs)

Human bone marrow derived stem cells were isolated from the femoral head obtained from patients undergoing total hip arthroplasty. This occurs under the approval of the Local Ethics Committee of the University of Würzburg. Each patient was informed and provided a written consent. Donors were aged between 43 and 79 years (in average 64.5). Trabecular bone pieces were harvested, mixed with DMEM Ham's F12 medium and strongly vortexed. After centrifugation (1200rpm/5min) the cell pellet was reconstituted in DMEM Ham's F12 medium supplemented with 10% foetal bovine serum (FCS), antibiotics (50 I.U. penicillin/ml and 50μg streptomycin/ml) and 50μg/ml ascorbate (complete medium). After repeated washing and vortexing, the stromal cells containing medium was filtered through a cell strainer to hold back bone fragments. The released cells were pelleted, suspended in complete medium and plated at a density of 2x10^8 cells per 150cm^2 tissue culture flask. Previously, cell number and vitality was determined by mixing 50μl cell suspension and 50μl trypan blue. A Neubauer counting chamber was used to determine the cell density (Lindl 2002). Seeded cells were incubated at 37°C in a humidified atmosphere enriched with 5% CO_2. Non-adherent cells were removed after two days and subsequently the medium was changed every three to four days until the cell cultures reached 90-100% confluence.

6.2. Culture and propagation of primary cells and cell lines

6.2.1. Subculturing

Culture medium was replaced every second-third day until the cells reached 90-100% confluence. Subsequently, cells were washed with PBS and detached by exposure of 1x trypsin/EDTA for 3-7min at 37°C. The addition of culture medium after exposure time was necessary to inactivate trypsin activity. Cells were pelleted by centrifugation (1200rpm for 5min), resuspended in fresh culture medium and subcultured at the specific ratio (Tab. 6.1). For experimental settings, plating density depended on the further applications of the cells (see next sections).

Table 6.1.: *Summary of derivation and cultivation conditions of primary cells and cell lines.*

Name	Derivation	Subculturing (split ratio)	Temp. [°C]
C28I2	human (rib cartilage)	1:30	37, 32 [1]
HEK-293T	human (embryonic kidney)	1:8	37
hFOB	human	1:6	37
hMSC	human (bone marrow)	1:3	37
hTert4	human	1:4	37
hTert20	human	1:20	37
MG63	human (ostesarcoma)	1:30	37
SF21	insect (Spodoptera frugiperda)	1:2 - 1:10	37
TE85	human (ostesarcoma)	1:30	37
Tc28a2	human (rib cartilage)	1:30	37, 32 [1]
U2	human (ostesarcoma)	1:30	37

Depending on culture vessel size, different quantities of cell culture medium, PBS and 1x trypsin/EDTA were required (Tab. 6.2).

Subculturing SF21 cells

Culture medium was replaced every seven days until the cells reached nearly 90% confluence. To divide subcultures, used medium was removed and cells were scraped and mixed in fresh culture medium. The split ratio extended between 1:2 and 1:10. For experimental setting, cells were disseminated in Insect express SF9 medium.

6.3. Recombinant protein production

Recombinant (r)protein production describes the method of generating protein expressions that have been produced by recombinant DNA techniques. For this purpose, proteins were created through combining sequences that would not occur via the common process of gene splicing. Genes of interest were amplified and integrated into plasmids, which were used as viral vectors to reproduce the altered DNA by replication and infection of other cells. This increased the amount of cells with the recombinant DNA and enabled an efficient (r)protein

[1] cells were incubated at 32°C during experimental settings

Table 6.2.: *Summary of appropriate cell culture vessel types and their corresponding amount of culture medium, PBS and 1x trypsin/EDTA.*

Culture vessel	**Culture medium [ml]**	**PBS [ml]**	**1x trypsin/EDTA [ml]**
6 well (9,03cm^2)	3-5	1	0.5
25cm^2 flask	5	2	1
75cm^2 flask	15	10	4
150cm^2 flask	25	12	5
175cm^2 flask	30	15	6
chamber slide (4.2cm^2)	1.2 - 2.0	0.5	-
chamber slide (1.8cm^2)	0.5 - 0.9	0.25	-

production. In this study, (r)protein expression was achieved with the Baculovirus Expression System purchased from Clontech. Baculoviruses are a family of viruses that infect mostly moth species and the virus autographa californica nuclear polyhedrosis (AcMNPV) is commonly used to express foreign proteins in the insect cell line SF21, developed from the moth Spodoptera frugiperda. The stable integration of the target sequence in the virus genome was caused by gene replacement, encoding the polyhedrin protein p10, which is not useful for the virus in cell culture. The polyhedrin promotor induced a high-level transcription of the insert, resulting in an increased amount of (r)protein.

6.3.1. Proof-reading Polymerase chain reaction (PCR)

Full-length cDNA plasmid sequences of WISP1-T1, WISP1-T2 and WISP2 were amplified with the Pfx50^{TM}DNA Polymerase, containing a proof-reading 5' to 3' exonuclease activity in the provided buffer system. Pfx50^{TM}DNA Polymerase produces PCR products, which can be directly used for TOPO®Cloning. Specific primer pairs (Sec. 5.11) were designed containing restriction sites for XhoI (forward primer) and EcoRI (reverse primer) flanking the expected open reading frames of the three different cDNA clones. According to the manufacturer's instructions 1-100pg cDNA template was applied in three different dilutions (1:10, 1:100, 1:1000) to separated PCR reactions. Standard protocol and reaction steps for the PTC-200 thermal cycler purchased from Peltier MJ Research are listed in table 6.3. Subsequently, proof-reading PCR products were verified by gel electrophoresis and sequencing analyses (Subsec. 6.3.2 and 6.3.3).

6.3.2. Gel electrophoresis

Agarose gel electrophoresis was used to determine the presence of PCR products as well as RNA fragments and plasmid inserts. DNA (or RNA) was forced to migrate through a highly

Table 6.3.: *Standard reaction steps: proof-reading PCR*

Reagent	**Amount [μl]**	**Reaction steps**	**Temp. [°C]**	**Time [min]**
10x buffer	5	1) step: Initial denaturating	94	2
10mM dNTPs	1.5	2) step: Denaturing	94	0.25
5μM primer for	3	3) step: Annealing	60	0.5
5μM primer rev	3	4) step: Elongation	68	1.5
5U/μl Pfx50^{TM}	1	5) step: Final elongation	68	5
0.2ng/μl cDNA plasmide template	1	6) step: Cooling	4	inf
HPLC water	50			

cross-linked agarose matrix in response to an electric current with a voltage of 0.9 V/cm^2 agarose gel. Phosphates on the DNA are negatively charged and therefore migrate to the positive pole. 1-1.8% agarose gels were prepared by dissolving agarose powder in 0.5xTBE buffer. For visualisation, 5% ethidium bromide was added to the solution. It intercalates into double-stranded DNA or RNA and fluoresces when exposed to UV-light. After the gel polymerised at room temperature (RT), proof-reading PCR products, plasmid DNA and RNA were enriched with 1xloading dye and loaded onto the gel. cDNA PCR products were achieved with the MangoTaq^{TM}DNA polymerase and contained already a loading dye in the associated buffer system (Subsec. 6.4.5). Depending on the target DNA or RNA size, a 100bp or 1000bp ladder was used to verify the expected size. Small fragments run more quickly than large fragments at a rate proportional to their size and were visualized by exposure to UV-light in a UV-chamber. Transcript amounts were normalized with the housekeeping gene EF1α and evaluated with the densitometric software GelAnalyzer 2010a.

6.3.3. Sequencing analysis

DNA sequencing is a method to verify the precise sequence of nucleotides (dNTPs) in a sample of DNA. Dideoxy sequencing (Sanger's method or chain termination) is based on the use of dideoxynucleotides (ddNTP's) additional to the normal dNTPs during PCR. Each of the different ddNTPs (ddATP, ddCTP, ddGTP, and ddTTP) is labelled with a distinct fluorescent dye and contains a hydrogen group on the 3' carbon instead of a hydroxyl group. After integration into a new sequence a phosphodiester bond cannot accumulate between the ddNTP and the next incoming dNTP. This results in termination of DNA synthesis and generates fragments of random length. All sequencing analyses were performed with the ABI PRISM 310 Sequencer purchased from Applied Biosystems. The appropriate Big Dye Terminator v1.1 Cycle Sequencing Kit includes dye terminators, dNTPs, AmpliTaq DNA Polymerase, magnesium chloride and buffer. According to the manufacturer's instruction a PCR mix was generated containing 5pmol primer (forward or reverse) and 1-2μl PCR product or 100-150ng plasmid DNA per reaction. Standard PCR reaction steps for the PTC-200 thermal cycler are listed below in table 6.4.

Table 6.4.: *Standard reaction steps: sequencing analysis PCR*

Reaction steps	**Temp. [°C]**	**Time [min]**
Initial denaturation	94	4
Denaturation	94	0.5
Annealing	50	1
Elongation	60	1
Final elongation	72	5
Cooling	12	inf

The amplification products were loaded onto NucleoSeq columns and excess of salts, nucleotides and primers were retained through centrifugation, whereas the eluate contained the pure PCR product. 0.1M sodium acetate (pH 4.3) supplemented to 80% ethanol precipitated the DNA. After incubation at room temperature (15min) and centrifugation (13.000rpm for 20min), the pellet was washed with 70% ethanol and air-dried. The pellet was then resuspended in 15-30μl Template Suppression Reagent and denaturated at 94°C for 4min. Subsequently, the samples were chilled on ice for a few minutes and placed into the sequencer. A laser determined the identity of each band, since the four dyes fluorescence at different wavelength. Using the ABI PRISM 310 collection and Sequencing analysis 3.4 software, the results were depicted in form of a chromatogram of coloured peaks that correspond to the nucleotide in that location in the DNA. In conclusion, sequences were compared to the online database of NCBI by inserting into NCBI blast search.

6.3.4. TOPO®Cloning

The plasmid vector pCR®2.1-TOPO®(purchased from invitrogen) is based on the properties of the enzyme topoisomerase I to cleave and rejoin supercoiled DNA ends and facilitate replication. This enzyme specifically recognizes the sequence 5'-C/TCCTT-3' (Shuman 1991), which present the final bases at both ends of the linearized vector. The enzyme is covalently attached with its tyrosyl residue (Tyr-274) and the 3' phosphate of the cleaved strands.

Ligation of WISP1-T1, WISP1-T2 and WISP2 PCR products

Full-length cDNA sequences of WISP1-T1, WISP1-T2 and WISP2 were amplified with the Pfx50^{TM}DNA polymerase. Pure PCR product and salt solution (1μl of each) were diluted in 3μl HPLC water and subsequently mixed with 1μl of linearized pCR®2.1-TOPO®vector. During the incubation (5min, RT), the free 5' ends of the PCR product strands were ligated (catalysed by topoisomerase I) with the topoisomerase/3' end of each vector strand. Subsequently, the reaction was stored on ice until the transformation of the ligated vector into chemically competent E.coli cells was performed.

Transformation into chemically competent cells

Vectors including the inserts of WISP1-T1 or WISP1-T2 were transformed in chemically competent One Shot®TOP10 cells, while the WISP2 containing vector was transformed into One Shot®Stbl3 cells. PCR®2.1-TOPO®vectors are ampicillin resistant, thus it was necessary to prepare LB/ampicillin agar plates prior to transformation. The cells were stored at -80°C and immediately defrosted before the transformation procedure started. 2μl of each TOPO®reaction was added to 50μl cells and incubated for 30min on ice. Cells were shortly warmed up by 42°C for 30sec and immediately cooled down on ice for 2-3min. 250μl outgrowth SOC medium (preheated) was added to the vials and cells shook 1h at 37°C. During the incubation, LB/ampicillin agar plates were preheated and 40μl of a 40mg/ml X-gal stock solution (necessary for blue/white screening) was dispensed onto two of these plates. After 1h, 200μl/vial were plated onto LB/ampicillin agar plates. One Shot®TOP10 cells were plated on X-gal covered agar plates, while One Shot®Stbl3 cells are not convenient for blue/white screening and were plated on pure LB/ampicillin agar plates.

Blue/white screening

Additional to the clone selection via ampicillin resistance of the TOPO®vector, One Shot®-TOP10 cells are convenient for blue/white screening. This is a common method to detect successful ligation of vector based gene cloning. The TOPO®vector encodes a subunit of the LacZ protein (β-galactosidase) with an internal multiple cloning site (MCS). The One Shot®TOP10 cells encode the remaining subunit to form a functional β-galactosidase enzyme. During the TOPO®cloning procedure, the inserts were ligated into the MCS within the lacZ gene. This will disrupt protein expression, thus positive clones will lack functional β-galactosidase. X-gal is a modified galactose sugar that is metabolized by β-galactosidase following the characteristic blue colour in the colonies containing a vector without insert. Colonies without a vector were not able to grow on ampicillin agar plates, while white colonies contained a vector + insert. These colonies weren't able to metabolize X-gal, because they lack functional β-galactosidase.

Minipreperation of plasmid DNA

Agar plates were incubated over night at 37°C. Respective and white coloured clone colonies were picked and cultivated in 2ml LB/amp-medium at 37°C with constant shaking for 12-16h. The medium contained 100mg/ml ampicillin to ensure plasmid propagation. Glycerol stock solutions of each clone in a 3:1 (glycerol/germs) ratio were constituted and stored at -80°C for further experiments. According to the manufacturer's instructions of the NucleoSpin®Plasmid kit (Marcherey & Nagel), 1ml of the saturated E. coli-LB culture was used to isolate the plasmid DNA in a provided buffer system. First, the culture was pelleted via centrifugation (30s at 11.000xg) and subsequently resuspended. Plasmid DNA was separated from the E. coli host cells by a SDS containing alkaline lysis buffer. Neutralization buffer was added to the lysate to creates appropriate conditions for binding of plasmid DNA to the silica membrane of the NucleoSpin®Plasmid binding column. Precipitated protein, genomic DNA, and cell debris were then pelleted by centrifugation and the supernatant was loaded onto the binding column. An additional centrifugation step was necessary for binding plasmid DNA onto the silica membrane. Washing with provided ethanolic buffer removed contaminations like salts, metabolites and soluble macromolecular cellular components. Pure plasmid DNA was finally eluted under low ionic conditions with a slightly alkaline buffer (5mM Tris/HCl, pH 8.5).

Concentration of plasmid DNA was determined by 1:25 dilution of plasmid suspension in HPLC. Absorption was measured at 260nm using UV-light permeable cuvettes. Purity was estimated by the quotients E_{260}/E_{280} and E_{260}/E_{230}, since the absorption of proteins occurs

at 280nm while contaminants like carbohydrates and peptides absorb at 230nm. To exclude contaminants, E_{260}/E_{280} should be 2.0 and E_{260}/E_{230} should be larger than 2.0.

Restriction enzymes were used to cut plasmid DNA at specific sequences to verify successful plasmid preparation. Previously, modified primer pairs enclosed restriction sites for XhoI (forward primer) and EcoRI (reverse primer) flanked the expected open reading frames of the three cDNA clones. These restriction sites were amplified during the proof reading PCR of the open reading frames and cloned into the TOPO®vector. 1U enzyme was used to restrict 1μg plasmid DNA in the appropriate buffer system. The restriction suspension was incubated for 2h at 37°C and subsequently verified using agarose gel electrophoresis. The expected sizes of the WISP1-T1, WISP1-T2 and WISP2 sequences are stated in section 5.11, table 5.11.

Midipreperation of plasmid DNA

Clones containing an insert with the expected size were amplified to achieve higher quantities of plasmid DNA. Using a diluting loop, marginal amounts of the glycerol stocks sufficed to inoculate 50ml LB/ampicillin medium. The suspension was incubated over night with constant shaking at 37°C. Following the manufacturer's instructions of the PureYield®plasmid midi preparation kit (promega), the saturated E. coli-LB culture was pelleted via centrifugation. Subsequently, the pellet was resuspended, lysed and neutralized to ensure appropriate conditions for removing cellular debris. The lysate was added onto the provided PureYield®Clearing Column and centrifugation separated cellular debris and plasmid DNA. An additional centrifugation step was performed for binding the plasmid DNA onto the membrane of the PureYield®Binding Column. Several washing steps, like endotoxin removal wash, removed substantial amounts of protein, RNA and endotoxin contaminants from purified plasmid DNA. 600μl nuclease-free water was added onto the membrane of the binding column to elute purified plasmid DNA. Concentration of plasmid DNA was determined depicted in subsection 6.3.4, page 52. Insert plasmid DNA were verified by sequencing analysis (Subsec. 6.3.3) to ensure a completely correct progression of bases within the open reading frame.

6.3.5. pBacPAK8 Cloning

Vector linearization and restriction of WISP1-T1, -T2 and WISP2 target sequence

The AcMNP virus genome is very large (134kb), thus the small transfer vector pBacPAK8 (<10kb) was used to integrate the target sequences of WISP1-T1, -T2 or WISP2 into the viral genome. 3μg of each target sequence (verified by sequencing analyses) and the transfer vector were restricted seperately with EcoRI and XhoI (1U/μg) over night at 37°C. To obviate recircularization and religation of the linearized vector, 1μl calf intestinal alkaline phosphatase (CIAP) and 5μl dephosphorylation buffer were added to the pBacPAK8 restriction reaction. The enzyme catalysed the 5' phosphate group's removal, thus DNA fragments that lack the 5' phosphoryl termini cannot self-ligate. After incubation for 1h at 37°C each target sequence and the linearized transfer vector were loaded onto a 1% agarose gel with a constant current of 145V for 1h. The visualization of specific DNA fragments took place by exposure to UV-light.

Purification of DNA from TBE-agarose gels

DNA bands of the target sequences were excised with a scalpel and size of the gel slice was minimized by removing excess of agarose. According to the manufacturer's instruction of the NucleoSpin® Extract II kit (purchased from Machery & Nagel), the gel slice was weight and 2 volumes of the dedicated buffer was added to 1 volume gel (e.g. 200μl buffer/100mg gel). The gel was incubated at 50°C for 10min and occasionally vortexed to solubilize the

agarose. Especially binding columns were used to bind DNA fragments onto silica-gel-based membranes during centrifugation (13000xg, 1min). The membrane was washed with desalting buffer and dried by centrifugation (13000xg, 2min). Pre-heated elution buffer was added onto the membrane to dissolve DNA fragments via an additional centrifugation step (13000xg, 1min).

Integration of target sequences into the transfer vector pBacPAK8 with subsequent transformation and plasmid purification

The restriction endonucleases EcoRI and XhoI produced palindromic, sticky ends in the pBacPAK8 vector and the WISP target sequences. Instantaneous after gel extraction, the cohesive ends were ligated according to the manufacturer's instructions of the Fast-Link DNA Ligation Kit (Biozym). The required amount of a 10kb sized vector is 75-150ng and the ratio between vector and insert should be 2:1. The reactions were incubated at RT for 5min and subsequently heated at 70°C (15min) to stop the enzyme activity of the ligase. The pBacPAK8 vectors including the inserts of WISP1-T1, -T2 or WISP2 were transformed in chemically competent One Shot®TOP10 cells. Transformation was performed (Subsec. 6.3.4, page 52) and bacteria suspension was plated on LB/amp-agar plates and incubated at 37°C over night. After plasmid mini preparation, the restriction enzymes EcoRI and XhoI were employed to verify successful ligation, transformation and plasmid preparation. Further restriction and cloning steps were conducted to integrate an additional Fc-tag into the pBacPAK8 vector. This tag has the sequence encoding for the Fc domain of human immunoglobulin protein IgG1 (740bp) and was cloned in frame at the C terminus of the WISP protein sequences. The Fc domain binds well to protein G and purification of Fc tagged fusion proteins were later performed using protein G coupled to sepharose columns (Subsec. 6.3.6, page 55). For cloning the tag in frame behind the WISP sequence into the pBacPAK8 vector, both (vector and Fc-tag) were restricted with EcoRI and NotI in a provided buffer system at 37°C over night. Recircularization and religation of the linearized vector was avoid by dephsophorylation before the reaction was loaded onto a 1% agarose gel. DNA bands were excised with a scalpel and gel extraction, ligation and tranformation were performed described previously. Sequencing analysis approved the correct sequences of WISP1-T1, -T2, WISP2 and the attached Fc-tag within the open reading frames.

6.3.6. Recombinant protein expression and purification

AcMNP virus transfection of SF21 cells

The transfer vector pBacPAK8 and an additional expression vector were cotransfected into SF21 cells. Double recombination between viral sequences in the transfer vector and conformable sequences in the expression vector transferred the target cDNAs of WISP1-T1, -T2 or WISP2 into the viral genome. Cells were cultivated as monolayers in 150cm^2 cell culture flasks with BacPak complete medium. For transfection, SF21 cells were seeded onto 6 well plates at a density of 1x10^6 cells/well and incubated at 27°C for 1.5h. After cells attached at the bottom of the 6 well plates, previous medium was replaced with serum free Grace's basic medium and incubated at RT for 20min. During this incubation, the transfection reagents were prepared according to the manufacturer's instructions of the BacPAK^{TM}Baculovirus Expression System (Tab. 6.5). The kit included the positive control pBacPak8GUS. Recombination between this specific transfer vector and the expression vector generated recombinant viruses that express β-glucuronidase (GUS). GUS expression was later detected by application of X-Gluc, which produced a blue precipitate in the presence of β-glucuronidase.

Reaction tubes were incubated at RT for 15min and medium was removed from the wells. 1.5ml fresh serum free Grace's basic medium was added onto the cells and the Bacfectin-DNA

Table 6.5.: *Standard transfection assay for (r)protein production with the Baculovirus Expression System*

	Experiment 1-3 [μl]	**Positive control [μl]**	**Negative control [μl]**
HPLC water	86	86	91
Transfer vector (100ng/μl)	5	-	5
pBacPak8GUS (100ng/μl)	-	5	-
Expression vector (Bsu36 I digest)	5	5	-
Bacfectin	4	4	4
Final volume	100	100	100

mixture was pipetted dropwise to the medium and incubated for 5h at 27°C. Subsequently, old medium was replaced with Insect Express SF9 medium and X-gluc (300μg/ml) was added to the control dishes.

AcMNP virus amplification in SF21 cells

After 72h at 27°C, blue colour of the positive control was inspected. The medium, containing the produced viruses (P0), was collected six days after transfection and stored at 4°C until the first virus amplification was performed. Using Insect Express SF9 medium, SF21 cells were seeded with a density of 1x10^6 cell/well in a 6 well plate and incubated for 2h at 27°C. Different concentrations of P0 viruses (1:10, 1:100, 1:1000) were added to the cells and incubated at 27°C for virus amplification. After seven days, medium was removed and centrifuged at 1200xg (5min). Supernatants (P1 viruses) were replaced in new caps and stored at 4°C for the second amplification step. Because WISP1-T1, -T2 and WISP2 proteins were secreted into the medium, western blotting analyses with a primary antibody against the Fc-Tag were performed to detect the efficientest P1 virus concentration for the following amplification procedure (Subsec. 6.3.8). After seven days, 5x10^6 SF21 cells were disseminated in 5ml Insect express SF9 medium/25ml cell culture flask and incubated at 27°C for several hours. The P1 virus concentration, which yielded most target protein was diluted 1:25, 1:62.5 and 1:500 and added to the Insect express SF9 medium upon the recently seeded cells. After further seven days, all P2 virus supernatants were collected and western blotting analyses were retried to identify the efficientest P2 virus titer. Finally, 200μl of the efficientest virus supernatant was added into 20ml medium to infect 1,6x10^7 cells, seeded as monolayers in 150cm^2 cell culture flasks. Cells incubated at 27°C for 5-7 days, before protein purification procedures were implemented.

Purification of secreted rWISP proteins

All rWISP proteins were expressed as fusion proteins tagged with an Fc-tag. However, the secreted proteins were purified using 1ml HiTrap Protein G Sepharose columns. Protein G

is a Type III Fc receptor and belongs to the group G cell surface proteins of Streptococci. This receptor binds to the Fc region of IgG and is matrix-bound within the HiTrap Sepharose columns. Cross-reactions with albumin in the medium were avoided, since the native albumin-binding region of protein G was genetically deleted. SF21 cells were able to produce the rWISP proteins four-seven days after transfection. The medium of three major cell culture flasks (150cm^2) was collected and centrifuged 5min by 4500xg. The supernatant, containing the specific (r)protein, was transferred into a new falcon and incubated on ice until the purification procedure started. The equilibration of the HiTrap Protein G Sepharose column was achieved with 10ml PBS. After equilibration, 60ml supernatant was loaded step by step onto the column carefully followed that a maximum of 2ml/min was filtered. Subsequently, the column was washed with 10ml PBS upside down. The strong affinity between protein G and IgG at pH 7.0 was dissolved by decreasing the pH of the elution reagent glycine to pH 2.2. Different protein fractions were collected in eppendorff caps. The first fraction contained 500μl eluate and 20μl Tris (3M, pH 8.0) for neutralization while further fractions consisted of 1ml eluate and 40μl Tris (3M, pH 8.0). The purified protein fractions were adjusted to pH 7.0 and stored at 4°C. The columns were washed with 10ml PBS and charged with 6ml ethanol to prevent desiccation.

6.3.7. Determination of protein concentration

Concentrations of the (r)protein fractions were determined after each purification and prior to each application by the Micro-Bradford method. This assay relies on binding of the dye Coomassie Blue G250 to proteins, based on the method originally described by (Bradford 1976). The dye can exist in three charged forms, the cationic red and green forms (absorbance max. at 470nm and 650nm) and the anionic blue form (absorbance max. at 590nm). Since only the anionic blue form binds to proteins, the quantity can be estimated by determining the amount of blue dye. Since it was necessary to gain a calibration curve before protein measurement took place, different calibration standards with of 25, 50, 75, 100, 150, and 250μg/ml BSA were diluted in 100mM glycine. Thus, a blank of 10μl 100nM glycine and 10μl per standard were vortexed and measured two times. 5x Roti-Quant (contained Coomassie Blue G250) was diluted 1:4 in distilled water and 500μl 1x Roti-Quant was mixed with 10μl (r)protein in a micro cuvette. After 10min at room temperature measurement of absorption was performed at 595nm in a photometer, which calculated absolute protein concentrations according to the obtained calibration curve.

6.3.8. Western blotting

Western blotting (immuno blotting) was used to determine expected size and purity of the rWISP-Fc proteins. Protein samples (250-300ng) were first loaded on a SDS page and separated during gel electrophoresis according to their size. Therefore, proteins were denaturated with SDS (sodium dodecyl sulfate). It dissolves hydrophobic molecules to reduce proteins to their primary structure (linearize) and covers the proteins with uniform negative charge by binding to disulfide linkages of the amino acids. A polyacrylamide gel (polymer of acrylamide monomers) was used to separate different sized proteins by moving at different rates during the application of a direct current. The gel consisted of two compartments (Tab. 6.6). The upper was formed by the stacking gel and yielded lower acrylamide concentration and different pockets, which were needed to accumulate the loaded proteins. The lower compartment (separating gel) consisted more acrylamide to separate different sized proteins by their mass.

It was important to add TEMED and APS immediately before use to the mixture, because they act as radical starters for gelling. One short glass plate and one spacer glass plate were

Table 6.6.: *Standard composition for two SDS-acrylamide gels*

	5% stacking gel [ml]	**12.5% separating gel [ml]**
distilled water	2.40	4.80
Rotiphorese gel 40 (29:1) acryl-amide/bisacrylamide mix	0.50	3.75
stacking gel buffer	1.00	–
separating gel buffer	–	1.25
10% SDS	0.04	0.10
TEMED	0.004	0.004
10% APS	0.04	0.10

clamped into a special fastener, which sealed bottom and lateral rims of the plates. The mixture of the separating gel was added between the glass plates (filling 2|3 of the space) and covered with 2-propanol until polymerization. After 20min, the 2-propanol was removed and the stacking gel mixture was loaded onto the polymerized separating gel. Combs were used to generate pockets into the stacking gel during its polymerization. After additional 20min, both glass plates (including the gel) were fitted into an electrophoresis cell, designed to hold two gels, which was inserted into a buffer tank. Two different buffers were needed to generate an electric field for protein separation. Upper buffer was filled between the gel trays while lower buffer was filled into the buffer tank up to the bottom of the gel trays. Equal amounts of protein were diluted with distilled water to a final volume of 10μl and added to 10μl sample buffer (yielded bromphenol blue). After an additional denaturating step (5min at 70°C), the samples and a rainbow marker were loaded onto the stacking gel and a direct current at a voltage of 190V was applied for about 40min. Migration of the proteins was controlled by location of bromphenol blue. After the separation was finished, two blotting papers and a nitrocellulose membrane were moistened with transfer buffer and placed on the bottom of the blotting chamber. One gel and two further wet blotting paper were placed onto the nitrocellulose membrane. The upper plate electrode was placed on top and a current of 150mA per membrane was applied for 2h. The proteins were transferred onto the nitrocellulose membrane via migration according to their negative charge towards the anode. Subsequently the membrane was incubated in a blocking solution for 2h to reduce non-specific protein interactions between the membrane and antibodies. A primary antibody against the Fc-tag was diluted 1:1000 in a buffer solution (PBS) containing the carrier protein BSA and incubation of the membrane was done over night at 4°C. The membrane was washed 4x 15min in washing solution I, before it was incubated with the anti-rabbit IgG secondary antibody for 1h. Anti rabbit IgG was diluted 1:2000 in PBS/BSA and labelled with the reporter enzyme horseradish peroxidase that allows visual identification by producing fluorescence. After rinsing the membrane 4x 15min in washing solution II, unbound secondary antibody was removed and the membrane was prepared

for detection by using the ECL Plus kit (purchased from Amersham). The kit contains the Lumigen PS-3 acridan substrate, which is converted into acridinium ester intermediated by the horseradish peroxidase activity of the secondary antibody. The resulted emission of light was detected by autoradiography. Every membrane was, according to the manufacturer's instruction, incubated in ECL Plus reagents for several minutes. Subsequently, the solution was removed and the membrane was placed (covered in cling film) in an X-ray film cassette. An autoradiography film was placed onto the membrane in a dark room for 2min to 2h, depending on the estimated exposure time. Detected proteins were visualized as dark bands and the size standard was copied by overlaying on the respective membrane.

6.3.9. Silver staining

In addition, silver staining was used to valid the purity of our (r)protein fractions. This is a highly sensitive method for visualization of separated protein bands on polyacrylamide gels. Therefore, 10-50ng amount of protein suffice for detection. Proteins bind silver ions, which can be reduced under appropriate conditions to build up a visible image made of finely divided silver metal (Chevallet et al. 2006). Following the manufacturer's instruction of the Silver staining kit (purchased from Amersham) the polyacrylamide gels were first fixed 30min in a solution of acetic acid and ethanol (1:3) to get rid of interfering compounds. For an increased sensitivity and contrast of the staining, the gel was slewed for additional 30min in a sensitization solution. Rinsing with distilled water (3x 5min) and incubation in silver nitrate staining solution for 20min (in the dark) was necessary for binding silver ions to the proteins. After quick washing with distilled water (2x 1min), the gel was incubated with developer. It was important to observe the gel during development, because duration to unveil bands varies between 2-10min. Subsequently after visualizing protein bands, the reaction was finished with stop solution for 10min and conserved in a vacuum dryer for at least 2h.

6.4. Reduction of gene expression through shRNA techniques

Gene-silencing includes methods by which the expression of one or more genes is reduced (in vivo or *in vitro*). This could be achieved by either the application of DNA or RNA oligonucleotides with a sequence complementary to a mRNA transcript, or through genetically modifications of the chromosomes. In this study, shRNA constructs, integrated into an expression vector of the lentiviral genome, were used to generate stable siRNA expression against WISP1 in different kind of cell types. A set of five different shRNA constructs against WISP1-T1 and -T2 was commercially supplied from the RNAi Consortium (TRC) of Thermo Fisher Scientific. These constructs were designed to include a 21bp hairpin stem (sense and antisense) flanking a loop of 6bp (Sec. 5.5). Each hairpin sequence was integrated into the lentiviral vector pLKO.1 (HIV-based) and provided as bacterial cultures of E.coli (DH5α) in LB-Lennox medium complemented with 8% glycerol.

Similarly, the TurboGFP^{TM}control vector (based on the TRC2-pLKO-puro vector) was used as a positive control for measuring transfection and transduction efficiency. After expression, GFP exhibits bright green fluorescence when exposed to blue light and therefore indicates successful virus infection of the target cells. The empty TRC2-pLKO-puro vector was used as a negative control. This pure vector control contains no shRNA insert and thus will not activate the RNAi pathway. The second negative control was a non-targeting shRNA vector (scrambled control). It contains a short hairpin sequence of 21bp (sense and antisense) flanking a loop of 6bp with mismatches to any known human gene (Sec. 5.5). Therefore, it activates RISC and the RNAi pathway, but doesn't affect the expression of any human gene. This

control allowed the examination of the effects of shRNA transduction and RNAi activation on the gene expression. Both negative controls were useful for observation of cellular effects of the transfection process. It was similarly necessary to generate envelope (pMD2.G) and packaging (psPAX2) plasmids with the consecutively described procedures. Cotransfection of either shRNA or control plasmids additional to envelope and packaging plasmids were required to generate efficient virus particles.

6.4.1. Amplification of shRNA and control constructs

The provided glycerol stock solutions were stored at -80°C. Using a dilution loop, marginal amounts were removed and plated on LB/ampicillin agar plates. After nearly 16h at 37°C, single colonies were picked and cultivated in 2.5ml LB/ampicillin medium at 37°C with constant shaking for 12-16h. Following plasmid mini preparation (Subsec. 6.3.4, page 52), positive clones were identified using restriction endonucleases. 1U enzyme was used to restrict 1μg plasmid DNA in the appropriate buffer system and restriction suspension was incubated for 1h at 37°C. Successful insertion of the shRNA construct into the MCS of the pLKO.1 vector, enabled double restriction with EcoRI and NcoI. Gel electrophoresis visualized two bands (∼2kb and ∼5kb) for plasmid DNA including the shRNA construct and only a linearized vector band (∼7kb) in shRNA negative plasmids. Positive samples were verified using sequencing analysis (subsection 6.3.3), amplified through transformation in chem. competent E.coli cells (Subsec. 6.3.4, page 52) and subsequent purified with plasmid midi preparation procedures (Subsec. 6.3.4, page 53).

6.4.2. Lentiviral transfection of HEK-293T cells

Approximately 24h prior to transfection, HEK-293T cells were seeded onto 6 well tissue culture plates at a density of 6x10^5 cells/well in 3ml DMEM Ham's F12 medium with L-glutamine and 10% FCS (without antibiotics). Cells were incubated over night at 37°C in a humidified atmosphere enriched with 5% CO_2 and transfected immediately after they reached a confluence of 60-80% (Tab. 6.7).

Subsequently, DMEM Ham's F12 medium was added to a final volume of 80μl per standard transfection assay. Lipofectamine™2000 treatment was used to alter the plasma membrane, which allows plasmids to enter the cytoplasm. Therefore, a lipofectamine master mix was prepared, containing 10μl lipofectamine and 90μl DMEM Ham's F12 medium for each reaction. Following an incubation of 5min at RT, 100μl lipofectamine mix was added to each reaction tube and incubated for 20min at RT. Afterwards, a total reaction volume of 180μl was pipetted dropwise into the medium of the seeded HEK-293T cells and incubated for nearly 18h at 37°C with 5% CO_2. All following procedures were accomplished according to the guidelines of the local S2 ethic commission of the University of Würzburg. After nearly 18h, used medium was removed from the HEK-293T cells and replaced with 5ml fresh DMEM Ham's F12 medium containing 30% FCS and 1% Pen/Strep. The GFP positive control was inspected under exposure to UV-light. It has a major excitation at a wavelength of 395nm, a minor one at 475nm and the emission peak is at 509nm, which is in the lower green portion of the visible spectrum.

6.4.3. Lentiviral transduction of target cells

Target cells were seeded in adequate plating densities, depending on cell type and culture vessel size (Tab. 6.8) in the provided medium (Subsec. 5.12.5, Tab. 5.18).

Target cells (except Tc28a2, C28I2) and transfected HEK-293T cells were incubated at 37°C (Tc28a2, C28I2 at 32°C) for further 24h. Transduction of the target cells took place on the

Table 6.7.: *Standard transfection assay for virus assembling for gene expression studies through shRNA constructs*

	shRNA construct [μg]	**Negative scrambled control [μg]**	**Negative pure vector control [μg]**	**Positive GFP control [μg]**
Packaging plasmid psPAX2	1.80	1.80	1.80	1.80
Envelope plasmid pMD2.G	0.25	0.25	0.25	0.25
shRNA/control plasmid	2.00	2.00	2.00	2.00

Table 6.8.: *Culture vessels dependent plating density of target cells used for lentiviral transduction*

Cell type	**Culture vessel**	**Plating density**
C28I2	6 well (9,03cm^2)	9.0x10^4
hFOB	6 well (9,03cm^2)	2.0x10^5
hMSC	6 well (9,03cm^2)	1.5x10^5
hMSC	25cm^2 flask	2.5x10^5
hTert4	6 well (9,03cm^2)	1.0x10^5
hTert20	6 well (9,03cm^2)	1.0x10^5
Tc28a2	6 well (9,03cm^2)	1.0x10^5
Tc28a2	25cm^2 flask	2.0x10^5

third day after HEK-293T cells were transfected. Therefore, total medium (5ml/sample) was removed from the HEK-293T cells and centrifuged at 4500xg for 5min to dissociate cell debris and virus supernatant. Subsequently, used medium was removed from the target cells and replaced with adequate amount of virus supernatant. Polybrene (8μg/ml) was added dropwise to the virus supernatant onto the target cells. This hexadimethrine bromide polymer was used to increase the efficiency of infection by neutralizing the charge repulsion between virions and sialic acid on the cell surface. Following, cells were incubated at 37°C (Tc28a2, C28I2 at 32°C) and used medium was replaced with fresh medium one day after transduction and additional every second day.

6.4.4. Isolation of cellular RNA

RNA isolation of WISP1 down-regulated and control cells took place simultaneously at several days to investigate the gradient of WISP1 gene-silencing. Total RNA from cultured cells was isolated following the manufacturer's instruction of the NucleoSpin®RNA II kit (Macherey-Nagel GmbH). Cells were disrupted and homogenized with a guanidine isothiocyanate- and β-mercaptoethanol-containing lysis buffer that inactivates RNases. Samples were loaded onto a filtration column to reduce viscosity by centrifugation. Subsequently, equal volumes of 70% ethanol was added to the filtrated lysate, to generate conditions that promote selective binding of RNA to a NucleoSpin column membrane. Especially binding columns were used to bind RNA to silica-gel-based membranes during centrifugation (8000xg, 30sec). The silica membrane was treated with membrane desalting buffer, to ensure appropriate conditions for the endonuclease DNase I. Since no RNA purification procedure removes 100% of the DNA, it is suitable to use DNase I for eliminating remaining DNA. Contaminants were washed out by appropriate buffers and purified RNA was eluted with 30μl HPLC by centrifugation (11000xg, 60sec). Samples were stored at -80°C. Concentration of mRNA specimens was determined by 1:25 dilution of RNA suspension in HPLC. RNA absorption was measured at 260nm using UV-light permeable cuvettes. The extinction of 1 E_{260} was conformed to 40μg/ml RNA. Purity was estimated by the quotients E_{260}/E_{280} and E_{260}/E_{230}, since the absorption of proteins occurs at 280nm while contaminants like carbohydrates and peptides absorb at 230nm. To exclude contaminants, E_{260}/E_{280} should be 2.0 and E_{260}/E_{230} should be larger than 2.0.

6.4.5. Reverse transcriptase polymerase chain reaction (RT-PCR)

Because mRNA is less stable than DNA, it is conventional to use cDNA to investigate gene expression patterns of specific genes in cells and tissues. cDNA is a single- or double strained DNA that is complementary to a certain sequence of mRNA.

After RNA isolation, cDNA was synthesized during reverse transcription, using the Bioscript reverse transcriptase (polymerase) purchased from Bioline. The cDNA synthesis was performed according to the manufacturer's instructions. Therefore, identical amounts of total RNA (1-2μg) were first incubated with random hexamer primers at 70°C to denaturate RNA secondary structures. Subsequently, the samples were chilled on ice were the random hexamers annealed to the RNA template. RNase inhibitor, dNTPs, reverse transcriptase and the corresponding buffer were added and the reactions extended at 25°C for 10min before the elongation starts at 42°C (1h). Enzyme inactivation at 70°C was necessary to stop the reaction. HPLC water diluted the samples to a final volume of 50μl. Subsequent semi-quantitative PCR analysis enabled the detection of specific gene expressions. Table 6.9 reflects a standard protocol and the corresponding reaction steps accommodated for the PTC-200 Peltier thermal cycler. Therefore, gene specific primers were used to anneal in the cDNA sequence of the gene of interest. This enabled the Taq DNA polymerase to elongate the sequences to double

stranded PCR products specific for the elected gene. MangoTaq™ DNA polymerase was used according to the manufacturers instruction with the respective, provided buffer system.

Steps 2-4 were repeated 22-39 times depending on the results of the following gel electrophoresis procedure. Modified assays, with higher amounts of $MgCl_2$ and/or by addition of DMSO, were performed as stated in section 5.11, table 5.11. PCR primers were either already established in the laboratory or designed using Primer3 software (Rozen and Skaletsky 2000). To exclude false positive detection of DNA contaminants, primer pairs were preferably selected, which anneal in DNA sequences of different exons (intron-spanning). PCR reaction conditions, like annealing temperature, cycle number and $MgCl_2$ and/or DMSO concentration were first optimized and subsequent sequencing analysis of the respective PCR product assessed gene specificity of each primer pair (Subsec. 6.3.3).

6.5. cDNA microarray

cDNA microarrays are small, solid supports onto which the sequences from thousands of different genes are attached at fixed locations. A microarray works by exploiting the ability of a given mRNA molecule to bind specifically to the DNA template from which it originated. Comparison of separate chips, loaded with different RNA specimens, enables the estimation of specific gene expression profiles. To investigate differences in the expression patterns of WISP1 depleted and control cells, knock-down experiments were performed in hMSCs (n=3) and the chondrocyte cell line Tc28a2 (n=5). In both cell types total RNA of WISP1 down-regulated and scrambled control cells was isolated on day six after transfection. The present down-regulation of WISP1 and a successful RNA isolation were verified by RT-PCR and gel electrophoresis.

6.5.1. Affymetrix GeneChip hybridization

Affymetrix GeneChip hybridization, staining, and scanning of the chips were performed by PD Dr. L. Klein-Hitpass at the Institute of Cell Biology, University of Duisburg-Essen, Germany. Therefore, the different mRNA samples were used to generate biotin-labelled, single-stranded cRNA samples, which were fragmented and hybridized onto the GeneChip Human Genome-U133+2.0 for 16h. The arrays were washed and stained according to the manufacturer's recommendation and finally scanned in a GeneChip scanner 3000 (Affymetrix). Thereby, the staining of hybridized cRNA by streptavidin phycoerythrin conjugate results in emission of light at 570nm, that is proportional to the bound cRNA. The software assigned the light emission to the respective probe sets and computed their intensities.

Microarray Analyses with the statistical software R

All further analyses were performed with the statistical software R (R Development Core Team 2010) and its additional component for microarray analyses, namely Bioconductor (Gentleman et al. 2004b). To analyse the Affymetrix GeneChips, we used the analysis add-on package Affy (Gautier et al. 2004). Raw data was visually quality controlled by looking for defective or inadequately spotted regions of the chip itself. Further, RNA degradation plots were used to determine the quality of all samples. All samples passed these controls and were used for further analyses. The raw data was normalised using the function expresso of the affy package. All of the three following normalisation steps were applied for each of the experiments: (1) Normalisation using quantiles (Q) without background correction, (2) using the robust multi-array average expression measure (RMA) with background correction and (3) variance

Table 6.9.: *Standard reaction steps: RT-PCR*

Reagent	**Amount [μl]**	**Reaction steps**	**Temp. [°C]**	**Time [min]**
5x Mango buffer	6	1) step: Initial denaturating	94	3
10mM dNTPs	1	2) step: Denaturing	94	0.75
50mM $MgCl_2$	1	3) step: Annealing	54	0.75
5μM primer for	1	4) step: Elongation	72	1
5μM primer rev	1	5) step: Final elongation	72	5
1U/μl Mango Taq^{TM}	0.3	6) step: Cooling	4	inf
cDNA template	1			
HPLC water	ad 30			

stabilization and normalization (VSN) with background correction using the package vsn (Huber et al. 2002). Methods included the pmonly correction and medianpolish options. However, only the method that yielded the best normalisation was used in the following analytical steps, which was determined by comparison of density plots. Linear models for microarray data were fit to expression data using the package limma (Smyth 2005). Empirical Bayes shrinkage was applied to compute moderated t-statistics, moderated F-statistic, and log-odds of differential expression. By these statistics, the AFFX cut-off filter was used to reduce the data to the most significantly differentially expressed probe sets (package genefilter, Gentleman et al. 2012). As on-chip AFFX probe sets are not expected to be significantly differentially expressed, their lowest p-value states a good cut-off point for significance and was used to filter out normal gene probe sets with a p-value above this threshold. A summary of definite parameters disposed during microarray analyses are stated in (Tab. 6.10).

For all remaining probe sets, annotation information was regarded (packages annotate and hgu133plus2.db, Carlson et al. 2012a; Gentleman 2012) and further gene ontologies (GO, package GOstats, Falcon and Gentleman 2007a) and KEGG (package KEGG.db, Carlson et al. 2012b) pathway classifications. We performed GO enrichment for cellular compounds (CC), molecular function (MF) and biological processes (BP) as well as KEGG enrichment analyses

Table 6.10.: *Summary of definite parameters disposed during microarray analyses*

	N	**Normalization**	**Filter**	**regulated probe sets**
Tc28a2	5	RMA	AFFX	1687
MSC	3	RMA	AFFX	522

with a hyper-geometric distribution to detect over- and under-represented GO and KEGG terms. Colour-coded heat maps that include significant probe sets of interesting pathways or functional groups of genes were plotted using the package gplots. We further displayed protein interaction networks within pathways to relate expression information to signalling cascades.

6.6. Application of (r)proteins onto target cells

To assess the effects of rWISP1 proteins, both transcript variants were added separately and combined with concentrations of 500ng to WISP1 down-regulated Tc28a2 chondrocytes. For this investigation, cells were seeded as monolayers in 6 well plates with a density of $1x10^5$ cells/well in 3ml hMSC culture medium. WISP1 gene-silencing procedures were performed described previously. Treatment with rWISP1-T1 and/or rWISP1-T2 took place a few hours after the virus transduction occurred and was repeated with every medium change until RNA isolation took place. Scrambled, GFP and pure vector transduced assays served as controls for the examination of differences in the endogenous WISP1 expression after (r)protein treatment. Protein treatment with rWISP2 was similarly performed with a protein concentration of 500ng. Therefore, Tc28a2 chondrocytes were first seeded with a plating density of $2x10^5$ cells/well in 6 well plates. Cells were incubated under normal cell culture conditions at 37°C until they reached 90-100% confluence. Prior to the protein treatment cells were cultivated with serum less medium (0%FCS) for 24h at 32°C and subsequently treated with 500ng rWISP2 for additional 24h. Following RNA isolation and RT-PCR analyses were performed to examine differential expression of endogenous WISP1-T1, -T2 and WISP2 with the corresponding control cells.

6.7. Immunocytochemistry

Apoptosis detection via Fluorochrome Inhibitor of Caspases (FLICA)

Apoptosis, or programmed cell death, is controlled by active cysteinyl aspartate-specific proteinases (caspases). Caspase enzymes are important mediators of apoptotic signals by cleaving a multitude of substrates, which consequently cause cellular demolition (Green and Reed 1998; Nuñez et al. 1998; Thornberry 1999). Methodology of FLICA is based on several cell permeable caspase inhibitors, which bind covalently to the sites of the corresponding active caspase. For visualization, inhibitors are fluorescence-labelled and staining procedures within this thesis were performed with the poly caspase inhibitor VAD-FMK labelled with sulforhodamine (SR). VAD is an amino acid sequence targeting by all caspases, exhibiting red fluorescence through the labelling with SR. The red signal is a direct measure for the number of active caspases, since unbound FLICA diffuses out of the cell and could be washed away. Hoechst, a cell permeable fluorescence marker, was additional used to counter stain nuclei of all cells (apoptotic and viable). Prior to staining procedures, hMSCs were seeded on glass cover slips in 24 well plates with a density of $4x10^4$ cells/well. Approximately 4h later cells were adherent and quiescent for apoptosis induction via zolendronic acid. Cells were treated with 100μM zolendronic acid between 48h and 72h and subsequent staining procedure were performed. For this purpose, staining protocols were observed according to the manufacturer's instructions concerning adherent cells. Thus, FLICA reagent was added at a 1:30 ratio in fresh medium onto the cells for 1h at 37°C. After incubation, medium was removed, 1.5μl Hoechst stain was added into 300μl fresh medium and mixture was used for the next cell incubation (5min at 37°C). Subsequently, cells were washed twice with washing solution and covered, facing down, with a slide containing one drop washing solution. Analysis was performed with fluorescence microscopy using a bandpass filter with excitation 55nm and emission >580nm to visualize red

fluorescence signals of active caspases.

Protein detection

Proteins, like cytochrome c and p53, can be visualized by immuno-cytochemistry labelling methods to infer their location within a cell. Therefor, protein specific primary antibodies were used to detect distinct proteins. Application of a second, fluorescence-labelled antibody against the primary one, was necessary for protein visualization via fluorescence microscopy. Staining procedure was performed according to the manufacturer's instructions for the corresponding specific antibodies. For this purpose, hMSC were seeded on glass cover slips in 24 well plates with a density of $4x10^5$ cells/well. Prior to the staining of specific proteins, cells could be stained with a counterstain (MitoTracker®Red) to visualize cellular mitochondrions. 100nM MitoTracker® Red was added onto the living cells for approximately 30min at 37°C. Subsequently, medium was removed and cells were twice washed with PBS to remove unbound counterstain. Cells were fixed with 4% PFA (paraformaldehyde) for additional 10min and following washed three times with PBS for 5min. It was necessary to permeabilize the cells with 0.1%Tween/PBS for 15min to enable cell entering of the specific antibodies. Possible unspecific binding sites within the cells were blocked with 2% BSA/PBS for 30min at RT. Incubation with the primary antibody (1:100 in 0.5% BSA/PBS for the mouse anti cytochrome c antibody and the rabbit FL393 antibody against p53) occurred at 4°C over night. Next day, antibody solution was removed and cells were washed three times for 5min at RT. Incubation with the secondary antibody (Cytochrome c: rabbit anti mouse IgG/FITC - F0261 1:100 in PBS; p53: goat anti rabbit IgG/FITC - sc2010 1:200 in PBS) was performed for a minimum of 1h at RT. Cells were covered face down with one drop of mounting medium onto a slide. To counterstain concurrently cellular nuclei, 4',6-Diamidino-2-phenylindole (DAPI) was integrated into the mounting medium. Cells were analysed immediately with fluorescence microscopy.

Part III.

Results

CHAPTER
SEVEN

RESULTS

Studies of this thesis comprised the investigation of molecular backgrounds concerning consequences of WISP1 and -2 signalling in primary cells (hMSCs) and different cell lines connected to the musculoskeletal system. The first experiments included the inspection of full-length WISP1 and WISP2 expression in different cell types of the musculoskeletal system to identify these cells as WISP target cells. Since a truncated isoform of WISP1, transcript variant 2 (-T2), has been identified by Yanagita et al. (2007) in non-transformed chondrocytes, primer pairs were designed to detect both variants separately. Depending on the presence of expression patterns, several experiments were designed to investigate WISP-signalling in detail. Figure 7.1 illustrates the workflow of experiments, starting with gene-silencing of a given WISP expression and subsequent microarray approaches in different cell types, over (r)protein production of WISP1-T1, WISP1-T2 and WISP2 up to (r)protein treatment of previously WISP down-regulated target cells.

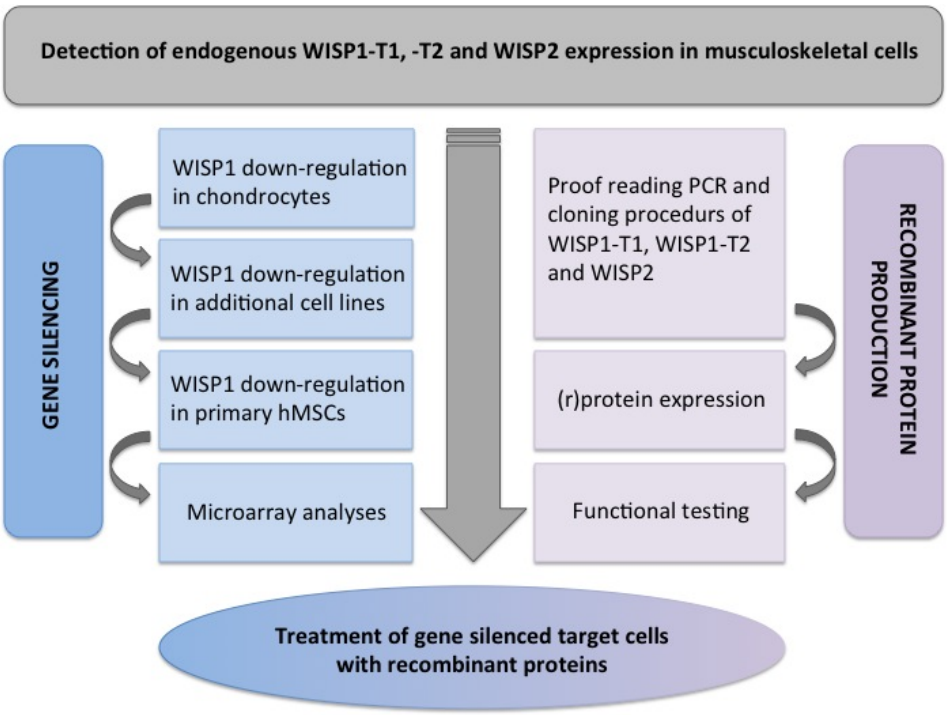

Figure 7.1.: *Schematic illustration of successional experiments.*

CHAPTER
EIGHT

WISP EXPRESSION PATTERNS

The expression of different WISP proteins was achieved by cultivation of monolayer cultures in different cell lines and primary hMSCs. Two different chondrocyte cell lines (Tc28a2; C28I2), three osteosarcoma cell lines (TE-85; MG-63; U2) the human foetal osteoblast cell line hFOB and 12 different hMSC donors were cultivated to investigate the endogenous amount of three different WISP proteins. Total RNA was isolated after cells reached confluence of 90-100%. RT-PCR analyses for both transcript variants of WISP1 showed a continuous expression in all appropriate hMSC donors (Fig. 8.1, A). High expression of WISP2 was only detectable in two different donors (MSC283; MSC354), whereas three different donors (MSC280; MSC486; MSC512) showed only a slight expression (Fig. 8.1, A). All remaining donors reflected no expression of WISP2 at all. A continuous WISP1-T1 expression was also detectable in the osteosarcoma cell lines MG-63 and U2 as well as in the osteoblast cell line hFOB and both chondrocyte cell lines (Fig. 8.1, B-C). Only the third osteosarcoma cell line TE-85 showed no expression of full-length WISP1. Similar expression patterns were detectable in the case of WISP1-T2 (Fig. 8.1, B-C). Except C28I2, which showed slight WISP1-T2 expression, all remaining cell lines expressed high amounts of the second transcript variant. By contrast, no expression of WISP2 was detectable in all examined cell lines. The mRNA levels of the housekeeping gene EF1α was used as an internal control.

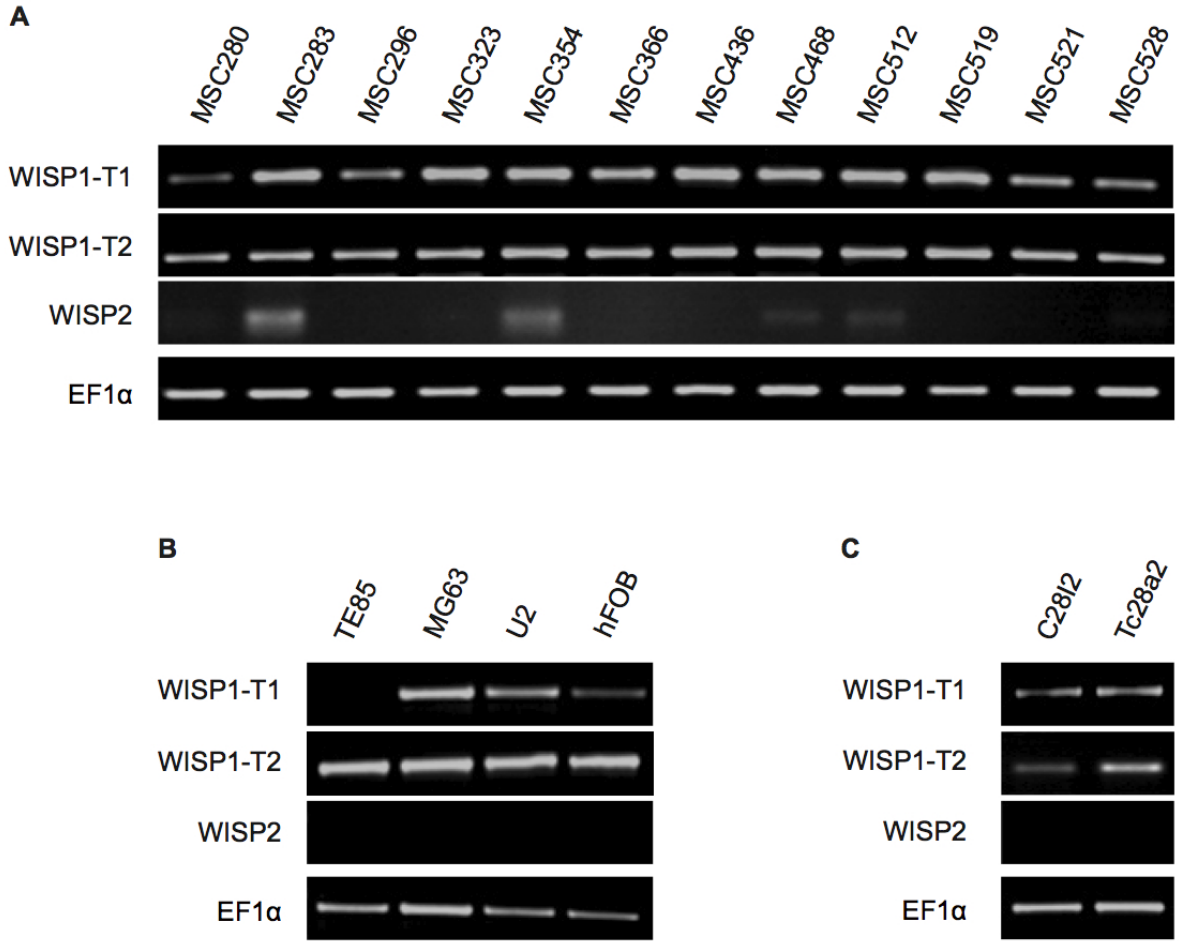

Figure 8.1.: *RT-PCR analysis of WISP expression in hMSCs and different cell lines. (A) constant expression of WISP1-T1 (row 1) and -T2 (row 2) among 12 different hMSC donors. WISP2, in contrast, was only in four of 12 different donors detectable. (B) expression of WISP1-T1/-T2 and WISP2 in three osteosarcoma cell lines (TE85; MG63; U2) and the osteoblast cell line hFOB. WISP1-T1 mRNA was detectable in MG63 and U2 cells as well as in the osteoblast cell line. Expression of the second transcript variant of WISP1 was detectable in all corresponding cell lines, whereas the mRNA of WISP2 could not be found in either of these cell lines. (C) Both transcript variants of WISP1 were expressed in C28I2 and Tc28a2 chondrocytes, while no expression of WISP2 was detectable.*

CHAPTER
NINE

WISP1 GENE-SILENCING

Depending on the presence of expression patterns in the previously described experiments, main focus of the subsequent experiments is dedicated to the functional dissection of WISP1-T1 and -T2. Therefore, gene-silencing studies were performed to examine the influence of WISP1-signalling in several cell types.

9.1. HEK-293T cell transfection and transduction of target cells

Successful gene-silencing of WISP1 by lentiviral transfection was confirmed with a cloning set of five different shRNA constructs. The constructs, integrated into the lentiviral pLKO.1 vector, as well as a GFP control vector, a non-targeting shRNA vector control (scrambled) and a pure vector control were used to transfect HEK-293T cells. Two days after transfection the cell supernatant, containing the recombinant lentiviral vectors, was used to transduce different target cells. The GFP control serves as a positive control for measuring transfection and transduction efficiency. After expression, GFP exhibits bright green fluorescence when exposed to UV-light (Fig. 9.1).

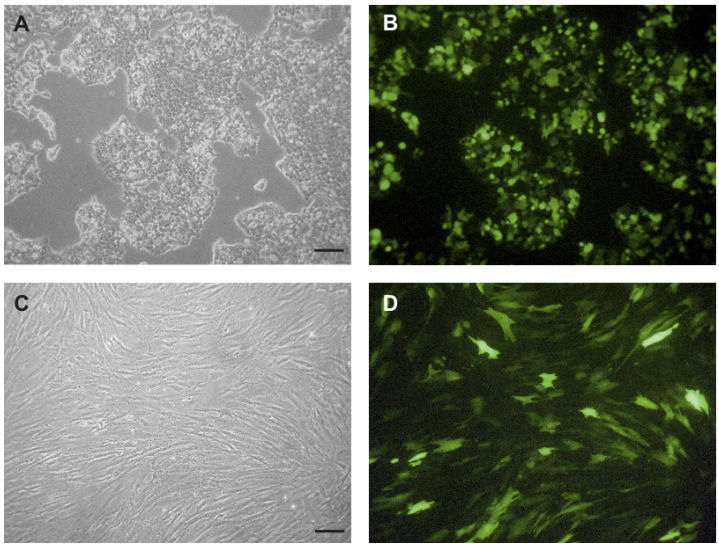

Figure 9.1.: *Lentiviral transfection of HEK-293T cells and transduction of hMSCs. (A) GFP transfected HEK-293T cells 48h after transfection. (B) Visualizing of transfection efficiency by exposure to UV-light. (C) GFP control five days after transduction and (D) equal section of the GFP control under exposure to UV-light. Scale bar=*$100\mu m$.

9.2. WISP1 gene-silencing in Tc28a2 chondrocytes

Virus supernatant, generated via HEK-293T cell transfection, was used to transduce monolayer cultures of different cell lines and primary hMSCs. First, the effectiveness of all five shRNA constructs was monitored by transducing the chondrocyte cell line Tc28a2. Concurrently, GFP and scrambled controls were transduced to discover transduction efficiency, morphological effects and differences in the endogenous amount of WISP1 mRNA. Total RNA was isolated five days after transduction and verified by RT-PCR analyses.

Figure 9.2 illustrates the mRNA level of both WISP1 transcript variants after their down-regulation compared to control cells (scrambled and GFP). A Specific primer pair was selected to detect both variants, thus the first row reflects the mRNA levels of WISP1-T1 and -T2 combined. Only four of five different shRNA constructs and both controls yielded enough mRNA to perform subsequent reverse transcription. Two constructs, shRNA2 and -5, reduced the endogenous amount remarkably, while shRNA1 and -4 transduction resulted in no or little reduction of the WISP1 mRNA. Scrambled and GFP controls revealed no down-regulation of the WISP1 mRNA level in this chondrocyte cell line. In all subsequent experiments, either shRNA2 and/or -5 were used to detect the mRNA levels of WISP1-T1 and -T2.

To clarify the date of an effective WISP1 down-regulation, total mRNA was isolated on day 1 to day 8 (d1-d8) after lentiviral transduction. Subsequently, reverse transcription and RT-PCR analyses were performed to validate the successful down-regulation of both transcript variants (Fig. 9.3). Therefore, the upper row illustrates the amount of WISP1-T1 mRNA in shRNA2 transduced cells, compared to the amount in the scrambled and GFP transduced control cells. Similarly, the second row reflects mRNA amounts of WISP1-T2 in shRNA2 transduced samples as well as in the corresponding control assays. The fourth day (d4) after transduction indicates the first day, with a detectable reduction of the WISP1-T1 mRNA. The successional days display a further decline in the endogenous amount of transcript variant T1. A similar outcome was detectable for the second transcript variant. Starting with the fourth day, the mRNA level was continuously reduced until the last day of the time series (d8). Both controls reflect a consistent expression of either transcript variant during the whole experiment.

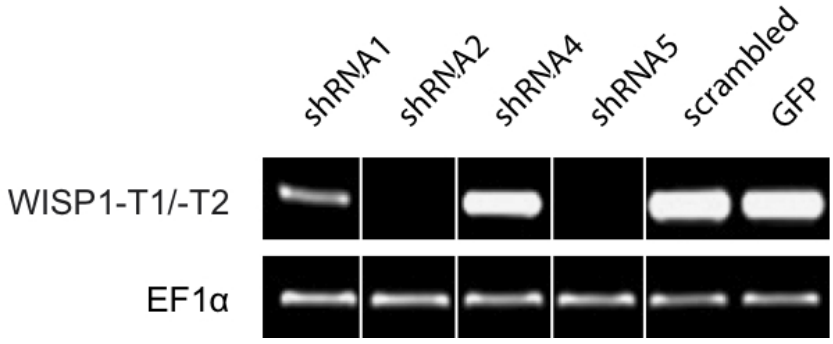

Figure 9.2.: *Range of function concerning four different shRNA constructs against WISP1. Total RNA was isolated five days after transduction. Two constructs, shRNA2 and -5 reduced the endogenous amount of WISP1 remarkably, while shRNA1 and -4 showed only slightly or no effects compared to the scrambled and GFP controls.*

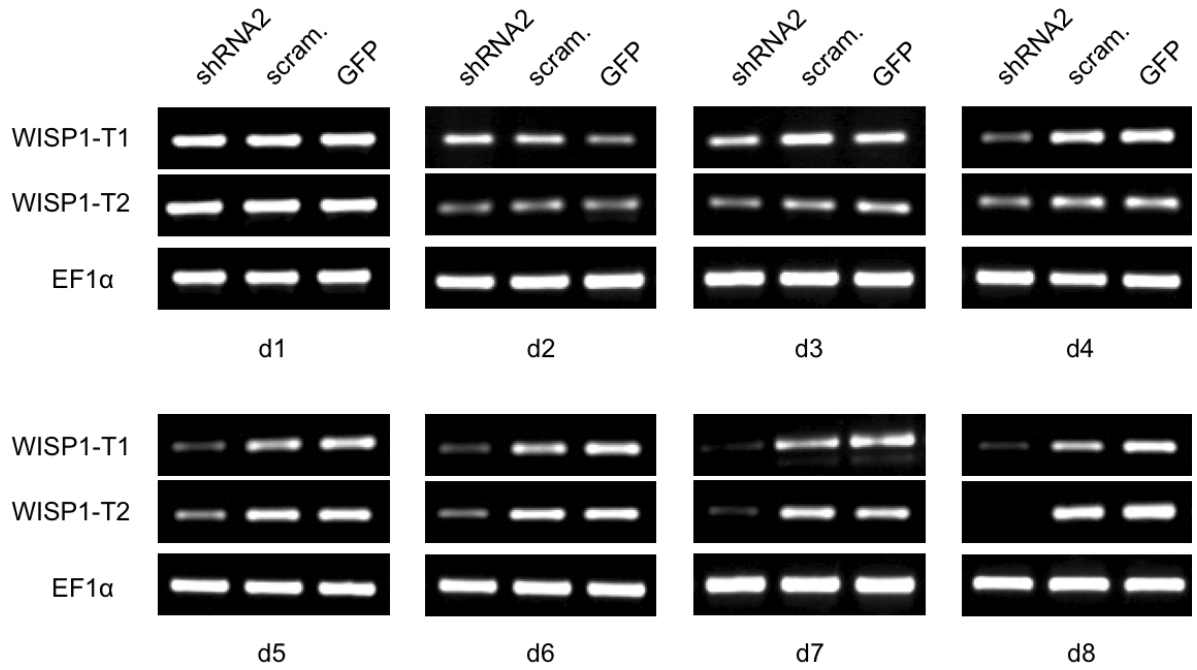

Figure 9.3.: *RT-PCR analysis of Tc28a2 chondrocytes on d1-d8 during WISP1 down-regulation. Total mRNA of shRNA2 transduced samples and two control samples (scrambled, GFP) were isolated on every day for one week. The shRNA2 construct reduced the endogenous amounts of WISP1-T1 and -T2 from the fourth day on, while both control samples showed no effects in the reduction of the WISP1 mRNA levels. Levels of EF1α mRNA were used as internal controls.*

9.3. WISP1 gene-silencing results in cell death in Tc28a2 chondrocytes

In addition to the reduction of the endogenous amounts of both transcript variants, optical differences were observable in WISP1 deficient chondrocytes compared to the control samples. Figure 9.4 reflects these optical differences in chondrocytes in a time series, initiated on the first day after lentiviral transduction. The time dependent optical differences between WISP1 deficient (shRNA2) and sufficient cells (scrambled; GFP) are visible in row 1 to 8. Cell death or proliferating effects within each sample could be observed in column 1-3 for each day of one week. Day 1, 2 and -3 after transduction, revealed no differences between shRNA2 (A1-A3) and scrambled control samples (B1-B3). Considering illustration A4, cell characteristics of shRNA2 transduced samples started to differ on the fourth day after transduction in comparison to the scrambled control samples (B4). Day 5 to 8 intensified these characteristics and chondrocytes containing shRNA2 constructs (A5-A8) showed remarkable differences combined with cell detachment in contrast to the control samples (B5-B8). Under UV-light exposure, sporadic cells slightly indicated GFP expression with green fluorescence on the third day (C3). Furthermore, cells intensified this illumination by GFP expression until the last day of the time series (C4-C8).

Cell death of WISP1 down-regulated chondrocytes was confirmed by transduction of the cells with a second functional shRNA construct (shRNA5). Further, a pure vector control was applied to clarify the optical differences between WISP1 down-regulated samples and their corresponding controls. All assays comprised the same conditions including medium, incubation and handling. Figure 9.5 illustrates Tc28a2 cells eight days after transduction. There were only slight differences observable comparing shRNA2 (A) and shRNA5 (B) transduced cells.

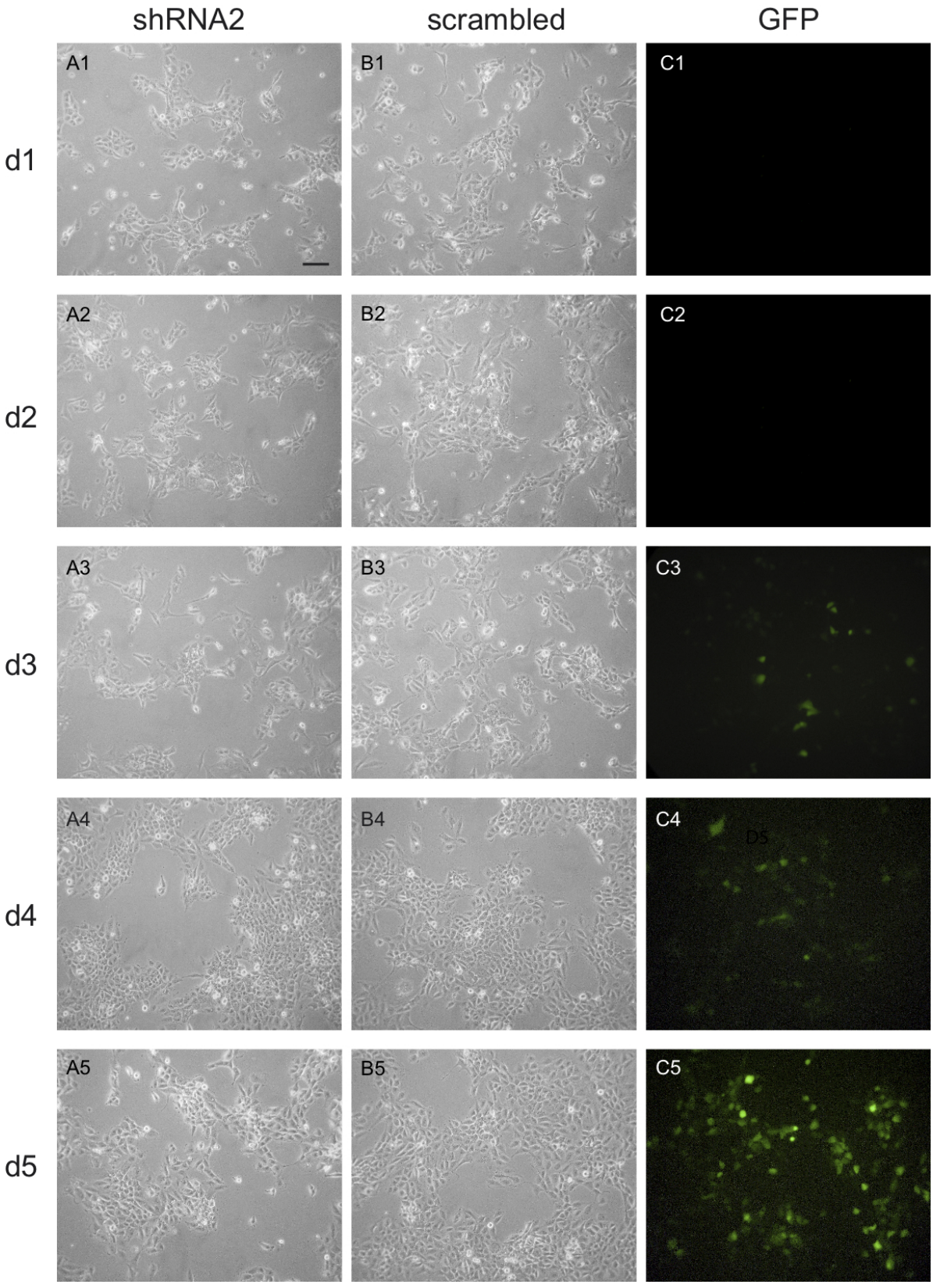
shRNA2
scrambled
GFP
d1
d2
d3
d4
d5
A1
B1
C1
A2
B2
C2
A3
B3
C3
A4
B4
C4
D5
A5
B5
C5

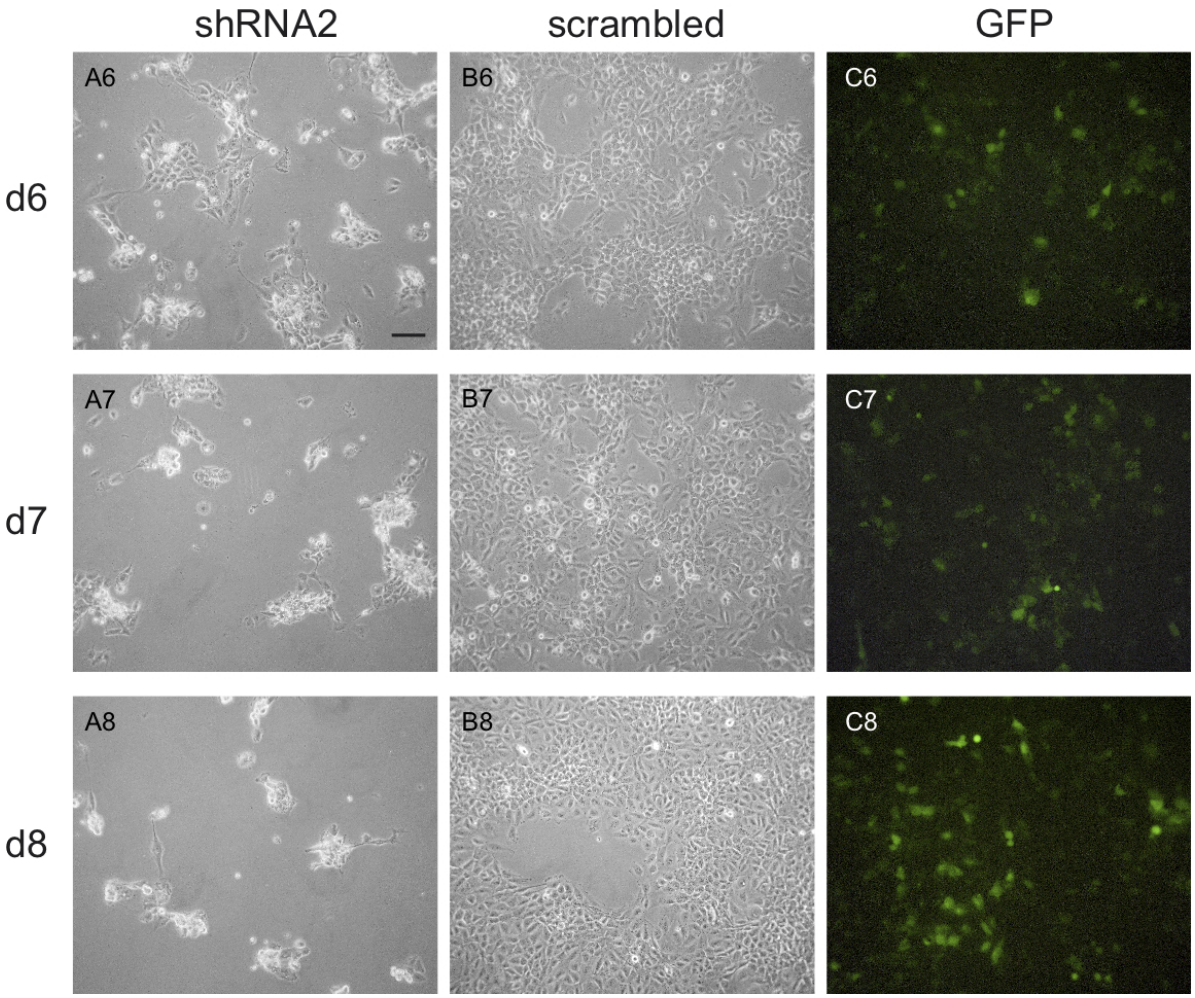

Figure 9.4.: *Cell death of WISP1 deficient Tc28a2 chondrocytes. Column 1 (A1-A6) showed, that WISP1 deficient cells died within one week after the transduction was performed. Day 1 to day 4 displayed a comparable proliferation of shRNA2-transduced cells (A1-A4) and the scrambled control sample (B1-B4). Day five is the first day that indicates optical differences between knock-down (A5) and scrambled control cells (B5). Day 6, 7 and 8 intensified these disparities remarkably (A6-A8, B6-B8). GFP expression was detectable under exposure to UV-light from the third day on (C3-C8). Scale bar=*$100\mu m$

However, in contrast to the scrambled- (C), pure vector- (D) and GFP control (E) both shRNA constructs manifested remarkably optical differences. Cells weren't able to survive in shRNA2 and -5 treated samples, while the three control samples reflected an expected proliferation. GFP expression was verified under exposure to UV-light (F). Total RNA of each sample was isolated on day 8 after transduction and RT-PCR analyses were performed immediately (G). Both shRNA constructs revealed an emersed reduction in the mRNA level of WISP1-T1 and -T2 compared to the control samples (scrambled, GFP and pure vector). Similar experiments, transduced with shRNA2-, scrambled- and GFP plasmids were repeated (n=7) and analysed by RT-PCR and densitometric analysis of the gel bands (Sec. 11.4, Fig. 11.3).

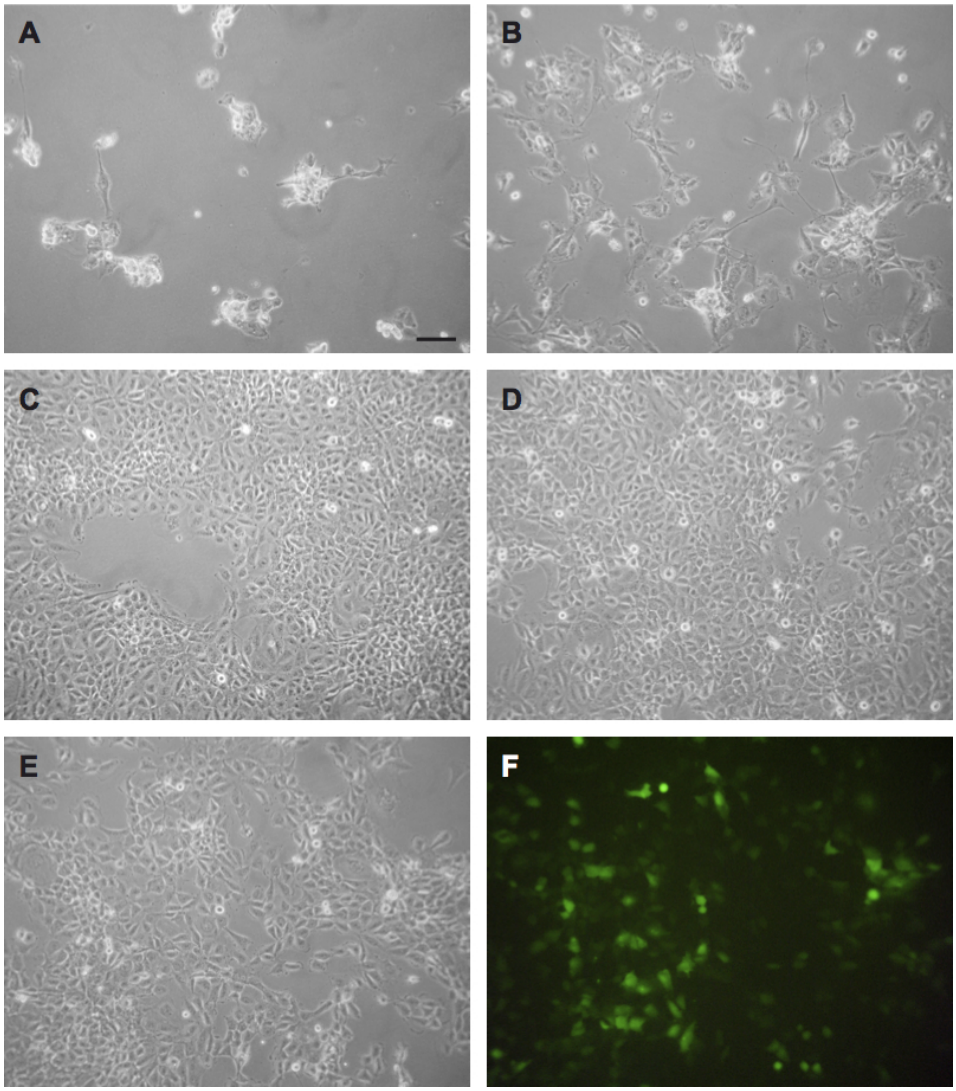

Figure 9.5.: *WISP1 gene-silencing in Tc28a2 chondrocytes on day 8 after transduction. (A) shRNA2 transduction results in cell death and thus reflect remarkable differences compared to the control samples (C, D, E). (B) shRNA5 transduced cells show similar effects, manifesting in cell death, but with slightly decelerated compared to the shRNA2 transduced cells. The scrambled (C), pure vector (D) and GFP control assays show entire proliferation and no optical differences among each other. Scale bar 100m.*

9.4. WISP1 gene-silencing in additional cell lines connected to the musculoskeletal system

Supplementary experiments of WISP1 gene-silencing were performed in the human chondrocyte cell line (C28I2), two immortalized MSC cell lines (Tert4, Tert20) and the human osteoblast cell line hFOB. During these experiments, same conditions including medium, incubation and handling were warranted. Two different shRNA constructs (shRNA2 and shRNA5) were used to reduce the endogenous amounts of both transcript variants of WISP1. Two negative controls (scrambled and pure vector) were used to observe cellular differences between WISP1 down-regulated and control assays. GFP was used as a positive control for measuring transfection and transduction efficiency. Figure 9.6 illustrates all corresponding experiments for each cell line. The first column (A1-A5) indicates cellular effects within C28I2 chondrocytes on the eighth day after transduction. Similar to the experiments in the Tc28a2 chondrocyte cell line, shRNA2 (A1) and shRNA5 (A2) transduced C28I2 cells died a few days after transduction. Both negative controls (scrambled A3, pure vector A5) showed an expected proliferation and the GFP control confirmed a successful transduction under exposure to UV-light (A4). Total RNA of all samples was isolated on day 8 to verify the down-regulation of both transcript variants of WISP1 with RT-PCR analysis (A6). Both, shRNA2 and -5 transduced cells show a remarkable reduction in the WISP1-T1 and -T2 mRNA levels, compared to the control samples. Similar outcomes were achieved for both immortalized MSC cell lines Tert4 (B1-B6) and Tert20 (C1-C6) and the osteoblast cell line hFOB (D1-D6). All cell types displayed the same cell characteristics in the absence of WISP1 compared to their control assays. RT-PCR analyses confirmed the reduction of the endogenous amounts of both transcript variants (B6, C6, D6).

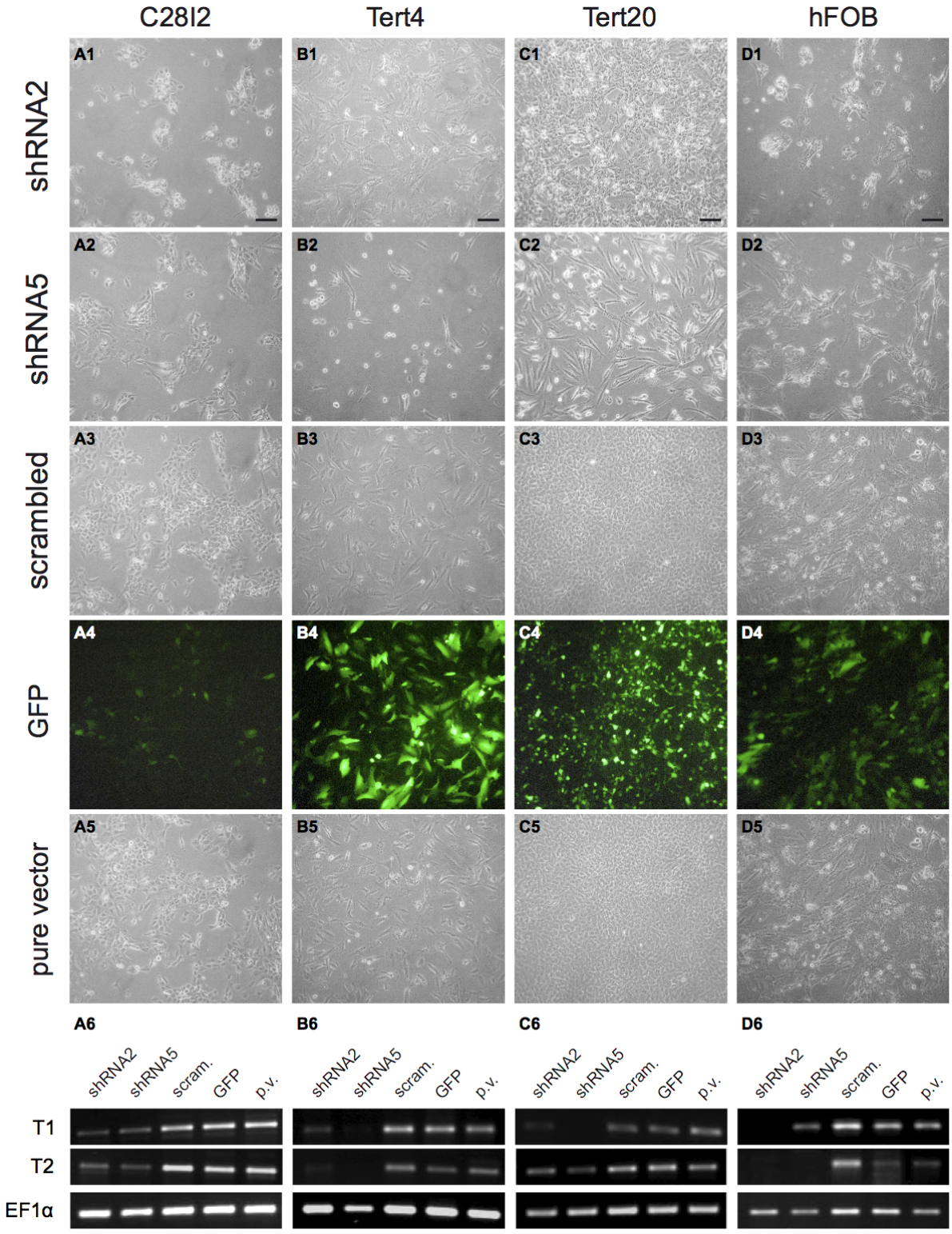

Figure 9.6.: *WISP1 down-regulation in the cell lines C28I2, Tert4, Tert20 and hFOB. In all present experiments, shRNA2 (A1, B1, C1 and D1) and shRNA5 (A2, B2, C2 and D2) transduced cells displayed the same cell characteristics. Eight days after transduction, scarcely viable cells were observable in all WISP1 down-regulated assays. In contrast, cells of the scrambled (A3, B3, C3 and D3) and pure vector (A5, B5, C5 and D5) control assays show an expected proliferation during the whole week. The GFP control confirmed a successful transduction in all cell lines (A4, B4, C4 and D4). Scale bar=100μm. RT-PCR analyses of total isolated RNA revealed a down-regulation of both transcript variants of WISP1 (A6, B6, C6 and D6). The mRNA levels of the housekeeping gene EF1α were used as internal controls.*

9.5. WISP1 gene-silencing in primary bone marrow derived hMSCs

To investigate cell characteristics of WISP1 depleted primary cells, additional experiments of WISP1-T1 and -T2 gene-silencing were performed in human bone marrow derived MSCs. Precedent work confirmed an continuous expression of both variants in 12 different hMSC donors (Fig. 8.1). Similar to the previously described experiments, two different shRNA constructs (shRNA2 and shRNA5) as well as three different controls (scrambled, GFP, pure vector) were used to compare WISP1 mRNA levels and cell characteristics. Figure 9.7 illustrates related optical differences between knock-down and control assays, like they were exhibited in the immortalized hMSC cell lines Tert4 and Tert20 (Fig. 9.6).

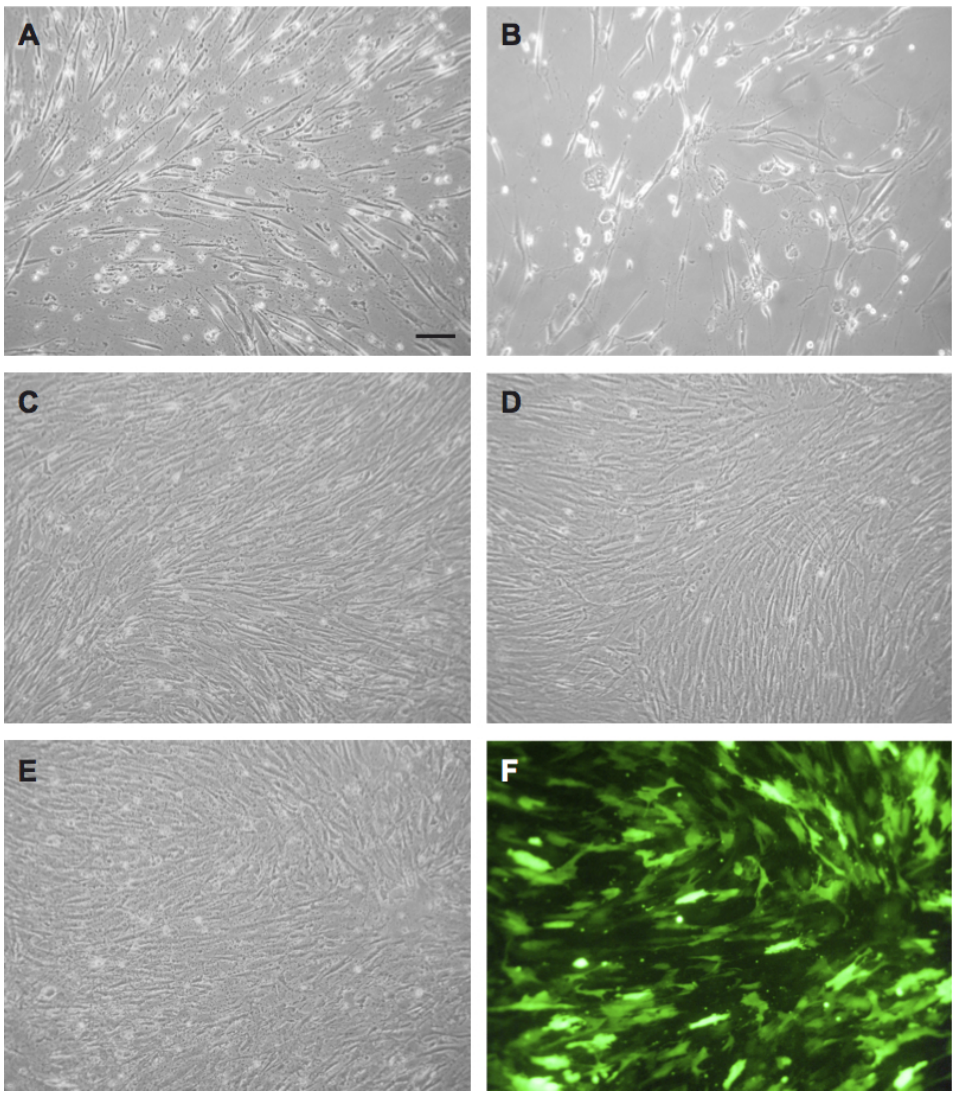

Figure 9.7.: *Microscopy of WISP1 down-regulation in primary hMSCs. Eight days after transduction, shRNA2 (A) and shRNA5 (B) transduced cells show distinct aberrant cell characteristics compared to the three control samples (C, D, E). Only few viable cells were observable while the scrambled (C), pure vector (D) and GFP control assays show entire proliferation and no optical differences among each other. Under exposure to UV-light GFP exhibits a bright, green fluorescence, which confirmed a successful virus transduction (F). Scale bar=*$100\mu m$.

However, shRNA2- and shRNA5 transduced hMSCs started to detach a few day after the transduction was performed. Cells transduced with shRNA5 (B) show slightly more optical differences than shRNA2 (A) transduced cells, but the optical effect was remarkably on day eight in both assays. All three controls (scrambled (C), pure vector (D) and GFP (F)) showed an expected proliferation within one week. Under exposure to UV-light, GFP visualized the successful transduction after eight days (F).

Total RNA of each sample was isolated and RT-PCR with subsequent densitometric analyses were performed to validate the successful down-regulation of WISP1-T1 and-T2 in the shRNA transduced assays (Fig. 9.8). The endogenous amounts of both transcript variants were significantly decreased in shRNA5 transduced cells. In contrast, all control samples showed expected mRNA levels of both transcript variants. Additional experiments were performed using shRNA5-, scrambled- and GFP constructs to confirm the down-regulation of WISP1 in four different hMSC donors. RT-PCR and subsequent densitometric analyses of the corresponding gel bands enabled a validation of a significant down-regulation of both WISP1 transcript variants (Fig. 9.8; Tab. 9.1).

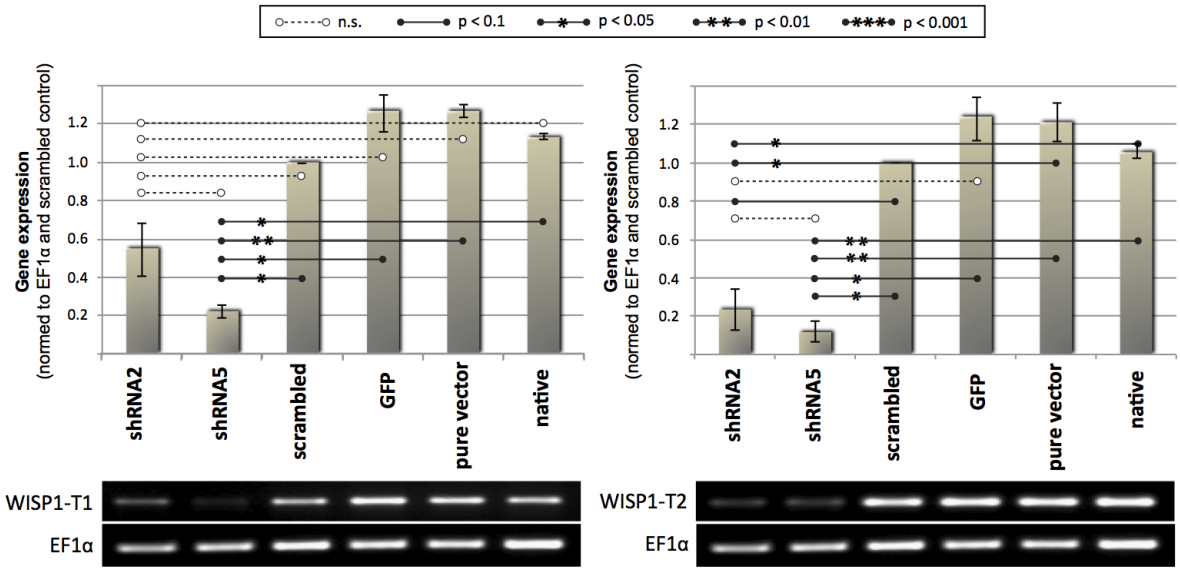

Figure 9.8.: *Densitometric analysis of RT-PCR bands from WISP1 down-regulation in primary hMSCs (n=4). Left: WISP-T1, right: WISP1-T2. The mRNA levels of the housekeeping gene EF1α were used as internal controls. Densitometric analysis of the corresponding gel bands revealed significant down-regulation of both transcript variants of WISP1. Displayed is the mean of densitometric measures, with the %SEM indicating error bars.*

Table 9.1.: *Results of the t-tests for all relevant comparisons between WISP1 down-regulation by shRNA2 and shRNA5 in hMSCs and the corresponding controls. The t-tests were conducted with paired samples and two sided. A p-value correction by fdr has been applied according to the number of comparisons. Differences were considered significant when the corrected p-value was <0.05 (∗), <0.01 (∗∗) and <0.001 (∗ ∗ ∗). N_S=Number of samples, df=degrees of freedom, p-adj.=corrected p-values, N_C=Number of comparisons corrected for p-adj.*

Data	**Comparisons**	$\mathbf{N}_S$	**t-val.**	**df**	**p-val.**	**p-adj.**	**sig.**	$\mathbf{N}_C$
WISP1-T1	shRNA2 - shRNA5	4	2.35	3	0.1008	0.9068	-	9
WISP1-T1	shRNA2 - scrambled	4	-3.84	3	0.0312	0.2810	-	9
WISP1-T1	shRNA2 - GFP	4	-3.83	3	0.0313	0.2820	-	9
WISP1-T1	shRNA2 - pure vector	4	-5.14	3	0.0143	0.1283	-	9
WISP1-T1	shRNA2 - native hMSCs	4	-4.40	3	0.0217	0.1955	-	9
WISP1-T1	shRNA5 - scrambled	4	-12.04	3	0.0012	0.0111	∗	9
WISP1-T1	shRNA5 - GFP	4	-9.96	3	0.0022	0.0194	∗	9
WISP1-T1	shRNA5 - pure vector	4	-14.54	3	0.0007	0.0064	∗∗	9
WISP1-T1	shRNA5 - native hMSCs	4	-8.26	3	0.0037	0.0335	∗	9
WISP1-T2	shRNA2 - shRNA5	4	0.94	3	0.4166	1.0000	-	9
WISP1-T2	shRNA2 - scrambled	4	-6.23	3	0.0084	0.0752	-	9
WISP1-T2	shRNA2 - GFP	4	-5.39	3	0.0125	0.1128	-	9
WISP1-T2	shRNA2 - pure vector	4	-8.20	3	0.0038	0.0342	∗	9
WISP1-T2	shRNA2 - native hMSCs	4	-8.74	3	0.0032	0.0284	∗	9
WISP1-T2	shRNA5 - scrambled	4	-9.44	3	0.0025	0.0227	∗	9
WISP1-T2	shRNA5 - GFP	4	-10.92	3	0.0016	0.0148	∗	9
WISP1-T2	shRNA5 - pure vector	4	-15.59	3	0.0006	0.0052	∗∗	9
WISP1-T2	shRNA5 - native hMSCs	4	-17.18	3	0.0004	0.0039	∗∗	9

CHAPTER
TEN

MICROARRAY ANALYSES

10.1. Microarray analysis of WISP1-T1 and -T2 silenced hMSCs

Assays with a reduced WISP1 expression (n=3) and the corresponding scrambled control assays (n=3) were performed in hMSCs simultaneous with the shRNA5- and scrambled control constructs. Total RNA was isolated at the fourth day after transduction to detect gene regulations in an early stage of cell death. RNA specimers were visualized and verified with gel electrophoresis. Figure 10.1 illustrates the purity of the 28s RNA (5.1kb) and 18s RNA (1.9kb) of all six samples.

Affymetrix microarray analyses were performed with the HG-U133+2.0 GeneChip and subsequent utilized with the statistical software R and its additional component for microarray analyses, namely Bioconductor (Gentleman et al. 2004b; R Development Core Team 2010). Raw data was visually quality controlled and the RNA degradation plot was used to determine the quality of all samples (Fig. 10.2 (A)). Mean intensities of all RNA specimens were lower in RNA parts of the 5' region compared to mean intensities of parts within the 3' region. However, all RNA samples reflect the same expected intensity gradients and were used for further analyses. In addition, Figure 10.2 illustrates box plot (B) and density plot (C) results of the raw data prior to the normalization steps.

Subsequently, three normalization steps were applied for each sample. Firstly, normalization using the robust multi-array average expression measure (RMA) with background correction; secondly, using the quantiles without background correction and thirdly the variance stabilization and normalization (VSN) with background correction. Figure 10.3 reflects box plot (A) and density plot (B) results of the raw data after the three normalization steps were per-

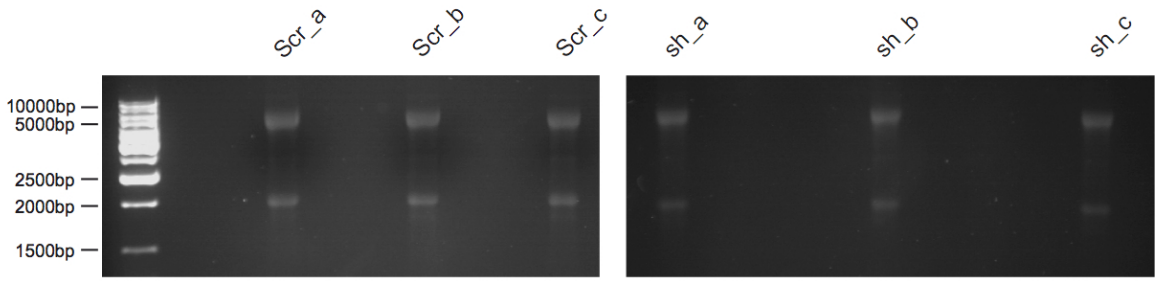

Figure 10.1.: *Gel electrophoresis results after RNA isolation from hMSCs. Displayed are 28s RNA (5.1kb) and 18s RNA (1.9kb) amounts, previously isolated from scrambled control transduced samples and shRNA5 transduced assays.*

formed. The RMA method yielded the best outcome, which was determined by comparison of the density plots, and was used for the following analyses.

10.1.1. Gene expression pattern after WISP1 gene-silencing in hMSCs

The Affymetrix GeneChip HG-U133+2.0 was able to detect regulation of 54.675 probe sets. Linear models for microarray data were fit to expression data using the R package limma. The AFFX cut-off (maximum differentially expressed AFFX labelled probe set as threshold) was used to reduce the data to the most significant probe sets. Thereby, comparison between WISP1 deficient (shRNA5) and sufficient (scrambled control) hMSCs revealed 522 differentially expressed probe sets corresponding to 456 genes. 210 probe sets (corresponding to 179 genes) were significantly up-regulated in shRNA5-transduced samples, while 312 probe sets revealed a significant down-regulation (corresponding to 277 genes). The top-ranked 25 differentially expressed genes detectable during the absence of WISP1 in hMSCs are listed according to their descending statistical score (logFc) in table 10.1.

Eight of the top ranked up-regulated genes were involved in immuno-regulatory processes. Additional, TNFSF10 (also known as TRAIL) - one of the major death ligands - is the fifth highest ranked up-regulated gene detected directly after WISP1 down-regulation. Detailed distribution of regulated probe sets including the logFc range and the adequate p-values are listed in the appendix A due to their degree of regulation (logFc) from highest up-regulation to highest down-regulation.

10.1.2. Gene ontology analysis

Significantly regulated genes of the array data were analysed for their affiliation regarding the main Gene Ontology (GO) categories biological process, cellular component and molecular function as well as for KEGG pathway over-representation (Ashburner et al. 2000; Falcon and Gentleman 2007b; Gentleman et al. 2004a; Harris et al. 2004; Ogata et al. 1999; R Development Core Team 2010). A detailed distribution regarding the different GO terms and KEGG pathway over-representation is listed in the appendix B due to the corresponding p-value for each subclass within the different terms. An overview of these results is provided in table 10.2. The analysis revealed several important cellular processes, affected subsequent to the down-regulation of WISP1. For example, a conspicuous cluster of differentially expressed genes belonged to different subclasses of immune-response (e.g. innate immune-response and positive regulation of interferon-beta production) was discovered in the GO-class of biological process. Similarly, regulations associated with e.g. apoptosis (induction of apoptosis and positive regulation of apoptosis) and focal adhesion could be assigned along the main GO-categories. Gene regulation in subclasses of higher interest will be observed in detail in subsequent sections.

10.1.3. Selection of regulated genes involved in immuno-regulatory processes

Microarray data analysis and additional GO classification, exhibited a remarkable cluster of gene regulations involved in immuno-regulatory processes. All differentially expressed genes were detected subsequently after the down-regulation of WISP1 took place in three different hMSC donors. Conspicuously, every probe set corresponding to the cluster of immune-responsive genes was up-regulated directly after the absence of WISP1 was enforced. Figure 10.4 illustrates these gene regulations by colour-coding in a so called heat map. The first three columns reflect regulations of the three scrambled control samples, whereas the following three columns display the corresponding WISP1 gene-silencing experiments. In this context, white represents high expression (over yellow and orange as medium expression) and red low

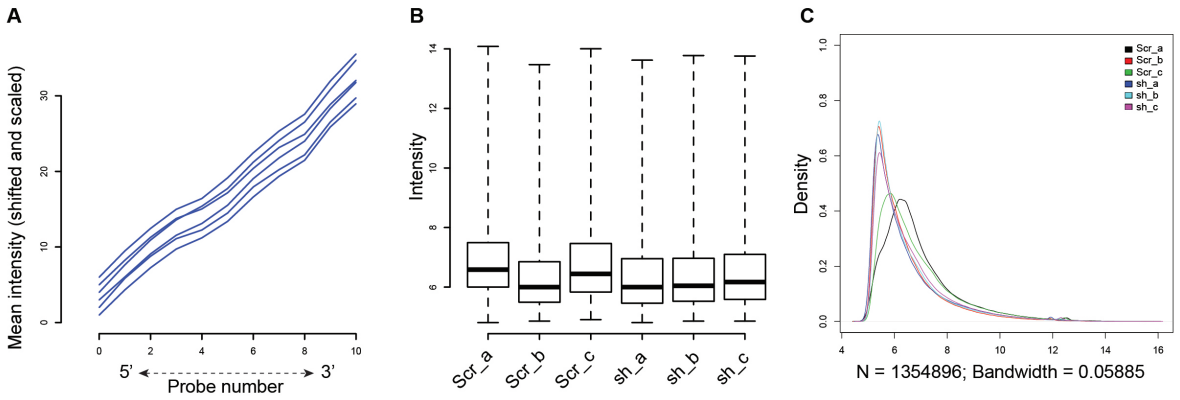

Figure 10.2.: *Diagnostic plots of microarray raw data prior to normalization. (A) RNA degradation from 5' to 3' end of the probe sets. Displayed are mean intensity values for each array. All samples were comparable according to their ascendent slope and parallelity. (B) and (C) displayed the distribution of raw expression intensities by box plot and density plot, respectively.*

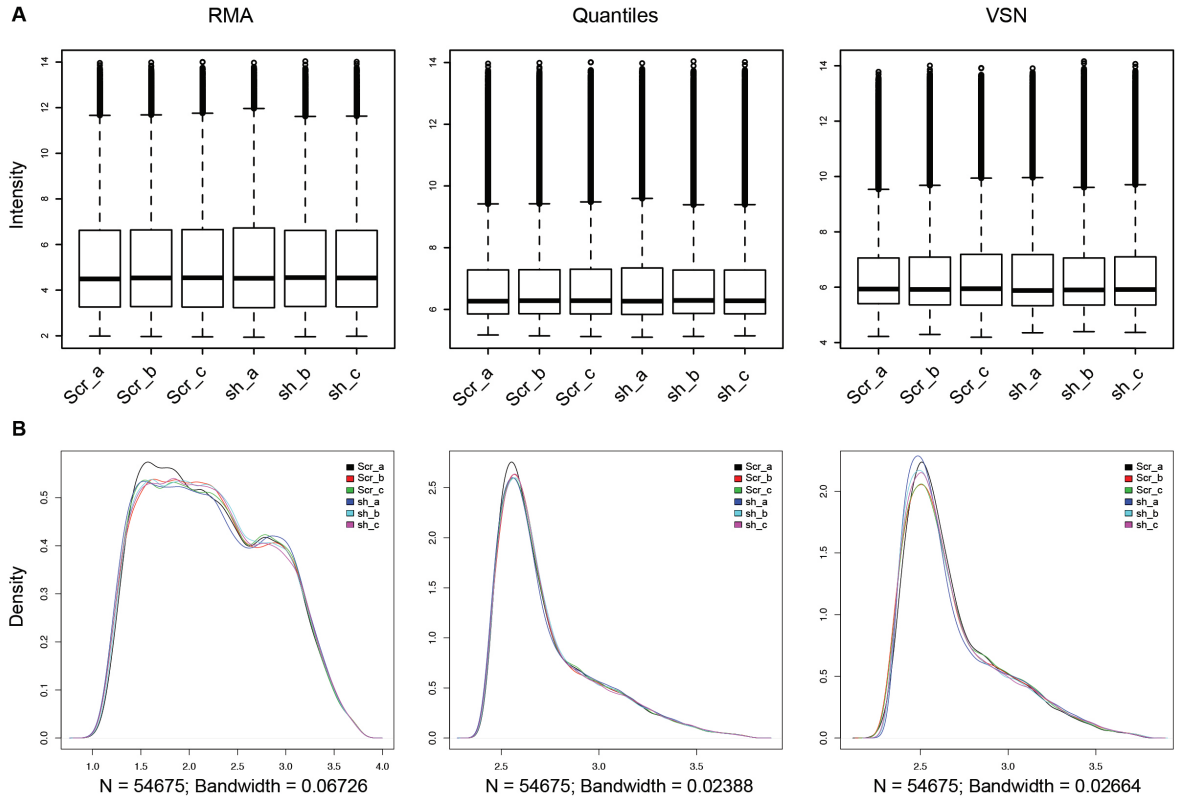

Figure 10.3.: *Diagnostic plots of microarray data after normalization. (A) Box plot distributions and (B) densities of normalized expression intensities. Within both subfigures, the three columns are the different applied normalization methods RMA, quantiles and VSN.*

Table 10.1.: *25 top-ranked genes differentially expressed after WISP1 down-regulation in hMSCs. Genes are listed according to their descending statistical score (logFc) with additional information regarding the number of regulated probe sets (N) and the corresponding adjusted (corrected for multiple comparisons) p-value. Thereby, positive values indicate fold changes of up-regulated whereas negative values state fold changes of down-regulated gene expression in shRNA5 transduced samples compared to the corresponding controls. Specified logFc and p-value belongs to the highest regulated probe set in case of more than one regulated probe set.*

Symbol	Gene name	logFC	adj. p-val.	N
RSAD2	radical S-adenosyl methionine domain containing 2	4.49	$2.1x10^{-5}$	2
CMPK2	cytidine monophosphate (UMP-CMP) kinase 2, mitochondrial	4.38	$9.0x10^{-6}$	1
IFIT2	interferon-induced protein with tetratricopeptide repeats 2	4.05	$1.2x10^{-6}$	2
OASL	2'-5'-oligoadenylate synthetase-like	3.88	$9.6x10^{-6}$	2
TNFSF10	tumour necrosis factor (ligand) superfamily, member 10	3.77	$3.2x10^{-5}$	3
TNFSF13B	tumour necrosis factor (ligand) superfamily, member 13b	3.69	$6.6x10^{-6}$	2
OAS1	2',5'-oligoadenylate synthetase 1. 40/46kDa	3.28	$8.1x10^{-6}$	2
ISG20	interferon stimulated exonuclease gene 20kDa	3.24	$3.8x10^{-5}$	1
CCL2	chemokine (C-C motif) ligand 2	3.06	$4.0x10^{-6}$	1
RTP4	receptor (chemosensory) transporter protein 4	2.94	$2.8x10^{-5}$	1
HERC5	hect domain and RLD 5	2.93	$9.3x10^{-6}$	1
IFI44L	interferon-induced protein 44-like	2.89	$1.7x10^{-5}$	1
DDX58	DEAD (Asp-Glu-Ala-Asp) box polypeptide 58	2.87	$8.7x10^{-7}$	1
LMOD1	leiomodin 1	-2.29	$4.1x10^{-5}$	1
FGF1	fibroblast growth factor 1	-2.29	$7.0x10^{-6}$	1
MAP1A	microtubule-associated protein 1A	-2.36	$2.7x10^{-6}$	1
PCYOX1	prenylcysteine oxidase 1	-2.44	$3.6x10^{-5}$	2
AAGAB	alpha- and gamma-adaptin binding protein	-2.50	$1.8x10^{-6}$	1
HSD17B6	hydroxysteroid (17-beta) dehydrogenase 6 homolog (mouse)	-2.53	$3.7x10^{-5}$	1
KIAA1715	KIAA1715	-2.55	$7.3x10^{-6}$	2
NACC2	NACC family member 2, BEN and BTB (POZ) domain containing	-2.56	$2.9x10^{-6}$	1
MRPL19	mitochondrial ribosomal protein L19	-2.60	$4.5x10^{-5}$	1
SEC63	SEC63 homolog (S. cerevisiae)	-2.70	$7.3x10^{-6}$	1
ACTA2	actin, alpha 2, smooth muscle, aorta	-3.01	$4.4x10^{-6}$	1
KCTD20	potassium channel tetramerisation domain containing 20	-3.06	$1.8x10^{-6}$	2

Table 10.2.: *Gene Ontology (GO) analysis and KEGG pathway over-representation. All 456 significantly regulated genes, detected during the WISP1 array data analysis in hMSCs, were continuative assigned to GO terms and KEGG signalling pathways. Illustrated are, in addition to the corresponding subclass name, the expected count, actual count and overall number of genes (N) associated to the GO/KEGG-term. These values are related to and corrected by the total number of all and differentially expressed corresponding genes present on the chip. Odds-ratio of corrected values is provided by the fraction (N/actual count). Corresponding p-values are results of the hyper-geometric tests.*

						— on chip —	
Go term	**p-value**	**Odds ratio**	**Exp. count**	**Act. count**	**N**	**Act. count**	**N**
Biological processes							
Innate immune-response	$4.2x10^{-8}$	3.58	9	29	382	9	212
Immune-response	$4.1x10^{-6}$	2.33	20	42	836	15	316
Cellular response to type I interferon	$5.1x10^{-5}$	12.03	2	15	68	1	1
Positive regulation of Interferon-beta production	0.038	7.44	0	2	13	2	13
Interferon-gamma-mediated signalling pathway	0.023	3.27	2	5	68	5	63
Induction of apoptosis	0.012	1.96	9	16	356	9	170
Positive regulation of apoptosis	0.048	1.59	12	18	489	4	122
Transforming growth factor beta receptor signalling pathway	0.014	2.92	3	7	106	3	62
Cellular components							
Focal adhesion	$8.3x10^{-7}$	6.21	2	13	102	13	102
Molecular functions							
GTP-Rho binding	0.019	11.42	0	2	9	2	9
Heat shock protein binding	0.042	2.74	2	5	78	5	60
Helicase activity	0.024	24.06	3	8	142	8	111
Ligase activity	0.007	1.92	11	20	447	13	342

expression of the specific probe set. The table beside the heat map illustrates additional information regarding probe set ID, degree of regulation (logFC) and the corresponding adjusted p-value of a specific probe set. Additional, individual genes of this cluster were successfully reevaluated by RT-PCR (Sec. 10.1.5).

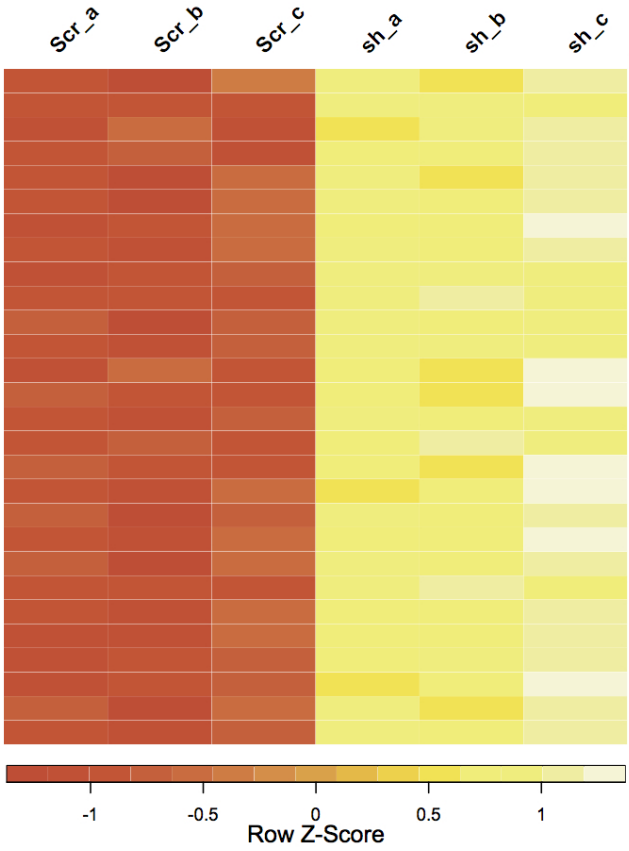

	probe set ID	logFC	p-val.
CCL5	01405_i_at	2.20	5.2×10^{-5}
DDX58	218943_s_at	2.87	2.3×10^{-5}
IFI16	208966_x_at	1.25	3.9×10^{-5}
IFI35	209417_s_at	2.03	8.1×10^{-6}
IFI44	214453_s_at	2.25	2.1×10^{-5}
IFI44L	204439_at	2.89	1.7×10^{-5}
IFIH1	219202_at	2.66	1.1×10^{-5}
IFIT1	203153_at	2.10	9.6×10^{-6}
IFIT2	226757_at	4.05	8.5×10^{-7}
IFIT2	217502_at	3.56	1.2×10^{-6}
IFIT3	204747_at	2.28	8.1×10^{-6}
IFIT3	229450_at	1.98	4.0×10^{-6}
IFNB1	208173_at	2.02	4.1×10^{-5}
IL18BP	222868_s_at	2.07	2.1×10^{-5}
IRF2	203275_at	1.19	2.1×10^{-5}
IRF7	208436_s_at	2.03	2.0×10^{-7}
ISG15	205483_s_at	1.37	4.2×10^{-5}
ISG20	33304_at	3.24	3.8×10^{-5}
MX1	202086_at	2.86	1.0×10^{-5}
MX2	204994_at	2.73	1.5×10^{-5}
OAS1	205552_s_at	3.28	8.1×10^{-6}
OAS1	202869_at	3.14	2.1×10^{-6}
OASL	210797_s_at	3.88	9.6×10^{-6}
OASL	205660_at	3.76	8.1×10^{-6}
PLSCR1	202446_s_at	2.29	4.0×10^{-6}
PLSCR1	202430_s_at	2.10	2.8×10^{-5}
RTP4	219684_at	2.94	2.8×10^{-5}
USP18	219211_at	2.12	4.9×10^{-6}

Figure 10.4.: *Selection of regulated genes involved in immuno-regulatory processes. Levels of gene expression are visualized by colour-coding, i.e. heat-colours with white representing high expression, over yellow and orange as medium expression and red representing low expression of the corresponding probe set. Values are normalized by rows (Z-score). Gene names are aligned beside the rows, with additional information regarding probe set IDs, degree of regulation (logFC) and the corresponding p-value. Sample names are presented over each column. Scr=scrambled control sample, sh=WISP1 down-regulated sample, logFC=logarithmic fold change, p-val.=adjusted p-value.*

10.1.4. Selection of regulated genes involved in cell survival and apoptosis

Eligible to the observed optical effect of cell death directly after the WISP1 down-regulation occurred, the bioinformatical investigation of the data sets identified also a cluster of differentially expressed genes associated with cell survival and/or apoptosis. In this section all statistical significant gene regulations were observed regarding their association with apoptosis and/or cell survival and independently of the previous used AFFX-cut off, but with high attention to the logFC and the corresponding adj. p-value. In all three comparisons, WISP1 down-regulation specifically affected genes important for both main apoptosis signalling cascades: the extrinsic- and intrinsic-mediated apoptosis.

Subsequent, the heat map clearly illustrates this cluster of gene regulations by colour-coding in all hMSC samples (Fig. 10.5). The first three columns reflect regulations in the control samples and the following three columns the corresponding gene regulation after the WISP1 down-regulation. Adapted to table 10.3, genes are listed according to their effectiveness connected to cell survival and/or apoptosis. Genes with regulations of more than one probe set were reduced to the probe set with the highest logFC. Not all genes in this cluster show regulations with the consequence of cell death. Three members (EIF2AK3, BOK and CASP2) are regulated in the opposite direction and are listed for the sake of completeness.

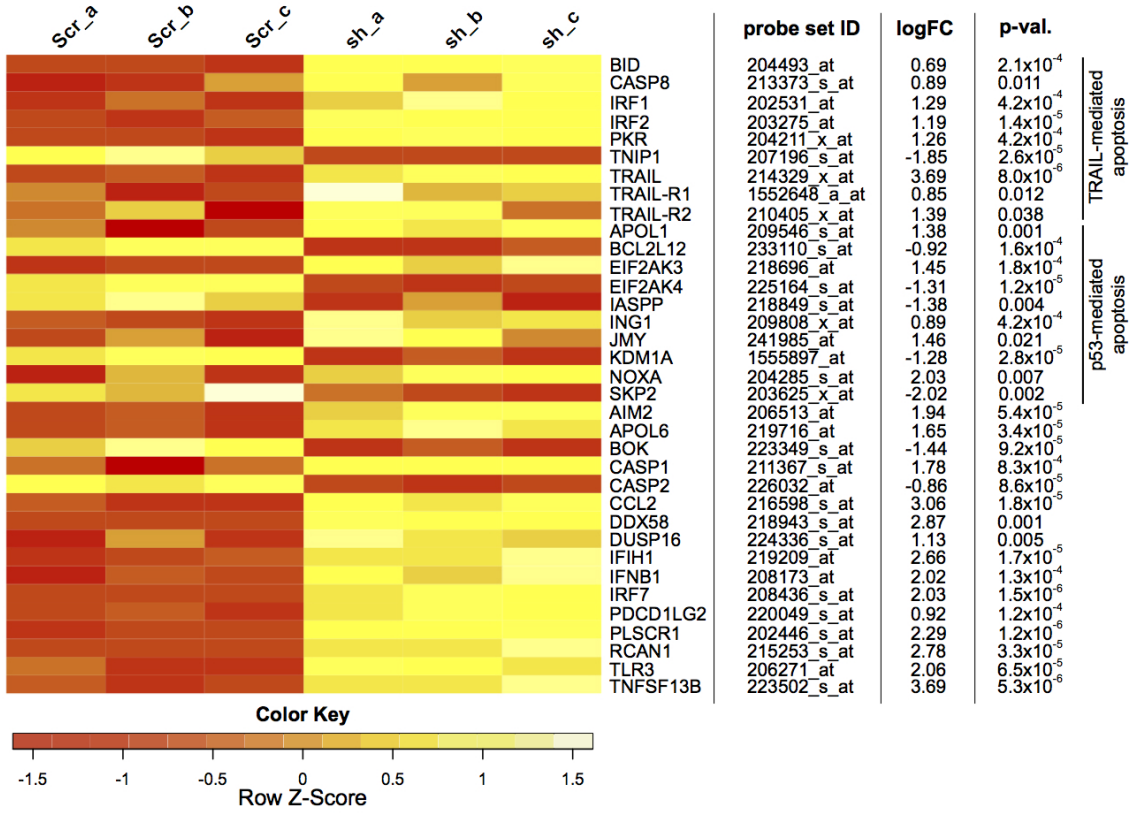

Figure 10.5.: *Selection of apoptosis responsive gene regulations. Genes are listed according to their effectiveness connected to cell survival and/or apoptosis. Levels of gene expression are visualized by colousubclassr-coding, i.e. heat-colours with white representing high expression, over yellow and orange as medium expression and red representing low expression of the corresponding probe set. Values are normalized by rows (Z-score). Gene names are aligned beside the rows, with additional information regarding probe set IDs, degree of regulation (logFC) and the corresponding p-value. Sample names are presented over each column. Scr=scrambled control sample, sh=WISP1 down-regulated sample, logFC=logarithmic fold change, p-val.=adjusted p-value.*

Table 10.3.: *Selection of apoptosis responsive gene regulations. Genes are listed according to their effectiveness connected to cell survival and/or apoptosis. The first nine members are assigned to the TRAIL mediated apoptosis, whereas the ten adjacent listed genes are clearly correlated to the p53 mediated apoptotic pathway. Columns (from left to right) describe gene symbols, gene names, number of regulated probe sets (N) and a short summary of the way of function in relation to cell death.*

Symbol	Gene name	N	Function Related to Cell Death
BID	BH3 interacting domain death agonist	1	pro-apoptotic member of the BCL2 family. Triggers cytochrome c release by shutteling to the outer mitochondrion membrane after CASP8 cleavage (Gross et al. 1999; Li et al. 1997; Liu et al. 1996; Renshaw et al. 2004)
CASP8	caspase 8, apoptosis-related cysteine peptidase	1	key component of the extrinsic mediated apoptosis (Ashkenazi and Dixit 1998; Budihardjo et al. 1999)
IRF1	interferon regulatory factor 1	2	expression of either IRF-1 or IRF-2 results in cleavage of caspase-8, -3 and -7 and promotes extrinsic mediated apoptosis (Chow et al. 2000; Stang et al. 2007; Wu et al. 2010)
IRF2	interferon regulatory factor 2	1	expression of either IRF-1 or IRF-2 results in cleavage of caspase-8, -3 and -7 and promotes extrinsic mediated apoptosis (Chow et al. 2000)
PKR	eukaryotic translation initiation factor 2-alpha kinase 2	2	over-expression induces apoptosis (Kibler et al. 1997; Lee and Esteban 1994), up-regulate the expression of the apoptotic receptor Fas (Takizawa et al. 1995)
TNIP1	TNFAIP3 interacting protein 1	1	inhibits TNF-induced apoptosis (Oshima et al. 2009; Wullaert et al. 2005)
TRAIL (TNSF10)	TNF-related apoptosis-inducing ligand	3	Major death ligand, rapidly induces apoptosis in a wide variety of transformed cell lines (Marsters et al. 1996; Wiley et al. 1995), TRAIL-expressing MSCs were able to significantly reduce tumor growth (Loebinger et al. 2009)

...continues on next page

Table 10.3.: (...continued)

Symbol	Gene name	N	Function Related to Cell Death
TRAIL-R1 DR4, TNSFRSF10A	TNF-related apoptosis-inducing ligand receptor 1	3	contains a cytoplasmic death domain and activates apoptosis by binding of TRAIL (Pan et al. 1997)
TRAIL-R2 DR5, TNSFRSF1B	TNF-related apoptosis-inducing ligand receptor 2	2	contains a cytoplasmic death domain and activates apoptosis by binding of TRAIL (Sheridan et al. 1997; Walczak et al. 1997)
APOL1	apolipoprotein L, 1	1	p53 downstreem target in p53 mediated apoptosis, induced autophagic cell death. (Wan et al. 2008; Zhaorigetu et al. 2008)
BCL2L12	BCL2-like 12 (proline rich)	1	anti-apoptotic member of the BCL2 family, inhibits caspases 3 and 7 in the cytoplasm and p53 in the nucleus (Stegh et al. 2007; Stegh and Depinho 2011)
EIF2AK3	eukaryotic translation initiation factor 2-alpha kinase 3	1	down-regulation promotes apoptosis via activation of p53 signal cascade (Liu et al. 2010)
EIF2AK4	eukaryotic translation initiation factor 2 alpha kinase 4	1	down-regulation promotes apoptosis via activation of p53 signal cascade (Liu et al. 2010)
IASPP	Inhibitor of ASPP protein	1	one of the most evolutionarily conserved inhibitors of p53 (Ahn et al. 2009)
ING1	inhibitor of growth family, member 1	2	Part of the p53 apoptotic pathway, stabilizes p53 by disrupting the the Interaction with p53 inhibitor MDM2 (Garkavtsev et al. 1998; Leung et al. 2002; Thalappilly et al. 2011)
JMY	junction mediating and regulatory protein, p53 cofactor	1	pro-apoptotic cofactor of p53 (Shikama et al. 1999)
KDM1A	lysine (K)-specific demethylase 1A	1	the histone lysine-specific demethylase mediates p53 demethylation and inhibts p53 mediated apoptosis (Huang et al. 2007; Scoumanne and Chen 2008)

...continues on next page

Table 10.3.: *(...continued)*

Symbol	Gene name	N	Function Related to Cell Death
NOXA	PMA-induced protein 1	2	pro-apoptotic member of the BCL2 family, mediator of p53-dependent apoptosis (Eferl et al. 2003; Kim et al. 2004; Oda et al. 2000; Seo et al. 2003)
SKP2	S-phase kinase-associated protein 2 (p45)	1	suppresses p300-mediated acetylation and activation of apoptosis via p53 (Kitagawa et al. 2008)
AIM2	absent in melanoma 2	1	Interaction with ASC (via pyrin-card-domain-binding) leads to an activated inflammasome and cell death via CASP1 (Fernandes-Alnemri et al. 2007; Hornung et al. 2009)
APOL6	apolipoprotein L, 6	4	induced mitochondria-mediated apoptosis in human colon cancer cells (Liu et al. 2005; Zhaorigetu et al. 2011)
BOK	BCL2-related ovarian killer	1	pro-apoptotic member of the BCL2 family, interacts with some anti-apoptotic members of the family like MCL1 (Hsu and Hsueh 1998; Hsu et al. 1997; Yang et al. 1995)
CASP1	caspase 1	5	is involved in inflammasome formation and cell death (Fernandes-Alnemri et al. 2007; Friedlander et al. 1996)
CASP2	caspase 2	2	activated by a variety of apoptotic stimuli of stress induced apoptosis (Harvey et al. 1997; Tinel and Tschopp 2004; Zhivotovsky and Orrenius 2005)
CCL2	chemokine (C-C motif) ligand 2	1	causes cell death by inducing oxidative stress (Xia et al. 2010; Younce and Kolattukudy 2010)
DDX58	DEAD (Asp-Glu-Ala-Asp) box polypeptide 58	3	triggers apoptosis as part of an antiviral host response (Besch et al. 2009; Hornung et al. 2009; Peng et al. 2009)

...continues on next page

Table 10.3.: *(...continued)*

Symbol	Gene name	N	Function Related to Cell Death
DUSP16	dual specificity phosphatase 16	2	inactivation via ROS mediates activation pro-apoptotic JNK signalling (Kiessling et al. 2010)
IFIH1	interferon induced with helicase C domain 1	1	triggers apoptosis as part of an antiviral host response (Peng et al. 2009)
IFNβ1	interferon, beta 1, fibroblast	1	produktion (triggered by TLR3 and IFIH1 signalling) leads to apoptosis via multiple BH3-only proteins (Marraco et al. 2011)
IRF7	interferon regulatory factor 7	1	function as an effector of BRCA1/IFNγ mediated apoptosis (Buckley et al. 2007)
PDCD1LG2	programmed cell death 1 ligand 2	2	programmed cell death 1 ligand 2 (genecards)
PLSCR1	phospholipid scramblase 1	2	expression through STAT1 requires activation of PKCδ and JNK. Increased intrinsic mediated apoptosis after DNA damage (Zhao et al. 2005)
RCAN1	regulator of calcineurin 1	2	facilitates neuronal apoptosis through caspase-3 activation (Sun et al. 2011)
TLR3	toll-like receptor 3	1	activation triggered the signalling of both the extrinsic and intrinsic apoptotic pathways (Marraco et al. 2011; Sun et al. 2011)
TNFSF13B	tumor necrosis factor (ligand) superfamily, member 13b	2	mediates apoptosis via caspase 3 activation, also activates NFκB and JNK (Mukhopadhyay et al. 1999)

10.1.5. Reevaluation by semi-quantitative RT-PCR

Amongst regulated genes, a selection of twelve were chosen for reevaluation by semi-quantitative RT-PCR and densitometric evaluation of RT-PCR bands on agarose gels. These genes, listed in table 10.4, were selected due to their high fold change obtained by microarray analysis with high attention to their functional properties that may be potentially relevant during apoptosis, immuno-regulatory processes or in consideration to their linkage concerning interactions with the ECM.

Reevaluation by RT-PCR was accomplished with the same RNA samples, previously used for the microarray analysis. The regulation of twelve gene products could be confirmed according to the microarray findings (Fig. 10.6; Tab. 10.5).

Table 10.4.: *Selection of genes for reevaluation. From left to right: probe set IDs, gene symbols, gene names, degree of regulation (logFC) and the corresponding p-value. Genes are listed alphabetically and according to their descendent statistical score in cases where more than one probe set is regulated.*

Probe set ID	Symbol	Gene name	logFC	adj. p-val.
209546_s_at	APOL1	apolioprotein L, 1	1.38	0.012
211813_x_at	DCN	decorin	-1.00	0.093
211896_s_at	DCN	decorin	-1.07	0.080
209335_at	DCN	decorin	-2.88	0.020
218943_s_at	DDX58	DEAD (Asp-Glu-Ala-Asp) box polypeptide 58	2.87	0.002
222793_at	DDX58	DEAD (Asp-Glu-Ala-Asp) box polypeptide 58	1.75	0.014
242961_x_at	DDX58	DEAD (Asp-Glu-Ala-Asp) box polypeptide 58	1.62	0.069
219209_at	IFIH1	interferon induced with helicase C domain 1	2.66	0.003
208173_at	IFNβ1	interferon, beta 1, fibroblast	2.02	4.1×10^{-5}
209808_x_at	ING1	inhibitor of growth family. member 1	0.89	4.2×10^{-4}
205483_s_at	ISG15	ISG15 ubiquitin-like modifier	1.37	0.005
227048_at	LAMA1	laminin, alpha 1	1.26	4.5×10^{-5}
204114_at	NID2	nidogen 2 (osteonidogen)	-1.80	0.005
204285_s_at	NOXA	phorbol-12-myristate-13-acetate-induced protein 1	2.03	0.028
204286_s_at	NOXA	phorbol-12-myristate-13-acetate-induced protein 1	1.96	0.037
206271_at	TLR3	toll-like receptor 3	2.06	2.8×10^{-5}
202687_s_at	TRAIL	TNF-related apoptosis inducing ligand	3.77	3.2×10^{-5}
214329_x_at	TRAIL	TNF-related apoptosis inducing ligand	3.69	8.1×10^{-6}
202688_at	TRAIL	TNF-related apoptosis inducing ligand	3.64	2.9×10^{-5}

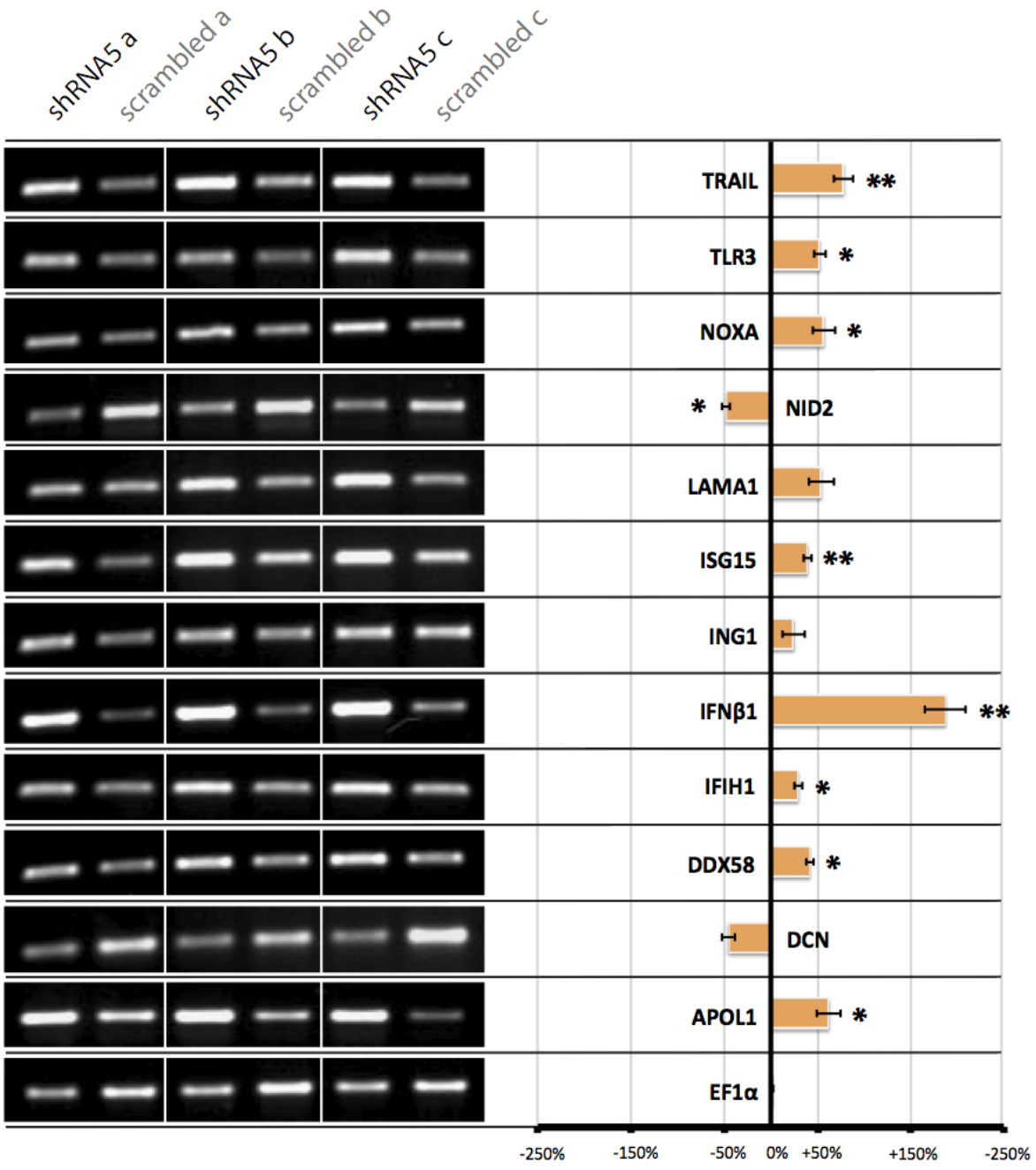

Figure 10.6.: *Reevaluation of selected genes after WISP1 down-regulation in hMSCs. In all RNA samples, previously used for microarray analysis, RT-PCR reactions of selected genes were performed. All inspected genes show an expected regulation according the previously ascertained logFC value. The mRNA levels of the housekeeping gene EF1α were used as internal controls. Densitometric analysis of the corresponding gel bands confirmed the RT-PCR findings. Displayed is the mean of densitometric measures, with the %SEM indicating error bars*

Table 10.5.: *Results of the t-tests for all relevant comparisons between WISP1 down-regulation by shRNA5 in MSCs and the corresponding scrambled control. The t-tests were conducted with paired samples and one-sided. Differences were considered significant when the p-value was <0.05 (∗), <0.01 (∗∗) and <0.001 (∗ ∗ ∗). N_S=Number of samples, df=degrees of freedom, N_C=Number of comparisons corrected for p-adj.*

Data	**Comparisons**	$\mathbf{N}_S$	**t-val.**	**df**	**p-val.**	**sig.**	$\mathbf{N}_C$
EF1α	shRNA5 - scrambled	3	1.65	2	0.2412	-	1
APOL1	shRNA5 - scrambled	3	5.61	2	0.0303	∗	1
DCN	shRNA5 - scrambled	3	-3.71	2	0.0657	-	1
DDX58	shRNA5 - scrambled	3	6.62	2	0.0221	∗	1
IFIH1	shRNA5 - scrambled	3	5.55	2	0.0310	∗	1
IFNβ1	shRNA5 - scrambled	3	18.60	2	0.0029	∗∗	1
ING1	shRNA5 - scrambled	3	1.66	2	0.2385	-	1
ISG15	shRNA5 - scrambled	3	17.26	2	0.0033	∗∗	1
LAMA1	shRNA5 - scrambled	3	3.95	2	0.0584	-	1
NID2	shRNA5 - scrambled	3	-9.40	2	0.0111	∗	1
NOXA	shRNA5 - scrambled	3	5.37	2	0.0329	∗	1
TLR3	shRNA5 - scrambled	3	4.53	2	0.0455	∗	1
TRAIL	shRNA5 - scrambled	3	13.88	2	0.0052	∗∗	1

Additional experiments of WISP1 gene-silencing were performed with a supplemental hMSC donor to determine gene regulations, of the previously validated genes, over time. Therefore, total RNA was isolated on d3 to d7 after transduction with shRNA5 and srambled control constructs. Thereby, day four reflects the gene expression patterns of the previously performed microarray analysis. RT-PCR analysis revealed time dependent regulations of APOL1, DDX58, IFIH1, IFNβ1, ISG15, NOXA and TRAIL. Interestingly, all of them are linked to apoptotic pathways and clearly increased in their up-regulation from d3 to d7 (Fig. 10.7).

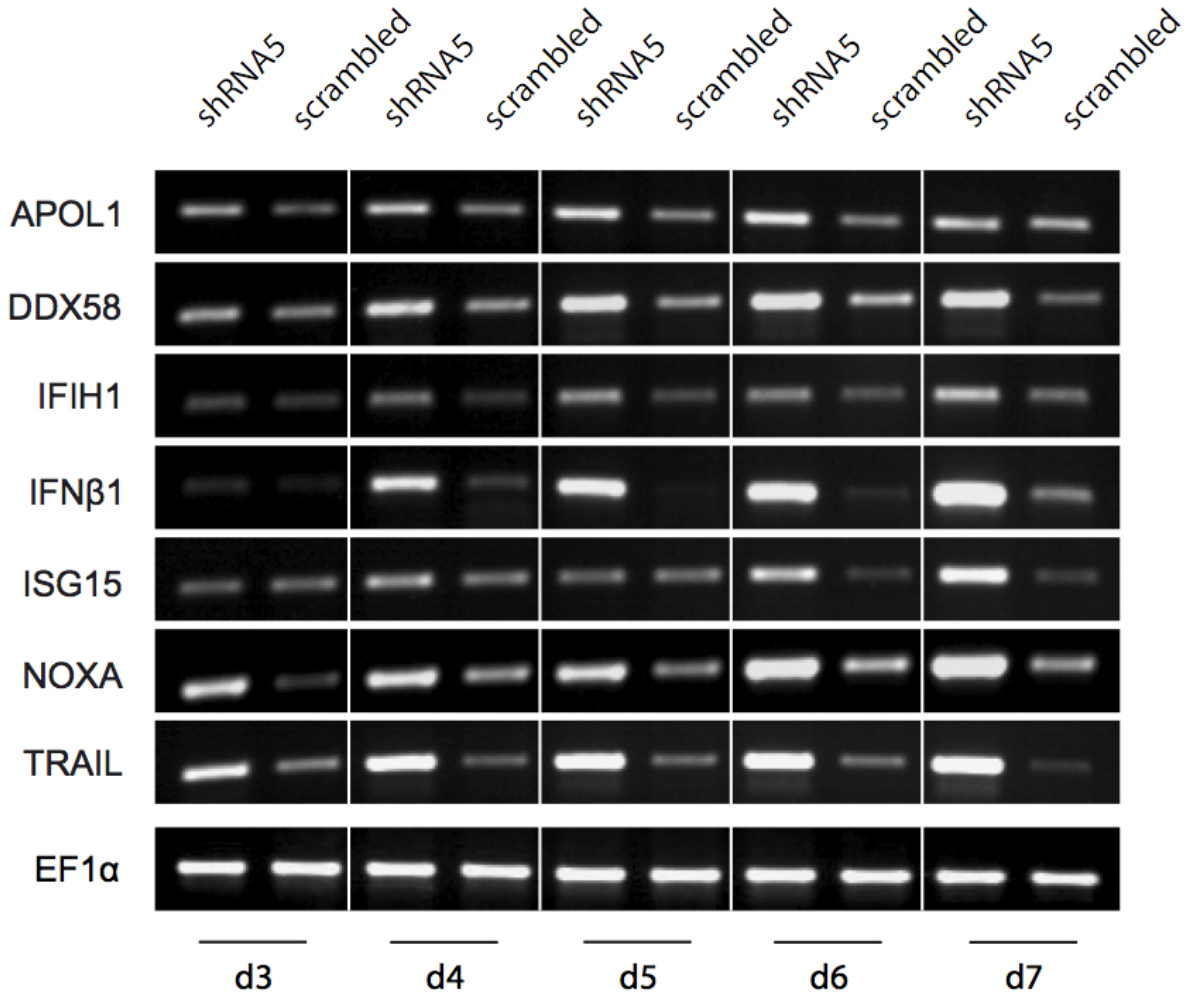

Figure 10.7.: *RT-PCR of gene regulations after WISP1 down-regulation in hMSCs over time. Total RNA was obtained on d3 to d7 after transduction with shRNA2 and scrambled control constructs. Seven of the previously reevaluated genes show additional an increased up-regulation over time. The mRNA levels of the housekeeping gene EF1α were used as internal controls.*

10.2. Microarray analysis of WISP1-T1 and -T2 down-regulated Tc28a2 chondrocytes compared to control cells

Further microarrays with HG-U133+2.0 GeneChips were performed by usage of RNA samples collected from WISP1 gene-silencing experiments (n=5) and scrambled control assays (n=5) in Tc28a2 chondrocytes. Previously, cells were transduced with the shRNA2- and scrambled control constructs and total RNA isolation took place on the fourth day after transduction. The RNA specimer visualization, as well as the raw data inspection was performed simultaneous to the procedure of the previously described microarray analysis in hMSCs (Sec. 10.1). All RNA samples shared the same expected intensity gradients and were used for further analyses. Three normalization steps were applied for each of the samples and comparison of the density plots revealed the RMA method as the best normalization. Using the R package limma and the AFFX cut-off, the analyses resulted in 1687 differentially regulated probe sets, corresponding to 1402 regulated genes. 493 of these probe sets (corresponding to 417 genes) show significantly up-regulation in WISP1 deficient chondrocytes whereas 1194 probe sets (corresponding to 985 genes) revealed a significant down-regulation. Detailed distribution of regulated probe sets including the logFC range and the adequate p-values are listed in the appendix C due to their degree of regulation from highest up-regulation to highest down-regulation. Table 10.6 reflects the top-ranked 25 differentially expressed genes, which were regulated directly after WISP1 down-regulation was present in the chondrocyte cell line Tc28a2.

10.2.1. Gene ontology analysis

Amongst regulated genes that were differentially expressed between WISP1 down-regulated (shRNA2) and control (scrambled) chondrocytes, microarray analyses detected several gene cluster with important cellular functions. Therefore, significantly regulated genes of the array data were analysed for their affiliation regarding the previously described main Gene Ontology (GO) categories and KEGG pathway over-representation. Table 10.7 shows a selection of these results with major attention to the corresponding p-values and odds-ratios. Many subclasses, associated with cartilage homeostasis, cell cycle-regulation and MAPK-signalling, could be detected in the main class of biological processes. Another interesting cluster comprised mitochondrion associated subclasses of cellular components and indicate a linkage of WISP1 depleted chondrocytes to mitochondrion interaction. Pathways, which can be directly linked to apoptosis or cell survival, like regulations within the apoptosis pathway as well as the regulation of MAPK-, ERB- and NOD-like receptor signalling were detected by KEGG pathway over-representation. Detailed distributions of different terms and KEGG pathway over-representation are listed in the appendix D due to the corresponding p-value for each subclass within the different terms.

Table 10.6.: *The 25 top-ranked genes differentially expressed after WISP1 down-regulation in chondrocytes. Genes are listed due to their degree of regulation from highest up-regulation to highest down-regulation. Similarly stated is information regarding the number of regulated probe sets and the corresponding adjusted p-value. The specified p-value belongs to the highest regulated probe set since more than one regulated probe set was detected.*

Symbol	Gene name	logFC	adj. p-val.	N
DCP2	DCP2 decapping enzyme homolog (S. cerevisiae)	1.76	$1.6x10^{-9}$	2
NUPL1	nucleoporin like 1	1.51	$1.9x10^{-9}$	1
PLSCR4	phospholipid scramblase 4	1.41	$1.9x10^{-8}$	1
ALG9	asparagine-linked glycosylation 9. alpha-1.2-mannosyltransferase homolog (S. cerevisiae)	1.31	$5.3x10^{-8}$	1
CASZ1	castor zinc finger 1	1.21	$8.1x10^{-7}$	1
ING3	inhibitor of growth family. member 3	1.17	$6.6x10^{-7}$	1
B4GALT4	UDP-Gal:betaGlcNAc beta 1.4- galactosyltransferase. polypeptide 4	1.15	$1.5x10^{-8}$	2
MED19	mediator complex subunit 19	1.12	$5.9x10^{-8}$	2
WDR33	WD repeat domain 33	1.12	$9.8x10^{-8}$	1
MED12L	mediator complex subunit 12-like	1.11	$1.5x10^{-6}$	1
HSPB8	heat shock 22kDa protein 8	1.07	$2.8x10^{-6}$	1
GFPT1	glutamine-fructose-6-phosphate transaminase 1	1.05	$1.4x10^{-8}$	2
GPR64	G protein-coupled receptor 64	1.04	$5.1x10^{-6}$	1
NIPA2	non imprinted in Prader-Willi/Angelman syndrome 2	-1.89	$4.1x10^{-9}$	1
PIGK	phosphatidylinositol glycan anchor biosynthesis, class K	-1.96	$3.4x10^{-9}$	1
TRHDE	thyrotropin-releasing hormone degrading enzyme	-1.98	$3.0x10^{-8}$	1
LTBP2	latent transforming growth factor beta binding protein 2	-2.00	$1.7x10^{-7}$	2
CYFIP1	cytoplasmic FMR1 interacting protein 1	-2.05	$1.2x10^{-8}$	1
SDC1	syndecan 1	-2.07	$3.9x10^{-9}$	2
AHNAK	AHNAK nucleoprotein	-2.08	$3.8x10^{-9}$	1
CDH6	cadherin 6, type 2, K-cadherin (fetal kidney)	-2.08	$6.6x10^{-7}$	1
HRSP12	heat-responsive protein 12	-2.14	$1.3x10^{-8}$	1
EDIL3	EGF-like repeats and discoidin I-like domains 3	-2.44	$2.6x10^{-7}$	1
PDLIM5	PDZ and LIM domain 5	-2.45	$1.8x10^{-9}$	4
COL4A1	collagen, type IV, alpha 1	-2.81	$3.8x10^{-9}$	2

Table 10.7.: *Gene Ontology (GO) analysis and KEGG pathway over-representation. All 1402 significantly regulated genes, detected during the WISP1 array data analysis in Tc28a2 chondrocytes, were continuatively assigned to GO terms and KEGG signalling pathways. Illustrated are, in addition to the corresponding subclass name, the expected count, actual count and overall number of genes (N) associated to the GO/KEGG-term. These values are related to and corrected by the total number of all and differentially expressed corresponding genes present on the chip. The corresponding odds-ratio of corrected values is provided by the fraction (N/actual count). Corresponding p-values are results of the hyper-geometric tests.*

						- on chip -	
Go term	**p-value**	**Odds ratio**	**Exp. count**	**Act. count**	**N**	**Act. count**	**N**
Biological processes							
Chondrocyte development	0.0027	21.02	0	3	5	3	5
Skeletal system morphogenesis	0.0225	1.99	7	13	105	3	24
Embryonic skeletal system morphogenesis	0.0287	2.39	4	8	55	4	37
Ossification	0.0349	1.70	11	17	158	4	46
Osteoblast differentiation	0.0363	2.14	5	9	68	3	20
Cell cycle	0.0030	1.42	61	82	910	35	439
Regulation of cell cycle	0.0386	1.47	21	29	308	5	37
Mitosis	0.0124	1.67	17	27	256	23	178
Mitotic spindle organization	0.0149	5.10	1	4	15	4	12
M phase	0.0148	1.53	25	36	370	1	2
G1 phase of mitotic cell cycle	0.0088	4.68	1	5	20	1	3
G2/M transition of mitotic cell cycle	0.0234	4.31	1	4	17	1	10
MAPKKK cascade	0.0352	1.55	16	24	243	5	29
Regulation of MAPKKK cascade	0.0273	1.88	8	14	119	2	7
Negative regulation of MAPKKK cascade	0.0234	4.31	1	4	17	1	7
Negative regulation of JNK cascade	0.0250	6.00	1	3	10	3	10
Induction of apoptosis	0.0447	1.44	22	30	325	13	157
Apoptotic protease activator activity	0.0244	4.25	1	4	17	1	2
Transforming growth factor beta receptor signalling pathway	0.0454	1.88	6	11	93	7	46
I-kappaB kinase/NF-kappaB cascade	0.0314	1.72	10	17	156	3	25
Mitochondrial e- transport. cytochrome c to oxygen	0.0045	Inf	0	2	2	2	2

...continues on next page

Table 10.7.: *(...continued)*

Go term	p-value	Odds ratio	Exp. count	Act. count	N	- on chip - Act. count	N
Cellular components							
Focal adhesion	0.0039	2.45	6	14	96	14	96
Mitochondrion	0.0009	1.46	67	92	1016	89	984
Mitochondrial membrane	0.0017	1.72	25	41	387	6	37
Mitochondrial outer membrane	0.0015	2.75	6	14	87	14	79
Mitochondrial envelope	0.0014	1.71	27	43	408	0	15
Molecular functions							
Proteoglycan binding	0.0429	4.60	1	3	12	1	2
MAP kinase kinase activity	0.0011	8.65	1	5	13	5	12
Growth factor binding	0.0120	2.11	7	14	106	2	17
Damaged DNA binding	0.0086	3.08	3	8	44	8	44
FAD binding	0.0457	2.04	5	9	70	9	70
KEGG pathway signalling							
Focal adhesion	0.0012	2.09	14	26	196	26	196
MAPK-signalling pathway	0.0174	1.62	19	28	262	28	262
ErbB-signalling pathway	0.0070	2.39	6	13	86	13	86
NOD-like receptor-signalling pathway	0.0292	2.26	4	9	62	9	62

Beside pathways, which can be directly linked to apoptosis or cell survival, some other interesting regulations could be detected within KEGG pathway over-representation. Figure 10.8 reflects all significant (p-value$<$0.1) over-represented pathway regulations directly after WISP1 down-regulation was achieved. Five of these pathways are associated with different cancer types (e.g. leukemia, lung- and prostata cancer) and are also of higher interest in consideration with apoptotic signals during the absence of WISP1. Similarly, the influence of important cellular processes like cell cycle decisions can trigger apoptotic signals and thus leading to cell death. Apart of pathways with regard to the optical phenotype of WISP1 deficient chondrocytes, focal adhesion, the most significantly over-represented pathway in this analysis, is of main interest, since it supports the knowledge of the CCN connection and interaction with the ECM.

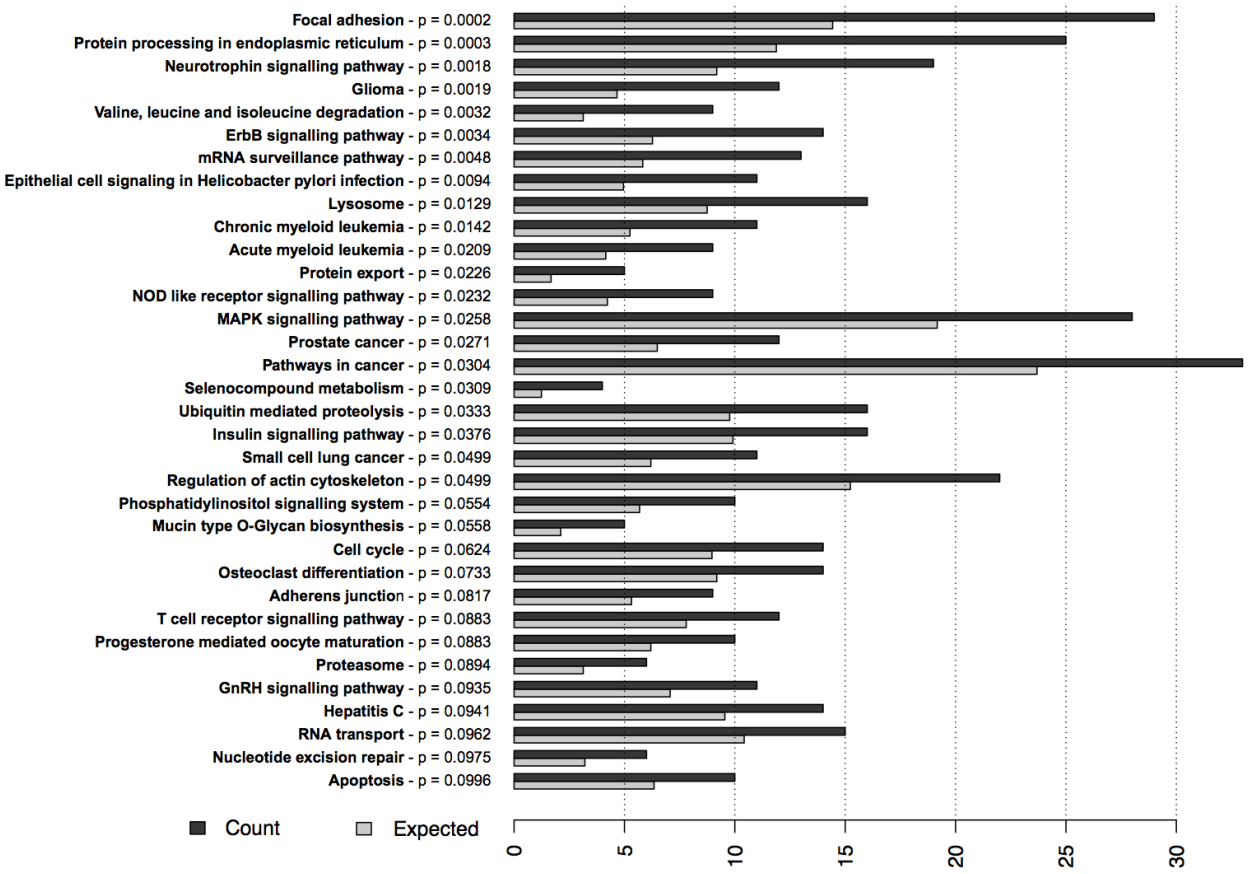

Figure 10.8.: *KEGG pathway over-representation. All 1402 significantly regulated genes were assigned to KEGG-signalling pathways. Illustrated are all pathways, which were over-represented according to their corresponding p-values. Grey bars indicate the expected count of gene regulations for each pathway, whereas black bars demonstrate the actual count. Corresponding p-values are results of the hyper-geometric tests.*

10.2.2. Differential expressed genes during MAPK-signalling cascades

Figure 10.9 comprises all gene regulations within the MAPK-signalling pathway (KEGG ID: 04010). This pathway regulation was detected with significance in several GO subclasses as well as by the KEGG pathway over-representation. The first five columns reflect regulations in the control samples and the following five columns the corresponding gene regulation after the WISP1 down-regulation. It is noticeable that the expression of most genes corresponding to the MAPK-signalling, are decreased directly after the down-regulation of WISP1 is apparent.

In supplement, we were able to visualize interaction patterns of the proteins corresponding to gene regulations on the basis of the KEGG database. Thus, not only overall regulation within a pathway, but also the interaction between the relevant molecules is of main interest. These interaction patterns are available for every pathway with the minimum of two different regulated genes per pathway. Not only the interaction itself between two or more pathway members is visualized, in fact the kind of interaction could be uncovered. Thus, we were able to exhibit e.g. indirect or direct effects, activation or inhibition, expression or repression as well as modifications like phosphorylation/dephosphorylation, methylation/ubiquitination and glycosylation. During the observation of the interaction patterns of all over-represented pathways, it was interesting that several of these pathways displayed no interaction of the corresponding differentially expressed molecules (data not shown). In contrast, the MAPK-signalling path-

way disclosed some interesting interactions between several differentially regulated members (Fig. 10.10). Some interactions could directly affect important cellular processes like proliferation and cell survival. Further, protein interactions that influence other pathways like cell cycle and apoptosis, which were over-represented in our analysis are of main interest and provide a foundation for further analysis.

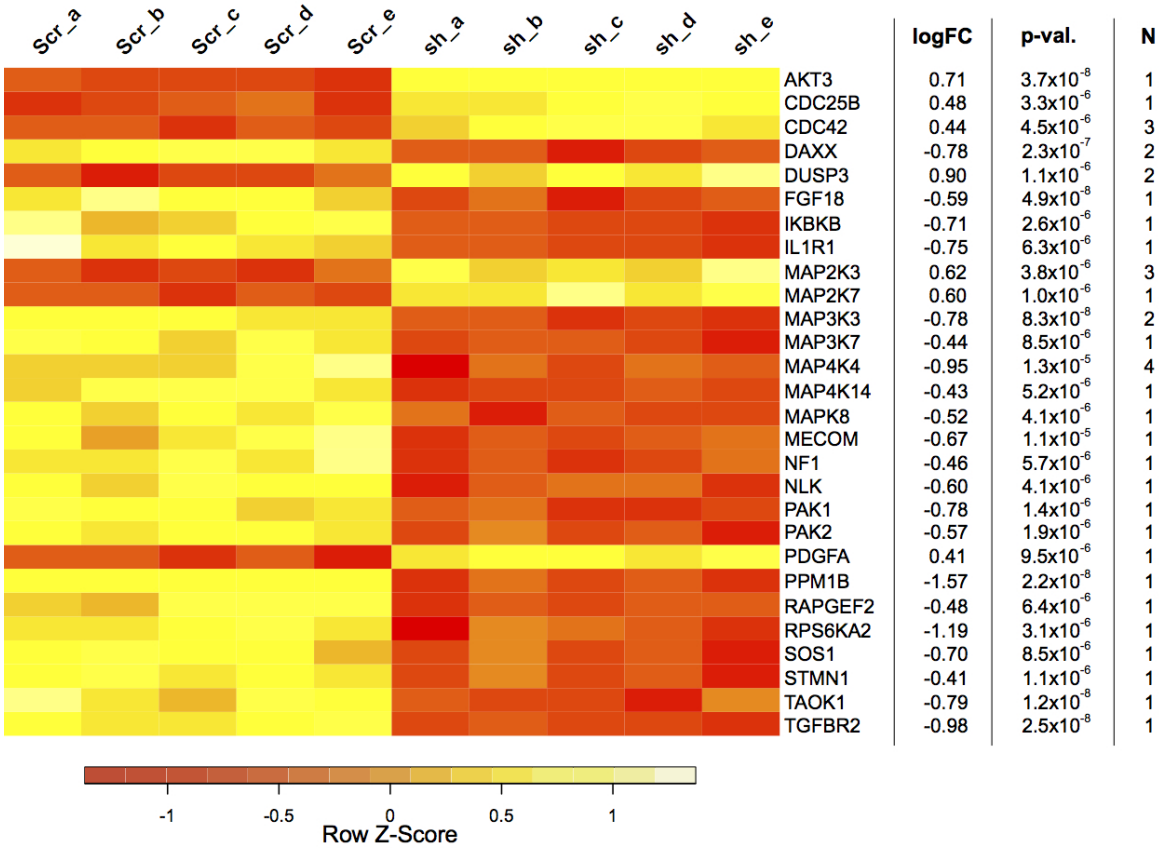

Figure 10.9.: *Heat map of gene regulations within the MAPK-signalling pathway. Levels of gene expression are visualized by colour-coding with white representing high expression, over yellow and orange as medium expression and red representing low expression of the corresponding probe set. Values are normalized by rows (Z-score). Gene names are aligned beside the rows, with additional information regarding degree of regulation (logFC), the corresponding adjusted p-value and the number of regulated probe sets. The highest regulated probe set was chosen for visualization in the case more than one regulated probe set was detected. Sample names are presented over each column. Scr=scrambled control sample, sh=WISP1 down-regulated sample, logFC=logarithmic fold change, p-val.=adjusted p-value.*

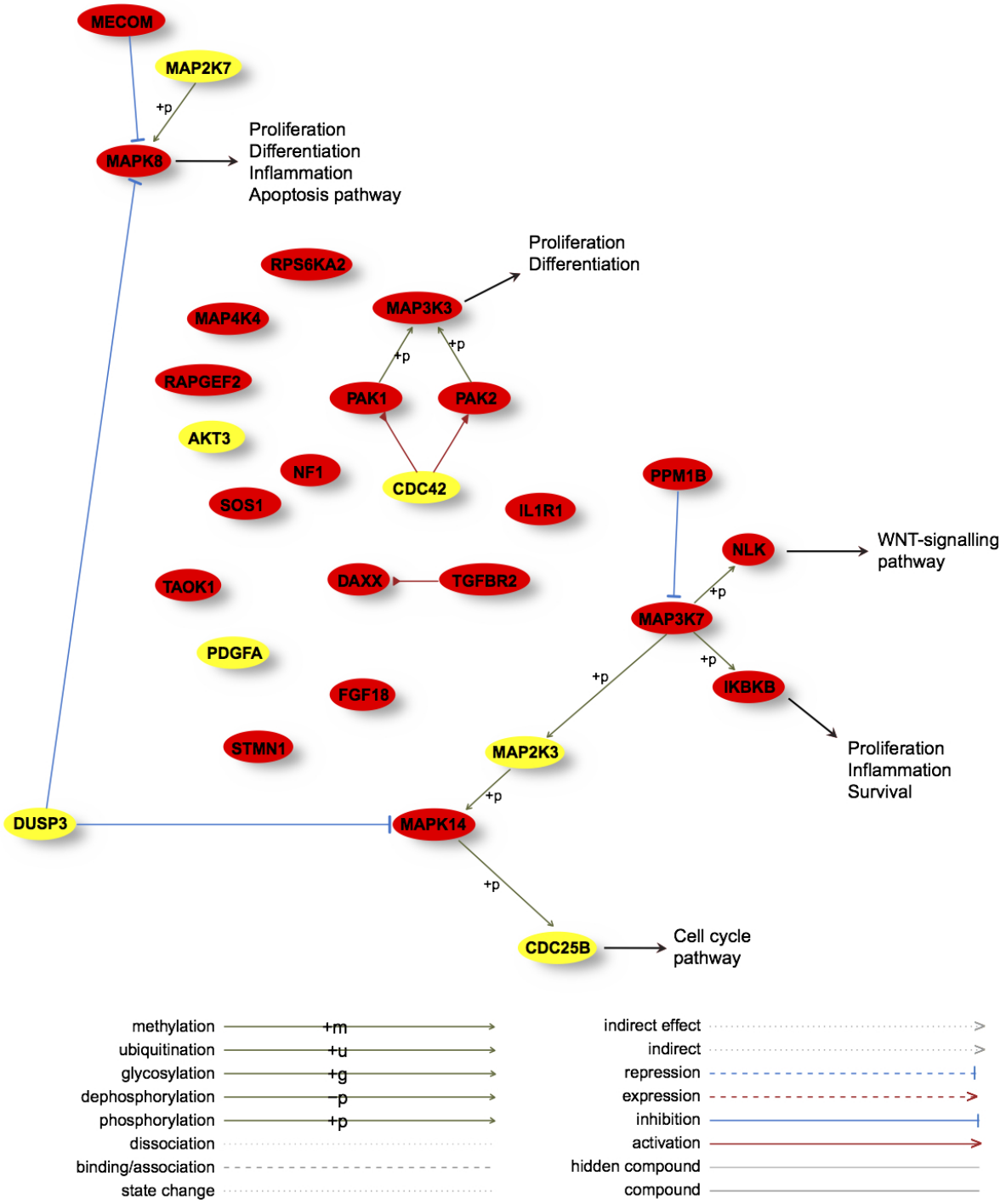

Figure 10.10.: *Interaction patterns within the MAPK-signalling pathway. Gene expressions are visualized by colour-coding with yellow representing up-regulation and red representing down-regulation of the corresponding gene in WISP1 depleted chondrocytes compared to scrambled control assays. Different interactions types are explained in the legend.*

10.2.3. Gene regulations important for cartilage homeostasis

Beside gene regulations, which can be directly linked to apoptosis, investigation of the data sets identified also a cluster of differentially expressed genes important for cartilage homeostasis. This involves mainly gene regulations important for ECM maintenance and replacement as well as regulations that may affect the chondrocyte phenotype. Therefore, all gene regulations were observed without the previous used AFFX cut-off, but with high attention to the logFC and the corresponding adjusted p-value. The heat map below (Fig. 10.11) illustrates this cluster by colour-coding in all chondrocyte samples. The first five columns of this heat map reflect regulations in the control samples and the following five columns the corresponding gene regulation after the WISP1 down-regulation. Affected genes are listed in alphabetical order and genes with regulations of more than one probe set were reduced to the probe set with the highest logFC.

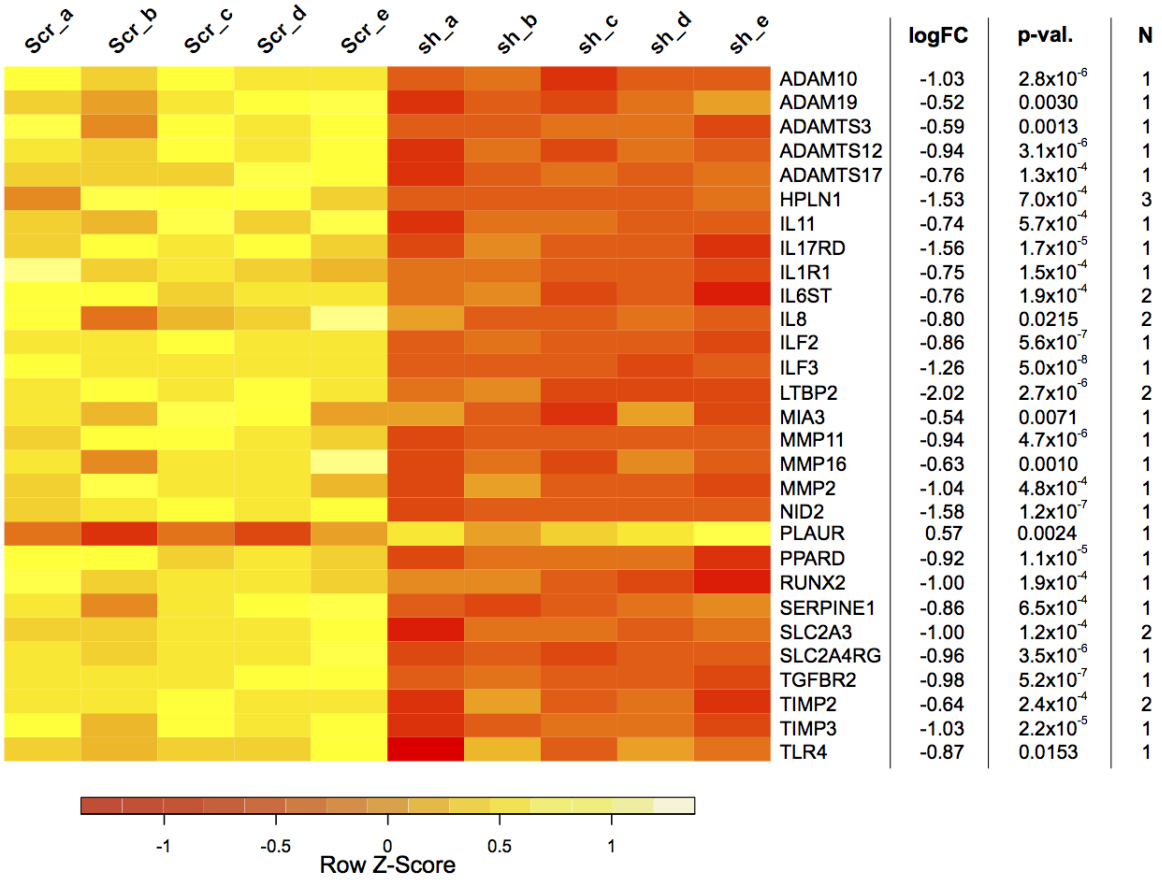

Figure 10.11.: *Heat map of gene regulations important for cartilage homeostasis. Levels of gene expression are visualized by colour-coding with white representing high expression, over yellow and orange as medium expression and red representing low expression of the corresponding probe set. Values are normalized by rows (Z-score). Gene names are aligned beside the rows, with additional information regarding degree of regulation (logFC), the corresponding p-value and the number of regulated probe sets. The highest regulated probe set was chosen for visualization, since more than one regulated probe set was detected. Sample names are presented over each column Scr=scrambled control sample, sh=WISP1 down-regulated sample, logFC=logarithmic fold change, p-val.=adjusted p-value.*

10.2.4. Reevaluation by semi-quantitative RT-PCR

The results of differential gene regulation, obtained during array analysis, were reevaluated by semi-quantitative RT-PCR and confirmed with densitometric analysis of the corresponding gel bands. Amongst all regulated genes, eleven were chosen for reevaluation due to their high fold change (logFC) and functional properties that may be potentially relevant during apoptosis or in consideration to their linkage concerning interactions with the ECM (Tab. 10.8).

Table 10.8.: *Selection of genes for reevaluation. Left to right: Probe set IDs, gene symbols, gene names, degree of regulation (logFC) and p-value. Genes are listed alphabetically according to their descendent statistical score as more than one probe set is regulated.*

Probe set ID	Symbol	Gene name	logFC	adj. p-val.
202766_s_at	FBN1	fibrillin 1	-1.27	3.4×10^{-9}
202765_s_at	FBN1	fibrillin 1	-1.16	1.4×10^{-8}
235318_at	FBN1	fibrillin 1	-1.09	2.6×10^{-6}
216326_s_at	HDAC3	histone deacetylase 3	-1.41	3.4×10^{-9}
218847_at	IGF2BP2	insulin-like growth factor 2 mRNA binding protein 2	-0.99	6.4×10^{-7}
211959_at	IGFBP5	insulin-like growth factor binding protein 5	-1.38	5.3×10^{-7}
212233_at	MAP1B	microtubule-associated protein 1B	-1.41	4.9×10^{-8}
226084_at	MAP1B	microtubule-associated protein 1B	-1.31	3.1×10^{-8}
214577_at	MAP1B	microtubule-associated protein 1B	-0.62	1.1×10^{-6}
229711_s_at	MDM2	Mdm2 p53 binding protein homolog (mouse)	0.74	1.5×10^{-6}
204114_at	NID2	nidogen 2 (osteonidogen)	-1.58	7.7×10^{-9}
228128_x_at	PAPPA	pregnancy-associated plasma protein A, pappalysin 1	-1.34	6.6×10^{-7}
224941_at	PAPPA	pregnancy-associated plasma protein A, pappalysin 1	-1.13	1.6×10^{-6}
224940_s_at	PAPPA	pregnancy-associated plasma protein A, pappalysin 1	-1.03	6.4×10^{-7}
200605_s_at	PRKAR1A	protein kinase, cAMP-dependent, regulatory, type I, alpha	-1.31	9.4×10^{-9}
200603_at	PRKAR1A	protein kinase, cAMP-dependent, regulatory, type I, alpha	-1.08	2.4×10^{-7}
200750_s_at	RAN	RAN, member RAS oncogene family	-1.54	1.3×10^{-8}
200749_at	RAN	RAN, member RAS oncogene family	-1.24	1.4×10^{-8}
201286_at	SDC1	syndecan 1	-2.07	3.9×10^{-9}
201287_s_at	SDC1	syndecan 1	-1.5	4.2×10^{-9}

Reevaluation by RT-PCR was accomplished with the same RNA samples, which were previously used for the microarray analysis. Eleven gene products could be confirmed according to the microarray analysis (Fig. 10.12; Tab. 10.9). MDM2 with logFC of -0.74 is located to detection limit and thus could not statistically confirmed.

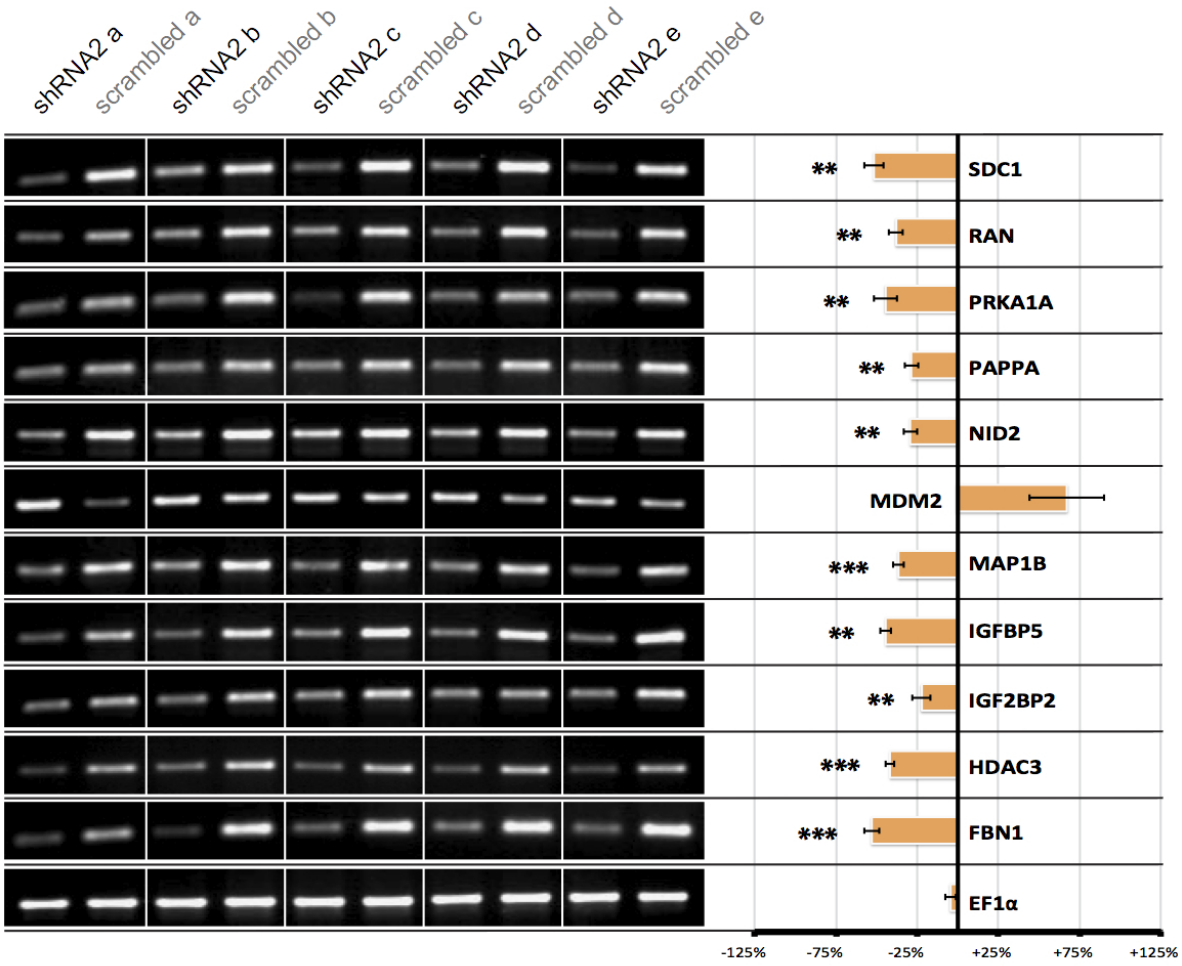

Figure 10.12.: *Reevaluation of selected genes after WISP1 down-regulation in Tc28a2 chondrocytes. In all RNA samples, previously used for microarray hybridization, RT-PCR reactions of selected genes were performed. All inspected genes show an expected regulation according the previously ascertained logFC value. The mRNA levels of the housekeeping gene EF1α were used as internal controls. Densitometric analysis of the corresponding gel bands confirmed the RT-PCR findings. Displayed is the mean of densitometric measures, with the %SEM indicating error bars.*

Table 10.9.: *Results of the t-tests for all relevant comparisons between WISP1 down-regulation by shRNA2 in chondrocytes and the corresponding scrambled control. The t-tests were conducted with paired samples and one-sided. Differences were considered significant when the corrected p-value was <0.05 (∗), <0.01 (∗∗) and <0.001 (∗ ∗ ∗). N_S=Number of samples, df=degrees of freedom, N_C=Number of comparisons corrected for p-adj.*

Data	**Comparisons**	$\mathbf{N}_S$	**t-val.**	**df**	**p-val.**	**sig.**	$\mathbf{N}_C$
EF1α	shRNA2 - scrambled	5	-1.31	4	0.2604	-	1
FBN1	shRNA2 - scrambled	5	-8.86	4	0.0009	***	1
HDAC3	shRNA2 - scrambled	5	-14	4	0.0002	***	1
IGFBP2	shRNA2 - scrambled	5	-4.65	4	0.0096	**	1
IGFBP5	shRNA2 - scrambled	5	-8.38	4	0.0011	**	1
MAP1B	shRNA2 - scrambled	5	-15.22	4	0.0001	***	1
MDM2	shRNA2 - scrambled	5	1.86	4	0.1359	-	1
NID2	shRNA2 - scrambled	5	-7.3	4	0.0019	**	1
PAPPA	shRNA2 - scrambled	5	-6.17	4	0.0035	**	1
PRKA1A	shRNA2 - scrambled	5	-6.04	4	0.0038	**	1
RAN	shRNA2 - scrambled	5	-7.56	4	0.0016	**	1
SDC1	shRNA2 - scrambled	5	-7.53	4	0.0017	**	1

CHAPTER
ELEVEN

RECOMBINANT PROTEIN PRODUCTION

11.1. Proof-reading PCR and cloning procedures of WISP1-T1, -T2 and WISP2

Full-length cDNA plasmid sequences of WISP1-T1, WISP1-T2 and WISP2, diluted 1:10,1:100 and 1:1000 in HPLC water, were amplified with the Pfx50^{TM} DNA Polymerase and subsequently verified by agarose gel electrophoresis. Figure 11.1 (A) reflects the proof-reading PCR outcome of the WISP1-T1 amplification under exposure to UV-light. All three dilutions show a considerable band of the expected size of 1103bp. The purest PCR product, the 1:1000 dilution in the case of WISP1-T1, was used for the TOPO®cloning amplification. Six putative WISP1-T1 TOPO®clones were selected and plasmid DNA was restricted with specific endonucleases to separate insert and vector DNA. Subsequently, gel electrophoresis (B) exhibit plasmid DNA of five clones (1,2,3,5 and 6,) with the expected WISP1-T1 insert size of 1103bp and plasmid DNA of one clone (4), which contained only unrestricted vector DNA. Insert DNA was verified with sequencing analysis (data not shown) and only confirmed sequences were utilized for cloning into the SF-21 expression vector pBacPAk8. Subsequent to the cloning and purification procedures, restriction of vector DNA and gel electrophoresis visualized the restricted vector and insert DNA. Referring to sequencing analysis of the insert DNA (data not shown), the Fc-tag was cloned N-terminal to the WISP1-T1 sequence into the bBacPAK8 vector. The left region of figure 11.1 (C) illustrates the plasmid DNA bands of six different pBacPAK8 vector containing clones (1a-6a). Plasmid DNA of four clones (1a, 3a, 4a and 5a) exhibit insert DNA of the expected size of WISP1-T1 (1103bp) and the pBacPAk8 vector (5500bp). The right region of figure 11.1 (C) reflects the identical six clones and similar to the previously described findings, the same four clones (1b, 3b, 4b and 5b) contained also the Fc-tag DNA with the expected size of 740bp. Subsequently, the Fc-tag insert DNA was verified with sequencing analysis as well, the expression vector was ready to use for the infection of the SF-21 cell line. Proof-reading PCR and cloning procedures of WISP1-T2 and WISP2 were performed analogous to WISP1-T1 (data not shown) and both were not used until appropriate base pare progression via sequencing analysis could be confirmed (data not shown).

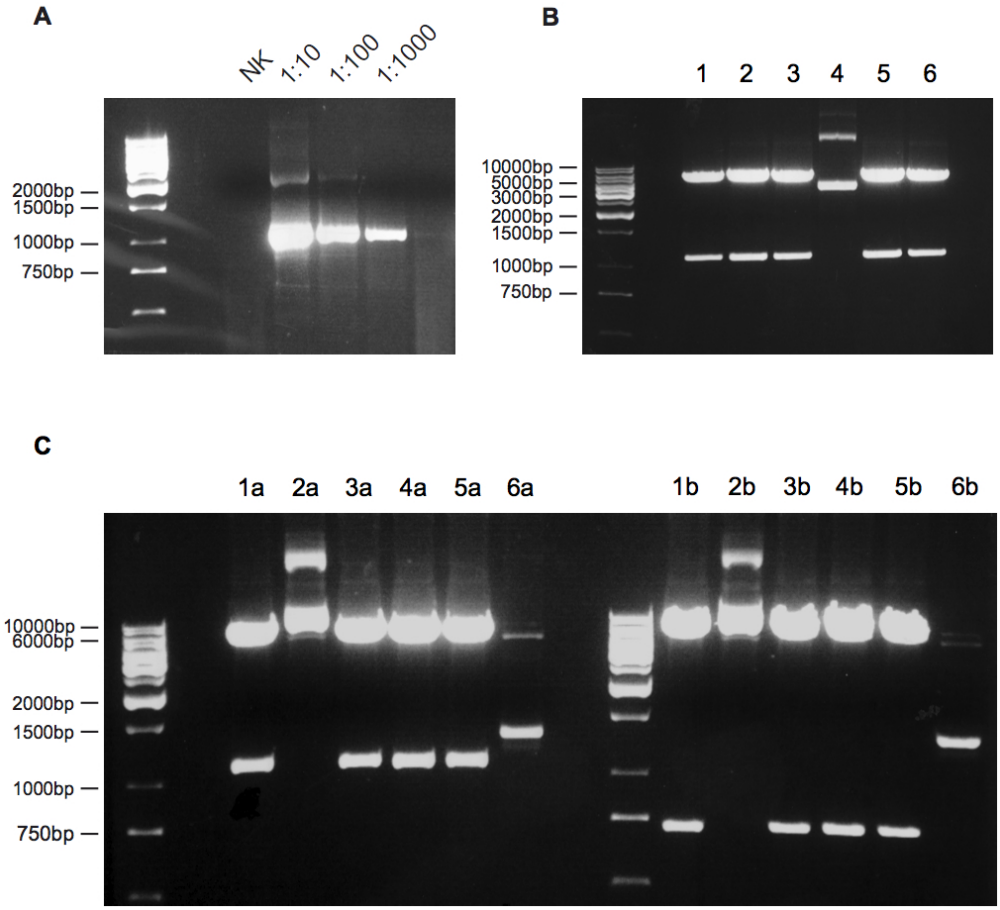

Figure 11.1.: *Proof-reading PCR and cloning procedures of WISP1-T1. (A) Proof reading PCR: three different concentrations of WISP1-T1 full-length cDNA sequence were amplified and visualized via gel electrophoresis. (B) TOPO® cloning: plasmid DNA of five clones (1,2,3,5 and 6,) show the expected WISP1-T1 insert size of 1103bp and plasmid DNA of one clone (4) contained only unrestricted vector DNA. (C) pBacPAK8 vector cloning: four clones (1a, 3a, 4a and 5a) exhibit insert DNA of the expected size of WISP1-T1 (1103bp) and the pBacPAk8 vector (5500bp). Additional, identical clones (1b, 3b, 4b and 5b) contained the Fc-tag DNA with the expected size of 740bp.*

11.2. Recombinant WISP1-T1, -T2 and WISP2 expression

The transfer vector pBacPAK8, containing the inserts of WISP1-T1/Fc-tag, WISP1/T2-Fc-tag or WISP2/Fc-tag, and an additional expression vector were co-transfected into SF-21 cells. Figure 11.2 shows the western blot findings, performed with a primary antibody against the Fc-tag. The upper region (A) reflects the different virus amplification steps, exemplarily for WISP1-T1. The virus amplification comprised p0 (six days after transfection), p1 based on p0 concentrations of 1:10, 1:100, 1:000 (seven days after retransfection) and p2 based on p1 concentrations of 1:25, 1:62.5 and 1:500 (seven days after reretransfection).

Autoradiography visualized two different protein bands per lane with the primary antibody against the Fc-tag. Only the lower one corresponds to the expected size of 67kd for WISP-T1/Fc-Tag. It was not possible to detect rWISP1-T1 in the p0 virus stock. The p1 virus stocks, in contrast, reflected a slight increase in the amount of secreted rWISP1-T1 protein and the p2 virus stock confirmed the virus amplification with an increase of rWISP1-T1. After virus amplification, three $150cm^2$ cell culture flasks were infected with 200μl p2 virus stock.

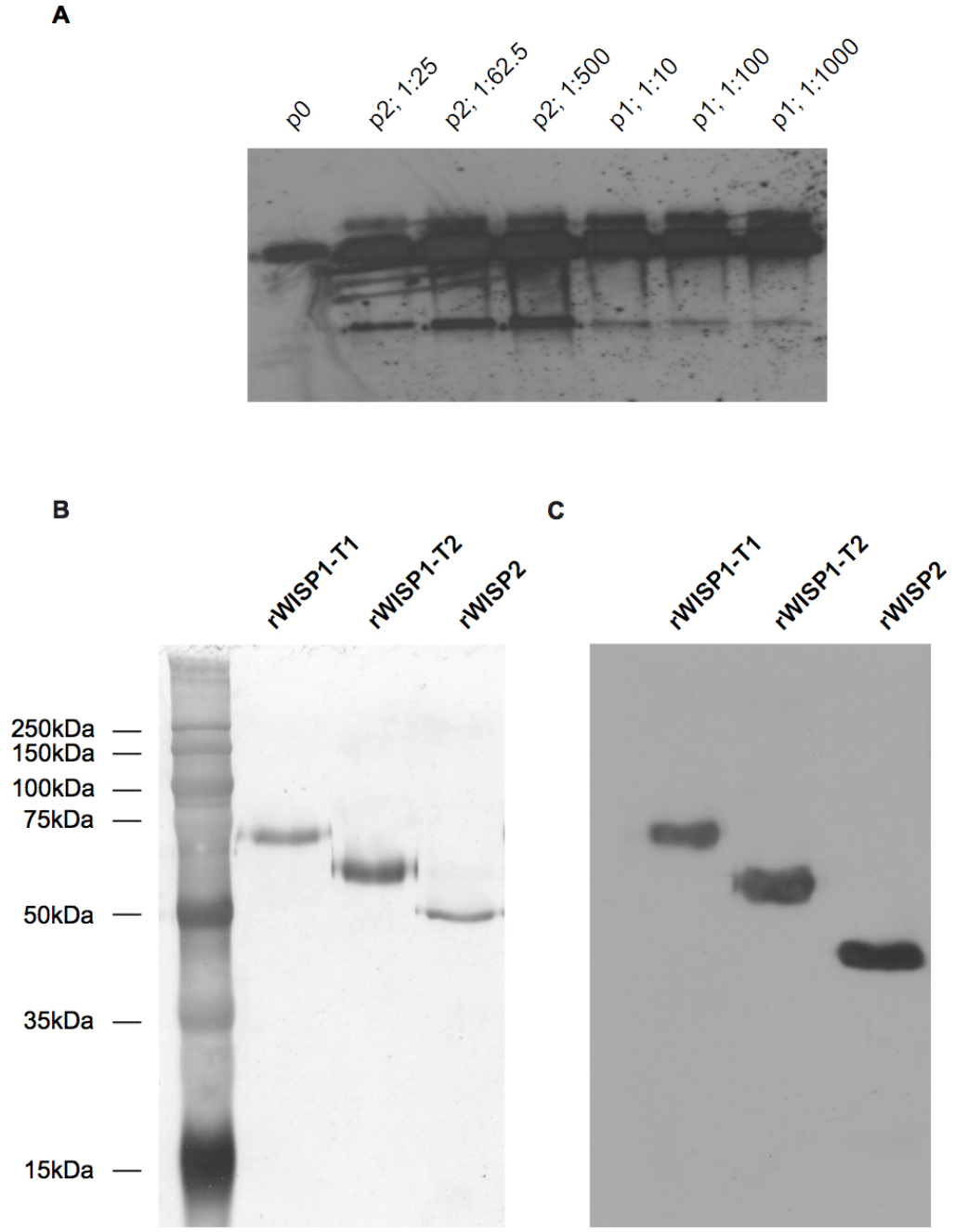

Figure 11.2.: *Western blotting and silver staining of rWISP1-T1, -T2 and rWISP2. (A) Western blot picture of virus amplification p0 (six days after transfection), p1 based on p0 concentrations of 1:10, 1:100, 1:000 (seven days after retransfection) and p2 based on p1 concentrations of 1:25, 1:62.5 and 1:500 (seven days after re-retransfection). The lower detected protein band corresponds with the expected size of 67kd for WISP-T1/Fc-Tag. (B) silver staining after expression and purification of rWISP1-T1, -T2 and rWISP2. Single protein bands of the expected size of 67kDa (rWISP1-T1), 57kDa (rWISP1-T2) and 53kDa (WISP2) were detectable. (C) Confirming of the same proteins with western blotting revealed protein bands in identical size and purity.*

Approximately seven days after transfection, cell supernatant yielded between 100 and 400μg of the respective (r)protein. Subsequently, 250μg of each protein was loaded onto a SDS page and proximate silver staining procedures (B) and western blotting analysis (C) revealed single protein bands of expected size and purity. rWISP1-T1 (67kDa), the largest of the three proteins, was detectable in the first lane of the blotting membrane. The 10kDa smaller second transcript variant was exhibit with a size of 57kDa in the second lane of both illustrations (B and C) and WISP2 (53kDa) in the third lane.

11.3. Functional testing of rWISP1-T1, -T2 and WISP2

The effectiveness of rWISP1-T1, -T2 and rWISP2 proteins was verified by treatment of Tc28a2 cells. With this experiment, it was possible to confirm a self-regulation of all three produced rWISP proteins in this chondrocyte cell line. To improve the function of rWISP1-T1 and -T2, the endogenous amount of both proteins were down-regulated. Three days after the transduction procedure was performed, 500ng rWISP1-T1 (pH: 7.0) was added into serum less medium (0%FCS) of the shRNA2 transduced Tc28a2 cells for 24h. Simultaneous, a second shRNA2 assay was treated with 500ng rWISP1-T2 (pH: 7.0). A scrambled control was used to compare the WISP1-T1 and -T2 mRNA levels with those of the knock-down experiments. Additionally, GFP was used first, as a positive control for measuring transfection and transduction efficiency and second, for comparison of the different WISP1-T1 and -T2 mRNA levels. Figure 11.3 illustrates an example of the RT-PCR analyses of the isolated mRNA from the fourth day after transduction. The mRNA level of both WISP1 transcript variants were remarkably down-regulated compared with the scrambled and GFP controls. In contrast, shRNA2-transduced cells, treated with 500ng rWISP1-T1, show an intensive increase of its own mRNA level during the knock-down experiments. The same findings could be observed by the application of the second recombinant transcript variant. 24h after treatment with 500ng rWISP1-T2, down-regulation induced by shRNA2 was compensated by an intensive increase in its own mRNA production. Total mRNA of seven independent experiments was isolated on day four after transduction and is illustrated by the densitometric analysis in table 11.1.

No expression of WISP2 was observable in 90-100% confluent Tc28a2 cells under normal cell culture conditions (Fig. 8.1, C). Therefore, the effectiveness of rWISP2 could be verified by application of the recombinant protein under standard cultivation procedures. Prior to the protein treatment cells were cultivated with serum less medium (0%FCS) for 24h and subsequently treated with 500ng rWISP2 for additional 24h. After isolation of total RNA, RT-PCR analyses revealed an intensive increase in the endogenous amount of the mRNA level of WISP2. These findings were confirmed by replicates (n=5) and the respective densitometric analysis (Fig. 11.4; Tab. 11.2).

11.4. rWISP1-T1 and -T2 treatment of Tc28a2 chondrocytes after WISP1 gene-silencing

Effects of the rWISP1-T1 and -T2 proteins were determined by application of these proteins to Tc28a2 chondrocytes after WISP1 gene-silencing. Previously, both recombinant transcript variants were verified of expected size and purity using western blot analysis and silver staining procedures (Fig. 11.2). According to the transduction, 500ng rWISP1-T1 (pH: 7.0) was added into 3ml medium of the shRNA2 transduced Tc28a2 cells. Simultaneous, one shRNA2 assay contained 500ng rWISP1-T2 (pH: 7.0) and a third shRNA2 transduced assay comprised 500ng of each recombinant produced transcript variants. The applications of (r)proteins were con-

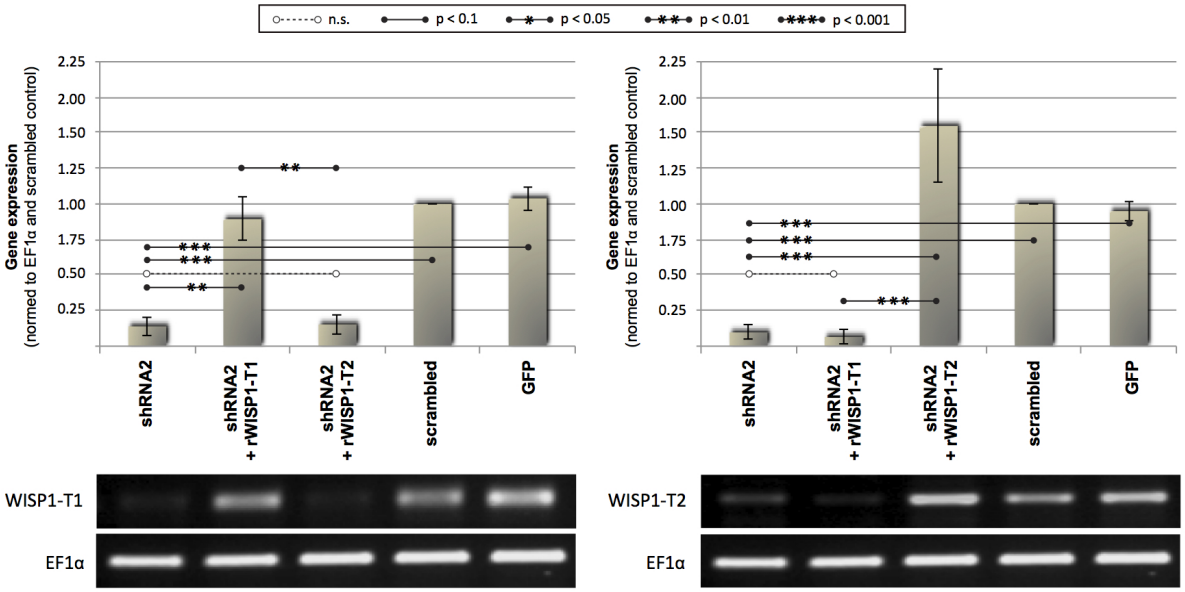

Figure 11.3.: *RT-PCR analysis of functional rWISP1-T1 and -T2 testing. Tc28a2 chondrocytes show remarkable self-regulation after treatment with rWISP1-T1 or -T2 during the WISP1 knock-down experiments. Densitometric analysis and t-test statistics confirmed these findings. Displayed is the mean of densitometric measures, with the %SEM indicating error bars.*

Table 11.1.: *Results of the t-tests for all relevant comparisons between WISP1 down-regulation by shRNA2 in chondrocytes, including samples treated with (r)proteins, and the corresponding control samples. The t-tests were conducted with paired samples and two sided. A p-value correction by fdr has been applied according to the number of comparisons. Differences were considered significant when the corrected p-value was <0.05 (∗), <0.01 (∗∗) and <0.001 (∗∗∗). N_S=Number of samples, df=degrees of freedom, p-adj.=corrected p-values, N_C=Number of comparisons corrected for p-adj.*

Data	Comparisons	N_S	t-val.	df	p-val.	p-adj.	sig.	N_C
WISP1-T1	shRNA2 - shRNA2T1	7	-8.12	5	0.0002	0.0011	∗∗	5
WISP1-T1	shRNA2 - shRNA2T2	7	-1.45	5	0.1038	0.5188	-	5
WISP1-T1	shRNA2 - scrambled	7	-7.52	6	0.0001	0.0007	∗∗∗	5
WISP1-T1	shRNA2 - GFP	7	-15.18	6	$2.6\text{x}10^{-6}$	$1.3\text{x}10^{-5}$	∗∗∗	5
WISP1-T1	shRNA2T2 - shRNA2T1	7	-6.46	5	0.0013	0.0066	∗∗	5
WISP1-T2	shRNA2 - shRNA2T1	7	-0.42	5	0.3453	1.0000	-	5
WISP1-T2	shRNA2 - shRNA2T2	7	-11.85	5	$3.8\text{x}10^{-5}$	0.0001	∗∗∗	5
WISP1-T2	shRNA2 - scrambled	7	-7.95	6	0.0001	0.0005	∗∗∗	5
WISP1-T2	shRNA2 - GFP	7	-10.02	6	$2.8\text{x}10^{-5}$	0.0001	∗∗∗	5
WISP1-T2	shRNA2T2 - shRNA2T1	7	11.30	5	$9.5\text{x}10^{-5}$	0.0001	∗∗∗	5

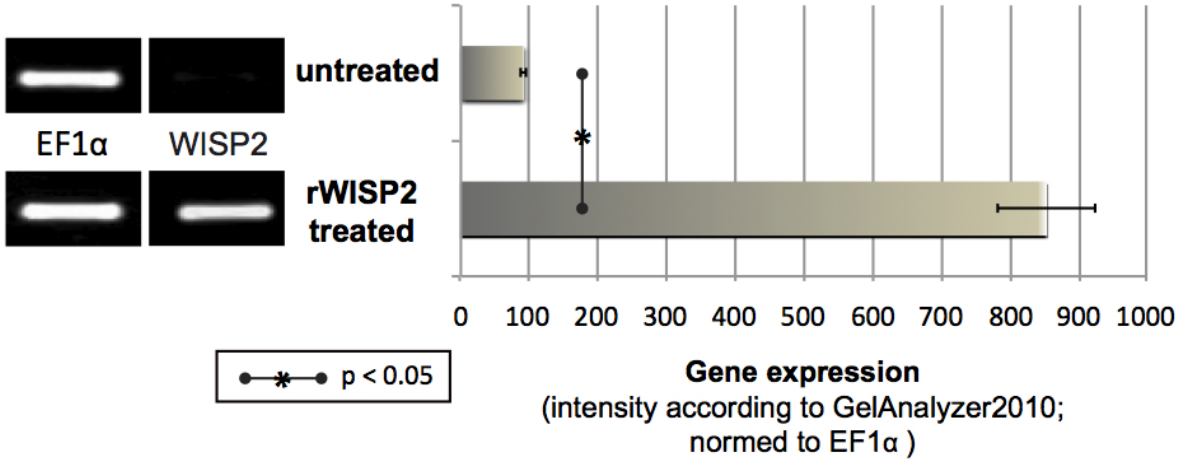

Figure 11.4.: *Densitometric analysis of functional rWISP2 testing. Tc28a2 chondrocytes show remarkable self-regulation after treatment with rWISP2. Densitometric analysis and t-test statistics confirmed these findings (p-value <0.05 (∗)). Displayed is the mean of densitometric measures, with the %SEM indicating error bars.*

Table 11.2.: *: Results of the t-test for the comparison between WISP2 treated and untreated (control) chondrocytes. The t-test was conducted with paired samples and one-sided. Differences were considered significant when the p-value was <0.05 (∗), <0.01 (∗∗) and <0.001 (∗∗∗). N_S=Number of samples, df=degrees of freedom, N_C=Number of comparisons corrected for p-adj.*

Data	Comparisons	N_S	t-val.	df	p-val.	sig.	N_C
WISP2	treated - untreated	5	3.74	4	0.0101	∗	1

tinued every two days with the addition of fresh medium to the cells. Supplemental controls were estimated at the same time. The first control was a pure shRNA2 transduced assay to compare optical differences between recombinant treated and untreated WISP1 knock-down cells. A scrambled control served as a negative control for effects of the lentivirus system and a GFP control was needed for validation of the transduction efficiency. Figure 11.5 illustrates the described assays following day 5 to day 8 after transduction of the cells. These four days were selected, because optical differences between shRNA2 transduced Tc28a2 cells and the scrambled control assays were clearly observable during the initiated time series. There were no optical differences detectable between pure shRNA2 transduced cells (A1-D1) and those who contained additional rWISP1-T1 (A2-D2), rWISP1-T2 (A3-D3) or both recombinant produced transcript variants (A4-B4) on each monitored day. The scrambled control shows normal proliferation during these four days (A5-D5) and the GFP control revealed an expected transduction efficiency under exposure to UV-light (A6-D6).

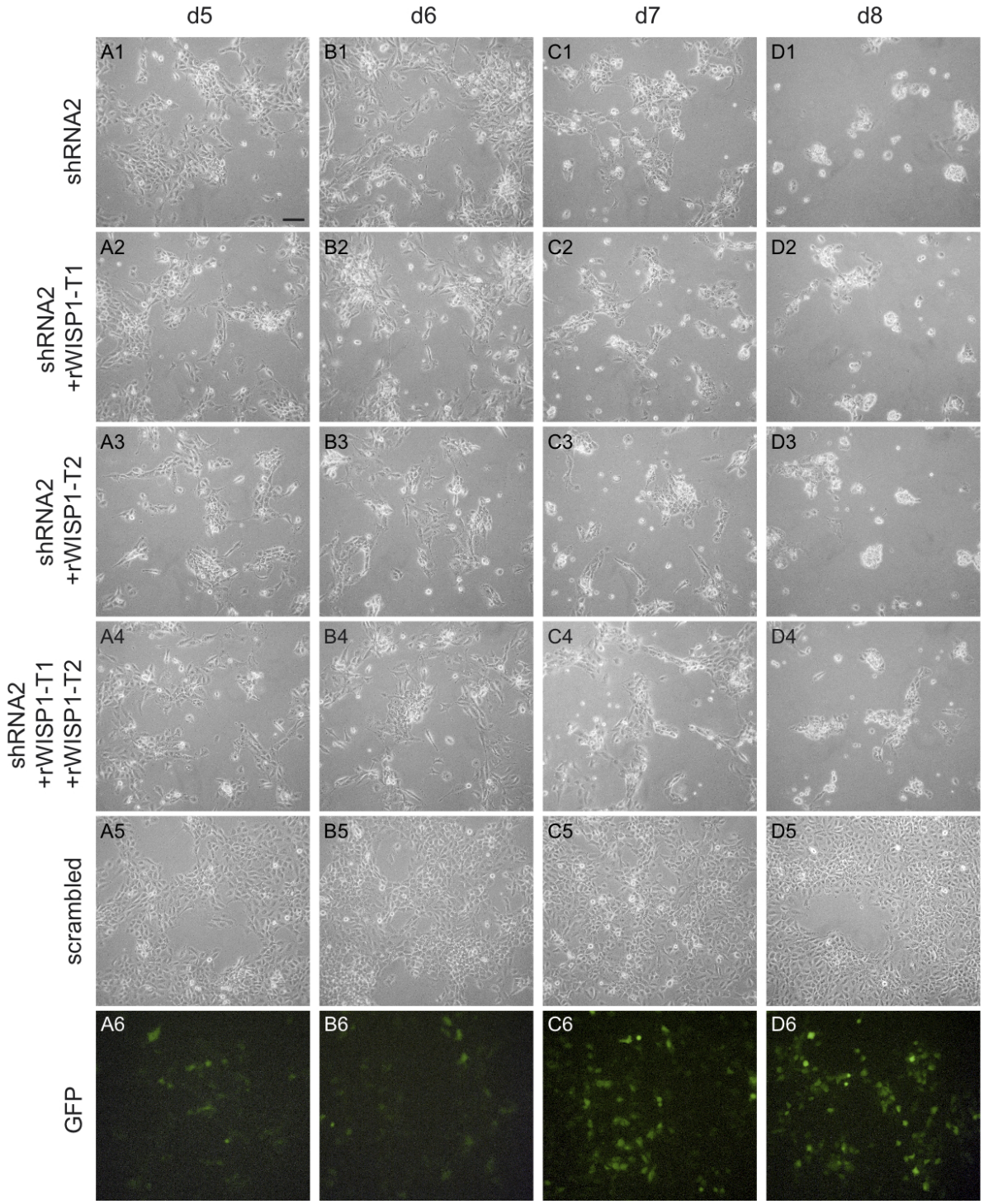

Figure 11.5.: *Treatment with rWISP1-T1 and -T2 of WISP1 down-regulated chondrocytes. Column 1-4 illustrates cell death of WISP1 within one week after the transduction was performed. Protein treatment with rWISP1-T1 (A2-D2), rWISP1-T2 (A3-D3) and both recombinant proteins (A4-D4) show no effect concerning cell survival or decelerated cell death. Control samples (scrambled and GFP) display expected proliferation and successful transduction of the chondrocyte cell line Tc28a2. Scale bar=*$100\mu m$.

CHAPTER

TWELVE

CONTINUATIVE EXPERIMENTS

12.1. Apoptosis detection with FLICA (fluorochrome inhibitor of caspase) in Tc28a2 chondrocytes

The FLICA assay was established to distinguish between apoptotic and healthy cells within the same cell population. Tc28a2 chondrocytes were seeded onto cover slips and subsequently treated with 100μM zolendronate for 72h. The apoptosis induction via zolendronate was confirmed by immuno-cytochemical staining procedures with sulforhodamine labelled FLICA. Figure 12.1 illustrates the different fluorescence marker under exposure to UV-light. Hoechst3334 stained all present nuclei with bright blue fluorescence (A and D), while the sulforhodamine FLICA stain, detected a broad range of active caspases. Zolendronate treated (apoptotic cells) exhibited a higher amount of active caspases (B) compared to untreated control cells (E). Both fluorescence stainings could be merged to quantify cells of respective active caspases (C and F).

12.2. Cytochrome c staining in hMSCs

When internal pro-apoptotic stimuli induce breakdown of the mitochondria, cytochrome c is released into the cytosol where it leads to activation of caspases and thus triggers apoptosis. Therefore, cytochrome c staining will be used to detect internal apoptosis stimuli via cytochrome c release. Bone marrow derived hMSCs were seeded on cover slips until they reached 50-60% confluence. Figure 12.2 shows the subsequent immune-cytochemical staining of hMSCs with a primary, fluorescence labelled antibody against cytochrome c (A-D) and the respective negative control (E-H). Nuclei of all cells were counterstained with DAPI (A and E) for displaying the whole cell population under exposure to UV-light. Because cytochrome c is located in the outer membrane of the mitochondria in viable, healthy cells, a second counterstain with MitoTracker® Red was performed to visualize the mitochondria of each cell (B and F). A FITC labelled secondary antibody against the primary cytochrome c detecting antibody, stained the respective protein with bright green fluorescence (C). An overlay of all stainings confirmed the cytochrome c location in the mitochondria of the cells (D). A negative control passed both counterstains and the incubation with the FITC labelled secondary antibody. No staining was observable in the absence of the primary antibody against cytochrome c (G and H).

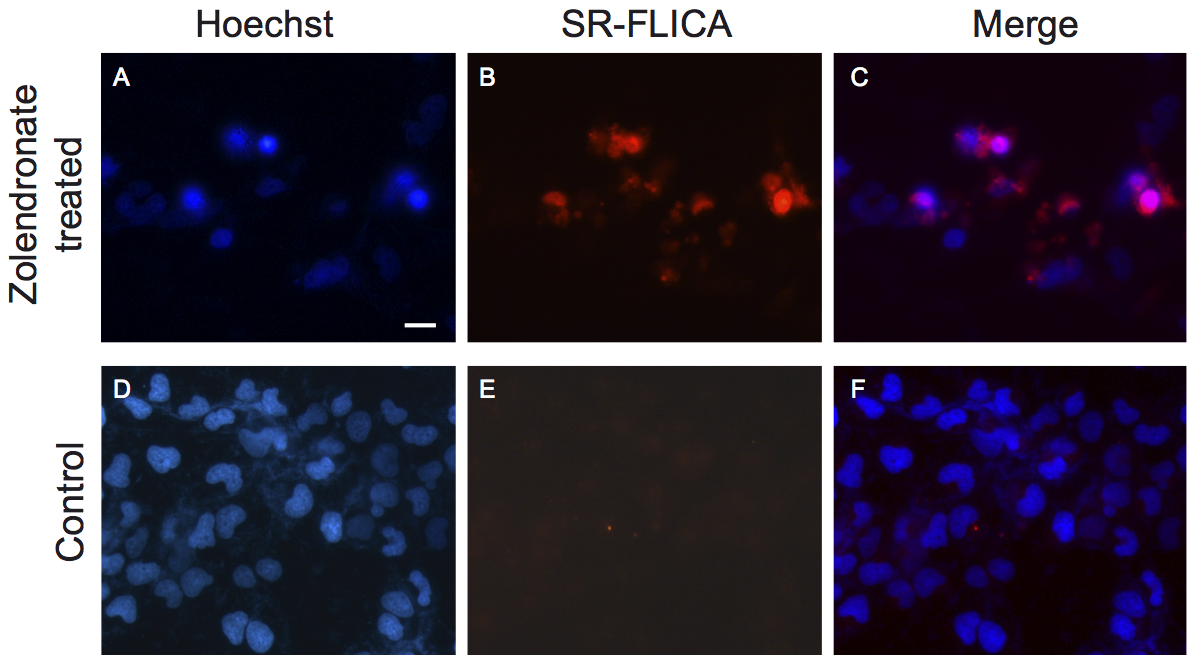

Figure 12.1.: *Detection of apoptotic Tc28a2 chondrocytes with FLICA. Fluorescence microscopy uncovered active caspases in zolendronate treated chondrocytes compared to non-zolendronate treated control cells. (A) Labelling of zolendronate treated cells with nucleus counterstain Hoechst, (B) staining with FLICA (sulforhodamine-VAD-FMK poly caspase inhibitor) reagent and the corresponding non zolendronate treated control saples (D, E). An overlay of both stainings is illustrated in (C) for zondronate treated and in (F) for untreated control cells. Scale bar=*$20\mu m$.

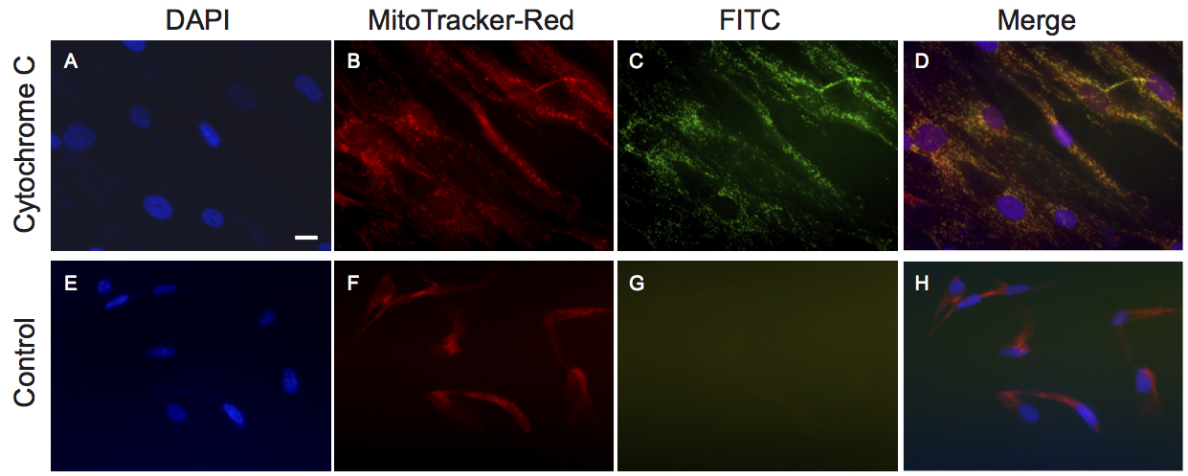

Figure 12.2.: *Cytochrome c immuno-staining of hMSCs. Cells were labelled with the nuclei counterstain DAPI (A, E), the mitochondria marker MitoTracker® Red (B, F) and antibodies against cytochrome c. The negative control (E-H) contained all described components, except the primary antibody against cytochrome c. Scale bar=*$20\mu m$.

12.3. P53 staining in hMSCs

The location of the tumour suppressor p53 in apoptotic hMSCs and chondrocytes will be visualized to verify one possible mechanism of apoptosis induction. Previously, hMSCs were seeded onto cover slips until they reached 50-60% confluence. Subsequent immuno-cytochemical staining with a primary antibody against p53 is illustrated in figure 12.3. DAPI was used as a counterstain to identify all nuclei of determined cells (A). A FITC labelled, secondary antibody visualized the tumour protein p53 within the cytoplasm of the cells (B and C), while the negative control remained widely unstained (E and F).

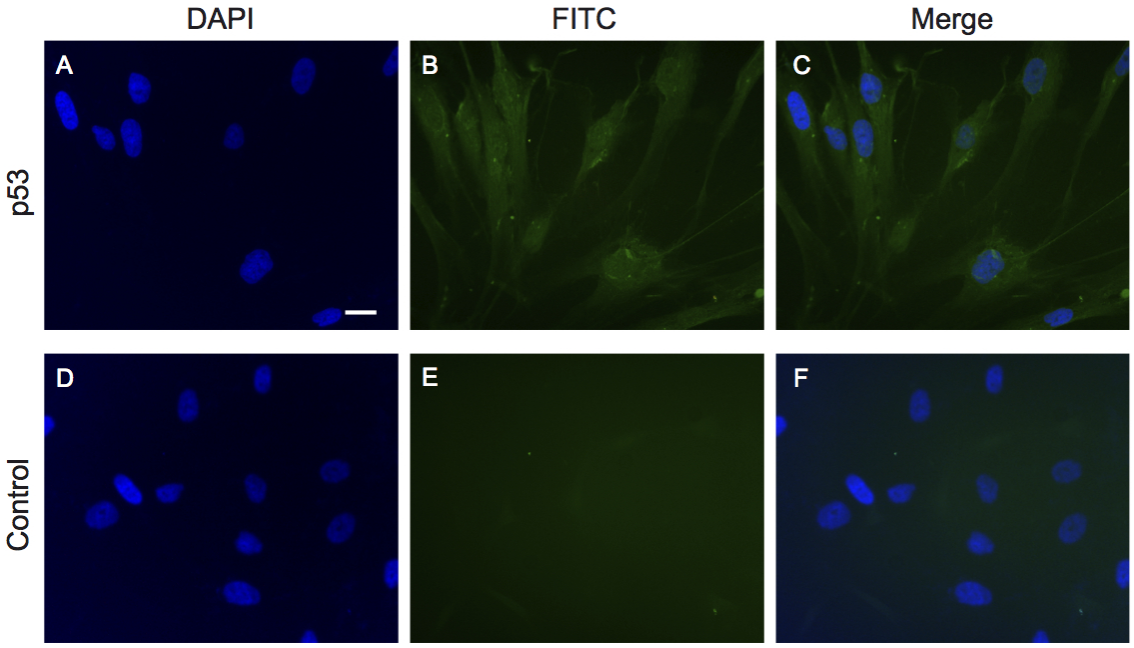

Figure 12.3.: *p53 immuno-staining in hMSCs. Cells were labelled with the nuclei counterstain DAPI (A, D). A FITC labelled, secondary antibody visualized the tumour protein p53 in the cytoplasm (B), while the negative control remained widely unstained (E). Scale bar=*$20\mu m$.

Part IV.

Discussion

CHAPTER
THIRTEEN

NATIVE EXPRESSION OF WISP1 AND WISP2 IN MUSCULOSKELETAL CELLS

Within the last decades, CCN protein family members have been identified as important ECM-associated, multifunctional regulators with significance in skeletal development and fracture repair (Hadjiargyrou et al. 2000; Nakata et al. 2002; O'Brien and Lau 1992). Previous studies of our working group already confirmed the differential expression of CYR61/CCN1, CTGF/CCN2, WISP2/CCN5 and WISP3/CCN6 during the differentiation of hMSCs in osteoblasts, chondrocytes or adipocytes (Schuetze et al. 2005), therefore indicating a prominent role during lineage progression. This investigation was supported by findings of French et al. (2004), who demonstrated the role of WISP1 as an osteogenic potentiating factor, which additionally represses the chondrocytic differentiation of MSCs. Apart from functional investigations of WISP1 within the musculoskeletal system, independent working groups depicted this protein as an important cellular survival factor. Thereby, it promotes cell growth and tumourigenesis (Su et al. 2002; Venkatesan et al. 2010). Considering the aforementioned examinations, several hypotheses were designed, established and investigated during this PhD thesis to provide a detailed view on WISP1-signalling in cells connected to the musculoskeletal system and its influence on cell survival and apoptosis.

The first hypothesis comprised the presumption that a natural expression of WISP1 (both transcript variants) and WISP2 exists in a variety of musculoskeletal cell types, i.e. primary hMSCs, osteoblasts and chondrocytes. The initial experiments confirmed the native expression of WISP1 in primary hMSCs as well as in different chondrocyte, osteosarcoma and osteoblast cell lines. Beside the expression of full-length WISP1 (-T1), we were able to detect the expression of a WISP1 isoform (-T2), which lacks the VWC domain, in all corresponding cell types as well. This isoform was first described by Yanagita et al. (2007) as naturally expressed in primary rabbit growth cartilage chondrocytes.

In contrast, the expression of WISP2 could not be confirmed. None of the examined cell lines displayed a continiously native expression of this protein. Accordingly, the expression of WISP2 in primary hMSCs seemed to be donor dependent and ranged from no expression, over little to an adequate expression. Neither age of donors nor their genders seem to be correlated with WISP2 expression. Due to privacy protection of donors, little is known about live and behaviour of the stem cell donors. Thus, it is difficult to explain a differential protein expression between donors, because it is not possible to exclude relevant medication or diseases, which may effect protein expression in such a case.

Subsequent to a successful validation of the natural expression of WISP1 in different cell types of the musculoskeletal system, the next approach included experiments to examine how cells can be affected by corresponding gene-silencing.

CHAPTER
FOURTEEN

WISP1 GENE-SILENCING

14.1. WISP1 gene-silencing leads to cell death in a variety of musculoskeletal cells

For the subsequent designed microarray comparisons of WISP1 down-regulated and control cells, it is important to apply specific shRNA constructs to engage target mRNAs of both detected transcript variants. Due to the fact that all CCN family members share several conserved sequence homologies, targeting a specific member by shRNA hairpins, like WISP1, is a difficult task. Therefore, experiments were confirmed with a second shRNA construct to exclude the observations of so called "off-target effects". These effects will occur if an assumed specific shRNA hairpin directly alters other genes. Appropriate shRNA constructs were selected due to their ability to target different domains existing in WISP1-T1 and -T2 (shRNA2 - TSP domain; shRNA5 - CT domain). A successful down-regulated expression of WISP1-T1 and -T2 was achieved in the chondrocyte cell line Tc28a2. Conspicuously, immediately after successful transduction, WISP1 depleted chondrocytes displayed optical differences in comparison to their control samples with the consequence of cell death. The application of shRNA5 onto the target cells induced a reduction of WISP1-T1, which was however not as intensive as the effect observed with shRNA2. This was confirmed by RT-PCR and the incidental difference in cell characteristics was comparably less acute, correspondingly. Off target effects can be excluded as both utilized shRNA constructs resulted in a down-regulation of WISP1-T1 and -T2 expression with subsequent cell floating. Although WISP1 shares 32% amino acid sequence identity with WISP3, additional RT-PCR analysis verified an unaffected expression of WISP3 in all samples compared to untreated cells (data not shown). Based on these methodically considerations, results of the gene-silencing studies are reliable and support the hypothesis of WISP1 as an essential survival factor for chondrocytes.

Further experiments, all performed with both effective shRNA constructs (shRNA2 and -5) and control constructs (scrambled, GFP and pure vector) were accomplished to investigate optical alterations after loss of WISP1 in several selected cell lines. To cover many areas of the musculoskeletal system, a second human chondrocyte cell line (C28I2), one human osteoblast cell line (hFOB) and two immortalized hMSC cell lines (hMSC-TERT4 and hMSC-TERT20) were chosen. Surprisingly, WISP1 seems to act as a general survival factor within the musculoskeletal system, due to the fact that every cell line in our investigation wasn't able to survive after down-regulation of WISP1. Both appropriated shRNA constructs revealed an effective down-regulation of both transcript variants of WISP1, confirmed by subsequent RT-PCR analyses. Similarly to the findings of the WISP1 down-regulation in Tc28a2 chondrocytes, little difference in the effectiveness of both shRNA constructs could be observed. The examined

osteoblast and chondrocyte cell lines displayed delayed optical difference in shRNA5 transduced samples compared to those transduced with shRNA2. In contrast, hMSC-Tert4 and hMSC-Tert20 cells deceases slightly faster after the transduction with the shRNA5 construct compared to the other one. An allocation between a specific shRNA construct and their effectiveness in WISP1 down-regulation could be observed through RT-PCR analyses. Except the chondrocyte cell line C28a2, all remaining cell lines seem to display stronger effects on cell survival by that shRNA construct, which exhibit a slightly increased down-regulation of WISP1-T1. This leads to the suggestion that the full-length variant of WISP1 could be more important for cell survival in majority of the selected cell lines.

In primary cells, both shRNA constructs were effective as well and similar to the immortalized hMSC cell lines shRNA5 displayed slightly more effect in WISP1-T1 down-regulation, which could also be confirmed by altered cell phenotype. Shortly after the effective down-regulation of WISP1 could be confirmed by RT-PCR analyses, cells weren't able to survive. These additional experiments of WISP1 gene-silencing exclude that the observed results are artefacts from a specific cell line and are furthermore the strongest evidence for the importance of WISP1-signalling in the human musculoskeletal system. The effect on cell survival by WISP1 gene-silencing has never been demonstrated in literature and is a novel finding. Therefore, microarray analyses were performed to give new insights in cell signalling concerning cell survival and -death in the enforced absence of WISP1 expression.

CHAPTER

FIFTEEN

WISP1 AND ITS CONNECTION TO CELL SURVIVAL

WISP1 seems to be important for cell survival in human musculoskeletal cells, but how could it affect viability? Several questions arouse concerning WISP1 as an important survival factor in different tissues of the musculoskeletal system. The protein is described as a general survival factor that prevents several cell types for undergoing apoptosis (Su et al. 2002; Venkatesan et al. 2010). Is it possible that WISP1 acts through different survival mechanisms in diverse cell types? Thus, it was very interesting to investigate WISP1-signalling in different cells of the musculoskeletal system. Primary hMSCs and the immortalized chondrocyte cell line Tc28a2 were chosen for this purpose.

Microarray comparisons were designed, shortly after WISP1 down-regulation took place, to exhibit initial effects of apoptotic signalling. Therefore, all samples were first inspected to reflect no optical differences between shRNA treated- and scrambled control cells. Second, all shRNA samples were subsequent validated to reflect a successful down-regulation of WISP1 expression. Raw data of the following gene expression analyses contained no defective or inadequately spotted regions of the chip itself and the quality of all RNA samples was adequate as well. Raw data were normalized by three different methods (Q, RMA, VSN), whereat RMA yielded the best normalization and was used for the following analyses in both cell types. Several differentially expressed genes, detected during the microarray analyses, were successfully validated with technical and biological replicates through RT-PCR, thus confirming the reliability of the microarray results.

15.1. Microarray analysis uncovered initial apoptosis effects in WISP1 down-regulated hMSCs

The term apoptosis was established by the research trio Kerr, Wyllie, and Currie in 1972 to distinguish a morphologically form of cell death, which was associated with normal physiology. In contrast to necrosis, a form of traumatic cell death, apoptosis is a highly conserved cell mechanism that enables metazoans to control their cell numbers in tissues and thus plays a central role in embryonic development and homeostasis (Jacobson et al. 1997; Wyllie et al. 1980). However, only two major apoptotic signalling pathways were classified: the intrinsic mitochondria-mediated pathway and the extrinsic death receptor-induced pathway (Fig. 15.1). Both major cell death pathways are controlled by cysteinyl aspartate-specific proteinases (caspases). This is an evolutionarily conserved family of cell death effector and cytokine-processing enzymes, which mediate apoptotic signals and cleave a multitude of substrates, thereby causing cellular demolition (Green and Reed 1998; Nuñez et al. 1998; Thornberry 1999).

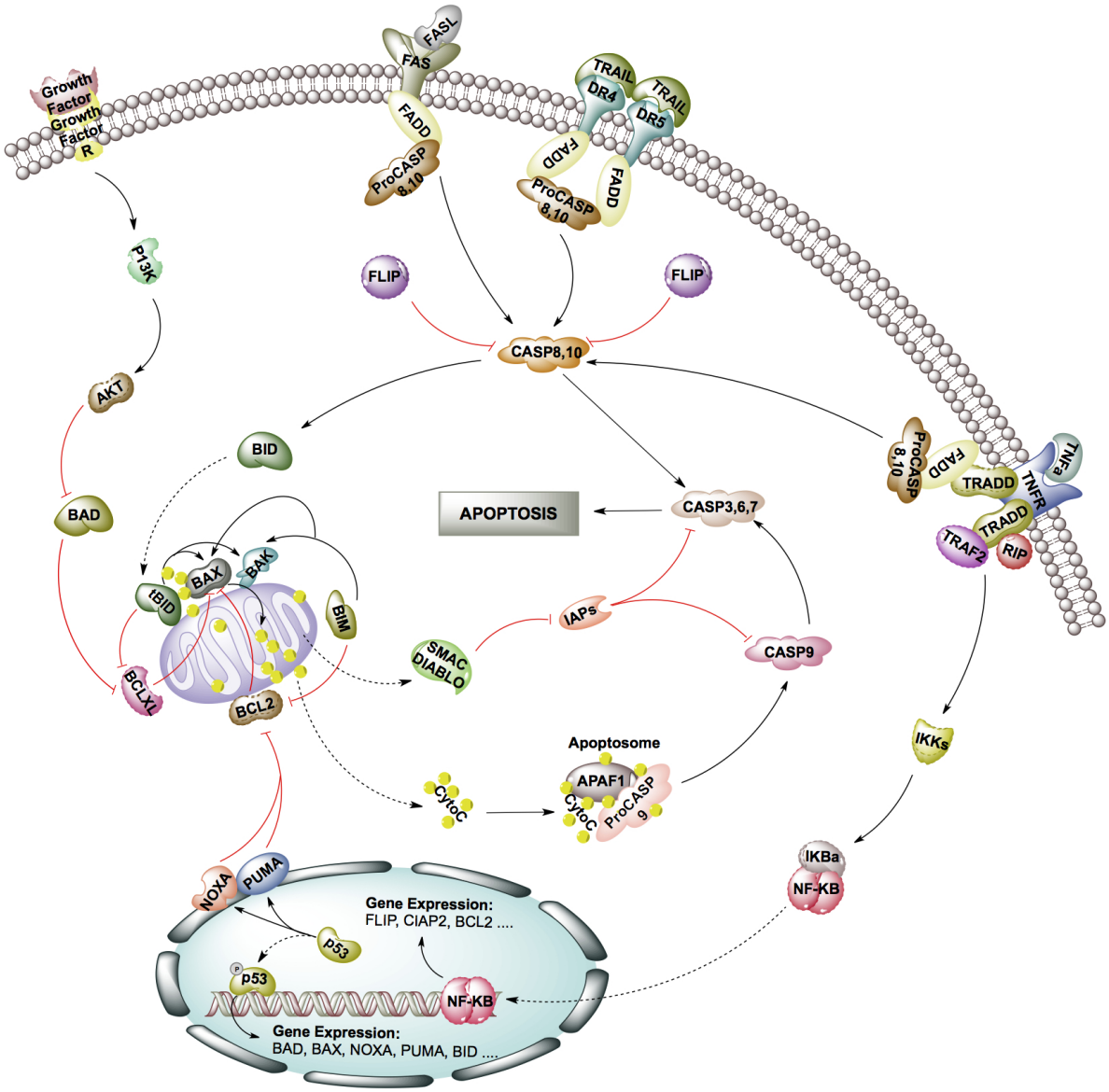

Figure 15.1.: *Extrinsic- and intrinsic-mediated apoptosis induction. Receptor-mediated (extrinsic) apoptosis is initiated by external stimuli like toxins, hormones and cytokines. Cell surface receptors transfer the signalling cascade into the cytosol where the activation of CASP8 and -10 leads to the cleavage of the effector caspases 3 , -6 and -7. Mitochondria-mediated (intrinsic) pathway can be initiated by oxidative stress, UV- or gamma-irradiation, kinase inhibitors and different cytotoxic compounds. Signalling is regulated by BCL2 family members, which lead to CASP9 activation and subsequent cleavage of CASP3, -6 and -7.*

15.1.1. Receptor mediated apoptosis via TRAIL

Genome wide microarray analysis of WISP1 down-regulated primary hMSCs, revealed a cluster of differential expressed genes important for cellular apoptosis induction. In contrast to the examined control samples, WISP1 down-regulation specifically affected genes important for both main apoptosis signalling cascades: the extrinsic- and intrinsic-mediated pathways. One of the most significant differentially expressed genes in this study is the tumor necrosis factor related apoptosis inducing ligand (TRAIL). TRAIL is known as a major cell-death inducing factor, which initiates the extrinsic-mediated apoptosis pathway by binding to its cell surface receptors DR4 and DR5 (Pan et al. 1997; Sheridan et al. 1997; Walczak et al. 1997).

The microarray data confirmed TRAIL-induced apoptosis by showing similarly upregulation of both corresponding death receptors, whereas no evidence for the apoptosis induction via other major death ligands (e.g. FAS ligand) was revealed. Following the extrinsic-mediated apoptosis cascade another key component, the expression of the effector caspase 8, is increased in all WISP1 deficient samples. CASP8 has two main functions during apoptosis. On the one hand, it can cleave downstream effector caspases (CASP3, -6 and -7) leading directly to apoptosis (Boldin et al. 1996). On the other hand, it has the ability to cleave BH3 interacting domain death agonist (BID), a pro-apoptotic member of the BCL2 family. Cleavage of BID generates the truncated active form tBID, which translocate to the mitochondrial membrane and initiates the intrinsic apoptotic pathway (Li et al. 1998; Luo et al. 1998). Accordingly, it was also possible to identify an intensified expression of this linker protein in WISP1 deficient hMSCs.

This study reflects for the first time a correlation between the TRAIL induced apoptosis cascade and WISP1-signalling in human cells. Detection of TRAIL, some of its important binding partners and subsequent signalling proteins is further interesting concerning the question, whether WISP-signalling has implications for anti-tumour strategies. In general, apoptosis induction has become an important approach for the development of new anti-cancer treatments. TRAIL has thereby emerged as one of the most promising apoptosis inducer for death receptor targeted cancer therapy.

In vivo, TRAIL reflects the remarkable feature of selectively inducing apoptosis in tumours without effecting non-transformed cells (Walczak et al. 1999). However, several primary tumour cells show resistance to TRAIL-induced apoptosis and various mechanisms have been suggested to evoke this resistance (Wang 2008). Development of chemotherapeutics or other biological agents are important to sensitize primary tumour cells to TRAIL induced apoptosis. Detection of proteins involved in this signalling cascades, like WISP1, are essential parts and constitute a premise for these strategies.

Beside the importance of TRAIL concerning anti-tumour strategies, its signalling is also suggested to be important for bone resorption and the osteoclastogenesisis of human peripheral blood cells (Zauli et al. 2004). Therefore, TRAIL has the ability to bind a third receptor, which is called osteoprotegerin (OPG) (Emery et al. 1998). This is one of the known decoy receptors, which protect cells against TRAIL-induced apoptotic signalling (Emery et al. 1998; Sheridan et al. 1997). However, main function of OPG is the regulation of osteoclastogenesis (Tsuda et al. 1997).

One key factor for mediating osteoclastogenesis is the osteoclast differentiation factor RANKL (Yasuda et al. 1998). This protein has also the ability to bind OPG. By competing with TRAIL for OPG binding, RANKL may be enforced to bind its second receptor activator of nuclear factor kappa B (RANK). Subsequent binding of RANKL to RANK finally results in osteoclast-mediated bone resorption (Simonet et al. 1997). Thus, it seems likely that differential WISP1 expression may also influence osteoclastogenesis by regulating the availability of TRAIL.

15.1.2. Intrinsic mediated apoptosis via p53

Several stimuli including oxidative stress, UV or gamma irradiation as well as kinase inhibitors and different cytotoxic compounds have been shown to activate the alternative mitochondrial (intrinsic) pathway of apoptosis. It is controlled by members of the BCL2 family that regulate cytochrome c release from the inter-membranous space of the mitochondria into the cytosol (Cory, Adams, et al. 2002). Following this major pathway, further important apoptotic factors were as well significantly differentially expressed between WISP1 down-regulated hMSCs and their control samples. Mostly, regulated genes concerning the second major pathway can be connected to p53-initiated apoptosis.

The tumour protein p53 is known as an essential transcription factor, regulating cell growth by repressing aberrant cell proliferation in response to multiple stimuli, like DNA damage and oncogene activation (Giaccia and Kastan 1998). Activation of p53 enhances DNA binding, thus triggering its transcriptional activity subsequent leading to cell cycle arrest and apoptosis induction. Initiation of an increased transcription of apoptosis responsive genes, often occur via p53 specific co-factors. One of those essential co-factors, the junction mediating and regulatory protein (JMY), is highly up-regulated in all examined WISP1 down-regulated samples. This protein acts by its complex formation with p300 in the nucleus, therefore enhancing the transcription activity of p53 apoptosis relevant target genes (Shikama et al. 1999).

Microarray data exhibited a differential expression of several p53 target genes. They can be divided in three subgroups, depending on their location within the cell membrane, cytoplasm or nucleus (Benchimol 2001). During the absence of WISP1 an increased expression of members of all three subgroups could be identified. First, the expression of apoptosis responsive membrane proteins, like the TRAIL binding death receptor DR5. Wu et al. (1997) discovered firstly an increased expression of this pro-apoptotic receptor, enabled through p53 after DNA damage (Wu et al. 1997). But also the transcription of the previously described protein BID, which is located in the cytoplasm, is clearly regulated through p53 (Sax et al. 2002). The third group comprises p53 target genes that encode proteins localized to the mitochondria. PMA-induced protein 1 (better known as NOXA), is an extensive characterized mediator of p53-dependent apoptosis (Oda et al. 2000) and was similarly up-regulated shortly after the down-regulation of WISP1 took place.

BID and NOXA are not only connected through their induced expression via p53, rather they are both pro-apoptotic BH3-only members of the BCL2 family. This family has been divided, based on structural similarities and functional criteria, in members with anti-apoptotic activity, e.g. B-cell lymphoma 2 (BCL2), BCL2 like 1 (BCLX) and members that promote cell death, e.g. NOXA, p53 up-regulated modulator of apoptosis (PUMA), bcl-2 interacting mediator of cell death (BIM), BCL2-associated X (BAX), BCL2-associated agonist of cell death (BAD) and BID (Gross et al. 1999; Puthalakath et al. 1999; Thomadaki and Scorilas 2006; Wolter et al. 1997). Activation of these proteins is affected by proteolysis, dephosphorylation and several other mechanisms (Adams 1998; Antonsson and Martinou 2000). After their activation, the pro-apoptotic proteins permeabilize the outer mitochondrial membrane and trigger the release of pro-apoptotic proteins, including cytochrome c (Kroemer and Reed 2000). Interestingly, cells with more pro-apoptotic BCL2 proteins are sensitive to death, whereas cells with an excess of protective family members are usually resistant. Yet, it is not well understood how cytochrome c release takes place, but Seo et al. (2003) assumed different mechanisms caused by either NOXA or BID. Mitochondrial breakdown and cytochrome c release through BID cleavage into tBID is mediated by BCL2-antagonist/killer 1 (BAK) or BAX oligomerization (Wang 2001; Wei et al. 2000, 2001), whereas NOXA-induced cytochrome c release is not dependent upon BAK oligomerization. Permeability transient related pore components seem to be responsible for NOXA-induced permeabilization of the mitochondrial outer membrane (Seo et al. 2003).

Interestingly, the previously described gene expression patterns, concerning p53-induced apoptosis in the absence of WISP1, are to a large part in accordance with findings of Su et al. (2002). They demonstrated the ability of WISP1 to prevent human lung carcinoma cells (H460) and human breast adenocarcinoma cells (MCF7) from undergoing apoptosis after DNA damage. Both cell types (containing wild type p53) were transfected with full-length Flag-tagged WISP1 and subsequent apoptosis induction via DNA damage clearly demonstrated an enhanced survival of WISP1 containing cells. Furthermore WISP1 thereby inhibits the mitochondrial release of cytochrome c and seems to circumvent cell death at a late stage in the p53-mediated apoptosis pathway. Another interesting and relevant study concerning p53 induced apoptosis and WISP1-signalling was published by Venkatesan et al. (2010). They characterized WISP1, similar to Su et al. (2002) as a survival factor, which has the ability to influence diverse survival pathways within a cell. The studies of Venkatesan et al. (2010) are based on the knowledge that WISP1 is over-expressed in several cancer cell lines and human tumours (Chen and Lau 2009; Yeger and Perbal 2007). Additionally, it is known that a forced expression of WISP1 initiates transformation and tumour formation of normal rat kidney fibroblast cells and nude mice (Pennica et al. 1998). Based on these facts, WISP1 seems to play a central role in tumour development. The research group of Venkatesan et al. (2010) used anthracycline antibiotic doxorubicin (DOX), a potent cancer chemotherapeutic agent, to induce cell death in adult mouse cardiomyocytes. DOX activates extrinsic- as well as intrinsic-mediated apoptotic signalling, which ultimately leads to cell death (Carvalho et al. 2009; Kotamraju et al. 2000; Olson and Mushlin 1990). Preincubation of mouse cardiomyocytes with full-length rWISP1 significantly attenuated DOX-mediated cell death (Venkatesan et al. 2010). DOX is also known to activate p53-dependent signalling pathways through DNA damage (Chua et al. 2006; L'Ecuyer et al. 2006). Venkatesan et al. (2010) clearly demonstrated that WISP1 suppressed DOX- mediated p53 activation. Similarly, WISP1 inhibited translocation of BAX to the mitochondria and circumvented DOX-induced cytochrome c release.

15.2. Initial apoptosis effects in WISP1 down-regulated Tc28a2 chondrocytes

15.2.1. WISP1 gene-silencing leads to differential gene expression patterns connected to the MAPK-signalling pathway

Additional microarray experiments were performed to investigate the effect of WISP1 gene-silencing on cell survival in the chondrocyte cell line Tc28a2. Similar to the procedure in hMSCs, microarray comparisons were designed to exhibit initial effects of apoptotic signalling shortly after WISP1 down-regulation took place. Surprisingly, the array data revealed remarkably differences compared to the findings concerning cell survival and apoptosis during WISP1 down-regulation in hMSCs. In Tc28a2 chondrocytes mainly genes connected to the mitogen-activated protein kinases (MAPK)-signalling pathway show differential expression patterns. These MAPKs are a group of serine/threonine kinases that are activated in response to a variety of extracellular stimuli. Activation results in three major types of MAP-kinase-cascades, usually named according to the main MAPK component of the cascades. The first cascade comprises signalling via extracellular signal regulated kinase 1 and -2 (ERK1/2), and is inducible by extracellular growth factor signals. The second one is mainly controlled by the stress-activated protein kinases p38-MAPK (α, β, γ and δ), inducible by cytokines and cellular stress. The third major MAPK cascade is mainly regulated through c-Jun amino-terminal kinases 1-3 (JNK1-3)-signalling, which is activated through hormones or cytokines, likewise to members of the TNF family.

Transmission of the signal via each cascade is mediated by sequential phosphorylation and activation of the components through various extracellular stimuli. MAPK-signalling thereby controls a large number of distinct and even opposing cellular processes such as proliferation, differentiation, survival, development, stress response, and apoptosis. Concerning apoptosis and cell survival, signalling through the JNK and p38 MAP-kinase cascades are, in general, associated with induction of cell death, whereas signalling through the ERK MAP-kinase cascade promotes cell growth and survival (Davis 2000; Yang et al. 1997). The impact of CCN family members on MAPK-signalling was first demonstrated by the activation of p38-MAPK and/or ERK cascades after stimulation with CYR61 and CTGF (Chen et al. 2001; Yosimichi et al. 2001). Furthermore, Kawaki et al. (2011) described an increased phosphorylation of ERK1/2 directly after osteoblast treatment with different recombinant CCN proteins. Thereby, WISP1 (as well as WISP2, CYR61 and CTGF) significantly activated ERK1/2. During this study, array analysis of the WISP1 down-regulated Tc28a2 chondrocytes identified several factors that finally point towards p38 and JNK phosphorylation as well as ERK1/2 inhibition. MAP2K7 for example, also known as JNK activating kinase 2 or MKK7, specifically activates JNK1 and -2 (Tournier et al. 2001). Deng et al. (2003) suggested that JNK activation via MAP2K7 is required for TNFα-induced CASP8 activation and apoptosis. There was no evidence for TNFα-induced apoptosis concerning the array data of WISP1 down-regulated chondrocytes, but some gene regulations seem to indicate an inhibition of NFκB (e.g. MAP3K3 and MAP3k7). NFκB activation also occurs via TNFα and the TNF-receptor and Javelaud and Besançon (2001) depict first a correlation between the NFκB and JNK pathways. Following the JNK or p38 pathway, both kinases translocate to the nucleus to activate transcription factors through phosphorylation (Davis 2000). Microarray data didn't confirm an increased gene expression of down-stream partners like ATF2, ELK1 or MEF2C, but it might be important to mention, that every array analysis reflects only one particular time point within a cell.

CHAPTER

SIXTEEN

EFFECT OF RECOMBINANT WISP PROTEINS ON TC28A2 CHONDOCYTES

WISP1 depleted Tc28a2 chondrocytes were partially treated with our previously produced (r)proteins of WISP1-T1 and WISP1-T2. Surprisingly, a highly significant self-regulation for both rWISP1 transcript variants was detectable after 24h. Furthermore it could be demonstrated that both transcript variants significantly increased their own expression, without affecting the down-regulation of the other one. This is a strong evidence for the effectiveness of both recombinant produced WISP1 protein variants in human cells. Additionally, Tc28a2 chondrocytes were treated with rWISP2. This cell line reflected no native WISP2 expression, thus it was unnecessary to reduce the endogenous protein amount prior to the treatment with rWISP2. Similar to the findings concerning WISP1 treatment, chondrocytes initiated their own WISP2 expression 24h after treatment. Thus, it is likewise a demonstration for the effectiveness of rWISP2 and moreover a novel finding in the research field comprising this CCN protein. To my knowledge, no other working group demonstrated an enforced endogenous WISP2 expression of cells that lack a native expression. How does en enforced endogenous WISP2 expression influence the chondrocyte cell line? Microarray analysis (n=3) were performed to investigate this question (data not shown). Unfortunately, no differentially gene expression patterns could be observed. Thus it is important to discuss, whether an enforced WISP2 expression has no effect on chondrocytes or maybe a change in experimental settings will help to exhibit gene regulations based on WISP2 expression. Isolation of WISP2 treated and native chondrocytes took place after cells reached nearly 100% confluence. Similarly, the native expression of different cells of the musculoskeletal system was validated. It is known that CCN proteins often are involved in proliferating processes. Therefore, further experiments are planned to examine WISP2 expression at different stages of confluence and during cell proliferation combined with several treatment experiments. Until then it cannot surely excluded that a native WISP2 expression exists, or an enforced expression constitutes to cellular differences compared to native cells.

16.1. rWISP1-T1 and -T2 don't prevent Tc28a2 chondrocytes for undergoing apoptosis after WISP1 gene-silencing

It was not possible to observe direct effects on cell survival after (r)protein treatment of the WISP1 down-regulated chondrocytes via microscopy. Why was it not possible to revert the process of cell death towards an enhanced vitality of the cells? Since our (r)proteins are able to induce their own endogenous expression, it can be excluded that the Fc-tag may disrupt

regulatory processes. Rather it is difficult to find the convenient time point to circumvent or reduce cell death induction. Protein treatment was performed a few hours subsequent to the transduction procedure, but an enhanced endogenous protein production was generally verified after additional 24h. Thus, it is possible that the time slot between treatment and resumption of endogenous protein production is too large to revert already induced cell death. Once apoptotic signalling has started, it may be difficult to obstruct the cascades before a point of no return is achieved. Additional, global gene expression patterns were examined using isolated mRNA of the previously described WISP1-T1 and -T2 treated cells (data not shown). Microarray analysis revealed no appreciable differences between shRNA5 transduced chondrocytes and such additional treated with rWISP1-T1 and -T2. Though, all shRNA5 transduced assays reflect similar regulations compared to their corresponding scrambled control samples - regardless if comparisons were performed with shRNA5 transduced samples or shRNA5 + rWISP1-T1 or -T2 treated samples (data not shown). This may supports the suggestion that self-regulation processes were initiated too late by protein treatments subsequent to the transduction procedure. It is also important to mention, that a time depend (r)protein treatment was performed without replicates and with only one concentration. Furthermore a certain assay to quantify apoptotic and viable cells was not available. Therefore, experiments should be repeated with improved experimental settings.

CHAPTER

SEVENTEEN

WISP1 AND ITS CONNECTION TO HUMAN HEALTH

Human WISP1 acts as a downstream factor of the canonical WNT-signalling pathway and its expression is regulated by β-catenin (Königshoff et al. 2009; Pennica et al. 1998; Xu et al. 2000). The canonical WNT-signalling pathway is known for the regulation of important cellular processes and aberrant expression of connected proteins is often described in combination with several medical conditions. However, WISP1 expression has been found in several cell types and prevalently an abnormal and increased WISP1 expression seems often to be responsible for different tumour types spreading over the whole human body. In vivo experiments exhibited an increased amount of full-length WISP1 mRNA and protein in colon adenocarcinomas, breast cancer, lung carcinoma and hepatocellular carcinoma (Calvisi et al. 2005; Margalit et al. 2003; Pennica et al. 1998; Xie et al. 2001). On the one hand, these findings clearly support the presumption for WISP1 as a survival factor for several cell types, because dysregulation of those proteins facilitate the formation of degenerated cell pools. On the other hand it might be an assertion for the distinct cluster of genes (23 interferon-inducible genes) connected to immuno-regulatory processes in the absence of WISP1.

Surprisingly, expression of all genes corresponding to this cluster is highly increased subsequent to the WISP1 down-regulation. It is known that hMSCs, derived from the bone marrow, constitutively secrete several cytokines important for haematopoiesis and immuno-modulatory processes (in 't Anker et al. 2003; Krampera et al. 2003). However, this study affords for the first time the influence of WISP1 on the activation of immuno-regulation through hMSCs. Microarray data suggests the importance for IFN1b signalling during this process. Interferon (IFN) inducing receptors, like the membrane bound toll like receptor 3 (TLR3) and receptors localized in the cytoplasm e.g. DDX58 and IFIH1, show an remarkable increase in regulation as well as the interferon IFNβ1 itself. In general, IFNs have been characterized as anti-proliferative cytokines, which act inter alia via the induction of cell cycle arrest in G1/G0 phase. IFNβ1 is such a member of the type I IFN family and has the ability to suppress tumour cell growth by induction of S-phase accumulation and apoptosis (Dong et al. 1999; Lokshin et al. 1995; Qin et al. 1997). These regulations support the previously described findings, which identified WISP1 as an important survival factor in hMSCs as well as its influence of immuno-regulatory processes mediated through primary cells.

17.1. WISP1 and its importance for the musculoskeletal system

The human musculoskeletal system persists of bones, cartilage, muscles, ligaments and associated connective tissues. A wide range of cell types, like multipotent stem cells (mesenchymals and haematopoetics), osteoblasts, chondrocytes, myoblasts and fibroblasts, are needed to es-

tablish and sustain this essential part of the human body. WNT-signalling is one of the most involved pathways to favour directly the regulation of skeletal development and tissue remodelling by modulating chondrocyte and osteoblast differentiation as well as joint formation (Hartmann and Tabin 2000, 2001; Rudnicki and Brown 1997). Given that WISP1 act as a downstream factor during WNT-signalling, assumption accrued this protein could play an important regulatory role in vertebrate skeletal development. A prominent role for WISP1 could be already confirmed for the signalling in primary hMSCs. French et al. (2004) illustrates the importance for full length WISP1 as an osteogenic potentiating factor, promoting MSC proliferation, osteoblast differentiation as well as repressing chondrocytic differentiation. This outcome is supported by Inkson et al. (2008) who further demonstrated the necessity of an additional trigger, like TGFβ or BMPs, to induce hMSC differentiation into osteoblasts. They further suggested the interaction of WISP1 with the proteoglycan biglycan (BGN) to control each other's activity in the regulation during osteoblast differentiation and proliferation (Inkson et al. 2009). Microarray data of WISP1 down-regulated hMSCs couldn't confirm an effect on the expression of TGFβ, BMPs or BGN. Instead of that, a second important binding partner of WISP1, the proteoglycan decorin (DCN) exhibits a strongly decreased expression during the absence of WISP1. The structure of DCN is closely related to that of biglycan and both proteins are highly expressed in bone tissues, but with observed differences in their distribution, indicating different roles during bone mineralization (Bianco et al. 1990; Ingram et al. 1993). In addition, the expression of the splicing variant WISP1-T2, lacking the VWC domain, could be observed in hMSCs (Inkson et al. 2008), osteoblasts and chondrocytes. (Yanagita et al. 2007) also confirmed an increased amount of WISP1-T2 during terminal chondrocyte differentiation. Compared to findings of French et al. (2004), who described a repressed chondrocytic differentiation mediated by full-length WISP1, differences in the effectiveness of both proteins could be assumed.

17.1.1. Influence of WISP1 on cartilage homeostasis

Adult cartilage is an avascular tissue composed mainly of chondrocytes, collagens and proteoglycans (Buckwalter and Mankin 1998; Palfrey and Davies 1966). Thereby, one major function of chondrocytes is the production and maintenance of the cartilaginous ECM by replacement of distinct matrix proteins. Influences on chondrocyte function are considered to be important in different human diseases, like the pathogenesis of osteoarthritis (OA) or rheumatoid arthritis (RA). A disruption of cartilage homeostasis may implicate the loss of collagens and proteoglycans from the ECM, which consequently impede the deposition of newly synthesized molecules. Thus, the pathogenesis of OA could be constrained by abnormal WNT-signalling that influences cartilage homeostasis (Loughlin et al. 2004). In this context, Blom et al. (2009) characterized expression patterns of WNT-inducible genes during experimental OA in mice and human OA. Interestingly, WISP1 expression was strongly increased in the synovium and cartilage of both examined OA types. Subsequent functional studies with rWISP1 in macrophages and chondrocytes led to the induction of different matrix metalloproteinases (MMPs) and aggrecanases (ADAMTSs) (Blom et al. 2009). Both are known to be mediating breakdown of extracellular cartilage matrix (Smith 1999).

Microarray analysis of WISP1 down-regulated Tc28a2 chondrocytes compared to their control samples revealed a remarkable cluster of distinct gene regulations that may affect cartilage homeostasis. Several expression patterns are in accordance with observations of Blom et al. (2009), e.g. the decrease of different extracellular proteases, like MMPS (MMP2, MMP11 and MMP16) and ADAMTSs (ADAMTS3, ADAMTS12 and ADAMTS17). MMP16 and ADAMTS17, a TNFα-converting enzyme, are both highly expressed in cartilage, but their specific roles in cartilage damage are still unclear (Leppert et al. 2001; Murphy and Lee 2005).

Further gene expression patterns, detectable during the absence of WISP1 in chondrocytes, seem to be important for cartilage homeostasis. Interestingly, all detected mRNA levels in this context are decreased in WISP1 down-regulated Tc28a2 chondrocytes compared to the corresponding control samples. The expression level of the cartilage linking protein HAPLN1, one major component of the cartilage extracellular matrix, was one of strongest effected transcripts in the absence of WISP1. Loss of HAPLN1 protein is associated with reduced aggrecan deposition and decreased numbers of hypertrophic chondrocytes in mice (Watanabe and Yamada 1999). It may also function as an inductor of the aggrecan and collagen type II synthesis in cartilage (McKenna et al. 1998). Therefore, dysregulated HAPLN1 expression seems crucial to proteoglycan aggregate formation and hypertrophic chondrocyte organization. Another protein, important in maintaining the chondrocyte phenotype is the transcription factor RUNX2. RUNX2 is a positive regulator of the transition from proliferating to hypertrophic chondrocytes, thus known as a hypertrophic marker. Interestingly, this protein is also strongly increased during the pathogenesis of OA (Martinez-Sanchez et al. 2012). At least we were able to detect significant over-representations of pathways important for cartilage homeostasis, like the MAPK-signalling pathway and focal adhesion. Both play essential roles in important biological processes including cell motility, cell proliferation, cell differentiation and regulation of gene expression. Focal adhesion, for example, controls cell-matrix adhesion via several ECM contact points, like trans-membrane receptors of the integrin family. Thereby, signalling cascades induce re-organization of the actin cytoskeleton, which constitutes the basis for changes in cell shape, motility, and gene expression. Focal adhesion is the most significant affected pathway detected through the KEGG pathway over-representation in WISP1 down-regulated chondrocytes. In contrast, MAPK-signalling is primary assumed to initiate apoptosis in chondrocytes as a result of the enforced down-regulation of WISP1 (Subsec. 15.2.1). Otherwise, it plays also an important role in cartilage homeostasis by affecting transcription levels of specific MMPs and cartilage-selective ECM associated proteins (Rockel et al. 2009; Séguin and Bernier 2003). Considering the fact that microarray analysis was actually performed to detect initial apoptotic effects in WISP1 down-regulated chondrocytes, findings concerning a disrupted cartilage homeostasis maybe closely linked to apoptosis in this chondrocyte cell line.

CHAPTER
EIGHTEEN

CONCLUSIONS

Recent studies have shown that WISP1 expression could mainly associate with development and disease by affecting cell survival, proliferation and cell differentiation. Results of this thesis emphasize the importance of regulatory mechanisms that influence cell survival of primary hMSCs and chondrocytes in the enforced absence of WISP1. For the first time, the dramatically effect of cell death, shortly after down-regulation of WISP1 could be confirmed in human musculoskeletal cells. In this context we were able to give new insights into gene expression changes, which indicate signalling of different apoptotic pathways, e.g. receptor- or p53-mediated apoptosis as well as MAPK-signalling. Since TRAIL and IFNβ, both remarkably increased in WISP1 down-regulated hMSCs, act as potent inhibitors for malignant cell growth *in vitro* knowledge about the connection with WISP1-signalling could help to find new therapeutic approaches concerning cancerogenesis and tumour growth. Moreover, the importance for WISP1-signalling in cartilage homeostasis seems to be manifested, since microarray data of WISP1 deficient chondrocytes revealed a distinct cluster of regulated genes important for ECM maintenance and hypertrophic chondrocyte organization. Several follow-up experiments are needed to investigate the role of WISP1-signalling in cartilage homeostasis and cell death, but this thesis generated an essential fundament for further examinations.

CHAPTER
NINETEEN

PERSPECTIVES

A difficult separation: Are the extrinsic- or intrinsic cascades responsible for apoptosis in WISP1 deficient hMSCs... or even both?

The affymetrix gene expression profile revealed different genes associated with both, the extrinsic- and intrinsic-mediated apoptosis pathways, after WISP1 down-regulation took place in MSCs. This is not exceptional, because different linker proteins like BID and p53, which directly connect the extrinsic and intrinsic mediated apoptosis, complicate a clearly separated examinations of both pathways. Nevertheless, it is important to molecularly dissect both major pathways for a better understanding of WISP1-signalling. Thus, different sets of experiments are planned to further investigate the role of extrinsic- and intrinsic-mediated apoptosis signals. One aim is the successful application of caspase inhibitors. They bind to the active site of a specific protease, e.g. CASP8 (extrinsic) or CASP9 (intrinsic), thereby inhibiting apoptosis in the absence of WISP1. Thus, the effective application of caspase inhibitors should enhance the cell viability during the WISP1 down-regulation. Additional, it is possible to stain CASP8 and CASP9 with specific fluorescence labelled caspase inhibitors (e.g. apoptosis detection assay FLICA) to distinguish between both initiator caspases. Due to the fact that both caspases are connected to one of both major apoptotic pathways, this staining procedure will give new insights in whether extrinsic or intrinsic stimuli are mainly responsible for hMSCS undergoing apoptosis in the absence of WISP1. We already established the general sulforhodamine-labelled VAD-FMK poly caspase inhibitor, detecting CASP1, -3, -4, -5, -6, -7, -8 and -9.

Furthermore, proteins that are involved in different apoptosis cascades can be visualized by immuno-cytochemistry labelling methods to infer their location within a cell. Cytochrome c, for example, promotes cell survival or death depending upon its intracellular location. In healthy cells it is a peripheral membrane protein of the mitochondria. When internal pro-apoptotic stimuli induce breakdown of the mitochondria, cytochrome c is released into the cytosol. There it leads to activation of caspases and thus triggers apoptosis. Another very interesting protein in this investigation could be the pro-apoptotic linker protein BID, which directly connects the mitochondrial pathway of apoptosis to the extrinsic pathway (Newsom-Davis et al. 2009). To investigate the protein localization, it is necessary to counterstain concurrently mitochondria and nuclei of the different cell types. Within this thesis, it was possible to establish the successful application of MitoTracker®Red to stain selective mitochondria in addition to the common nuclei marker DAPI. MitoTracker®Red is concentrated by active mitochondria and well retained during cell fixation.

Binding of TRAIL to its cell surface receptors results similarly in the activation of different caspases, which in turn inevitably initiate apoptosis. TRAIL has the ability to bind also to several decoy receptors that lack the death effector domain and thus are unable to promote

apoptosis-inducing signalling. OPG, for example, is one of the known decoy receptors, which protect cells against the apoptotic effects of TRAIL (Emery et al. 1998; Sheridan et al. 1997). A few years after OPG was identified as a modulator of osteoclastogenesis (Tsuda et al. 1997), it becomes more important as a survival factor for human breast and prostate cancer cells *in vivo* through inhibition of TRAIL induced apoptosis (Holen et al. 2002, 2005). Rachner et al. (2009) showed that differences in OPG expression affect the ability of breast cancer cell lines to evade TRAIL induced apoptosis. IL1β is one of the cytokines that has been shown to induce the OPG expression in breast cancer cells (Kapoor et al. 2008). Therefore, the apoptotic effect of IL1β-treated MSCs and chondrocytes, during WISP1 down-regulation, will be analysed in relation to the amount of endogenous expressed OPG. Additionally, gene-silencing of WISP1 with supplementary treatment of recombinant OPG are planned to discover survival effects between the shift in the TRAIL/OPG ratio. Depending on the knowledge that an increased amount of TRAIL enforces osteoclast differentiation, WISP1-signalling should also examined in detail concerning its role during the osteoclastogenesis.

In accordance to the literature, microarray data also support the importance of WISP1 for p53-dependent apoptotic signalling, thereby increasing the interest for further investigations of WISP1-signalling in future projects. It is well known that DNA damage initiates the stabilization of the p53 protein. This occurs, via phosphorylation or acetylation at several N-terminal residues, including Ser15, -20, -33 and -37 (Sakaguchi et al. 1998; Shieh et al. 1997, 1999; Siliciano et al. 1997). This knowledge is important for the use of specific antibodies against different activation sites and to examine the impact of p53 induction during the absence of WISP1 in hMSCs. After activation, p53 can either stimulate the death receptor pathway or the mitochondrial-mediated apoptosis signals. To further investigate the impact of p53 signalling during the absence of WISP1 in hMSCs, it is important to visualise its localization in WISP1 down-regulated cells in comparison to control cells. We already established the successful application of p53 specific, fluorescence labelled antibodies in hMSCs. The next step will include multiple staining experiments with double counterstain of mitochondria (MitoTracker®Red) and nuclei (DAPI), as soon as the p53 labelling is successful in MSCs during the WISP1 down-regulation. The findings concerning the impact of WISP1 on MAPK-signalling will be extended to the protein level by analysing possible alterations in phosphorylation levels of kinases and/or protein levels of regulating factors by western blotting. We will analyse phosphorylation of these kinases in addition to time- and concentration dependent application of (r)proteins. Kawaki et al. (2011) also demonstrated a successful annihilation of ERK1/2 activation through the application of specific MAPK inhibitors prior to the treatment with rCCN proteins. We plan to investigate the effect of three different MAPK inhibitors (MEK inhibitor PD98059, p38-MAPK inhibitor SB 203580 and JNK inhibitor 1; Merck) during the WISP1 down-regulation in Tc28a2 cells. The inhibitors will be used in independent and combined experiments with working concentration based on literature revue (Badger et al. 1998; Bain et al. 2003; Hung et al. 2008). Separated inhibition of the three major MAPK cascades will give new insights in the effectiveness of WISP1 on cell survival in chondrocytes.

It was not possible to revert the process of cell death in Tc28a2 chondrocytes through protein treatments with rWISP1-T1 or/and -T2. Improved experimental settings will therefore include different concentration steps of the (r)proteins that range from 100ng-1000ng. Treatments will be performed prior to and during the transduction to ensure a constant effectiveness of rWISP1-T1 and -T2. RNA isolation will be performed regularly to examine states of endogenous protein existence combined with subsequent apoptosis assays, like the previously described FLICA assay for a better validation of cell viability.

Part V.

Bibliography and additional Information

BIBLIOGRAPHY

Adams, J. M (1998). "The Bcl-2 Protein Family: Arbiters of Cell Survival". In: *Science* 281.5381, pp. 1322–1326 (cit. on p. 132).

Ahn, J, I.-J. L Byeon, C.-H Byeon, and A. M Gronenborn (2009). "Insight into the Structural Basis of Pro- and Antiapoptotic p53 Modulation by ASPP Proteins". In: *Journal of Biological Chemistry* 284.20, pp. 13812–13822 (cit. on p. 93).

Altschul, S., W. Gish, W. Miller, E. Myers, D. Lipman, et al. (1990). "Basic local alignment search tool". In: *Journal of molecular biology* 215.3, pp. 403–410 (cit. on p. 45).

Antonsson, B and J. C. Martinou (2000). "The Bcl-2 protein family". In: *Experimental Cell Research* 256.1, pp. 50–7 (cit. on p. 132).

Ashburner, M., C. Ball, J. Blake, D. Botstein, H. Butler, J. Cherry, A. Davis, K. Dolinski, S. Dwight, J. Eppig, et al. (2000). "Gene Ontology: tool for the unification of biology". In: *Nature genetics* 25.1, p. 25 (cit. on p. 86).

Ashkenazi, A and V. M. Dixit (1998). "Death receptors: signaling and modulation". In: *Science* 281.5381, pp. 1305–8 (cit. on p. 92).

Babic, A. M., M. L. Kireeva, T. V. Kolesnikova, and L. F. Lau (1998). "CYR61, a product of a growth factor-inducible immediate early gene, promotes angiogenesis and tumor growth". In: *Proc Natl Acad Sci USA* 95.11, pp. 6355–60 (cit. on p. 7).

Badger, A., M. Cook, M. Lark, T. Newman-Tarr, B. Swift, A. Nelson, F. Barone, and S. Kumar (1998). "SB 203580 inhibits p38 mitogen-activated protein kinase, nitric oxide production, and inducible nitric oxide synthase in bovine cartilage-derived chondrocytes". In: *The Journal of Immunology* 161.1, p. 467 (cit. on p. 144).

Bain, J., H. McLauchlan, M. Elliott, and P. Cohen (2003). "The specificities of protein kinase inhibitors: an update." In: *Biochemical Journal* 371.Pt 1, p. 199 (cit. on p. 144).

Baksh, D, L Song, and R. S. Tuan (2004). "Adult mesenchymal stem cells: characterization, differentiation, and application in cell and gene therapy". In: *J Cell Mol Med* 8.3, pp. 301–16 (cit. on pp. 3, 4).

Barry, F. P. and J. M. Murphy (2004). "Mesenchymal stem cells: clinical applications and biological characterization". In: *Int J Biochem Cell Biol* 36.4, pp. 568–84 (cit. on p. 3).

Baum, C. M., I. L. Weissman, A. S. Tsukamoto, A. M. Buckle, and B Peault (1992). "Isolation of a candidate human hematopoietic stem-cell population". In: *Proc Natl Acad Sci USA* 89.7, pp. 2804–8 (cit. on p. 3).

Benchimol, S (2001). "p53-dependent pathways of apoptosis". In: *Cell Death Differ* 8.11, pp. 1049–51 (cit. on p. 132).

Benson, D., M. Boguski, D. Lipman, and J. Ostell (1997). "GenBank". In: *Nucleic acids research* 25.1, pp. 1–6 (cit. on p. 45).

Besch, R., H. Poeck, T. Hohenauer, D. Senft, G. Häcker, C. Berking, V. Hornung, S. Endres, T. Ruzicka, S. Rothenfusser, and G. Hartmann (2009). "Proapoptotic signaling induced by RIG-I and MDA-5 results in type I interferon–independent apoptosis in human melanoma cells". In: *J. Clin. Invest.* Pp. 1–13 (cit. on p. 94).

Bianco, P and P. G. Robey (2001). "Stem cells in tissue engineering". In: *Nature* 414.6859, pp. 118–21 (cit. on p. 4).

Bianco, P, L. W Fisher, M. F Young, J. D Termine, and P. G Robey (1990). "Expression and localization of the two small proteoglycans biglycan and decorin in developing human skeletal and non-skeletal tissues." In: *Journal of Histochemistry & Cytochemistry* 38.11, pp. 1549–1563 (cit. on p. 138).

Bianco, P, M Riminucci, S Gronthos, and P. G. Robey (2001). "Bone marrow stromal stem cells: nature, biology, and potential applications". In: *Stem Cells* 19.3, pp. 180–92 (cit. on p. 4).

Blom, A. B., S. M. Brockbank, P. L. V. Lent, H. M. V. Beuningen, J. Geurts, N. Takahashi, P. M. V. D. Kraan, F. A. V. D. Loo, B. W. Schreurs, K. Clements, P. Newham, and W. B. V. D. Berg (2009). "Involvement of the Wnt signaling pathway in experimental and human osteoarthritis: Prominent role of Wnt-induced signaling protein 1". In: *Arthritis Rheum* 60.2, pp. 501–512 (cit. on pp. 9, 138).

Boldin, M. P., T. M. Goncharov, Y. V. Goltsev, and D Wallach (1996). "Involvement of MACH, a novel MORT1/FADD-interacting protease, in Fas/APO-1- and TNF receptor-induced cell death". In: *Cell* 85.6, pp. 803–15 (cit. on p. 131).

Bork, P (1993). "The modular architecture of a new family of growth regulators related to connective tissue growth factor". In: *FEBS Letters* 327.2, pp. 125–30 (cit. on p. 7).

Bradford, M. M. (1976). "A rapid and sensitive method for the quantitation of microgram quantities of protein utilizing the principle of protein-dye binding". In: *Anal Biochem* 72, pp. 248–54 (cit. on p. 56).

Bradham, D. M., A Igarashi, R. L. Potter, and G. R. Grotendorst (1991). "Connective tissue growth factor: a cysteine-rich mitogen secreted by human vascular endothelial cells is related to the SRC-induced immediate early gene product CEF-10". In: *J Cell Biol* 114.6, pp. 1285–94 (cit. on p. 7).

Brigstock, D. R. (2003). "The CCN family: a new stimulus package". In: *J Endocrinol* 178.2, pp. 169–75 (cit. on pp. 7, 9).

Buckley, N. E, A. M Hosey, J. J Gorski, J. W Purcell, J. M Mulligan, D. P Harkin, and P. B Mullan (2007). "BRCA1 Regulates IFN- Signaling through a Mechanism Involving the Type I IFNs". In: *Molecular Cancer Research* 5.3, pp. 261–270 (cit. on p. 95).

Buckwalter, J. A. and H. J. Mankin (1998). "Articular cartilage: tissue design and chondrocyte-matrix interactions". In: *Instr Course Lect* 47, pp. 477–86 (cit. on pp. 4, 138).

Budihardjo, I, H Oliver, M Lutter, X Luo, and X Wang (1999). "Biochemical pathways of caspase activation during apoptosis". In: *Annu Rev Cell Dev Biol* 15, pp. 269–90 (cit. on p. 92).

Calvisi, D. F., E. A. Conner, S. Ladu, E. R. Lemmer, V. M. Factor, and S. S. Thorgeirsson (2005). "Activation of the canonical Wnt/beta-catenin pathway confers growth advantages in c-Myc/E2F1 transgenic mouse model of liver cancer". In: *J Hepatol* 42.6, pp. 842–9 (cit. on p. 137).

Caplan, A. I. (1991). "Mesenchymal stem cells". In: *J Orthop Res* 9.5, pp. 641–50 (cit. on p. 3).

Caplan, A. (2005). "Review: mesenchymal stem cells: cell-based reconstructive therapy in orthopedics". In: *Tissue Engineering* 11.7-8, pp. 1198–1211 (cit. on p. 4).

Cardone, M. H., N Roy, H. R. Stennicke, G. S. Salvesen, T. F. Franke, E Stanbridge, S Frisch, and J. C. Reed (1998). "Regulation of cell death protease caspase-9 by phosphorylation". In: *Science* 282.5392, pp. 1318–21 (cit. on p. 11).

Carlson, M., S. Falcon, H. Pages, and N. Li (2012a). *hgu133plus2.db: Affymetrix Human Genome U133 Plus 2.0 Array annotation data (chip hgu133plus2)*. R package version 2.5.0 (cit. on p. 63).

– (2012b). *KEGG.db: A set of annotation maps for KEGG*. R package version 2.5.0 (cit. on p. 63).

Carvalho, C., R. X. Santos, S. Cardoso, S. Correia, P. J. Oliveira, M. S. Santos, and P. I. Moreira (2009). "Doxorubicin: the good, the bad and the ugly effect". In: *Curr Med Chem* 16.25, pp. 3267–85 (cit. on p. 133).

Chen, C. C., N Chen, and L. F. Lau (2001). "The angiogenic factors Cyr61 and connective tissue growth factor induce adhesive signaling in primary human skin fibroblasts". In: *J Biol Chem* 276.13, pp. 10443–52 (cit. on p. 134).

Chen, C.-C. and L. F. Lau (2009). "Functions and mechanisms of action of CCN matricellular proteins". In: *Int J Biochem Cell Biol* 41.4, pp. 771–783 (cit. on p. 133).

– (2010). "Deadly liaisons: fatal attraction between CCN matricellular proteins and the tumor necrosis factor family of cytokines". In: *J. Cell Commun. Signal.* 4.1, pp. 63–69 (cit. on p. 5).

Chevallet, M., S. Luche, and T. Rabilloud (2006). "Silver staining of proteins in polyacrylamide gels". In: *Nat Protoc* 1.4, pp. 1852–8 (cit. on p. 58).

Chow, W. A., J. J. Fang, and J. K. Yee (2000). "The IFN regulatory factor family participates in regulation of Fas ligand gene expression in T cells". In: *J Immunol* 164.7, pp. 3512–8 (cit. on p. 92).

Chua, C. C., X. Liu, J. Gao, R. C. Hamdy, and B. H. L. Chua (2006). "Multiple actions of pifithrin-alpha on doxorubicin-induced apoptosis in rat myoblastic H9c2 cells". In: *Am J Physiol Heart Circ Physiol* 290.6, H2606–13 (cit. on p. 133).

Cory, S., J. Adams, et al. (2002). "The Bcl2 family: regulators of the cellular life-or-death switch". In: *Nature Reviews Cancer* 2.9, pp. 647–656 (cit. on p. 132).

Datta, S. R., H Dudek, X Tao, S Masters, H Fu, Y Gotoh, and M. E. Greenberg (1997). "Akt phosphorylation of BAD couples survival signals to the cell-intrinsic death machinery". In: *Cell* 91.2, pp. 231–41 (cit. on p. 11).

Davis, L., Y. Chen, and M. Sen (2006). "WISP-3 functions as a ligand and promotes superoxide dismutase activity". In: *Biochem Biophys Res Commun* 342.1, pp. 259–65 (cit. on p. 11).

Davis, R. J. (2000). "Signal transduction by the JNK group of MAP kinases". In: *Cell* 103.2, pp. 239–52 (cit. on p. 134).

Delague, V., E. Chouery, S. Corbani, I. Ghanem, S. Aamar, J. Fischer, E. Levy-Lahad, J. Urtizberea, and A. Mégarbané (2005). "Molecular study of WISP3 in nine families originating from the Middle-East and presenting with progressive pseudorheumatoid dysplasia: Identification of two novel mutations, and description of a founder effect". In: *American Journal of Medical Genetics Part A* 138.2, pp. 118–126 (cit. on p. 11).

Deng, Y., X. Ren, L. Yang, Y. Lin, and X. Wu (2003). "A JNK-dependent pathway is required for TNFalpha-induced apoptosis". In: *Cell* 115.1, pp. 61–70 (cit. on p. 134).

Desnoyers, L, D Arnott, and D Pennica (2001). "WISP-1 binds to decorin and biglycan". In: *J Biol Chem* 276.50, pp. 47599–607 (cit. on p. 9).

Dong, Z, G Greene, C Pettaway, C. P. Dinney, I Eue, W Lu, C. D. Bucana, M. D. Balbay, D Bielenberg, and I. J. Fidler (1999). "Suppression of angiogenesis, tumorigenicity, and metastasis by human prostate cancer cells engineered to produce interferon-beta". In: *Cancer Res* 59.4, pp. 872–9 (cit. on p. 137).

Eferl, R., R. Ricci, L. Kenner, R. Zenz, J.-P. David, M. Rath, and E. F. Wagner (2003). "Liver tumor development. c-Jun antagonizes the proapoptotic activity of p53". In: *Cell* 112.2, pp. 181–92 (cit. on p. 94).

Ehl, S., M. Uhl, R. Berner, L. Bonafe, A. Superti-Furga, and A. Kirchhoff (2004). "Clinical, radiographic, and genetic diagnosis of progressive pseudorheumatoid dysplasia in a patient with severe polyarthropathy". In: *Rheumatology international* 24.1, pp. 53–56 (cit. on p. 11).

Emery, J. G., P McDonnell, M. B. Burke, K. C. Deen, S Lyn, C Silverman, E Dul, E. R. Appelbaum, C Eichman, R DiPrinzio, R. A. Dodds, I. E. James, M Rosenberg, J. C. Lee, and P. R. Young (1998). "Osteoprotegerin is a receptor for the cytotoxic ligand TRAIL". In: *J Biol Chem* 273.23, pp. 14363–7 (cit. on pp. 131, 144).

Falcon, S and R Gentleman (2007a). "Using GOstats to test gene lists for GO term association." In: *Bioinformatics* 23.2, pp. 257–8 (cit. on p. 63).

Falcon, S. and R. Gentleman (2007b). "Using GOstats to test gene lists for GO term association". In: *Bioinformatics* 23.2, p. 257 (cit. on p. 86).

Fernandes-Alnemri, T, J Wu, J.-W. Yu, P Datta, B Miller, W Jankowski, S Rosenberg, J Zhang, and E. S. Alnemri (2007). "The pyroptosome: a supramolecular assembly of ASC dimers mediating inflammatory cell death via caspase-1 activation". In: *Cell Death Differ* 14.9, pp. 1590–1604 (cit. on p. 94).

French, D. M., R. J. Kaul, A. L. D'Souza, C. W. Crowley, M. Bao, G. D. Frantz, E. H. Filvaroff, and L. Desnoyers (2004). "WISP-1 is an osteoblastic regulator expressed during skeletal development and fracture repair". In: *The American Journal of Pathology* 165.3, pp. 855–67 (cit. on pp. 8, 9, 125, 138).

Friedlander, R. M., V Gagliardini, R. J. Rotello, and J Yuan (1996). "Functional role of interleukin 1 beta (IL-1 beta) in IL-1 beta-converting enzyme-mediated apoptosis". In: *J Exp Med* 184.2, pp. 717–24 (cit. on p. 94).

Fuchs, E., T. Tumbar, and G. Guasch (2004). "Socializing with the neighbors: stem cells and their niche". In: *Cell* 116.6, pp. 769–78 (cit. on p. 3).

Fukunaga, T., T. Yamashiro, S. Oya, N. Takeshita, M. Takigawa, and T. Takano-Yamamoto (2003). "Connective tissue growth factor mRNA expression pattern in cartilages is associated with their type I collagen expression". In: *Bone* 33.6, pp. 911–8 (cit. on p. 5).

Galli, C, G Passeri, and G. M Macaluso (2010). "Osteocytes and WNT: the Mechanical Control of Bone Formation". In: *Journal of Dental Research* 89.4, pp. 331–343 (cit. on p. 4).

Garkavtsev, I, I. A. Grigorian, V. S. Ossovskaya, M. V. Chernov, P. M. Chumakov, and A. V. Gudkov (1998). "The candidate tumour suppressor p33ING1 cooperates with p53 in cell growth control". In: *Nature* 391.6664, pp. 295–8 (cit. on p. 93).

Gautier, L., L. Cope, B. M. Bolstad, and R. A. Irizarry (2004). "affy—analysis of Affymetrix GeneChip data at the probe level". In: *Bioinformatics* 20.3, pp. 307–315. ISSN: 1367-4803 (cit. on p. 62).

Gentleman, R. (2012). *annotate: Annotation for microarrays*. R package version 1.30.0 (cit. on p. 63).

Gentleman, R., V. Carey, W. Huber, and F. Hahne (2012). *genefilter: genefilter: methods for filtering genes from microarray experiments*. R package version 1.34.0 (cit. on p. 63).

Gentleman, R., V. Carey, D. Bates, B. Bolstad, M. Dettling, S. Dudoit, B. Ellis, L. Gautier, Y. Ge, J. Gentry, et al. (2004a). "Bioconductor: open software development for computational biology and bioinformatics". In: *Genome biology* 5.10, R80 (cit. on p. 86).

Gentleman, R. C., V. J. Carey, D. M. Bates, and others (2004b). "Bioconductor: Open software development for computational biology and bioinformatics". In: *Genome Biology* 5, R80 (cit. on pp. 62, 85).

Giaccia, A. J and M. B Kastan (1998). "The complexity of p53 modulation: emerging patterns from divergent signals". In: *Genes & Development* 12.19, pp. 2973–2983 (cit. on p. 132).

Green, D. R. and J. C. Reed (1998). "Mitochondria and apoptosis". In: *Science* 281.5381, pp. 1309–12 (cit. on pp. 64, 129).

Gronthos, S. and P. Simmons (1996). "The biology and application of human bone marrow stromal cell precursors". In: *Journal of hematotherapy* 5.1, pp. 15–23 (cit. on p. 4).

Gross, A, X. M. Yin, K Wang, M. C. Wei, J Jockel, C Milliman, H Erdjument-Bromage, P Tempst, and S. J. Korsmeyer (1999). "Caspase cleaved BID targets mitochondria and is required for cytochrome c release, while BCL-XL prevents this release but not tumor necrosis factor-R1/Fas death". In: *J Biol Chem* 274.2, pp. 1156–63 (cit. on pp. 92, 132).

Habisch, H.-J., J Fiedler, A. Ludolph, A Storch, and R. Brenner (2008). "Altered migration and adhesion potential of pro-neurally converted human bone marrow stromal cells". In: *Cytotherapy* 10.8, pp. 824–833 (cit. on p. 4).

Hadjiargyrou, M, W Ahrens, and C. T. Rubin (2000). "Temporal expression of the chondrogenic and angiogenic growth factor CYR61 during fracture repair". In: *J Bone Miner Res* 15.6, pp. 1014–23 (cit. on p. 125).

Hadjidakis, D. J and I. I Androulakis (2006). "Bone Remodeling". In: *Ann N Y Acad Sci* 1092.1, pp. 385–396 (cit. on p. 4).

Harris, M., J. Clark, A. Ireland, J. Lomax, M. Ashburner, R. Foulger, K. Eilbeck, S. Lewis, B. Marshall, C. Mungall, et al. (2004). "The Gene Ontology (GO) database and informatics resource". In: *Nucleic acids research* 32.Database issue, p. D258 (cit. on p. 86).

Hartmann, C and C. J. Tabin (2000). "Dual roles of Wnt signaling during chondrogenesis in the chicken limb". In: *Development* 127.14, pp. 3141–59 (cit. on p. 138).

– (2001). "Wnt-14 plays a pivotal role in inducing synovial joint formation in the developing appendicular skeleton". In: *Cell* 104.3, pp. 341–51 (cit. on p. 138).

Harvey, N. L., A. J. Butt, and S Kumar (1997). "Functional activation of Nedd2/ICH-1 (caspase-2) is an early process in apoptosis". In: *J Biol Chem* 272.20, pp. 13134–9 (cit. on p. 94).

Hashimoto, G., I. Inoki, Y. Fujii, T. Aoki, E. Ikeda, and Y. Okada (2002). "Matrix metalloproteinases cleave connective tissue growth factor and reactivate angiogenic activity of vascular endothelial growth factor 165". In: *J Biol Chem* 277.39, pp. 36288–95 (cit. on p. 9).

Hill, T. P., D. Später, M. M. Taketo, W. Birchmeier, and C. Hartmann (2005). "Canonical Wnt/beta-catenin signaling prevents osteoblasts from differentiating into chondrocytes". In: *Dev Cell* 8.5, pp. 727–38 (cit. on p. 5).

Hojo, H., S. Ohba, F. Yano, and U.-I. Chung (2010). "Coordination of chondrogenesis and osteogenesis by hypertrophic chondrocytes in endochondral bone development". In: *J Bone Miner Metab* 28.5, pp. 489–502 (cit. on p. 5).

Holen, I., P. I. Croucher, F. C. Hamdy, and C. L. Eaton (2002). "Osteoprotegerin (OPG) is a survival factor for human prostate cancer cells". In: *Cancer Res* 62.6, pp. 1619–23 (cit. on p. 144).

Holen, I., S. S. Cross, H. L. Neville-Webbe, N. A. Cross, S. P. Balasubramanian, P. I. Croucher, C. A. Evans, J. M. Lippitt, R. E. Coleman, and C. L. Eaton (2005). "Osteoprotegerin (OPG) Expression by Breast Cancer Cells *in vitro* and Breast Tumours *in vivo* – A Role in Tumour Cell Survival?" In: *Breast Cancer Res Treat* 92.3, pp. 207–215 (cit. on p. 144).

Holloway, S. E., A. W. Beck, L. Girard, M. R. Jaber, C. C. Barnett, R. A. Brekken, and J. B. Fleming (2005). "Increased expression of Cyr61 (CCN1) identified in peritoneal metastases from human pancreatic cancer". In: *J Am Coll Surg* 200.3, pp. 371–7 (cit. on p. 7).

Hornung, V., A. Ablasser, M. Charrel-Dennis, F. Bauernfeind, G. Horvath, D. R. Caffrey, E. Latz, and K. A. Fitzgerald (2009). "AIM2 recognizes cytosolic dsDNA and forms a caspase-1-activating inflammasome with ASC". In: *Nature* 458.7237, pp. 514–8 (cit. on p. 94).

Horowitz, M. C., Y Xi, K Wilson, and M. A. Kacena (2001). "Control of osteoclastogenesis and bone resorption by members of the TNF family of receptors and ligands". In: *Cytokine Growth Factor Rev* 12.1, pp. 9–18 (cit. on p. 4).

Hsu, S. Y. and A. J. Hsueh (1998). "A splicing variant of the Bcl-2 member Bok with a truncated BH3 domain induces apoptosis but does not dimerize with antiapoptotic Bcl-2 proteins *in vitro*". In: *J Biol Chem* 273.46, pp. 30139–46 (cit. on p. 94).

Hsu, S. Y., A Kaipia, E McGee, M Lomeli, and A. J. Hsueh (1997). "Bok is a pro-apoptotic Bcl-2 protein with restricted expression in reproductive tissues and heterodimerizes with selective anti-apoptotic Bcl-2 family members". In: *Proc Natl Acad Sci USA* 94.23, pp. 12401–6 (cit. on p. 94).

Huang, J., R. Sengupta, A. B. Espejo, M. G. Lee, J. A. Dorsey, M. Richter, S. Opravil, R. Shiekhattar, M. T. Bedford, T. Jenuwein, and S. L. Berger (2007). "p53 is regulated by the lysine demethylase LSD1". In: *Nature* 449.7158, pp. 105–108 (cit. on p. 93).

Huber, W., A. von Heydebreck, H. Sueltmann, A. Poustka, and M. Vingron (2002). "Variance Stabilization Applied to Microarray Data Calibration and to the Quantification of Differential Expression". In: *Bioinformatics* 18 Suppl. 1, S96–S104 (cit. on p. 63).

Hung, L., J. Lai, L. Lin, S. Wang, T. Hou, D. Chang, C. Liang, and L. Ho (2008). "Retinoid acid inhibits IL-1-induced iNOS, COX-2 and chemokine production in human chondrocytes". In: *Immunological Investigations* 37.7, pp. 675–693 (cit. on p. 144).

Hurvitz, J. R., W. M. Suwairi, W. V. Hul, H El-Shanti, A Superti-Furga, et al. (1999). "Mutations in the CCN gene family member WISP3 cause progressive pseudorheumatoid dysplasia". In: *Nat Genet* 23.1, pp. 94–8 (cit. on p. 11).

In 't Anker, P. S., W. A. Noort, A. B. Kruisselbrink, S. A. Scherjon, W. Beekhuizen, R. Willemze, H. H. H. Kanhai, and W. E. Fibbe (2003). "Nonexpanded primary lung and bone marrow-derived mesenchymal cells promote the engraftment of umbilical cord blood-derived CD34(+) cells in NOD/SCID mice". In: *Exp Hematol* 31.10, pp. 881–9 (cit. on p. 137).

Ingram, R. T., B. L. Clarke, L. W. Fisher, and L. A. Fitzpatrick (1993). "Distribution of noncollagenous proteins in the matrix of adult human bone: evidence of anatomic and functional heterogeneity". In: *J Bone Miner Res* 8.9, pp. 1019–29 (cit. on p. 138).

Inkson, C. A., M. Ono, S. A. Kuznetsov, L. W. Fisher, P. G. Robey, and M. F. Young (2008). "TGF-β1 and WISP-1/CCN-4 can regulate each other's activity to cooperatively control osteoblast function". In: *J. Cell. Biochem.* 104.5, pp. 1865–1878 (cit. on pp. 9, 138).

Inkson, C. A., M. Ono, Y. Bi, S. A. Kuznetsov, L. W. Fisher, and M. F. Young (2009). "The Potential Functional Interaction of Biglycan and WISP-1 in Controlling Differentiation and Proliferation of Osteogenic Cells". In: *Cells Tissues Organs* 189.1-4, pp. 153–157 (cit. on pp. 9, 138).

Jacobson, M. D., M Weil, and M. C. Raff (1997). "Programmed cell death in animal development". In: *Cell* 88.3, pp. 347–54 (cit. on p. 129).

Javelaud, D and F Besançon (2001). "NF-kappa B activation results in rapid inactivation of JNK in TNF alpha-treated Ewing sarcoma cells: a mechanism for the anti-apoptotic effect of NF-kappa B". In: *Oncogene* 20.32, pp. 4365–72 (cit. on p. 134).

Joliot, V, C Martinerie, G Dambrine, G Plassiart, M Brisac, J Crochet, and B Perbal (1992). "Proviral rearrangements and overexpression of a new cellular gene (nov) in myeloblastosis-associated virus type 1-induced nephroblastomas". In: *Mol Cell Biol* 12.1, pp. 10–21 (cit. on p. 7).

Kapoor, P., L. J. Suva, D. R. Welch, and H. J. Donahue (2008). "Osteoprotegrin and the bone homing and colonization potential of breast cancer cells". In: *J Cell Biochem* 103.1, pp. 30–41 (cit. on p. 144).

Kawaki, H., S. Kubota, A. Suzuki, M. Suzuki, K. Kohsaka, K. Hoshi, T. Fujii, N. Lazar, T. Ohgawara, T. Maeda, B. Perbal, T. Takano-Yamamoto, and M. Takigawa (2011). "Differential roles of CCN family proteins during osteoblast differentiation: Involvement of Smad and MAPK signaling pathways". In: *Bone*, pp. 1–15 (cit. on pp. 134, 144).

Kerr, J. F., A. H. Wyllie, and A. R. Currie (1972). "Apoptosis: a basic biological phenomenon with wide-ranging implications in tissue kinetics". In: *Br J Cancer* 26.4, pp. 239–57 (cit. on p. 129).

Kibler, K. V., T Shors, K. B. Perkins, C. C. Zeman, M. P. Banaszak, J Biesterfeldt, J. O. Langland, and B. L. Jacobs (1997). "Double-stranded RNA is a trigger for apoptosis in vaccinia virus-infected cells". In: *J Virol* 71.3, pp. 1992–2003 (cit. on p. 92).

Kiessling, M. K., B. Linke, M. Brechmann, D. Süss, P. H. Krammer, and K. Gülow (2010). "Inhibition of NF-kappaB induces a switch from CD95L-dependent to CD95L-independent and JNK-mediated apoptosis in T cells". In: *FEBS Letters* 584.22, pp. 4679–88 (cit. on p. 95).

Kim, J.-Y., H.-J. Ahn, J.-H. Ryu, K. Suk, and J.-H. Park (2004). "BH3-only protein Noxa is a mediator of hypoxic cell death induced by hypoxia-inducible factor 1alpha". In: *J Exp Med* 199.1, pp. 113–24 (cit. on p. 94).

Kitagawa, M., S. H. Lee, and F. McCormick (2008). "Skp2 suppresses p53-dependent apoptosis by inhibiting p300". In: *Mol Cell* 29.2, pp. 217–31 (cit. on p. 94).

Königshoff, M., M. Kramer, N. Balsara, J. Wilhelm, O. V. Amarie, A. Jahn, F. Rose, L. Fink, W. Seeger, L. Schaefer, A. Günther, and O. Eickelberg (2009). "WNT1-inducible signaling protein-1 mediates pulmonary fibrosis in mice and is upregulated in humans with idiopathic pulmonary fibrosis". In: *J Clin Invest* 119.4, pp. 772–87 (cit. on p. 137).

Kotamraju, S, E. A. Konorev, J Joseph, and B Kalyanaraman (2000). "Doxorubicin-induced apoptosis in endothelial cells and cardiomyocytes is ameliorated by nitrone spin traps and ebselen. Role of reactive oxygen and nitrogen species". In: *J Biol Chem* 275.43, pp. 33585–92 (cit. on p. 133).

Krampera, M., S. Glennie, J. Dyson, D. Scott, R. Laylor, E. Simpson, and F. Dazzi (2003). "Bone marrow mesenchymal stem cells inhibit the response of naive and memory antigen-specific T cells to their cognate peptide". In: *Blood* 101.9, pp. 3722–9 (cit. on p. 137).

Kroemer, G and J. C. Reed (2000). "Mitochondrial control of cell death". In: *Nat Med* 6.5, pp. 513–9 (cit. on p. 132).

Kubota, S. and M. Takigawa (2011). "The role of CCN2 in cartilage and bone development". In: *J. Cell Commun. Signal.* 5.3, pp. 209–217 (cit. on p. 5).

Lau, L. F. and S. C. Lam (1999). "The CCN family of angiogenic regulators: the integrin connection". In: *Experimental Cell Research* 248.1, pp. 44–57 (cit. on p. 7).

Leask, A and D. J Abraham (2006). "All in the CCN family: essential matricellular signaling modulators emerge from the bunker". In: *Journal of Cell Science* 119.23, pp. 4803–4810 (cit. on p. 7).

L'Ecuyer, T., S. Sanjeev, R. Thomas, R. Novak, L. Das, W. Campbell, and R. V. Heide (2006). "DNA damage is an early event in doxorubicin-induced cardiac myocyte death". In: *Am J Physiol Heart Circ Physiol* 291.3, H1273–80 (cit. on p. 133).

Lee, S. B. and M Esteban (1994). "The interferon-induced double-stranded RNA-activated protein kinase induces apoptosis". In: *Virology* 199.2, pp. 491–6 (cit. on p. 92).

Leppert, D, R. L. Lindberg, L Kappos, and S. L. Leib (2001). "Matrix metalloproteinases: multifunctional effectors of inflammation in multiple sclerosis and bacterial meningitis". In: *Brain Res Brain Res Rev* 36.2-3, pp. 249–57 (cit. on p. 138).

Leung, K. M., L. S. Po, F. C. Tsang, W. Y. Siu, A. Lau, H. T. B. Ho, and R. Y. C. Poon (2002). "The candidate tumor suppressor ING1b can stabilize p53 by disrupting the regulation of p53 by MDM2". In: *Cancer Res* 62.17, pp. 4890–3 (cit. on p. 93).

Li, H, H Zhu, C. J. Xu, and J Yuan (1998). "Cleavage of BID by caspase 8 mediates the mitochondrial damage in the Fas pathway of apoptosis". In: *Cell* 94.4, pp. 491–501 (cit. on p. 131).

Li, P, D Nijhawan, I Budihardjo, S. M. Srinivasula, M Ahmad, E. S. Alnemri, and X Wang (1997). "Cytochrome c and dATP-dependent formation of Apaf-1/caspase-9 complex initiates an apoptotic protease cascade". In: *Cell* 91.4, pp. 479–89 (cit. on p. 92).

Lin, C. G., S.-J. Leu, N. Chen, C. M. Tebeau, S.-X. Lin, C.-Y. Yeung, and L. F. Lau (2003). "CCN3 (NOV) is a novel angiogenic regulator of the CCN protein family". In: *J Biol Chem* 278.26, pp. 24200–8 (cit. on p. 7).

Lin, C. G., C.-C. Chen, S.-J. Leu, T. M. Grzeszkiewicz, and L. F. Lau (2005). "Integrin-dependent functions of the angiogenic inducer NOV (CCN3): implication in wound healing". In: *J Biol Chem* 280.9, pp. 8229–37 (cit. on p. 7).

Lindl, T. (2002). *Zell-und Gewebekultur*. Spektrum Akademischer Verlag, Heidelberg, Germany (cit. on p. 47).

Liu, X, C. N. Kim, J Yang, R Jemmerson, and X Wang (1996). "Induction of apoptotic program in cell-free extracts: requirement for dATP and cytochrome c". In: *Cell* 86.1, pp. 147–57 (cit. on p. 92).

Liu, Y., C. László, Y. Liu, W. Liu, X. Chen, S. C. Evans, and S. Wu (2010). "Regulation of G(1) arrest and apoptosis in hypoxia by PERK and GCN2-mediated eIF2alpha phosphorylation". In: *Neoplasia* 12.1, pp. 61–8 (cit. on p. 93).

Liu, Z., H. Lu, Z. Jiang, A. Pastuszyn, and C. an A Hu (2005). "Apolipoprotein l6, a novel proapoptotic Bcl-2 homology 3-only protein, induces mitochondria-mediated apoptosis in cancer cells". In: *Mol Cancer Res* 3.1, pp. 21–31 (cit. on p. 94).

Loebinger, M. R, A Eddaoudi, D Davies, and S. M Janes (2009). "Mesenchymal Stem Cell Delivery of TRAIL Can Eliminate Metastatic Cancer". In: *Cancer Research* 69.10, pp. 4134–4142 (cit. on p. 92).

Lokshin, A, J. E. Mayotte, and M. L. Levitt (1995). "Mechanism of interferon beta-induced squamous differentiation and programmed cell death in human non-small-cell lung cancer cell lines". In: *J Natl Cancer Inst* 87.3, pp. 206–12 (cit. on p. 137).

Longo, K. A., J. A. Kennell, M. J. Ochocinska, S. E. Ross, W. S. Wright, and O. A. MacDougald (2002). "Wnt signaling protects 3T3-L1 preadipocytes from apoptosis through induction of insulin-like growth factors". In: *J Biol Chem* 277.41, pp. 38239–44 (cit. on p. 11).

Loughlin, J., B. Dowling, K. Chapman, L. Marcelline, Z. Mustafa, L. Southam, A. Ferreira, C. Ciesielski, D. A. Carson, and M. Corr (2004). "Functional variants within the secreted frizzled-related protein 3 gene are associated with hip osteoarthritis in females". In: *Proc Natl Acad Sci USA* 101.26, pp. 9757–62 (cit. on p. 138).

Luo, X, I Budihardjo, H Zou, C Slaughter, and X Wang (1998). "Bid, a Bcl2 interacting protein, mediates cytochrome c release from mitochondria in response to activation of cell surface death receptors". In: *Cell* 94.4, pp. 481–90 (cit. on p. 131).

Mancuso, D. J., E. A. Tuley, L. A. Westfield, N. K. Worrall, B. B. Shelton-Inloes, J. M. Sorace, Y. G. Alevy, and J. E. Sadler (1989). "Structure of the gene for human von Willebrand factor". In: *J Biol Chem* 264.33, pp. 19514–27 (cit. on p. 9).

Margalit, O, L Eisenbach, N Amariglio, N Kaminski, A Harmelin, R Pfeffer, M Shohat, G Rechavi, and R Berger (2003). "Overexpression of a set of genes, including WISP-1, common to pulmonary metastases of both mouse D122 Lewis lung carcinoma and B16-F10.9 melanoma cell lines". In: *Br J Cancer* 89.2, pp. 314–9 (cit. on p. 137).

Marraco, S. A. F., C. L. Scott, P. Bouillet, A. Ives, S. Masina, D. Vremec, E. S. Jansen, L. A. O'reilly, P. Schneider, N. Fasel, K. Shortman, A. Strasser, and H. Acha-Orbea (2011). "Type I Interferon Drives Dendritic Cell Apoptosis via Multiple BH3-Only Proteins following Activation by PolyIC In Vivo". In: *PLoS ONE* 6.6, e20189 (cit. on p. 95).

Marsters, S. A., R. M. Pitti, C. J. Donahue, S Ruppert, K. D. Bauer, and A Ashkenazi (1996). "Activation of apoptosis by Apo-2 ligand is independent of FADD but blocked by CrmA". In: *Curr Biol* 6.6, pp. 750–2 (cit. on p. 92).

Martin, T. J. (1983). "Drug and hormone effects on calcium release from bone". In: *Pharmacol Ther* 21.2, pp. 209–28 (cit. on pp. 3, 4).

Martinez-Sanchez, A., K. A. Dudek, and C. L. Murphy (2012). "Regulation of Human Chondrocyte Function through Direct Inhibition of Cartilage Master Regulator SOX9 by MicroRNA-145 (miRNA-145)". In: *J Biol Chem* 287.2, pp. 916–24 (cit. on p. 139).

McKenna, L. A., H Liu, P. A. Sansom, and M. F. Dean (1998). "An N-terminal peptide from link protein stimulates proteoglycan biosynthesis in human articular cartilage *in vitro*". In: *Arthritis Rheum* 41.1, pp. 157–62 (cit. on p. 139).

Mukhopadhyay, A, J Ni, Y Zhai, G. L. Yu, and B. B. Aggarwal (1999). "Identification and characterization of a novel cytokine, THANK, a TNF homologue that activates apoptosis, nuclear factor-kappaB, and c-Jun NH2-terminal kinase". In: *J Biol Chem* 274.23, pp. 15978–81 (cit. on p. 95).

Muraglia, A, R Cancedda, and R Quarto (2000). "Clonal mesenchymal progenitors from human bone marrow differentiate *in vitro* according to a hierarchical model". In: *J Cell Sci* 113 (Pt 7), pp. 1161–6 (cit. on p. 3).

Murphy, G and M. H. Lee (2005). "What are the roles of metalloproteinases in cartilage and bone damage?" In: *Annals of the Rheumatic Diseases* 64 Suppl 4, pp. iv44–7 (cit. on p. 138).

Nakamura, I., N. Takahashi, E. Jimi, N. Udagawa, and T. Suda (2011). "Regulation of osteoclast function". In: *Mod Rheumatol* (cit. on p. 4).

Nakamura, Y., G. Weidinger, J. O. Liang, A. Aquilina-Beck, K. Tamai, R. T. Moon, and M. L. Warman (2007). "The CCN family member Wisp3, mutant in progressive pseudorheumatoid dysplasia, modulates BMP and Wnt signaling". In: *J. Clin. Invest.* 117.10, pp. 3075–3086 (cit. on p. 11).

Nakanishi, T, T Nishida, T Shimo, K Kobayashi, T Kubo, T Tamatani, K Tezuka, and M Takigawa (2000). "Effects of CTGF/Hcs24, a product of a hypertrophic chondrocyte-specific gene, on the proliferation and differentiation of chondrocytes in culture". In: *Endocrinology* 141.1, pp. 264–73 (cit. on p. 7).

Nakata, E, T Nakanishi, A Kawai, K Asaumi, T Yamaai, M Asano, T Nishida, S Mitani, H Inoue, and M Takigawa (2002). "Expression of connective tissue growth factor/hypertrophic chondrocyte-specific gene product 24 (CTGF/Hcs24) during fracture healing". In: *Bone* 31.4, pp. 441–7 (cit. on p. 125).

Newsom-Davis, T., S. Prieske, and H. Walczak (2009). "Is TRAIL the holy grail of cancer therapy?" In: *Apoptosis* 14.4, pp. 607–623 (cit. on p. 143).

Nishida, T, T Nakanishi, M Asano, T Shimo, and M Takigawa (2000). "Effects of CTGF/Hcs24, a hypertrophic chondrocyte-specific gene product, on the proliferation and differentiation of osteoblastic cells *in vitro*". In: *J Cell Physiol* 184.2, pp. 197–206 (cit. on p. 7).

Nöth, U., R. Tuli, A. M. Osyczka, K. G. Danielson, and R. S. Tuan (2002). "In vitro engineered cartilage constructs produced by press-coating biodegradable polymer with human mesenchymal stem cells". In: *Tissue Eng* 8.1, pp. 131–44 (cit. on p. 4).

Nuñez, G, M. A. Benedict, Y Hu, and N Inohara (1998). "Caspases: the proteases of the apoptotic pathway". In: *Oncogene* 17.25, pp. 3237–45 (cit. on pp. 64, 129).

O'Brien, T. P. and L. F. Lau (1992). "Expression of the growth factor-inducible immediate early gene cyr61 correlates with chondrogenesis during mouse embryonic development". In: *Cell Growth Differ* 3.9, pp. 645–54 (cit. on p. 125).

O'Brien, T. P., G. P. Yang, L Sanders, and L. F. Lau (1990). "Expression of cyr61, a growth factor-inducible immediate-early gene". In: *Mol Cell Biol* 10.7, pp. 3569–77 (cit. on p. 7).

Oda, E, R Ohki, H Murasawa, J Nemoto, T Shibue, T Yamashita, T Tokino, T Taniguchi, and N Tanaka (2000). "Noxa, a BH3-only member of the Bcl-2 family and candidate mediator of p53-induced apoptosis". In: *Science* 288.5468, pp. 1053–8 (cit. on pp. 94, 132).

Ogata, H., S. Goto, K. Sato, W. Fujibuchi, H. Bono, and M. Kanehisa (1999). "KEGG: Kyoto encyclopedia of genes and genomes". In: *Nucleic acids research* 27.1, p. 29 (cit. on p. 86).

Olson, R. D. and P. S. Mushlin (1990). "Doxorubicin cardiotoxicity: analysis of prevailing hypotheses". In: *FASEB J* 4.13, pp. 3076–86 (cit. on p. 133).

Ono, M., C. A. Inkson, T. M. Kilts, and M. F. Young (2011). "WISP-1/CCN4 regulates osteogenesis by enhancing BMP-2 activity". In: *J Bone Miner Res* 26.1, pp. 193–208 (cit. on p. 9).

Oshima, S., E. E. Turer, J. A. Callahan, S. Chai, R. Advincula, J. Barrera, N. Shifrin, B. Lee, B. Yen, T. Woo, B. A. Malynn, and A. Ma (2009). "ABIN-1 is a ubiquitin sensor that restricts cell death and sustains embryonic development". In: *Nature* 457.7231, pp. 906–909 (cit. on p. 92).

Palfrey, A. and D. Davies (1966). "The fine structure of chondrocytes." In: *Journal of anatomy* 100.Pt 2, p. 213 (cit. on pp. 4, 138).

Pan, G, K O'Rourke, A. M. Chinnaiyan, R Gentz, R Ebner, J Ni, and V. M. Dixit (1997). "The receptor for the cytotoxic ligand TRAIL". In: *Science* 276.5309, pp. 111–3 (cit. on pp. 93, 131).

Pederson, L., M. Ruan, J. J. Westendorf, S. Khosla, and M. J. Oursler (2008). "Regulation of bone formation by osteoclasts involves Wnt/BMP signaling and the chemokine sphingosine-1-phosphate". In: *Proc Natl Acad Sci USA* 105.52, pp. 20764–9 (cit. on p. 4).

Peng, S., J. Geng, R. Sun, Z. Tian, and H. Wei (2009). "Polyinosinic-polycytidylic acid liposome induces human hepatoma cells apoptosis which correlates to the up-regulation of RIG-I like receptors". In: *Cancer Science* 100.3, pp. 529–536 (cit. on pp. 94, 95).

Pennica, D, T. A. Swanson, J. W. Welsh, M. A. Roy, D. A. Lawrence, et al. (1998). "WISP genes are members of the connective tissue growth factor family that are up-regulated in wnt-1-transformed cells and aberrantly expressed in human colon tumors". In: *Proc Natl Acad Sci USA* 95.25, pp. 14717–22 (cit. on pp. 9, 11, 133, 137).

Perbal, B (2001). "NOV (nephroblastoma overexpressed) and the CCN family of genes: structural and functional issues". In: *MP, Mol Pathol* 54.2, pp. 57–79 (cit. on p. 7).

Perbal, B. (2004). "CCN proteins: multifunctional signalling regulators". In: *Lancet* 363.9402, pp. 62–4 (cit. on p. 7).

Pereira, R. F., K. W. Halford, M. D. O'Hara, D. B. Leeper, B. P. Sokolov, M. D. Pollard, O Bagasra, and D. J. Prockop (1995). "Cultured adherent cells from marrow can serve as long-lasting precursor

cells for bone, cartilage, and lung in irradiated mice". In: *Proc Natl Acad Sci USA* 92.11, pp. 4857–61 (cit. on p. 3).
Pittenger, M. F., A. M. Mackay, S. C. Beck, R. K. Jaiswal, R Douglas, J. D. Mosca, M. A. Moorman, D. W. Simonetti, S Craig, and D. R. Marshak (1999). "Multilineage potential of adult human mesenchymal stem cells". In: *Science* 284.5411, pp. 143–7 (cit. on pp. 3, 4).
Ponte, A. L., E. Marais, N. Gallay, A. Langonné, B. Delorme, O. Hérault, P. Charbord, and J. Domenech (2007). "The In Vitro Migration Capacity of Human Bone Marrow Mesenchymal Stem Cells: Comparison of Chemokine and Growth Factor Chemotactic Activities". In: *Stem Cells* 25.7, pp. 1737–1745 (cit. on p. 4).
Prockop, D. J. (1997). "Marrow stromal cells as stem cells for nonhematopoietic tissues". In: *Science* 276.5309, pp. 71–4 (cit. on p. 3).
Puthalakath, H, D. C. Huang, L. A. O'Reilly, S. M. King, and A Strasser (1999). "The proapoptotic activity of the Bcl-2 family member Bim is regulated by interaction with the dynein motor complex". In: *Mol Cell* 3.3, pp. 287–96 (cit. on p. 132).
Qin, X. Q., L Runkel, C Deck, C DeDios, and J Barsoum (1997). "Interferon-beta induces S phase accumulation selectively in human transformed cells". In: *J Interferon Cytokine Res* 17.6, pp. 355–67 (cit. on p. 137).
R Development Core Team (2010). "R: A language and environment for statistical computing". In: *R Foundation for Statistical Computing Vienna Austria* 01/19 (cit. on pp. 46, 62, 85, 86).
Rachner, T. D., P. Benad, M. Rauner, C. Goettsch, S. K. Singh, M. Schoppet, and L. C. Hofbauer (2009). "Osteoprotegerin production by breast cancer cells is suppressed by dexamethasone and confers resistance against TRAIL-induced apoptosis". In: *J. Cell. Biochem.* 108.1, pp. 106–116 (cit. on p. 144).
Renshaw, S. A., C. E. Dempsey, F. A. Barnes, S. M. Bagstaff, S. K. Dower, C. D. Bingle, and M. K. B. Whyte (2004). "Three novel Bid proteins generated by alternative splicing of the human Bid gene". In: *J Biol Chem* 279.4, pp. 2846–55 (cit. on p. 92).
Reya, T. (2003). "Regulation of hematopoietic stem cell self-renewal". In: *Recent Prog Horm Res* 58, pp. 283–95 (cit. on p. 3).
Rockel, J. S., S. M. Bernier, and A. Leask (2009). "Egr-1 inhibits the expression of extracellular matrix genes in chondrocytes by TNFalpha-induced MEK/ERK signalling". In: *Arthritis Res Ther* 11.1, R8 (cit. on p. 139).
Ross, S. E., N Hemati, K. A. Longo, C. N. Bennett, P. C. Lucas, R. L. Erickson, and O. A. MacDougald (2000). "Inhibition of adipogenesis by Wnt signaling". In: *Science* 289.5481, pp. 950–3 (cit. on p. 11).
Rozen, S and H Skaletsky (2000). "Primer3 on the WWW for general users and for biologist programmers". In: *Methods Mol Biol* 132, pp. 365–86 (cit. on pp. 28, 46, 62).
Rudnicki, J. A. and A. M. Brown (1997). "Inhibition of chondrogenesis by Wnt gene expression *in vivo* and *in vitro*". In: *Dev Biol* 185.1, pp. 104–18 (cit. on p. 138).
Sacchetti, B., A. Funari, S. Michienzi, S. D. Cesare, S. Piersanti, I. Saggio, E. Tagliafico, S. Ferrari, P. G. Robey, M. Riminucci, and P. Bianco (2007). "Self-renewing osteoprogenitors in bone marrow sinusoids can organize a hematopoietic microenvironment". In: *Cell* 131.2, pp. 324–36 (cit. on p. 4).
Sakaguchi, K, J. E. Herrera, S Saito, T Miki, M Bustin, A Vassilev, C. W. Anderson, and E Appella (1998). "DNA damage activates p53 through a phosphorylation-acetylation cascade". In: *Genes & Development* 12.18, pp. 2831–41 (cit. on p. 144).
Sax, J. K., P. Fei, M. E. Murphy, E. Bernhard, S. J. Korsmeyer, and W. S. El-Deiry (2002). "BID regulation by p53 contributes to chemosensitivity". In: *Nat Cell Biol* 4.11, pp. 842–9 (cit. on p. 132).
Schilling, T., R. Küffner, L. Klein-Hitpass, R. Zimmer, F. Jakob, and N. Schütze (2008). "Microarray analyses of transdifferentiated mesenchymal stem cells". In: *J. Cell. Biochem.* 103.2, pp. 413–433 (cit. on p. 4).
Schuetze, N., U. Noeth, J. Schneidereit, C. Hendrich, and F. Jakob (2005). "Differential expression of CCN-family members in primary human bone marrow-derived mesenchymal stem cells during osteogenic, chondrogenic and adipogenic differentiation". In: *Cell Commun Signal* 3.1, p. 5 (cit. on pp. 4, 7–9, 11, 125).
Scoumanne, A and X Chen (2008). "Protein methylation: a new mechanism of p53 tumor suppressor regulation". In: *Histol Histopathol* 23.9, pp. 1143–9 (cit. on p. 93).

Séguin, C. A. and S. M. Bernier (2003). "TNFalpha suppresses link protein and type II collagen expression in chondrocytes: Role of MEK1/2 and NF-kappaB signaling pathways". In: *J. Cell. Physiol.* 197.3, pp. 357–69 (cit. on p. 139).

Sen, M., Y.-H. Cheng, M. B. Goldring, M. K. Lotz, and D. A. Carson (2004). "WISP3-dependent regulation of type II collagen and aggrecan production in chondrocytes". In: *Arthritis Rheum* 50.2, pp. 488–497 (cit. on p. 11).

Seo, Y.-W., J. N. Shin, K. H. Ko, J. H. Cha, J. Y. Park, B. R. Lee, C.-W. Yun, Y. M. Kim, D. wu Seol, D. wook Kim, X.-M. Yin, and T.-H. Kim (2003). "The molecular mechanism of Noxa-induced mitochondrial dysfunction in p53-mediated cell death". In: *J Biol Chem* 278.48, pp. 48292–9 (cit. on pp. 94, 132).

Sheridan, J. P., S. A. Marsters, R. M. Pitti, A Gurney, M Skubatch, D Baldwin, L Ramakrishnan, C. L. Gray, K Baker, W. I. Wood, A. D. Goddard, P Godowski, and A Ashkenazi (1997). "Control of TRAIL-induced apoptosis by a family of signaling and decoy receptors". In: *Science* 277.5327, pp. 818–21 (cit. on pp. 93, 131, 144).

Shieh, S. Y., M Ikeda, Y Taya, and C Prives (1997). "DNA damage-induced phosphorylation of p53 alleviates inhibition by MDM2". In: *Cell* 91.3, pp. 325–34 (cit. on p. 144).

Shieh, S. Y., Y Taya, and C Prives (1999). "DNA damage-inducible phosphorylation of p53 at N-terminal sites including a novel site, Ser20, requires tetramerization". In: *EMBO J* 18.7, pp. 1815–23 (cit. on p. 144).

Shikama, N, C. W. Lee, S France, L Delavaine, J Lyon, M Krstic-Demonacos, and N. B. L. Thangue (1999). "A novel cofactor for p300 that regulates the p53 response". In: *Mol Cell* 4.3, pp. 365–76 (cit. on pp. 93, 132).

Shu, B., M. Zhang, R. Xie, M. Wang, H. Jin, W. Hou, D. Tang, S. E. Harris, Y. Mishina, R. J. O'Keefe, M. J. Hilton, Y. Wang, and D. Chen (2011). "BMP2, but not BMP4, is crucial for chondrocyte proliferation and maturation during endochondral bone development". In: *Journal of Cell Science* 124.Pt 20, pp. 3428–40 (cit. on p. 5).

Shuman, S (1991). "Site-specific DNA cleavage by vaccinia virus DNA topoisomerase I. Role of nucleotide sequence and DNA secondary structure". In: *J Biol Chem* 266.3, pp. 1796–803 (cit. on p. 51).

Siliciano, J. D., C. E. Canman, Y Taya, K Sakaguchi, E Appella, and M. B. Kastan (1997). "DNA damage induces phosphorylation of the amino terminus of p53". In: *Genes & Development* 11.24, pp. 3471–81 (cit. on p. 144).

Simmons, P., S. Gronthos, A. Zannettino, S. Ohta, and S. Graves (1994). "Isolation, characterization and functional activity of human marrow stromal progenitors in hemopoiesis." In: *Progress in clinical and biological research* 389, p. 271 (cit. on p. 4).

Simonet, W. S., D. L. Lacey, C. R. Dunstan, M Kelley, M. S. Chang, et al. (1997). "Osteoprotegerin: a novel secreted protein involved in the regulation of bone density". In: *Cell* 89.2, pp. 309–19 (cit. on p. 131).

Sims, N. A. and J. H. Gooi (2008). "Bone remodeling: Multiple cellular interactions required for coupling of bone formation and resorption". In: *Semin Cell Dev Biol* 19.5, pp. 444–51 (cit. on p. 4).

Smith, R. L. (1999). "Degradative enzymes in osteoarthritis". In: *Front Biosci* 4, pp. D704–12 (cit. on p. 138).

Smyth, G. K. (2005). "Limma: linear models for microarray data". In: *Bioinformatics and Computational Biology Solutions using R and Bioconductor*. Ed. by R. Gentleman, V. Carey, S. Dudoit, R. Irizarry, and W. Huber. New York: Springer, pp. 397–420 (cit. on p. 63).

Stang, M. T., M. J. Armstrong, G. A. Watson, K. Y. Sung, Y Liu, B Ren, and J. H. Yim (2007). "Interferon regulatory factor-1-induced apoptosis mediated by a ligand-independent fas-associated death domain pathway in breast cancer cells". In: *Oncogene* 26.44, pp. 6420–6430 (cit. on p. 92).

Stegh, A. H, H Kim, R. M Bachoo, K. L Forloney, J Zhang, H Schulze, K Park, G. J Hannon, J Yuan, D. N Louis, R. A Depinho, and L Chin (2007). "Bcl2L12 inhibits post-mitochondrial apoptosis signaling in glioblastoma". In: *Genes & Development* 21.1, pp. 98–111 (cit. on p. 93).

Stegh, A. H. and R. A. Depinho (2011). "Beyond effector caspase inhibition: Bcl2L12 neutralizes p53 signaling in Glioblastoma". In: *cc* 10.1, pp. 33–38 (cit. on p. 93).

Su, F., M. Overholtzer, D. Besser, and A. J. Levine (2002). "WISP-1 attenuates p53-mediated apoptosis in response to DNA damage through activation of the Akt kinase". In: *Genes & Development* 16.1, pp. 46–57 (cit. on pp. 11, 125, 129, 133).

Suda, T, N Takahashi, N Udagawa, E Jimi, M. T. Gillespie, and T. J. Martin (1999). "Modulation of osteoclast differentiation and function by the new members of the tumor necrosis factor receptor and ligand families". In: *Endocr Rev* 20.3, pp. 345–57 (cit. on p. 4).

Sun, R., Y. Zhang, Q. Lv, B. Liu, M. Jin, et al. (2011). "Toll-like receptor 3 (TLR3) induces apoptosis via death receptors and mitochondria by up-regulating the transactivating p63 isoform alpha (TAP63alpha)". In: *J Biol Chem* 286.18, pp. 15918–28 (cit. on p. 95).

Takizawa, T, R Fukuda, T Miyawaki, K Ohashi, and Y Nakanishi (1995). "Activation of the apoptotic Fas antigen-encoding gene upon influenza virus infection involving spontaneously produced beta-interferon". In: *Virology* 209.2, pp. 288–96 (cit. on p. 92).

Ten Dijke, P., C. Krause, D. J. J. de Gorter, C. W. G. M. Löwik, and R. L. van Bezooijen (2008). "Osteocyte-derived sclerostin inhibits bone formation: its role in bone morphogenetic protein and Wnt signaling". In: *J Bone Joint Surg Am* 90 Suppl 1, pp. 31–5 (cit. on p. 4).

Thalappilly, S., X. Feng, S. Pastyryeva, K. Suzuki, D. Muruve, D. Larocque, S. Richard, M. Truss, A. V. Deimling, K. Riabowol, and G. Tallen (2011). "The p53 Tumor Suppressor Is Stabilized by Inhibitor of Growth 1 (ING1) by Blocking Polyubiquitination". In: *PLoS ONE* 6.6, e21065 (cit. on p. 93).

Thomadaki, H. and A. Scorilas (2006). "BCL2Family of Apoptosis-Related Genes: Functions and Clinical Implications in Cancer". In: *Critical Reviews in Clinical Laboratory Sciences* 43.1, pp. 1–67 (cit. on p. 132).

Thompson, J., T. Gibson, and D. Higgins (2002). "Multiple sequence alignment using ClustalW and ClustalX". In: *Current protocols in bioinformatics* (cit. on p. 45).

Thornberry, N. A. (1999). "Caspases: a decade of death research". In: *Cell Death Differ* 6.11, pp. 1023–7 (cit. on pp. 64, 129).

Till, J. E. and E. A. McCulloch (2011). "A direct measurement of the radiation sensitivity of normal mouse bone marrow cells. 1961". In: *Radiat Res* 175.2, pp. 145–9 (cit. on p. 3).

Tinel, A. and J. Tschopp (2004). "The PIDDosome, a protein complex implicated in activation of caspase-2 in response to genotoxic stress". In: *Science* 304.5672, pp. 843–6 (cit. on p. 94).

Tournier, C., C. Dong, T. Turner, S. Jones, R. Flavell, and R. Davis (2001). "MKK7 is an essential component of the JNK signal transduction pathway activated by proinflammatory cytokines". In: *Genes & development* 15.11, p. 1419 (cit. on p. 134).

Tsuda, E., M. Goto, S. Mochizuki, K. Yano, F. Kobayashi, T. Morinaga, and K. Higashio (1997). "Isolation of a novel cytokine from human fibroblasts that specifically inhibits osteoclastogenesis". In: *Biochemical and biophysical research communications* 234.1, pp. 137–142 (cit. on pp. 131, 144).

Tuan, R. S., G. Boland, and R. Tuli (2003). "Adult mesenchymal stem cells and cell based tissue engineering". In: *Arthritis Res Ther* 5.1, p. 32 (cit. on p. 3).

Urano, T., K. Narusawa, M. Shiraki, T. Usui, N. Sasaki, T. Hosoi, Y. Ouchi, T. Nakamura, and S. Inoue (2007). "Association of a single nucleotide polymorphism in the WISP1 gene with spinal osteoarthritis in postmenopausal Japanese women". In: *J Bone Miner Metab* 25.4, pp. 253–258 (cit. on p. 9).

Väänänen, H. K., H Zhao, M Mulari, and J. M. Halleen (2000). "The cell biology of osteoclast function". In: *J Cell Sci* 113 (Pt 3), pp. 377–81 (cit. on p. 4).

Venkatesan, B., S. D. Prabhu, K. Venkatachalam, S. Mummidi, A. J. Valente, R. A. Clark, P. Delafontaine, and B. Chandrasekar (2010). "WNT1-inducible signaling pathway protein-1 activates diverse cell survival pathways and blocks doxorubicin-induced cardiomyocyte death". In: *Cellular Signalling* 22.5, pp. 809–820 (cit. on pp. 11, 125, 129, 133).

Verfaillie, C. M. (2002). "Adult stem cells: assessing the case for pluripotency". In: *Trends Cell Biol* 12.11, pp. 502–8 (cit. on p. 3).

Voorberg, J, R Fontijn, J Calafat, H Janssen, J. A. van Mourik, and H Pannekoek (1991). "Assembly and routing of von Willebrand factor variants: the requirements for disulfide-linked dimerization reside within the carboxy-terminal 151 amino acids". In: *J Cell Biol* 113.1, pp. 195–205 (cit. on p. 9).

Walczak, H, M. A. Degli-Esposti, R. S. Johnson, P. J. Smolak, J. Y. Waugh, N Boiani, M. S. Timour, M. J. Gerhart, K. A. Schooley, C. A. Smith, R. G. Goodwin, and C. T. Rauch (1997). "TRAIL-R2: a novel apoptosis-mediating receptor for TRAIL". In: *EMBO J* 16.17, pp. 5386–97 (cit. on pp. 93, 131).

Walczak, H, R. E. Miller, K Ariail, B Gliniak, T. S. Griffith, et al. (1999). "Tumoricidal activity of tumor necrosis factor-related apoptosis-inducing ligand *in vivo*". In: *Nat Med* 5.2, pp. 157–63 (cit. on p. 131).

Wan, G., S. Zhaorigetu, Z. Liu, R. Kaini, Z. Jiang, and C. an A Hu (2008). "Apolipoprotein L1, a novel Bcl-2 homology domain 3-only lipid-binding protein, induces autophagic cell death". In: *J Biol Chem* 283.31, pp. 21540–9 (cit. on p. 93).

Wang, S (2008). "The promise of cancer therapeutics targeting the TNF-related apoptosis-inducing ligand and TRAIL receptor pathway". In: *Oncogene* 27.48, pp. 6207–15 (cit. on p. 131).

Wang, X (2001). "The expanding role of mitochondria in apoptosis". In: *Genes Dev* 15.22, pp. 2922–33 (cit. on p. 132).

Watanabe, H and Y Yamada (1999). "Mice lacking link protein develop dwarfism and craniofacial abnormalities". In: *Nat Genet* 21.2, pp. 225–9 (cit. on p. 139).

Wei, M. C., T Lindsten, V. K. Mootha, S Weiler, A Gross, M Ashiya, C. B. Thompson, and S. J. Korsmeyer (2000). "tBID, a membrane-targeted death ligand, oligomerizes BAK to release cytochrome c". In: *Genes Dev* 14.16, pp. 2060–71 (cit. on p. 132).

Wei, M. C., W. X. Zong, E. H. Cheng, T Lindsten, V Panoutsakopoulou, A. J. Ross, K. A. Roth, G. R. MacGregor, C. B. Thompson, and S. J. Korsmeyer (2001). "Proapoptotic BAX and BAK: a requisite gateway to mitochondrial dysfunction and death". In: *Science* 292.5517, pp. 727–30 (cit. on p. 132).

Wiley, S. R., K Schooley, P. J. Smolak, W. S. Din, C. P. Huang, J. K. Nicholl, G. R. Sutherland, T. D. Smith, C Rauch, and C. A. Smith (1995). "Identification and characterization of a new member of the TNF family that induces apoptosis". In: *Immunity* 3.6, pp. 673–82 (cit. on p. 92).

Wolter, K. G., Y. T. Hsu, C. L. Smith, A Nechushtan, X. G. Xi, and R. J. Youle (1997). "Movement of Bax from the cytosol to mitochondria during apoptosis". In: *J Cell Biol* 139.5, pp. 1281–92 (cit. on p. 132).

Wu, G. S., T. F. Burns, E. R. McDonald, W Jiang, R Meng, I. D. Krantz, G Kao, D. D. Gan, J. Y. Zhou, R Muschel, S. R. Hamilton, N. B. Spinner, S Markowitz, G Wu, and W. S. el Deiry (1997). "KILLER/DR5 is a DNA damage-inducible p53-regulated death receptor gene". In: *Nat Genet* 17.2, pp. 141–3 (cit. on p. 132).

Wu, X., J. Shi, Y. Wu, Y. Tao, J. Hou, X. Meng, X. Hu, Y. Han, W. Jiang, S. Tang, M. Zangari, G. Tricot, and F. Zhan (2010). "Arsenic trioxide-mediated growth inhibition of myeloma cells is associated with an extrinsic or intrinsic signaling pathway through activation of TRAIL or TRAIL receptor 2". In: *cbt* 10.11, pp. 1201–1214 (cit. on p. 92).

Wullaert, A., B. Wielockx, S. V. Huffel, V. Bogaert, B. D. Geest, P. Papeleu, P. Schotte, K. E. Bakkouri, K. Heyninck, C. Libert, and R. Beyaert (2005). "Adenoviral gene transfer of ABIN-1 protects mice from TNF/galactosamine-induced acute liver failure and lethality". In: *Hepatology* 42.2, pp. 381–9 (cit. on p. 92).

Wyllie, A. H., J. F. Kerr, and A. R. Currie (1980). "Cell death: the significance of apoptosis". In: *Int Rev Cytol* 68, pp. 251–306 (cit. on p. 129).

Xia, X., E. Park, B. Liu, J. Willette-Brown, W. Gong, J. Wang, D. Mitchell, S. M. Fischer, and Y. Hu (2010). "Reduction of IKKα Expression Promotes Chronic Ultraviolet B Exposure-Induced Skin Inflammation and Carcinogenesis". In: *The American Journal of Pathology* 176.5, pp. 2500–2508 (cit. on p. 94).

Xie, D, K Nakachi, H Wang, R Elashoff, and H. P. Koeffler (2001). "Elevated levels of connective tissue growth factor, WISP-1, and CYR61 in primary breast cancers associated with more advanced features". In: *Cancer Res* 61.24, pp. 8917–23 (cit. on p. 137).

Xu, L, R. B. Corcoran, J. W. Welsh, D Pennica, and A. J. Levine (2000). "WISP-1 is a Wnt-1- and beta-catenin-responsive oncogene". In: *Genes Dev* 14.5, pp. 585–95 (cit. on p. 137).

Yanagita, T., S. Kubota, H. Kawaki, K. Kawata, S. Kondo, T. Takano-Yamamoto, S. Tanaka, and M. Takigawa (2007). "Expression and physiological role of CCN4/Wnt-induced secreted protein mRNA splicing variants in chondrocytes". In: *FEBS Journal* 274.7, pp. 1655–1665 (cit. on pp. 7, 69, 125, 138).

Yang, D. D., C. Y. Kuan, A. J. Whitmarsh, M Rincón, T. S. Zheng, R. J. Davis, P Rakic, and R. A. Flavell (1997). "Absence of excitotoxicity-induced apoptosis in the hippocampus of mice lacking the Jnk3 gene". In: *Nature* 389.6653, pp. 865–70 (cit. on p. 134).

Yang, T, K. M. Kozopas, and R. W. Craig (1995). "The intracellular distribution and pattern of expression of Mcl-1 overlap with, but are not identical to, those of Bcl-2". In: *J Cell Biol* 128.6, pp. 1173–84 (cit. on p. 94).

Yasuda, H, N Shima, N Nakagawa, K Yamaguchi, M Kinosaki, et al. (1998). "Osteoclast differentiation factor is a ligand for osteoprotegerin/osteoclastogenesis-inhibitory factor and is identical to TRANCE/RANKL". In: *Proc Natl Acad Sci USA* 95.7, pp. 3597–602 (cit. on p. 131).

Yeger, H. and B. Perbal (2007). "The CCN family of genes: a perspective on CCN biology and therapeutic potential". In: *J. Cell Commun. Signal.* 1.3-4, pp. 159–164 (cit. on pp. 8, 133).

Yosimichi, G, T Nakanishi, T Nishida, T Hattori, T Takano-Yamamoto, and M Takigawa (2001). "CTGF/Hcs24 induces chondrocyte differentiation through a p38 mitogen-activated protein kinase (p38MAPK), and proliferation through a p44/42 MAPK/extracellular-signal regulated kinase (ERK)". In: *Eur J Biochem* 268.23, pp. 6058–65 (cit. on p. 134).

Younce, C. W. and P. E. Kolattukudy (2010). "MCP-1 causes cardiomyoblast death via autophagy resulting from ER stress caused by oxidative stress generated by inducing a novel zinc-finger protein, MCPIP". In: *Biochem. J.* 426.1, pp. 43–53 (cit. on p. 94).

Young, H. E., C. Duplaa, R. Katz, T. Thompson, K. C. Hawkins, et al. (2005). "Adult-derived stem cells and their potential for use in tissue repair and molecular medicine". In: *J Cell Mol Med* 9.3, pp. 753–69 (cit. on p. 4).

Zauli, G., E. Rimondi, V. Nicolin, E. Melloni, C. Celeghini, and P. Secchiero (2004). "TNF-related apoptosis-inducing ligand (TRAIL) blocks osteoclastic differentiation induced by RANKL plus M-CSF". In: *Blood* 104.7, pp. 2044–50 (cit. on p. 131).

Zha, J, H Harada, E Yang, J Jockel, and S. J. Korsmeyer (1996). "Serine phosphorylation of death agonist BAD in response to survival factor results in binding to 14-3-3 not BCL-X(L)". In: *Cell* 87.4, pp. 619–28 (cit. on p. 11).

Zhang, Y., Q. Pan, H. Zhong, S. D. Merajver, and C. G. Kleer (2005). "Inhibition of CCN6 (WISP3) expression promotes neoplastic progression and enhances the effects of insulin-like growth factor-1 on breast epithelial cells". In: *Breast Cancer Res* 7.6, R1080–9 (cit. on p. 7).

Zhao, K.-W., D. Li, Q. Zhao, Y. Huang, R. H. Silverman, P. J. Sims, and G.-Q. Chen (2005). "Interferon-alpha-induced expression of phospholipid scramblase 1 through STAT1 requires the sequential activation of protein kinase Cdelta and JNK". In: *J Biol Chem* 280.52, pp. 42707–14 (cit. on p. 95).

Zhaorigetu, S., G. Wan, R. Kaini, Z. Jiang, and C. an A Hu (2008). "ApoL1, a BH3-only lipid-binding protein, induces autophagic cell death". In: *Autophagy* 4.8, pp. 1079–82 (cit. on p. 93).

Zhaorigetu, S., Z. Yang, I. Toma, T. A. McCaffrey, and C.-A. A. Hu (2011). "Apolipoprotein L6, induced in atherosclerotic lesions, promotes apoptosis and blocks Beclin 1-dependent autophagy in atherosclerotic cells". In: *J Biol Chem* 286.31, pp. 27389–98 (cit. on p. 94).

Zhivotovsky, B. and S. Orrenius (2005). "Caspase-2 function in response to DNA damage". In: *Biochem Biophys Res Commun* 331.3, pp. 859–67 (cit. on p. 94).

LIST OF FIGURES

LIST OF TABLES

APPENDIX

A

DIFFERENTIALLY EXPRESSED PROBE SETS DURING MICROARRAY ANALYSIS OF WISP1 DOWN-REGULATED HMSCS

Table A.1.: *Listed are all 522 differentially expressed probe sets between shRNA5 transduced hMSC samples and their corresponding scrambled control assays (n=3). Probe sets are ordered according to their descending statistical score (logFc) from highest up-regulation to highest down-regulation. Additional information reflects the probe set ID, their corresponding gene symbol and name as well as the adjusted (corrected for multiple comparisons) p-value.*

Probe set ID	Gene symbol	Gene name	logFc	adj.p-val
242625_at	RSAD2	radical S-adenosyl methionine domain containing 2	4,49	$2{,}07 \times 10^{-5}$
213797_at	RSAD2	radical S-adenosyl methionine domain containing 2	4,41	$7{,}03 \times 10^{-6}$
226702_at	CMPK2	cytidine monophosphate (UMP-CMP) kinase 2, mitochondrial	4,38	$9{,}80 \times 10^{-6}$
226757_at	IFIT2	interferon-induced protein with tetratricopeptide repeats 2	4,05	$1{,}15 \times 10^{-6}$
210797_s_at	OASL	2'-5'-oligoadenylate synthetase-like	3,88	$9{,}61 \times 10^{-6}$
202687_s_at	TNFSF10	tumor necrosis factor (ligand) superfamily, member 10	3,77	$3{,}24 \times 10^{-5}$
205660_at	OASL	2'-5'-oligoadenylate synthetase-like	3,76	$8{,}08 \times 10^{-6}$
214329_x_at	TNFSF10	tumor necrosis factor (ligand) superfamily, member 10	3,69	$8{,}12 \times 10^{-6}$
223502_s_at	TNFSF13B	tumor necrosis factor (ligand) superfamily, member 13b	3,69	$6{,}59 \times 10^{-6}$
202688_at	TNFSF10	tumor necrosis factor (ligand) superfamily, member 10	3,64	$2{,}91 \times 10^{-5}$
217502_at	IFIT2	interferon-induced protein with tetratricopeptide repeats 2	3,56	$8{,}49 \times 10^{-7}$
223501_at	TNFSF13B	tumor necrosis factor (ligand) superfamily, member 13b	3,42	$2{,}28 \times 10^{-5}$
205552_s_at	OAS1	2',5'-oligoadenylate synthetase 1, 40/46kDa	3,28	$8{,}12 \times 10^{-6}$
33304_at	ISG20	interferon stimulated exonuclease gene 20kDa	3,24	$3{,}82 \times 10^{-5}$
202869_at	OAS1	2',5'-oligoadenylate synthetase 1, 40/46kDa	3,14	$2{,}08 \times 10^{-6}$
216598_s_at	CCL2	chemokine (C-C motif) ligand 2	3,06	$3{,}96 \times 10^{-6}$
219684_at	RTP4	receptor (chemosensory) transporter protein 4	2,94	$2{,}77 \times 10^{-5}$
219863_at	HERC5	hect domain and RLD 5	2,93	$9{,}33 \times 10^{-6}$
204439_at	IFI44L	interferon-induced protein 44-like	2,89	$1{,}73 \times 10^{-5}$
218943_s_at	DDX58	DEAD (Asp-Glu-Ala-Asp) box polypeptide 58	2,87	$8{,}71 \times 10^{-7}$

...continues on next page

Table A.1.: *(...continued)*

Probe set ID	Gene symbol	Gene name	logFc	adj.p-val
202086_at	MX1	myxovirus (influenza virus) resistance 1, interferon-inducible protein p78 (mouse)	2,86	$1{,}04 \times 10^{-5}$
215253_s_at	RCAN1	regulator of calcineurin 1	2,78	$1{,}75 \times 10^{-5}$
204502_at	SAMHD1	SAM domain and HD domain 1	2,74	$9{,}61 \times 10^{-6}$
204994_at	MX2	myxovirus (influenza virus) resistance 2 (mouse)	2,73	$1{,}47 \times 10^{-5}$
235456_at	NA	NA	2,70	$4{,}24 \times 10^{-5}$
224225_s_at	ETV7	ets variant 7	2,68	$4{,}35 \times 10^{-5}$
219209_at	IFIH1	interferon induced with helicase C domain 1	2,66	$1{,}12 \times 10^{-5}$
229622_at	NA	NA	2,63	$1{,}81 \times 10^{-5}$
217497_at	TYMP	thymidine phosphorylase	2,63	$4{,}41 \times 10^{-6}$
1559883_s_at	SAMHD1	SAM domain and HD domain 1	2,61	$2{,}28 \times 10^{-5}$
204224_s_at	GCH1	GTP cyclohydrolase 1	2,41	$1{,}38 \times 10^{-5}$
228439_at	BATF2	basic leucine zipper transcription factor, ATF-like 2	2,38	$2{,}77 \times 10^{-5}$
202446_s_at	PLSCR1	phospholipid scramblase 1	2,29	$3{,}96 \times 10^{-6}$
204747_at	IFIT3	interferon-induced protein with tetratricopeptide repeats 3	2,28	$8{,}12 \times 10^{-6}$
214453_s_at	IFI44	interferon-induced protein 44	2,25	$2{,}07 \times 10^{-5}$
1405_i_at	CCL5	chemokine (C-C motif) ligand 5	2,23	$5{,}18 \times 10^{-5}$
1555759_a_at	CCL5	chemokine (C-C motif) ligand 5	2,19	$5{,}06 \times 10^{-5}$
219352_at	HERC6	hect domain and RLD 6	2,15	$9{,}80 \times 10^{-6}$
214472_at	NA	NA	2,13	$4{,}03 \times 10^{-5}$
219211_at	USP18	ubiquitin specific peptidase 18	2,12	$4{,}93 \times 10^{-6}$
203153_at	IFIT1	interferon-induced protein with tetratricopeptide repeats 1	2,10	$9{,}61 \times 10^{-6}$
202430_s_at	PLSCR1	phospholipid scramblase 1	2,10	$2{,}77 \times 10^{-5}$
214290_s_at	NA	NA	2,10	$1{,}98 \times 10^{-5}$
235061_at	PPM1K	protein phosphatase 1K (PP2C domain containing)	2,08	$3{,}96 \times 10^{-6}$
219593_at	SLC15A3	solute carrier family 15, member 3	2,08	$1{,}12 \times 10^{-5}$
222868_s_at	IL18BP	interleukin 18 binding protein	2,08	$2{,}10 \times 10^{-5}$
234987_at	NA	NA	2,07	$3{,}37 \times 10^{-5}$
206271_at	TLR3	toll-like receptor 3	2,06	$2{,}75 \times 10^{-5}$
209417_s_at	IFI35	interferon-induced protein 35	2,03	$8{,}12 \times 10^{-6}$
208436_s_at	IRF7	interferon regulatory factor 7	2,03	$4{,}41 \times 10^{-6}$
208173_at	IFNB1	interferon, beta 1, fibroblast	2,02	$4{,}09 \times 10^{-5}$
229450_at	IFIT3	interferon-induced protein with tetratricopeptide repeats 3	1,98	$3{,}96 \times 10^{-6}$
204205_at	APOBEC3G	apolipoprotein B mRNA editing enzyme, catalytic polypeptide-like 3G	1,98	$6{,}04 \times 10^{-6}$
231769_at	FBXO6	F-box protein 6	1,98	$1{,}57 \times 10^{-5}$
225291_at	PNPT1	polyribonucleotide nucleotidyltransferase 1	1,95	$9{,}80 \times 10^{-6}$
224680_at	TMED4	transmembrane emp24 protein transport domain containing 4	1,94	$4{,}41 \times 10^{-6}$
206513_at	AIM2	absent in melanoma 2	1,94	$2{,}57 \times 10^{-5}$

...continues on next page

Table A.1.: *(...continued)*

Probe set ID	Gene symbol	Gene name	logFc	adj.p-val
204655_at	CCL5	chemokine (C-C motif) ligand 5	1,91	$2{,}91 \times 10^{-5}$
210785_s_at	C1orf38	chromosome 1 open reading frame 38	1,91	$1{,}12 \times 10^{-5}$
230036_at	SAMD9L	sterile alpha motif domain containing 9-like	1,90	$3{,}96 \times 10^{-6}$
235529_x_at	NA	NA	1,88	$5{,}73 \times 10^{-5}$
241916_at	NA	NA	1,86	$4{,}48 \times 10^{-5}$
1554462_a_at	DNAJB9	DnaJ (Hsp40) homolog, subfamily B, member 9	1,83	$2{,}84 \times 10^{-5}$
207510_at	BDKRB1	bradykinin receptor B1	1,82	$1{,}25 \times 10^{-5}$
217933_s_at	LAP3	leucine aminopeptidase 3	1,82	$3{,}46 \times 10^{-5}$
1555167_s_at	NAMPT	nicotinamide phosphoribosyltransferase	1,81	$9{,}61 \times 10^{-6}$
218280_x_at	NA	NA	1,80	$1{,}39 \times 10^{-5}$
238025_at	MLKL	mixed lineage kinase domain-like	1,77	$1{,}08 \times 10^{-5}$
204279_at	PSMB9	proteasome (prosome, macropain) subunit, beta type, 9 (large multifunctional peptidase 2)	1,77	$5{,}93 \times 10^{-5}$
205773_at	CPEB3	cytoplasmic polyadenylation element binding protein 3	1,76	$1{,}78 \times 10^{-5}$
203823_at	RGS3	regulator of G-protein signalling 3	1,73	$1{,}78 \times 10^{-5}$
207571_x_at	C1orf38	chromosome 1 open reading frame 38	1,72	$4{,}41 \times 10^{-6}$
217739_s_at	NAMPT	nicotinamide phosphoribosyltransferase	1,71	$1{,}73 \times 10^{-5}$
1554334_a_at	DNAJA4	DnaJ (Hsp40) homolog, subfamily A, member 4	1,70	$4{,}24 \times 10^{-5}$
230314_at	NA	NA	1,70	$4{,}42 \times 10^{-5}$
204804_at	TRIM21	tripartite motif-containing 21	1,67	$2{,}77 \times 10^{-5}$
219716_at	APOL6	apolipoprotein L, 6	1,65	$2{,}23 \times 10^{-5}$
226603_at	SAMD9L	sterile alpha motif domain containing 9-like	1,64	$2{,}29 \times 10^{-5}$
243271_at	NA	NA	1,64	$1{,}12 \times 10^{-5}$
225295_at	SLC39A10	solute carrier family 39 (zinc transporter), member 10	1,62	$1{,}86 \times 10^{-5}$
228817_at	ALG9	asparagine-linked glycosylation 9, alpha-1,2-mannosyltransferase homolog (S. cerevisiae)	1,62	$3{,}24 \times 10^{-5}$
223220_s_at	PARP9	poly (ADP-ribose) polymerase family, member 9	1,62	$2{,}10 \times 10^{-5}$
203964_at	NMI	N-myc (and STAT) interactor	1,61	$2{,}34 \times 10^{-5}$
218999_at	TMEM140	transmembrane protein 140	1,60	$4{,}53 \times 10^{-5}$
214995_s_at	NA	NA	1,60	$1{,}75 \times 10^{-5}$
202282_at	HSD17B10	hydroxysteroid (17-beta) dehydrogenase 10	1,59	$5{,}44 \times 10^{-5}$
213361_at	TDRD7	tudor domain containing 7	1,56	$1{,}12 \times 10^{-5}$
218543_s_at	PARP12	poly (ADP-ribose) polymerase family, member 12	1,55	$1{,}57 \times 10^{-5}$
204858_s_at	TYMP	thymidine phosphorylase	1,53	$3{,}57 \times 10^{-5}$
237105_at	NA	NA	1,53	$4{,}00 \times 10^{-5}$
213716_s_at	SECTM1	secreted and transmembrane 1	1,52	$2{,}40 \times 10^{-5}$
241342_at	TMEM65	transmembrane protein 65	1,51	$2{,}58 \times 10^{-5}$
217226_s_at	SFXN3	sideroflexin 3	1,50	$8{,}24 \times 10^{-6}$
220974_x_at	SFXN3	sideroflexin 3	1,49	$9{,}61 \times 10^{-6}$
223264_at	MESDC1	mesoderm development candidate 1	1,48	$5{,}68 \times 10^{-5}$
230405_at	C5orf56	chromosome 5 open reading frame 56	1,47	$1{,}12 \times 10^{-5}$
205875_s_at	TREX1	three prime repair exonuclease 1	1,47	$1{,}61 \times 10^{-5}$

...continues on next page

Table A.1.: *(...continued)*

Probe set ID	Gene symbol	Gene name	logFc	adj.p-val
228230_at	PRIC285	peroxisomal proliferator-activated receptor A interacting complex 285	1,46	$4{,}24x10^{-5}$
204172_at	CPOX	coproporphyrinogen oxidase	1,45	$2{,}28x10^{-5}$
218696_at	EIF2AK3	eukaryotic translation initiation factor 2-alpha kinase 3	1,45	$5{,}72x10^{-5}$
220104_at	ZC3HAV1	zinc finger CCCH-type, antiviral 1	1,44	$5{,}16x10^{-5}$
222642_s_at	TMEM33	transmembrane protein 33	1,43	$1{,}73x10^{-5}$
201649_at	UBE2L6	ubiquitin-conjugating enzyme E2L 6	1,41	$3{,}44x10^{-5}$
238765_at	ATP6V1G1	ATPase, H+ transporting, lysosomal 13kDa, V1 subunit G1	1,41	$1{,}61x10^{-5}$
222150_s_at	PION	pigeon homolog (Drosophila)	1,39	$4{,}53x10^{-5}$
205842_s_at	JAK2	Janus kinase 2	1,39	$9{,}13x10^{-6}$
206432_at	HAS2	hyaluronan synthase 2	1,38	$1{,}10x10^{-5}$
216236_s_at	NA	NA	1,38	$5{,}94x10^{-5}$
221432_s_at	SLC25A28	solute carrier family 25, member 28	1,38	$2{,}84x10^{-5}$
205483_s_at	ISG15	ISG15 ubiquitin-like modifier	1,37	$4{,}24x10^{-5}$
205282_at	LRP8	low density lipoprotein receptor-related protein 8, apolipoprotein e receptor	1,36	$4{,}35x10^{-5}$
209762_x_at	SP110	SP110 nuclear body protein	1,35	$9{,}80x10^{-6}$
218004_at	BSDC1	BSD domain containing 1	1,35	$1{,}58x10^{-5}$
224797_at	ARRDC3	arrestin domain containing 3	1,35	$2{,}62x10^{-5}$
239909_at	ADAMTSL1	ADAMTS-like 1	1,34	$1{,}12x10^{-5}$
211366_x_at	CASP1	caspase 1, apoptosis-related cysteine peptidase (interleukin 1, beta, convertase)	1,33	$6{,}21x10^{-5}$
222200_s_at	BSDC1	BSD domain containing 1	1,32	$1{,}82x10^{-5}$
223192_at	SLC25A28	solute carrier family 25, member 28	1,32	$2{,}57x10^{-5}$
210540_s_at	B4GALT4	UDP-Gal:betaGlcNAc beta 1,4- galactosyltransferase, polypeptide 4	1,31	$3{,}33x10^{-5}$
229163_at	CAMK2N1	calcium/calmodulin-dependent protein kinase II inhibitor 1	1,31	$3{,}24x10^{-5}$
208012_x_at	SP110	SP110 nuclear body protein	1,31	$1{,}04x10^{-5}$
219364_at	DHX58	DEXH (Asp-Glu-X-His) box polypeptide 58	1,29	$2{,}57x10^{-5}$
241869_at	APOL6	apolipoprotein L, 6	1,27	$2{,}40x10^{-5}$
238327_at	ODF3B	outer dense fiber of sperm tails 3B	1,27	$3{,}90x10^{-5}$
227048_at	LAMA1	laminin, alpha 1	1,26	$4{,}53x10^{-5}$
218986_s_at	DDX60	DEAD (Asp-Glu-Ala-Asp) box polypeptide 60	1,26	$3{,}65x10^{-5}$
204211_x_at	EIF2AK2	eukaryotic translation initiation factor 2-alpha kinase 2	1,26	$1{,}78x10^{-5}$
208966_x_at	IFI16	interferon, gamma-inducible protein 16	1,25	$3{,}88x10^{-5}$
229091_s_at	CCNJ	cyclin J	1,25	$4{,}09x10^{-5}$
218817_at	SPCS3	signal peptidase complex subunit 3 homolog (S. cerevisiae)	1,23	$4{,}24x10^{-5}$
1557236_at	APOL6	apolipoprotein L, 6	1,22	$2{,}77x10^{-5}$
200901_s_at	M6PR	mannose-6-phosphate receptor (cation dependent)	1,21	$3{,}24x10^{-5}$
235384_at	NUDT19	nudix (nucleoside diphosphate linked moiety X)-type motif 19	1,20	$6{,}37x10^{-5}$
229350_x_at	PARP10	poly (ADP-ribose) polymerase family, member 10	1,20	$4{,}60x10^{-5}$

...continues on next page

Table A.1.: *(...continued)*

Probe set ID	Gene symbol	Gene name	logFc	adj.p-val
201818_at	LPCAT1	lysophosphatidylcholine acyltransferase 1	1,19	$4{,}21 \times 10^{-5}$
203275_at	IRF2	interferon regulatory factor 2	1,19	$2{,}10 \times 10^{-5}$
202307_s_at	TAP1	transporter 1, ATP-binding cassette, sub-family B (MDR/TAP)	1,18	$5{,}90 \times 10^{-5}$
219691_at	SAMD9	sterile alpha motif domain containing 9	1,16	$3{,}41 \times 10^{-5}$
213142_x_at	PION	pigeon homolog (Drosophila)	1,16	$4{,}79 \times 10^{-5}$
213782_s_at	MYOZ2	myozenin 2	1,16	$6{,}61 \times 10^{-5}$
229437_at	MIR155HG	MIR155 host gene (non-protein coding)	1,15	$4{,}89 \times 10^{-5}$
217918_at	DYNLRB1	dynein, light chain, roadblock-type 1	1,15	$2{,}23 \times 10^{-5}$
221816_s_at	PHF11	PHD finger protein 11	1,15	$1{,}65 \times 10^{-5}$
208829_at	TAPBP	TAP binding protein (tapasin)	1,15	$4{,}35 \times 10^{-5}$
209300_s_at	NECAP1	NECAP endocytosis associated 1	1,15	$2{,}77 \times 10^{-5}$
217917_s_at	DYNLRB1	dynein, light chain, roadblock-type 1	1,15	$2{,}77 \times 10^{-5}$
206451_at	TBCCD1	TBCC domain containing 1	1,13	$5{,}37 \times 10^{-5}$
226300_at	MED19	mediator complex subunit 19	1,13	$3{,}14 \times 10^{-5}$
203957_at	E2F6	E2F transcription factor 6	1,12	$5{,}93 \times 10^{-5}$
34689_at	TREX1	three prime repair exonuclease 1	1,11	$7{,}60 \times 10^{-5}$
207375_s_at	IL15RA	interleukin 15 receptor, alpha	1,11	$7{,}35 \times 10^{-5}$
240277_at	NA	NA	1,10	$2{,}62 \times 10^{-5}$
203710_at	ITPR1	inositol 1,4,5-triphosphate receptor, type 1	1,10	$4{,}24 \times 10^{-5}$
219470_x_at	CCNJ	cyclin J	1,09	$3{,}24 \times 10^{-5}$
203598_s_at	WBP4	WW domain binding protein 4 (formin binding protein 21)	1,09	$6{,}33 \times 10^{-5}$
209761_s_at	SP110	SP110 nuclear body protein	1,09	$3{,}41 \times 10^{-5}$
53720_at	C19orf66	chromosome 19 open reading frame 66	1,08	$3{,}81 \times 10^{-5}$
225999_at	RIMKLB	ribosomal modification protein rimK-like family member B	1,06	$6{,}91 \times 10^{-5}$
209282_at	PRKD2	protein kinase D2	1,06	$8{,}13 \times 10^{-5}$
236487_at	SCLT1	sodium channel and clathrin linker 1	1,05	$4{,}92 \times 10^{-5}$
214541_s_at	QKI	quaking homolog, KH domain RNA binding (mouse)	1,05	$8{,}23 \times 10^{-5}$
205746_s_at	ADAM17	ADAM metallopeptidase domain 17	1,04	$4{,}00 \times 10^{-5}$
212622_at	TMEM41B	transmembrane protein 41B	1,04	$4{,}48 \times 10^{-5}$
226261_at	ZNRF2	zinc and ring finger 2	1,03	$4{,}00 \times 10^{-5}$
228617_at	XAF1	XIAP associated factor 1	1,02	$4{,}24 \times 10^{-5}$
235086_at	THBS1	thrombospondin 1	1,02	$4{,}97 \times 10^{-5}$
226293_at	MED19	mediator complex subunit 19	1,01	$6{,}04 \times 10^{-5}$
222459_at	AKIRIN1	akirin 1	1,01	$4{,}76 \times 10^{-5}$
221653_x_at	APOL2	apolipoprotein L, 2	1,01	$8{,}01 \times 10^{-5}$
242138_at	DLX1	distal-less homeobox 1	0,99	$8{,}94 \times 10^{-5}$
52940_at	NA	NA	0,99	$4{,}24 \times 10^{-5}$
211935_at	ARL6IP1	ADP-ribosylation factor-like 6 interacting protein 1	0,99	$5{,}65 \times 10^{-5}$
219357_at	GTPBP1	GTP binding protein 1	0,98	$6{,}89 \times 10^{-5}$

...continues on next page

Table A.1.: *(...continued)*

Probe set ID	Gene symbol	Gene name	logFc	adj.p-val
223497_at	FAM135A	family with sequence similarity 135, member A	0,95	$7{,}65 \times 10^{-5}$
204068_at	STK3	serine/threonine kinase 3 (STE20 homolog, yeast)	0,95	$4{,}21 \times 10^{-5}$
202875_s_at	PBX2	pre-B-cell leukemia homeobox 2	0,95	$6{,}59 \times 10^{-5}$
228531_at	SAMD9	sterile alpha motif domain containing 9	0,94	$7{,}10 \times 10^{-5}$
219356_s_at	CHMP5	chromatin modifying protein 5	0,94	$8{,}97 \times 10^{-5}$
240873_x_at	DAB2	disabled homolog 2, mitogen-responsive phosphoprotein (Drosophila)	0,94	$8{,}67 \times 10^{-5}$
228736_at	HELQ	helicase, POLQ-like	0,94	$4{,}24 \times 10^{-5}$
243296_at	NAMPT	nicotinamide phosphoribosyltransferase	0,94	$1{,}00 \times 10^{-4}$
236224_at	RIT1	Ras-like without CAAX 1	0,93	$8{,}37 \times 10^{-5}$
220178_at	C19orf28	chromosome 19 open reading frame 28	0,93	$9{,}39 \times 10^{-5}$
218597_s_at	CISD1	CDGSH iron sulfur domain 1	0,93	$7{,}10 \times 10^{-5}$
225931_s_at	RNF213	ring finger protein 213	0,92	$7{,}35 \times 10^{-5}$
218429_s_at	C19orf66	chromosome 19 open reading frame 66	0,92	$7{,}12 \times 10^{-5}$
220049_s_at	PDCD1LG2	programmed cell death 1 ligand 2	0,92	$7{,}66 \times 10^{-5}$
208737_at	ATP6V1G1	ATPase, H+ transporting, lysosomal 13kDa, V1 subunit G1	0,90	$7{,}11 \times 10^{-5}$
213379_at	COQ2	coenzyme Q2 homolog, prenyltransferase (yeast)	0,89	$6{,}37 \times 10^{-5}$
221586_s_at	E2F5	E2F transcription factor 5, p130-binding	0,89	$7{,}54 \times 10^{-5}$
226233_at	B3GALNT2	beta-1,3-N-acetylgalactosaminyltransferase 2	0,89	0,0001
220668_s_at	DNMT3B	DNA (cytosine-5-)-methyltransferase 3 beta	0,88	$5{,}34 \times 10^{-5}$
218802_at	CCDC109B	coiled-coil domain containing 109B	0,88	$8{,}13 \times 10^{-5}$
205241_at	SCO2	SCO cytochrome oxidase deficient homolog 2 (yeast)	0,86	$8{,}37 \times 10^{-5}$
208081_s_at	ZNF442	zinc finger protein 442	0,85	$9{,}52 \times 10^{-5}$
238476_at	C5orf41	chromosome 5 open reading frame 41	0,85	$7{,}25 \times 10^{-5}$
207374_at	PLSCR2	phospholipid scramblase 2	0,84	0,0001
218066_at	SLC12A7	solute carrier family 12 (potassium/chloride transporters), member 7	0,83	$7{,}00 \times 10^{-5}$
217427_s_at	HIRA	HIR histone cell cycle regulation defective homolog A (S. cerevisiae)	0,82	0,0001
202260_s_at	STXBP1	syntaxin binding protein 1	0,81	$8{,}37 \times 10^{-5}$
229962_at	LRRC37A3	leucine rich repeat containing 37, member A3	0,78	0,0001
222203_s_at	RDH14	retinol dehydrogenase 14 (all-trans/9-cis/11-cis)	0,78	0,0001
205745_x_at	ADAM17	ADAM metallopeptidase domain 17	0,77	0,0001
235012_at	LRCH1	leucine-rich repeats and calponin homology (CH) domain containing 1	0,77	0,0001
225868_at	TRIM47	tripartite motif-containing 47	0,74	0,0002
204274_at	EBAG9	estrogen receptor binding site associated, antigen, 9	0,73	0,0001
222557_at	STMN3	stathmin-like 3	0,71	0,0002
208229_at	FGFR2	fibroblast growth factor receptor 2	0,71	0,0002
223705_s_at	GPBP1	GC-rich promoter binding protein 1	0,70	0,0002
204493_at	BID	BH3 interacting domain death agonist	0,69	0,0002
226042_at	EDC3	enhancer of mRNA decapping 3 homolog (S. cerevisiae)	-0,71	0,0002

...continues on next page

Table A.1.: *(...continued)*

Probe set ID	Gene symbol	Gene name	logFc	adj.p-val
201030_x_at	LDHB	lactate dehydrogenase B	-0,72	0,0002
202573_at	CSNK1G2	casein kinase 1, gamma 2	-0,72	0,0002
232172_at	NCRNA00103	non-protein coding RNA 103	-0,74	0,0002
222887_s_at	TMEM127	transmembrane protein 127	-0,74	0,0001
210879_s_at	RAB11FIP5	RAB11 family interacting protein 5 (class I)	-0,75	0,0001
217798_at	CNOT2	CCR4-NOT transcription complex, subunit 2	-0,76	0,0001
225778_at	RBMS2	RNA binding motif, single stranded interacting protein 2	-0,76	0,0001
222568_at	UGGT1	UDP-glucose glycoprotein glucosyltransferase 1	-0,77	$9{,}76 \times 10^{-5}$
32836_at	AGPAT1	1-acylglycerol-3-phosphate O-acyltransferase 1 (lysophosphatidic acid acyltransferase, alpha)	-0,77	0,0001
216095_x_at	MTMR1	myotubularin related protein 1	-0,77	0,0001
218060_s_at	C16orf57	chromosome 16 open reading frame 57	-0,79	0,0001
202128_at	KIAA0317	KIAA0317	-0,80	0,0001
223009_at	C11orf59	chromosome 11 open reading frame 59	-0,80	0,0001
221831_at	LUZP1	leucine zipper protein 1	-0,80	0,0001
210672_s_at	C16orf35	chromosome 16 open reading frame 35	-0,80	0,0001
217773_s_at	NDUFA4	NADH dehydrogenase (ubiquinone) 1 alpha subcomplex, 4, 9kDa	-0,81	0,0001
213859_x_at	SMARCA5	SWI/SNF related, matrix associated, actin dependent regulator of chromatin, subfamily a, member 5	-0,81	$9{,}15 \times 10^{-5}$
212979_s_at	FAM115A	family with sequence similarity 115, member A	-0,81	0,0001
211938_at	EIF4B	eukaryotic translation initiation factor 4B	-0,81	$9{,}52 \times 10^{-5}$
203038_at	PTPRK	protein tyrosine phosphatase, receptor type, K	-0,82	0,0001
221755_at	EHBP1L1	EH domain binding protein 1-like 1	-0,82	$8{,}37 \times 10^{-5}$
218606_at	ZDHHC7	zinc finger, DHHC-type containing 7	-0,82	0,0001
202381_at	ADAM9	ADAM metallopeptidase domain 9 (meltrin gamma)	-0,83	0,0001
212484_at	FAM89B	family with sequence similarity 89, member B	-0,84	0,0001
229735_s_at	NA	NA	-0,84	$7{,}35 \times 10^{-5}$
213511_s_at	MTMR1	myotubularin related protein 1	-0,85	0,0001
218640_s_at	PLEKHF2	pleckstrin homology domain containing, family F (with FYVE domain) member 2	-0,85	$6{,}67 \times 10^{-5}$
214212_x_at	FERMT2	fermitin family homolog 2 (Drosophila)	-0,86	0,0001
226032_at	CASP2	caspase 2, apoptosis-related cysteine peptidase	-0,86	$7{,}12 \times 10^{-5}$
213371_at	LDB3	LIM domain binding 3	-0,86	0,0001
212403_at	UBE3B	ubiquitin protein ligase E3B	-0,87	$6{,}89 \times 10^{-5}$
225068_at	KLHL12	kelch-like 12 (Drosophila)	-0,87	$9{,}52 \times 10^{-5}$
44696_at	TBC1D13	TBC1 domain family, member 13	-0,87	$5{,}30 \times 10^{-5}$
218460_at	HEATR2	HEAT repeat containing 2	-0,88	$6{,}91 \times 10^{-5}$
213448_at	NA	NA	-0,88	$6{,}04 \times 10^{-5}$
201549_x_at	KDM5B	lysine (K)-specific demethylase 5B	-0,89	$8{,}49 \times 10^{-5}$
225776_at	RBMS2	RNA binding motif, single stranded interacting protein 2	-0,89	$5{,}61 \times 10^{-5}$
225390_s_at	KLF13	Kruppel-like factor 13	-0,90	$8{,}13 \times 10^{-5}$
223917_s_at	SLC39A3	solute carrier family 39 (zinc transporter), member 3	-0,91	$7{,}92 \times 10^{-5}$

...continues on next page

Table A.1.: *(...continued)*

Probe set ID	Gene symbol	Gene name	logFc	adj.p-val
32209_at	FAM89B	family with sequence similarity 89, member B	-0,91	$6{,}24 \times 10^{-5}$
208407_s_at	CTNND1	catenin (cadherin-associated protein), delta 1	-0,92	$8{,}41 \times 10^{-5}$
225010_at	CCDC6	coiled-coil domain containing 6	-0,92	$6{,}43 \times 10^{-5}$
213787_s_at	EBP	emopamil binding protein (sterol isomerase)	-0,92	$5{,}56 \times 10^{-5}$
233110_s_at	BCL2L12	BCL2-like 12 (proline rich)	-0,92	$8{,}76 \times 10^{-5}$
200919_at	PHC2	polyhomeotic homolog 2 (Drosophila)	-0,93	$5{,}72 \times 10^{-5}$
224890_s_at	C7orf59	chromosome 7 open reading frame 59	-0,93	$4{,}11 \times 10^{-5}$
238865_at	PABPC4L	poly(A) binding protein, cytoplasmic 4-like	-0,94	$8{,}13 \times 10^{-5}$
224742_at	ABHD12	abhydrolase domain containing 12	-0,94	0,0001
65884_at	MAN1B1	mannosidase, alpha, class 1B, member 1	-0,94	$5{,}27 \times 10^{-5}$
208029_s_at	LAPTM4B	lysosomal protein transmembrane 4 beta	-0,95	$5{,}66 \times 10^{-5}$
44702_at	SYDE1	synapse defective 1, Rho GTPase, homolog 1 (C. elegans)	-0,96	$5{,}37 \times 10^{-5}$
32502_at	GDPD5	glycerophosphodiester phosphodiesterase domain containing 5	-0,96	$6{,}24 \times 10^{-5}$
208890_s_at	PLXNB2	plexin B2	-0,97	$4{,}35 \times 10^{-5}$
238477_at	NA	NA	-0,97	$6{,}91 \times 10^{-5}$
203920_at	NR1H3	nuclear receptor subfamily 1, group H, member 3	-0,97	$6{,}11 \times 10^{-5}$
232493_at	NA	NA	-0,97	$4{,}03 \times 10^{-5}$
217778_at	SLC39A1	solute carrier family 39 (zinc transporter), member 1	-0,98	$8{,}42 \times 10^{-5}$
212256_at	GALNT10	UDP-N-acetyl-alpha-D-galactosamine:polypeptide N-acetylgalactosaminyltransferase 10 (GalNAc-T10)	-0,98	$6{,}89 \times 10^{-5}$
209065_at	UQCRB	ubiquinol-cytochrome c reductase binding protein	-0,99	$7{,}29 \times 10^{-5}$
228920_at	ZNF260	zinc finger protein 260	-0,99	$6{,}38 \times 10^{-5}$
223530_at	TDRKH	tudor and KH domain containing	-0,99	$5{,}56 \times 10^{-5}$
225022_at	GOPC	golgi-associated PDZ and coiled-coil motif containing	-1,00	$5{,}30 \times 10^{-5}$
212112_s_at	STX12	syntaxin 12	-1,00	$9{,}05 \times 10^{-5}$
221515_s_at	LCMT1	leucine carboxyl methyltransferase 1	-1,00	$3{,}41 \times 10^{-5}$
224186_s_at	RNF123	ring finger protein 123	-1,00	$6{,}38 \times 10^{-5}$
224874_at	POLR1D	polymerase (RNA) I polypeptide D, 16kDa	-1,00	$5{,}90 \times 10^{-5}$
208662_s_at	TTC3	tetratricopeptide repeat domain 3	-1,00	$9{,}98 \times 10^{-5}$
204619_s_at	VCAN	versican	-1,01	$8{,}23 \times 10^{-5}$
218632_at	HECTD3	HECT domain containing 3	-1,01	$9{,}38 \times 10^{-5}$
202137_s_at	ZMYND11	zinc finger, MYND domain containing 11	-1,01	$3{,}78 \times 10^{-5}$
224926_at	EXOC4	exocyst complex component 4	-1,01	$7{,}20 \times 10^{-5}$
228402_at	ZBED3	zinc finger, BED-type containing 3	-1,01	$4{,}53 \times 10^{-5}$
225228_at	DRAM2	DNA-damage regulated autophagy modulator 2	-1,02	$3{,}37 \times 10^{-5}$
214039_s_at	LAPTM4B	lysosomal protein transmembrane 4 beta	-1,02	$7{,}08 \times 10^{-5}$
225967_s_at	C17orf89	chromosome 17 open reading frame 89	-1,02	$8{,}09 \times 10^{-5}$
225308_s_at	TANC1	tetratricopeptide repeat, ankyrin repeat and coiled-coil containing 1	-1,03	$4{,}87 \times 10^{-5}$
238652_at	NA	NA	-1,03	$4{,}24 \times 10^{-5}$
222244_s_at	TUG1	taurine upregulated 1 (non-protein coding)	-1,03	$9{,}19 \times 10^{-5}$

...continues on next page

Table A.1.: *(...continued)*

Probe set ID	Gene symbol	Gene name	logFc	adj.p-val
212089_at	LMNA	lamin A/C	-1,03	$4{,}53 \times 10^{-5}$
1554016_a_at	C16orf57	chromosome 16 open reading frame 57	-1,03	$6{,}33 \times 10^{-5}$
235346_at	FUNDC1	FUN14 domain containing 1	-1,04	$5{,}16 \times 10^{-5}$
228240_at	NA	NA	-1,04	$6{,}12 \times 10^{-5}$
238868_at	UACA	uveal autoantigen with coiled-coil domains and ankyrin repeats	-1,04	$6{,}37 \times 10^{-5}$
202645_s_at	MEN1	multiple endocrine neoplasia I	-1,04	$4{,}11 \times 10^{-5}$
225230_at	DRAM2	DNA-damage regulated autophagy modulator 2	-1,04	$5{,}58 \times 10^{-5}$
212502_at	ADO	2-aminoethanethiol (cysteamine) dioxygenase	-1,04	$4{,}31 \times 10^{-5}$
219842_at	ARL15	ADP-ribosylation factor-like 15	-1,04	$6{,}89 \times 10^{-5}$
213263_s_at	PCBP2	poly(rC) binding protein 2	-1,05	$8{,}13 \times 10^{-5}$
219158_s_at	NAA15	N(alpha)-acetyltransferase 15, NatA auxiliary subunit	-1,05	$5{,}16 \times 10^{-5}$
203259_s_at	HDDC2	HD domain containing 2	-1,05	$4{,}48 \times 10^{-5}$
208900_s_at	TOP1	topoisomerase (DNA) I	-1,05	$8{,}23 \times 10^{-5}$
223594_at	TMEM117	transmembrane protein 117	-1,06	$6{,}04 \times 10^{-5}$
223266_at	STRADB	STE20-related kinase adaptor beta	-1,06	$6{,}29 \times 10^{-5}$
200931_s_at	VCL	vinculin	-1,07	$8{,}76 \times 10^{-5}$
208661_s_at	TTC3	tetratricopeptide repeat domain 3	-1,07	$5{,}90 \times 10^{-5}$
228031_at	TTPAL	tocopherol (alpha) transfer protein-like	-1,07	$6{,}89 \times 10^{-5}$
226820_at	ZNF362	zinc finger protein 362	-1,07	$4{,}87 \times 10^{-5}$
209691_s_at	DOK4	docking protein 4	-1,08	$4{,}09 \times 10^{-5}$
238523_at	KLHL36	kelch-like 36 (Drosophila)	-1,08	$4{,}48 \times 10^{-5}$
219571_s_at	ZNF12	zinc finger protein 12	-1,08	$4{,}99 \times 10^{-5}$
227514_at	ITPRIPL2	inositol 1,4,5-triphosphate receptor interacting protein-like 2	-1,08	$5{,}56 \times 10^{-5}$
215535_s_at	AGPAT1	1-acylglycerol-3-phosphate O-acyltransferase 1 (lysophosphatidic acid acyltransferase, alpha)	-1,08	$8{,}13 \times 10^{-5}$
230108_at	ERCC6	excision repair cross-complementing rodent repair deficiency, complementation group 6	-1,08	$2{,}77 \times 10^{-5}$
201207_at	TNFAIP1	tumor necrosis factor, alpha-induced protein 1 (endothelial)	-1,09	$2{,}77 \times 10^{-5}$
222258_s_at	SH3BP4	SH3-domain binding protein 4	-1,09	$3{,}60 \times 10^{-5}$
1567014_s_at	NFE2L2	nuclear factor (erythroid-derived 2)-like 2	-1,09	$5{,}23 \times 10^{-5}$
222826_at	PLDN	pallidin homolog (mouse)	-1,10	$8{,}13 \times 10^{-5}$
202117_at	ARHGAP1	Rho GTPase activating protein 1	-1,10	$8{,}01 \times 10^{-5}$
212113_at	LOC552889	hypothetical protein LOC552889	-1,10	$4{,}24 \times 10^{-5}$
201956_s_at	GNPAT	glyceronephosphate O-acyltransferase	-1,10	$2{,}77 \times 10^{-5}$
227319_at	NA	NA	-1,13	$5{,}75 \times 10^{-5}$
228065_at	BCL9L	B-cell CLL/lymphoma 9-like	-1,14	$7{,}26 \times 10^{-5}$
204544_at	HPS5	Hermansky-Pudlak syndrome 5	-1,15	$5{,}58 \times 10^{-5}$
220765_s_at	LIMS2	LIM and senescent cell antigen-like domains 2	-1,15	$7{,}30 \times 10^{-5}$
221824_s_at	MARCH8	membrane-associated ring finger (C3HC4) 8	-1,15	$4{,}09 \times 10^{-5}$
222116_s_at	TBC1D16	TBC1 domain family, member 16	-1,15	$7{,}14 \times 10^{-5}$

...continues on next page

Table A.1.: *(...continued)*

Probe set ID	Gene symbol	Gene name	logFc	adj.p-val
221748_s_at	TNS1	tensin 1	-1,15	$6{,}57\text{x}10^{-5}$
236358_at	NA	NA	-1,15	$7{,}84\text{x}10^{-5}$
202401_s_at	SRF	serum response factor (c-fos serum response element-binding transcription factor)	-1,15	$6{,}91\text{x}10^{-5}$
221843_s_at	KIAA1609	KIAA1609	-1,16	$2{,}50\text{x}10^{-5}$
227261_at	KLF12	Kruppel-like factor 12	-1,16	$4{,}97\text{x}10^{-5}$
217367_s_at	ZHX3	zinc fingers and homeoboxes 3	-1,16	$6{,}91\text{x}10^{-5}$
65438_at	KIAA1609	KIAA1609	-1,16	$2{,}81\text{x}10^{-5}$
229268_at	FAM105B	family with sequence similarity 105, member B	-1,16	$2{,}57\text{x}10^{-5}$
227123_at	RAB3B	RAB3B, member RAS oncogene family	-1,16	$2{,}67\text{x}10^{-5}$
233986_s_at	PLEKHG2	pleckstrin homology domain containing, family G (with RhoGef domain) member 2	-1,17	$2{,}79\text{x}10^{-5}$
203514_at	MAP3K3	mitogen-activated protein kinase kinase kinase 3	-1,17	$2{,}23\text{x}10^{-5}$
207760_s_at	NCOR2	nuclear receptor co-repressor 2	-1,17	$6{,}91\text{x}10^{-5}$
230440_at	ZNF469	zinc finger protein 469	-1,17	$5{,}16\text{x}10^{-5}$
221059_s_at	NA	NA	-1,18	$3{,}65\text{x}10^{-5}$
212073_at	NA	NA	-1,19	$6{,}96\text{x}10^{-5}$
219529_at	CLIC3	chloride intracellular channel 3	-1,19	$4{,}00\text{x}10^{-5}$
34764_at	LARS2	leucyl-tRNA synthetase 2, mitochondrial	-1,19	$7{,}27\text{x}10^{-5}$
209088_s_at	UBN1	ubinuclein 1	-1,20	$6{,}91\text{x}10^{-5}$
225530_at	MOBKL2A	MOB1, Mps One Binder kinase activator-like 2A (yeast)	-1,20	$2{,}27\text{x}10^{-5}$
212109_at	HN1L	hematological and neurological expressed 1-like	-1,21	$2{,}28\text{x}10^{-5}$
212725_s_at	TUG1	taurine upregulated 1 (non-protein coding)	-1,21	$4{,}09\text{x}10^{-5}$
204357_s_at	LIMK1	LIM domain kinase 1	-1,21	$6{,}07\text{x}10^{-5}$
225243_s_at	SLMAP	sarcolemma associated protein	-1,21	$4{,}48\text{x}10^{-5}$
201219_at	NA	NA	-1,23	$2{,}02\text{x}10^{-5}$
213394_at	MAPKBP1	mitogen-activated protein kinase binding protein 1	-1,23	$4{,}30\text{x}10^{-5}$
223186_at	NA	NA	-1,23	$1{,}78\text{x}10^{-5}$
203157_s_at	GLS	glutaminase	-1,24	$7{,}35\text{x}10^{-5}$
200886_s_at	PGAM1	phosphoglycerate mutase 1 (brain)	-1,24	$3{,}41\text{x}10^{-5}$
222570_at	NCS1	neuronal calcium sensor 1	-1,24	$3{,}42\text{x}10^{-5}$
226517_at	BCAT1	branched chain aminotransferase 1, cytosolic	-1,25	$5{,}18\text{x}10^{-5}$
226408_at	TEAD2	TEA domain family member 2	-1,25	$7{,}29\text{x}10^{-5}$
201941_at	CPD	carboxypeptidase D	-1,25	$1{,}81\text{x}10^{-5}$
225875_s_at	NIPAL3	NIPA-like domain containing 3	-1,26	$2{,}58\text{x}10^{-5}$
201989_s_at	CREBL2	cAMP responsive element binding protein-like 2	-1,26	$3{,}81\text{x}10^{-5}$
218527_at	APTX	aprataxin	-1,26	$1{,}58\text{x}10^{-5}$
228456_s_at	LOC149832	hypothetical protein LOC149832	-1,26	$5{,}23\text{x}10^{-5}$
213198_at	ACVR1B	activin A receptor, type IB	-1,27	$3{,}14\text{x}10^{-5}$
218434_s_at	AACS	acetoacetyl-CoA synthetase	-1,27	$2{,}06\text{x}10^{-5}$
230254_at	NA	NA	-1,27	$4{,}48\text{x}10^{-5}$
226194_at	ZNF828	zinc finger protein 828	-1,27	$3{,}41\text{x}10^{-5}$

...continues on next page

Table A.1.: *(...continued)*

Probe set ID	Gene symbol	Gene name	logFc	adj.p-val
1555897_at	KDM1A	lysine (K)-specific demethylase 1A	-1,28	$2{,}57\text{x}10^{-5}$
235279_at	NA	NA	-1,28	$3{,}60\text{x}10^{-5}$
225285_at	BCAT1	branched chain aminotransferase 1, cytosolic	-1,28	$4{,}53\text{x}10^{-5}$
212897_at	CDK19	cyclin-dependent kinase 19	-1,29	$2{,}10\text{x}10^{-5}$
226793_at	LOC283267	hypothetical LOC283267	-1,29	$4{,}92\text{x}10^{-5}$
226648_at	HIF1AN	hypoxia inducible factor 1, alpha subunit inhibitor	-1,29	$2{,}13\text{x}10^{-5}$
202274_at	ACTG2	actin, gamma 2, smooth muscle, enteric	-1,29	$1{,}63\text{x}10^{-5}$
227131_at	MAP3K3	mitogen-activated protein kinase kinase kinase 3	-1,30	$2{,}12\text{x}10^{-5}$
229881_at	KLF12	Kruppel-like factor 12	-1,30	$4{,}35\text{x}10^{-5}$
208663_s_at	TTC3	tetratricopeptide repeat domain 3	-1,30	$3{,}24\text{x}10^{-5}$
222988_s_at	TMEM9	transmembrane protein 9	-1,30	$6{,}91\text{x}10^{-5}$
202548_s_at	ARHGEF7	Rho guanine nucleotide exchange factor (GEF) 7	-1,31	$4{,}97\text{x}10^{-5}$
225164_s_at	EIF2AK4	eukaryotic translation initiation factor 2 alpha kinase 4	-1,31	$1{,}78\text{x}10^{-5}$
202795_x_at	TRIOBP	TRIO and F-actin binding protein	-1,32	$5{,}30\text{x}10^{-5}$
224583_at	COTL1	coactosin-like 1 (Dictyostelium)	-1,32	$1{,}82\text{x}10^{-5}$
222530_s_at	MKKS	McKusick-Kaufman syndrome	-1,33	$3{,}07\text{x}10^{-5}$
224883_at	PLDN	pallidin homolog (mouse)	-1,33	$3{,}56\text{x}10^{-5}$
209627_s_at	OSBPL3	oxysterol binding protein-like 3	-1,33	$2{,}57\text{x}10^{-5}$
221740_x_at	LRRC37A2	leucine rich repeat containing 37, member A2	-1,33	$5{,}46\text{x}10^{-5}$
212337_at	TUG1	taurine upregulated 1 (non-protein coding)	-1,34	$5{,}18\text{x}10^{-5}$
226030_at	ACADSB	acyl-Coenzyme A dehydrogenase, short/branched chain	-1,34	$5{,}72\text{x}10^{-5}$
1557938_s_at	PTRF	polymerase I and transcript release factor	-1,34	$3{,}24\text{x}10^{-5}$
219460_s_at	TMEM127	transmembrane protein 127	-1,34	$2{,}57\text{x}10^{-5}$
217598_at	NA	NA	-1,35	$2{,}77\text{x}10^{-5}$
217762_s_at	RAB31	RAB31, member RAS oncogene family	-1,35	$3{,}37\text{x}10^{-5}$
217764_s_at	RAB31	RAB31, member RAS oncogene family	-1,36	$3{,}24\text{x}10^{-5}$
227021_at	KDM1B	lysine (K)-specific demethylase 1B	-1,36	$1{,}12\text{x}10^{-5}$
213552_at	GLCE	glucuronic acid epimerase	-1,36	$3{,}37\text{x}10^{-5}$
213233_s_at	KLHL9	kelch-like 9 (Drosophila)	-1,36	$4{,}06\text{x}10^{-5}$
203941_at	INTS9	integrator complex subunit 9	-1,36	$3{,}08\text{x}10^{-5}$
225807_at	JUB	jub, ajuba homolog (Xenopus laevis)	-1,37	$7{,}08\text{x}10^{-5}$
217974_at	TM7SF3	transmembrane 7 superfamily member 3	-1,37	$4{,}35\text{x}10^{-5}$
213123_at	MFAP3	microfibrillar-associated protein 3	-1,38	$1{,}34\text{x}10^{-5}$
209440_at	PRPS1	phosphoribosyl pyrophosphate synthetase 1	-1,38	$2{,}46\text{x}10^{-5}$
218473_s_at	GLT25D1	glycosyltransferase 25 domain containing 1	-1,38	$3{,}24\text{x}10^{-5}$
223184_s_at	AGPAT3	1-acylglycerol-3-phosphate O-acyltransferase 3	-1,38	$2{,}01\text{x}10^{-5}$
219384_s_at	ADAT1	adenosine deaminase, tRNA-specific 1	-1,39	$5{,}23\text{x}10^{-5}$
235685_at	NA	NA	-1,39	$2{,}77\text{x}10^{-5}$
202822_at	LPP	LIM domain containing preferred translocation partner in lipoma	-1,39	$1{,}38\text{x}10^{-5}$
212872_s_at	MED20	mediator complex subunit 20	-1,39	$1{,}12\text{x}10^{-5}$
239218_at	NA	NA	-1,39	$2{,}13\text{x}10^{-5}$

...continues on next page

Table A.1.: *(...continued)*

Probe set ID	Gene symbol	Gene name	logFc	adj.p-val
216210_x_at	TRIOBP	TRIO and F-actin binding protein	-1,40	$4{,}30\text{x}10^{-5}$
228151_at	NA	NA	-1,41	$1{,}12\text{x}10^{-5}$
222526_at	GATAD2A	GATA zinc finger domain containing 2A	-1,41	$4{,}00\text{x}10^{-5}$
202275_at	G6PD	glucose-6-phosphate dehydrogenase	-1,42	$5{,}30\text{x}10^{-5}$
226231_at	NA	NA	-1,42	$3{,}24\text{x}10^{-5}$
224598_at	MGAT4B	mannosyl (alpha-1,3-)-glycoprotein beta-1,4-N-acetylglucosaminyltransferase, isozyme B	-1,44	$1{,}07\text{x}10^{-5}$
204497_at	ADCY9	adenylate cyclase 9	-1,44	$4{,}19\text{x}10^{-5}$
228900_at	CYTSB	cytospin B	-1,44	$1{,}93\text{x}10^{-5}$
202897_at	SIRPA	signal-regulatory protein alpha	-1,44	$2{,}23\text{x}10^{-5}$
223349_s_at	BOK	BCL2-related ovarian killer	-1,44	$4{,}07\text{x}10^{-5}$
229669_at	NA	NA	-1,45	$3{,}80\text{x}10^{-5}$
225876_at	NIPAL3	NIPA-like domain containing 3	-1,46	$3{,}24\text{x}10^{-5}$
220189_s_at	MGAT4B	mannosyl (alpha-1,3-)-glycoprotein beta-1,4-N-acetylglucosaminyltransferase, isozyme B	-1,46	$1{,}12\text{x}10^{-5}$
201020_at	YWHAH	tyrosine 3-monooxygenase/tryptophan 5-monooxygenase activation protein, eta polypeptide	-1,47	$1{,}78\text{x}10^{-5}$
201729_s_at	KIAA0100	KIAA0100	-1,48	$2{,}28\text{x}10^{-5}$
1555037_a_at	IDH1	isocitrate dehydrogenase 1 (NADP+), soluble	-1,49	$2{,}62\text{x}10^{-5}$
200792_at	XRCC6	X-ray repair complementing defective repair in Chinese hamster cells 6	-1,49	$9{,}33\text{x}10^{-6}$
221832_s_at	LUZP1	leucine zipper protein 1	-1,50	$3{,}41\text{x}10^{-5}$
223182_s_at	AGPAT3	1-acylglycerol-3-phosphate O-acyltransferase 3	-1,50	$1{,}12\text{x}10^{-5}$
211976_at	NA	NA	-1,50	$2{,}67\text{x}10^{-5}$
226000_at	CTTNBP2NL	CTTNBP2 N-terminal like	-1,51	$5{,}18\text{x}10^{-5}$
225484_at	TSGA14	testis specific, 14	-1,51	$2{,}40\text{x}10^{-5}$
204004_at	PAWR	PRKC, apoptosis, WT1, regulator	-1,52	$2{,}58\text{x}10^{-5}$
201990_s_at	CREBL2	cAMP responsive element binding protein-like 2	-1,52	$5{,}72\text{x}10^{-5}$
212635_at	TNPO1	transportin 1	-1,52	$2{,}64\text{x}10^{-5}$
222450_at	PMEPA1	prostate transmembrane protein, androgen induced 1	-1,52	$4{,}35\text{x}10^{-5}$
213675_at	NA	NA	-1,52	$2{,}67\text{x}10^{-5}$
227004_at	NA	NA	-1,53	$3{,}44\text{x}10^{-5}$
227140_at	NA	NA	-1,53	$5{,}06\text{x}10^{-5}$
202136_at	ZMYND11	zinc finger, MYND domain containing 11	-1,54	$1{,}64\text{x}10^{-5}$
224928_at	SETD7	SET domain containing (lysine methyltransferase) 7	-1,55	$2{,}23\text{x}10^{-5}$
223183_at	AGPAT3	1-acylglycerol-3-phosphate O-acyltransferase 3	-1,55	$2{,}58\text{x}10^{-5}$
202119_s_at	CPNE3	copine III	-1,56	$3{,}76\text{x}10^{-5}$
210276_s_at	NA	NA	-1,56	$3{,}90\text{x}10^{-5}$
209153_s_at	TCF3	transcription factor 3 (E2A immunoglobulin enhancer binding factors E12/E47)	-1,56	$1{,}61\text{x}10^{-5}$
224659_at	SEPN1	selenoprotein N, 1	-1,56	$4{,}16\text{x}10^{-5}$
224937_at	PTGFRN	prostaglandin F2 receptor negative regulator	-1,56	$1{,}61\text{x}10^{-5}$
212040_at	TGOLN2	trans-golgi network protein 2	-1,56	$6{,}53\text{x}10^{-5}$

...continues on next page

Table A.1.: *(...continued)*

Probe set ID	Gene symbol	Gene name	logFc	adj.p-val
235109_at	NA	NA	-1,57	$5{,}72 \times 10^{-5}$
224906_at	ANO6	anoctamin 6	-1,58	$1{,}38 \times 10^{-5}$
225185_at	MRAS	muscle RAS oncogene homolog	-1,59	$9{,}61 \times 10^{-6}$
241879_at	NA	NA	-1,59	$1{,}78 \times 10^{-5}$
225485_at	TSGA14	testis specific, 14	-1,59	$3{,}46 \times 10^{-5}$
201462_at	SCRN1	secernin 1	-1,61	$4{,}09 \times 10^{-5}$
208790_s_at	PTRF	polymerase I and transcript release factor	-1,62	$2{,}29 \times 10^{-5}$
226518_at	KCTD10	potassium channel tetramerisation domain containing 10	-1,63	$3{,}24 \times 10^{-5}$
209608_s_at	ACAT2	acetyl-Coenzyme A acetyltransferase 2	-1,64	$2{,}66 \times 10^{-5}$
202369_s_at	TRAM2	translocation associated membrane protein 2	-1,65	$2{,}28 \times 10^{-5}$
202808_at	C10orf26	chromosome 10 open reading frame 26	-1,66	$1{,}38 \times 10^{-5}$
203185_at	RASSF2	Ras association (RalGDS/AF-6) domain family member 2	-1,66	$5{,}44 \times 10^{-5}$
205117_at	FGF1	fibroblast growth factor 1 (acidic)	-1,68	$2{,}10 \times 10^{-5}$
208614_s_at	FLNB	filamin B, beta	-1,68	$2{,}75 \times 10^{-5}$
55081_at	MICALL1	MICAL-like 1	-1,68	$4{,}09 \times 10^{-5}$
203159_at	GLS	glutaminase	-1,69	$3{,}41 \times 10^{-5}$
226103_at	NEXN	nexilin (F actin binding protein)	-1,69	$3{,}65 \times 10^{-5}$
231968_at	UGGT1	UDP-glucose glycoprotein glucosyltransferase 1	-1,69	$6{,}08 \times 10^{-5}$
1556646_at	NA	NA	-1,69	$4{,}92 \times 10^{-5}$
212099_at	RHOB	ras homolog gene family, member B	-1,71	$8{,}12 \times 10^{-6}$
222494_at	FOXN3	forkhead box N3	-1,73	$6{,}08 \times 10^{-5}$
224811_at	NA	NA	-1,74	$1{,}78 \times 10^{-5}$
227006_at	PPP1R14A	protein phosphatase 1, regulatory (inhibitor) subunit 14A	-1,74	$4{,}98 \times 10^{-5}$
229699_at	LOC100129550	hypothetical LOC100129550	-1,74	$3{,}82 \times 10^{-5}$
226421_at	AMMECR1	Alport syndrome, mental retardation, midface hypoplasia and elliptocytosis chromosomal region gene 1	-1,75	$1{,}04 \times 10^{-5}$
208757_at	TMED9	transmembrane emp24 protein transport domain containing 9	-1,76	$1{,}12 \times 10^{-5}$
224502_s_at	KIAA1191	KIAA1191	-1,76	$3{,}96 \times 10^{-6}$
200644_at	MARCKSL1	MARCKS-like 1	-1,78	$2{,}28 \times 10^{-5}$
202016_at	MEST	mesoderm specific transcript homolog (mouse)	-1,79	$8{,}34 \times 10^{-6}$
203062_s_at	MDC1	mediator of DNA-damage checkpoint 1	-1,79	$2{,}02 \times 10^{-5}$
226009_at	DPCD	deleted in primary ciliary dyskinesia homolog (mouse)	-1,79	$4{,}93 \times 10^{-6}$
204114_at	NID2	nidogen 2 (osteonidogen)	-1,80	$3{,}42 \times 10^{-5}$
209460_at	ABAT	4-aminobutyrate aminotransferase	-1,80	$6{,}01 \times 10^{-5}$
205547_s_at	TAGLN	transgelin	-1,80	$1{,}08 \times 10^{-5}$
1555724_s_at	TAGLN	transgelin	-1,81	$1{,}12 \times 10^{-5}$
201870_at	TOMM34	translocase of outer mitochondrial membrane 34	-1,81	$1{,}81 \times 10^{-5}$
238604_at	NA	NA	-1,82	$9{,}61 \times 10^{-6}$
207196_s_at	TNIP1	TNFAIP3 interacting protein 1	-1,85	$1{,}78 \times 10^{-5}$
200055_at	TAF10	TAF10 RNA polymerase II, TATA box binding protein (TBP)-associated factor, 30kDa	-1,85	$9{,}33 \times 10^{-6}$

...continues on next page

Table A.1.: *(...continued)*

Probe set ID	Gene symbol	Gene name	logFc	adj.p-val
201885_s_at	CYB5R3	cytochrome b5 reductase 3	-1,85	$8{,}12\text{x}10^{-6}$
212605_s_at	NA	NA	-1,88	$1{,}86\text{x}10^{-5}$
204352_at	TRAF5	TNF receptor-associated factor 5	-1,90	$2{,}28\text{x}10^{-5}$
209362_at	MED21	mediator complex subunit 21	-1,91	$9{,}61\text{x}10^{-6}$
225574_at	RWDD4A	RWD domain containing 4A	-1,92	$3{,}24\text{x}10^{-5}$
226752_at	FAM174A	family with sequence similarity 174, member A	-1,95	$1{,}12\text{x}10^{-5}$
226523_at	TAGLN	transgelin	-1,95	$3{,}24\text{x}10^{-5}$
200028_s_at	STARD7	StAR-related lipid transfer (START) domain containing 7	-1,97	$4{,}41\text{x}10^{-6}$
201615_x_at	CALD1	caldesmon 1	-1,98	$4{,}92\text{x}10^{-5}$
212899_at	CDK19	cyclin-dependent kinase 19	-2,00	$3{,}96\text{x}10^{-6}$
225342_at	AK3L1	adenylate kinase 3-like 1	-2,03	$4{,}48\text{x}10^{-5}$
228635_at	PCDH10	protocadherin 10	-2,05	$1{,}64\text{x}10^{-5}$
226777_at	NA	NA	-2,06	$9{,}61\text{x}10^{-6}$
225274_at	PCYOX1	prenylcysteine oxidase 1	-2,06	$1{,}86\text{x}10^{-5}$
1558173_a_at	LUZP1	leucine zipper protein 1	-2,07	$7{,}82\text{x}10^{-6}$
205812_s_at	NA	NA	-2,09	$5{,}72\text{x}10^{-6}$
225880_at	NA	NA	-2,13	$3{,}63\text{x}10^{-6}$
213790_at	ADAM12	ADAM metallopeptidase domain 12	-2,16	$7{,}03\text{x}10^{-6}$
225718_at	KIAA1715	KIAA1715	-2,17	$8{,}12\text{x}10^{-6}$
1553976_a_at	DPCD	deleted in primary ciliary dyskinesia homolog (mouse)	-2,20	$2{,}68\text{x}10^{-6}$
209459_s_at	ABAT	4-aminobutyrate aminotransferase	-2,21	$3{,}24\text{x}10^{-5}$
201792_at	AEBP1	AE binding protein 1	-2,26	$8{,}12\text{x}10^{-6}$
203766_s_at	LMOD1	leiomodin 1 (smooth muscle)	-2,29	$4{,}09\text{x}10^{-5}$
1552721_a_at	FGF1	fibroblast growth factor 1 (acidic)	-2,29	$7{,}03\text{x}10^{-6}$
203151_at	MAP1A	microtubule-associated protein 1A	-2,36	$2{,}68\text{x}10^{-6}$
203803_at	PCYOX1	prenylcysteine oxidase 1	-2,44	$3{,}57\text{x}10^{-5}$
235821_at	NA	NA	-2,49	$5{,}28\text{x}10^{-5}$
202852_s_at	AAGAB	alpha- and gamma-adaptin binding protein	-2,50	$1{,}81\text{x}10^{-6}$
37512_at	HSD17B6	hydroxysteroid (17-beta) dehydrogenase 6 homolog (mouse)	-2,53	$3{,}65\text{x}10^{-5}$
229173_at	KIAA1715	KIAA1715	-2,55	$7{,}31\text{x}10^{-6}$
212993_at	NACC2	NACC family member 2, BEN and BTB (POZ) domain containing	-2,56	$2{,}90\text{x}10^{-6}$
203465_at	MRPL19	mitochondrial ribosomal protein L19	-2,60	$4{,}45\text{x}10^{-5}$
229969_at	SEC63	SEC63 homolog (S. cerevisiae)	-2,70	$7{,}31\text{x}10^{-6}$
228299_at	KCTD20	potassium channel tetramerisation domain containing 20	-2,70	$1{,}81\text{x}10^{-6}$
229802_at	NA	NA	-2,75	$5{,}16\text{x}10^{-5}$
200974_at	ACTA2	actin, alpha 2, smooth muscle, aorta	-3,01	$4{,}41\text{x}10^{-6}$
223176_at	KCTD20	potassium channel tetramerisation domain containing 20	-3,06	$1{,}81\text{x}10^{-6}$

APPENDIX

B

GENE ONTOLOGY ANALYSIS OF ALL SIGNIFICANTLY REGULATED GENES IN WISP1 DOWN-REGULATED HMSCS

Table B.1.: *All 456 significantly regulated genes, detected during the WISP1 array data analysis in hMSCs, were continuative assigned to GO terms and KEGG-signalling pathways. Illustrated are: the corresponding subclass name, the expected count, actual count and overall number of genes (N) associated to the GO/KEGG-term. These values are related to and corrected by the total number of all and differentially expressed corresponding genes present on the chip. The corresponding odds-ratio of corrected values is provided by the fraction (N/actual count). Corresponding p-values are results of the hyper-geometric tests.*

					– on chip –	
Go term	**p-value**	**Odds ratio**	**Exp. count**	**Act. count**	**N**	**Act. count**	**N**
	Biological processes						
response to virus	$2{,}97 \times 10^{-11}$	6,24	4,58	24	191	21	123
type I interferon-mediated signalling pathway	$5{,}08 \times 10^{-11}$	12,03	1,63	15	68	15	64
cellular response to type I interferon	$5{,}08 \times 10^{-11}$	12,03	1,63	15	68	1	1
response to type I interferon	$6{,}35 \times 10^{-11}$	11,81	1,65	15	69	0	2
response to biotic stimulus	$7{,}28 \times 10^{-10}$	3,59	11,85	37	494	0	13
response to other organism	$8{,}26 \times 10^{-10}$	3,90	9,74	33	406	0	3
cytokine-mediated signalling pathway	$4{,}59 \times 10^{-9}$	5,15	4,94	22	206	19	154
cellular response to cytokine stimulus	$4{,}75 \times 10^{-9}$	4,91	5,40	23	225	0	3
response to cytokine stimulus	$2{,}13 \times 10^{-8}$	4,04	7,31	26	305	1	53
innate immune response	$4{,}21 \times 10^{-8}$	3,58	9,16	29	382	9	212
negative regulation of viral genome replication	$4{,}06 \times 10^{-7}$	68,89	0,19	5	8	4	6
negative regulation of viral reproduction	$4{,}06 \times 10^{-7}$	68,89	0,19	5	8	1	2
immune response	$4{,}09 \times 10^{-6}$	2,33	20,05	42	836	15	316
immune system process	$4{,}44 \times 10^{-6}$	2,06	31,08	57	1296	0	2
cellular response to organic substance	$5{,}47 \times 10^{-6}$	2,53	14,82	34	618	0	2
regulation of viral genome replication	$3{,}75 \times 10^{-5}$	17,21	0,41	5	17	0	2
histone H3-K4 demethylation	$5{,}37 \times 10^{-5}$	123,24	0,10	3	4	3	4
response to organic substance	$5{,}47 \times 10^{-5}$	1,94	28,39	50	1184	0	36
negative regulation of type I interferon production	$6{,}63 \times 10^{-5}$	10,35	0,72	6	30	6	30

...continues on next page

Table B.1.: *(...continued)*

Go term	p-value	Odds ratio	Exp. count	Act. count	N	– on chip – Act. count	N
viral genome replication	$9{,}71 \times 10^{-5}$	9,55	0,77	6	32	1	13
defense response	0,0001	2,06	20,12	38	839	4	72
cellular response to chemical stimulus	0,0004	1,92	21,39	38	892	0	4
defense response to virus	0,0006	4,68	1,89	8	79	4	28
positive regulation of gene-specific transcription from RNA polymerase II promoter	0,0009	3,32	3,57	11	149	10	143
glial cell migration	0,0010	20,53	0,22	3	9	1	5
negative regulation of cytokine production	0,0011	4,20	2,09	8	87	0	2
apoptotic cell clearance	0,0014	17,60	0,24	3	10	2	7
ribose phosphate biosynthetic process	0,0017	81,91	0,07	2	3	1	1
PMA-inducible membrane protein ectodomain proteolysis	0,0017	81,91	0,07	2	3	2	3
cellular response to exogenous dsRNA	0,0017	81,91	0,07	2	3	2	3
lymphocyte chemotaxis	0,0020	15,40	0,26	3	11	2	6
regulation of cytokine-mediated signalling pathway	0,0028	4,68	1,41	6	59	0	3
phospholipid scrambling	0,0033	40,95	0,10	2	4	2	4
astrocyte cell migration	0,0033	40,95	0,10	2	4	2	4
negative regulation of binding	0,0040	3,38	2,54	8	106	0	3
response to interferon-gamma	0,0040	3,76	2,01	7	84	1	13
NADPH regeneration	0,0041	11,20	0,34	3	14	2	2
histone lysine demethylation	0,0041	11,20	0,34	3	14	0	1
protein ubiquitination involved in ubiquitin-dependent protein catabolic process	0,0047	5,03	1,10	5	46	5	43
regulation of locomotion	0,0048	2,33	6,35	14	265	0	3
response to stress	0,0050	1,44	55,68	74	2322	0	117
modification-dependent protein catabolic process	0,0055	2,16	7,82	16	326	1	3
D-ribose metabolic process	0,0055	27,30	0,12	2	5	0	1
intracellular transport of viral proteins in host cell	0,0055	27,30	0,12	2	5	2	5
response to lipopolysaccharide	0,0055	2,94	3,26	9	136	5	107
histone demethylation	0,0061	9,47	0,38	3	16	0	2
positive regulation of transforming growth factor beta receptor signalling pathway	0,0061	9,47	0,38	3	16	3	16
protein autophosphorylation	0,0066	3,40	2,21	7	92	7	76
cell junction assembly	0,0066	2,85	3,36	9	140	5	87
positive regulation of signal transduction	0,0070	1,92	10,93	20	456	0	11
positive regulation of gene-specific transcription	0,0072	2,50	4,65	11	194	1	54
proteolysis involved in cellular protein catabolic process	0,0072	2,09	8,06	16	336	1	24
protein demethylation	0,0072	8,79	0,41	3	17	0	1

...continues on next page

Table B.1.: *(...continued)*

					– on chip –	
Go term	**p-value**	**Odds ratio**	**Exp. count**	**Act. count**	**N**	**Act. count**	**N**
macrophage chemotaxis	0,0072	8,79	0,41	3	17	2	10
regulation of defense response to virus by host	0,0072	8,79	0,41	3	17	0	4
positive regulation of T cell chemotaxis	0,0081	20,47	0,14	2	6	2	6
pentose biosynthetic process	0,0081	20,47	0,14	2	6	1	2
antigen processing and presentation of endogenous peptide antigen via MHC class I	0,0081	20,47	0,14	2	6	2	6
hormone catabolic process	0,0081	20,47	0,14	2	6	0	2
negative regulation of defense response to virus	0,0081	20,47	0,14	2	6	1	3
positive regulation of nitric-oxide synthase biosynthetic process	0,0081	20,47	0,14	2	6	2	6
chemokine-mediated signalling pathway	0,0081	20,47	0,14	2	6	2	3
cytokine production	0,0085	2,17	6,79	14	283	1	14
cellular protein catabolic process	0,0085	2,05	8,20	16	342	0	4
branched chain family amino acid catabolic process	0,0085	8,21	0,43	3	18	3	18
cellular response to interferon-gamma	0,0086	3,64	1,77	6	74	1	6
response to molecule of bacterial origin	0,0098	2,66	3,57	9	149	0	10
negative regulation of protein binding	0,0100	7,69	0,46	3	19	3	13
protein targeting to membrane	0,0104	5,14	0,86	4	36	3	11
regulation of transcription from RNA polymerase II promoter	0,0109	1,61	20,93	32	873	7	210
positive regulation of macrophage chemotaxis	0,0111	16,38	0,17	2	7	2	7
endosome to lysosome transport	0,0115	7,24	0,48	3	20	3	20
endoplasmic reticulum unfolded protein response	0,0115	7,24	0,48	3	20	3	19
cellular macromolecule catabolic process	0,0117	1,80	12,25	21	511	0	1
regulation of cellular component movement	0,0117	2,15	6,35	13	265	0	2
regulation of gene-specific transcription from RNA polymerase II promoter	0,0119	2,02	7,79	15	325	0	24
induction of apoptosis	0,0121	1,96	8,54	16	356	9	170
regulation of cell migration	0,0124	2,21	5,71	12	238	3	26
gene-specific transcription from RNA polymerase II promoter	0,0126	2,00	7,84	15	327	0	4
positive regulation of leukocyte migration	0,0126	4,84	0,91	4	38	1	8
cellular response to protein stimulus	0,0126	4,84	0,91	4	38	1	16
induction of programmed cell death	0,0128	1,95	8,58	16	358	0	1
NADP metabolic process	0,0132	6,84	0,50	3	21	0	5
cell adhesion mediated by integrin	0,0132	6,84	0,50	3	21	2	4
transforming growth factor beta receptor signalling pathway	0,0138	2,92	2,54	7	106	3	62
limbic system development	0,0138	4,70	0,94	4	39	0	2
one-carbon metabolic process	0,0145	2,48	3,81	9	159	0	23
pinocytosis	0,0146	13,65	0,19	2	8	1	5

...continues on next page

Table B.1.: *(...continued)*

Go term	p-value	Odds ratio	Exp. count	Act. count	N	– on chip – Act. count	N
antigen processing and presentation of endogenous antigen	0,0146	13,65	0,19	2	8	0	1
positive regulation of cell adhesion mediated by integrin	0,0146	13,65	0,19	2	8	1	5
activation of JAK2 kinase activity	0,0146	13,65	0,19	2	8	1	3
regulation of translational initiation in response to stress	0,0146	13,65	0,19	2	8	1	2
positive regulation of viral genome replication	0,0146	13,65	0,19	2	8	2	8
transcription from RNA polymerase II promoter	0,0155	1,52	25,68	37	1071	6	250
cellular response to lipopolysaccharide	0,0164	4,44	0,98	4	41	3	23
protein catabolic process	0,0172	1,84	9,64	17	402	1	32
methylation	0,0174	2,78	2,66	7	111	0	13
cholesterol biosynthetic process	0,0178	4,33	1,01	4	42	3	33
cell-cell adhesion mediated by integrin	0,0185	11,70	0,22	2	9	1	4
positive regulation of toll-like receptor signalling pathway	0,0185	11,70	0,22	2	9	1	4
vesicle docking involved in exocytosis	0,0190	5,86	0,58	3	24	2	19
antigen processing and presentation of peptide antigen	0,0190	5,86	0,58	3	24	0	1
regulation of cytokine production	0,0197	2,06	6,09	12	254	0	6
positive regulation of intracellular protein kinase cascade	0,0197	2,06	6,09	12	254	1	4
cellular amino acid catabolic process	0,0200	2,98	2,13	6	89	0	2
regulation of innate immune response	0,0200	2,34	4,03	9	168	1	5
regulation of immune system process	0,0206	1,63	15,37	24	641	0	1
protein methylation	0,0209	3,37	1,58	5	66	0	10
zinc ion transport	0,0213	5,59	0,60	3	25	1	16
protein modification process	0,0218	1,36	49,30	63	2056	8	144
regulation of translational initiation	0,0224	4,01	1,08	4	45	2	26
ubiquitin-dependent protein catabolic process	0,0225	1,90	7,67	14	320	2	139
response to stimulus	0,0225	1,26	134,88	153	5625	3	276
regulation of receptor recycling	0,0227	10,23	0,24	2	10	2	3
positive regulation of defense response to virus by host	0,0227	10,23	0,24	2	10	2	10
activation of Janus kinase activity	0,0227	10,23	0,24	2	10	0	1
interferon-gamma-mediated signalling pathway	0,0234	3,27	1,63	5	68	5	63
response to progesterone stimulus	0,0236	5,35	0,62	3	26	3	26
vesicle docking	0,0236	5,35	0,62	3	26	0	2
negative regulation of antigen processing and presentation of peptide or polysaccharide antigen via MHC class II	0,0240	Inf	0,02	1	1	1	1

...continues on next page

Table B.1.: *(...continued)*

Go term	p-value	Odds ratio	Exp. count	Act. count	N	– on chip – Act. count	N
negative regulation of dendritic cell antigen processing and presentation	0,0240	Inf	0,02	1	1	1	1
glutamine catabolic process	0,0240	Inf	0,02	1	1	1	1
glucocorticoid catabolic process	0,0240	Inf	0,02	1	1	1	1
detection of virus	0,0240	Inf	0,02	1	1	1	1
DNA methylation on cytosine within a CG sequence	0,0240	Inf	0,02	1	1	1	1
negative regulation of protein glutathionylation	0,0240	Inf	0,02	1	1	1	1
negative regulation of nitric oxide mediated signal transduction	0,0240	Inf	0,02	1	1	1	1
negative regulation of cGMP-mediated signalling	0,0240	Inf	0,02	1	1	1	1
regulation of synaptic vesicle priming	0,0240	Inf	0,02	1	1	1	1
negative regulation of keratinocyte proliferation	0,0240	Inf	0,02	1	1	1	1
orbitofrontal cortex development	0,0240	Inf	0,02	1	1	1	1
ventricular zone neuroblast division	0,0240	Inf	0,02	1	1	1	1
actin modification	0,0240	Inf	0,02	1	1	1	1
evasion by virus of host immune response	0,0240	Inf	0,02	1	1	1	1
sister chromatid biorientation	0,0240	Inf	0,02	1	1	1	1
mineralocorticoid receptor signalling pathway	0,0240	Inf	0,02	1	1	1	1
endosome localization	0,0240	Inf	0,02	1	1	1	1
response to vitamin B3	0,0240	Inf	0,02	1	1	1	1
positive regulation of macrophage fusion	0,0240	Inf	0,02	1	1	1	1
histone H3-K4 demethylation. trimethyl-H3-K4-specific	0,0240	Inf	0,02	1	1	1	1
histone H3-Y41 phosphorylation	0,0240	Inf	0,02	1	1	1	1
cellular response to interferon-alpha	0,0240	Inf	0,02	1	1	1	1
fibroblast growth factor receptor signalling pathway involved in negative regulation of apoptosis in bone marrow	0,0240	Inf	0,02	1	1	1	1
fibroblast growth factor receptor signalling pathway involved in hemopoiesis	0,0240	Inf	0,02	1	1	1	1
fibroblast growth factor receptor signalling pathway involved in positive regulation of cell proliferation in bone marrow	0,0240	Inf	0,02	1	1	1	1
fibroblast growth factor receptor signalling pathway involved in orbitofrontal cortex development	0,0240	Inf	0,02	1	1	1	1
protection from natural killer cell mediated cytotoxicity	0,0240	Inf	0,02	1	1	1	1
cytoplasmic sequestering of CFTR protein	0,0240	Inf	0,02	1	1	1	1
regulation of pentose-phosphate shunt	0,0240	Inf	0,02	1	1	1	1
engulfment of apoptotic cell	0,0240	Inf	0,02	1	1	1	1

...continues on next page

Table B.1.: *(...continued)*

Go term	p-value	Odds ratio	Exp. count	Act. count	N	– on chip – Act. count	N
regulation of DNA methylation	0,0240	Inf	0,02	1	1	1	1
negative regulation of virion penetration into host cell	0,0240	Inf	0,02	1	1	1	1
tetrahydrofolate biosynthetic process	0,0240	Inf	0,02	1	1	1	1
peptide antigen stabilization	0,0240	Inf	0,02	1	1	1	1
maintenance of Golgi location	0,0240	Inf	0,02	1	1	1	1
response to high density lipoprotein particle stimulus	0,0240	Inf	0,02	1	1	1	1
Golgi to transport vesicle transport	0,0240	Inf	0,02	1	1	1	1
epithelial cell differentiation involved in salivary gland development	0,0240	Inf	0,02	1	1	1	1
cellular response to interleukin-2	0,0240	Inf	0,02	1	1	1	1
cellular response to testosterone stimulus	0,0240	Inf	0,02	1	1	1	1
regulation of cellular ketone metabolic process by negative regulation of transcription from an RNA polymerase II promoter	0,0240	Inf	0,02	1	1	1	1
positive regulation of cell aging	0,0240	Inf	0,02	1	1	1	1
positive regulation of Wnt receptor signalling pathway. planar cell polarity pathway	0,0240	Inf	0,02	1	1	1	1
positive regulation of cholesterol homeostasis	0,0240	Inf	0,02	1	1	1	1
cellular response to molecule of bacterial origin	0,0240	3,91	1,10	4	46	0	1
response to bacterium	0,0244	2,06	5,56	11	232	1	20
negative regulation of transcription	0,0247	1,60	15,63	24	652	11	268
negative regulation of cellular metabolic process	0,0250	1,49	23,16	33	966	0	1
activation of protein kinase activity	0,0253	2,38	3,52	8	147	1	16
regulation of gene expression by genetic imprinting	0,0273	9,10	0,26	2	11	2	11
regulation of cholesterol efflux	0,0273	9,10	0,26	2	11	1	2
sterol biosynthetic process	0,0276	3,73	1,15	4	48	0	6
positive regulation of transcription from RNA polymerase II promoter	0,0287	1,73	10,24	17	427	9	294
salivary gland morphogenesis	0,0287	4,92	0,67	3	28	1	5
hippocampus development	0,0287	4,92	0,67	3	28	3	25
negative regulation of blood pressure	0,0287	4,92	0,67	3	28	3	22
proteolysis	0,0290	1,51	20,05	29	836	10	411
catabolic process	0,0315	1,37	36,74	48	1532	0	3
response to tumor necrosis factor	0,0315	3,57	1,20	4	50	3	19
receptor recycling	0,0323	8,19	0,29	2	12	0	2
homotypic cell-cell adhesion	0,0323	8,19	0,29	2	12	0	3
regulation of smooth muscle cell differentiation	0,0323	8,19	0,29	2	12	2	5
response to chemical stimulus	0,0324	1,32	50,36	63	2100	0	12
cellular protein metabolic process	0,0326	1,29	65,15	79	2717	6	279

...continues on next page

Table B.1.: *(...continued)*

						– on chip –	
Go term	**p-value**	**Odds ratio**	**Exp. count**	**Act. count**	**N**	**Act. count**	**N**
peptide transport	0,0344	2,23	3,74	8	156	1	4
positive regulation of leukocyte chemotaxis	0,0344	4,56	0,72	3	30	1	7
DNA methylation	0,0344	4,56	0,72	3	30	2	17
cholesterol efflux	0,0344	4,56	0,72	3	30	1	21
negative regulation of gene expression	0,0357	1,52	17,05	25	711	0	26
regulation of defense response to virus	0,0357	3,42	1,25	4	52	0	4
salivary gland development	0,0374	4,39	0,74	3	31	0	4
virus-host interaction	0,0374	4,39	0,74	3	31	1	10
monocyte chemotaxis	0,0376	7,44	0,31	2	13	1	7
pentose-phosphate shunt	0,0376	7,44	0,31	2	13	1	11
positive regulation of interferon-beta production	0,0376	7,44	0,31	2	13	2	13
regulation of activin receptor signalling pathway	0,0376	7,44	0,31	2	13	1	5
response to exogenous dsRNA	0,0376	7,44	0,31	2	13	0	10
genetic imprinting	0,0376	7,44	0,31	2	13	0	2
negative regulation of signal transduction	0,0386	1,72	9,04	15	377	2	48
negative regulation of biosynthetic process	0,0392	1,48	18,90	27	788	0	1
positive regulation of protein kinase activity	0,0396	1,84	6,76	12	282	1	20
negative regulation of metabolic process	0,0399	1,42	24,94	34	1040	0	1
glycoprotein metabolic process	0,0399	1,90	6,02	11	251	0	6
lysosomal transport	0,0406	4,24	0,77	3	32	0	6
regulation of signal transduction	0,0406	1,38	30,24	40	1261	0	21
cell migration	0,0425	1,57	13,19	20	550	4	66
chronic inflammatory response	0,0431	6,82	0,34	2	14	1	5
syncytium formation	0,0431	6,82	0,34	2	14	0	2
zinc ion transmembrane transport	0,0431	6,82	0,34	2	14	2	14
regulation of gene-specific transcription	0,0432	1,69	9,18	15	383	0	8
interspecies interaction between organisms	0,0448	1,72	8,44	14	352	12	302
cell motility	0,0449	1,54	14,10	21	588	1	7
regulation of transforming growth factor beta receptor signalling pathway	0,0450	3,16	1,34	4	56	0	13
negative regulation of cellular protein metabolic process	0,0461	1,91	5,42	10	226	0	1
ER-nucleus signalling pathway	0,0473	3,97	0,82	3	34	0	3
response to endoplasmic reticulum stress	0,0473	3,97	0,82	3	34	1	10
membranous septum morphogenesis	0,0474	40,83	0,05	1	2	1	2
5-phosphoribose 1-diphosphate biosynthetic process	0,0474	40,83	0,05	1	2	1	2
glyoxylate cycle	0,0474	40,83	0,05	1	2	1	2
dTDP biosynthetic process	0,0474	40,83	0,05	1	2	1	2
transcription. RNA-dependent	0,0474	40,83	0,05	1	2	1	2

...continues on next page

Table B.1.: *(...continued)*

Go term	p-value	Odds ratio	Exp. count	Act. count	N	– on chip – Act. count	N
leucyl-tRNA aminoacylation	0,0474	40,83	0,05	1	2	1	2
C-terminal protein methylation	0,0474	40,83	0,05	1	2	1	2
androgen catabolic process	0,0474	40,83	0,05	1	2	1	2
nicotinamide metabolic process	0,0474	40,83	0,05	1	2	1	2
protoporphyrinogen IX biosynthetic process	0,0474	40,83	0,05	1	2	1	2
branched chain family amino acid biosynthetic process	0,0474	40,83	0,05	1	2	1	2
gamma-aminobutyric acid catabolic process	0,0474	40,83	0,05	1	2	1	2
positive regulation of transcription via serum response element binding	0,0474	40,83	0,05	1	2	1	2
positive regulation of fibroblast migration	0,0474	40,83	0,05	1	2	1	2
regulation of lung blood pressure	0,0474	40,83	0,05	1	2	1	2
synaptic vesicle priming	0,0474	40,83	0,05	1	2	0	1
regulation of transcription from RNA polymerase II promoter involved in forebrain neuron fate commitment	0,0474	40,83	0,05	1	2	1	2
cerebral cortex GABAergic interneuron fate commitment	0,0474	40,83	0,05	1	2	1	2
prenylated protein catabolic process	0,0474	40,83	0,05	1	2	1	2
prenylcysteine catabolic process	0,0474	40,83	0,05	1	2	1	2
prenylcysteine metabolic process	0,0474	40,83	0,05	1	2	1	1
paranodal junction assembly	0,0474	40,83	0,05	1	2	1	2
negative regulation of myelination	0,0474	40,83	0,05	1	2	1	2
secretion of lysosomal enzymes	0,0474	40,83	0,05	1	2	1	2
positive regulation of cell-cell adhesion mediated by integrin	0,0474	40,83	0,05	1	2	1	2
beta-amyloid formation	0,0474	40,83	0,05	1	2	1	2
urate biosynthetic process	0,0474	40,83	0,05	1	2	1	2
negative regulation of Rac protein signal transduction	0,0474	40,83	0,05	1	2	1	2
helper T cell extravasation	0,0474	40,83	0,05	1	2	1	2
positive regulation of amyloid precursor protein biosynthetic process	0,0474	40,83	0,05	1	2	1	2
negative regulation of Golgi to plasma membrane protein transport	0,0474	40,83	0,05	1	2	0	1
Golgi to plasma membrane CFTR protein transport	0,0474	40,83	0,05	1	2	0	1
regulation of MHC class I biosynthetic process	0,0474	40,83	0,05	1	2	1	1
negative regulation of retroviral genome replication	0,0474	40,83	0,05	1	2	1	2
negative regulation of natural killer cell mediated cytotoxicity	0,0474	40,83	0,05	1	2	0	1
S-adenosylmethioninamine metabolic process	0,0474	40,83	0,05	1	2	1	2
regulation of virion penetration into host cell	0,0474	40,83	0,05	1	2	0	1

...continues on next page

Table B.1.: *(...continued)*

					– on chip –	
Go term	**p-value**	**Odds ratio**	**Exp. count**	**Act. count**	**N**	**Act. count**	**N**
cytosol to ER transport	0,0474	40,83	0,05	1	2	1	2
negative regulation of pinocytosis	0,0474	40,83	0,05	1	2	1	2
dihydrobiopterin metabolic process	0,0474	40,83	0,05	1	2	1	2
attachment of spindle microtubules to kinetochore involved in mitotic sister chromatid segregation	0,0474	40,83	0,05	1	2	1	2
Golgi localization	0,0474	40,83	0,05	1	2	0	1
maintenance of centrosome location	0,0474	40,83	0,05	1	2	1	2
maternal process involved in parturition	0,0474	40,83	0,05	1	2	1	2
positive regulation of growth hormone receptor signalling pathway	0,0474	40,83	0,05	1	2	1	2
squamous basal epithelial stem cell differentiation involved in prostate gland acinus development	0,0474	40,83	0,05	1	2	1	2
fibroblast growth factor receptor signalling pathway involved in mammary gland specification	0,0474	40,83	0,05	1	2	1	2
mammary gland bud formation	0,0474	40,83	0,05	1	2	1	2
branch elongation involved in salivary gland morphogenesis	0,0474	40,83	0,05	1	2	1	2
cell differentiation involved in salivary gland development	0,0474	40,83	0,05	1	2	0	1
mesenchymal cell differentiation involved in lung development	0,0474	40,83	0,05	1	2	1	2
positive regulation of cell proliferation in bone marrow	0,0474	40,83	0,05	1	2	0	1
negative regulation of apoptosis in bone marrow	0,0474	40,83	0,05	1	2	0	1
negative regulation of protein deubiquitination	0,0474	40,83	0,05	1	2	1	2
positive regulation of non-canonical Wnt receptor signalling pathway	0,0474	40,83	0,05	1	2	0	1
antigen processing and presentation	0,0475	3,10	1,37	4	57	0	29
erythrocyte differentiation	0,0475	3,10	1,37	4	57	1	22
positive regulation of apoptosis	0,0477	1,59	11,73	18	489	4	122
posttranscriptional regulation of gene expression	0,0481	1,83	6,21	11	259	0	1
antigen processing and presentation of peptide or polysaccharide antigen via MHC class II	0,0490	6,29	0,36	2	15	0	10
positive regulation of type I interferon production	0,0490	6,29	0,36	2	15	0	1
regulation of cell adhesion mediated by integrin	0,0490	6,29	0,36	2	15	0	2
cellular response to heat	0,0490	6,29	0,36	2	15	2	14
hippo signalling cascade	0,0490	6,29	0,36	2	15	2	13
positive regulation of kinase activity	0,0493	1,77	7,00	12	292	0	4
histone modification	0,0494	1,97	4,75	9	198	0	2

...continues on next page

Table B.1.: *(...continued)*

Go term	p-value	Odds ratio	Exp. count	Act. count	N	– on chip – Act. count	N
positive regulation of transcription. DNA-dependent	0,0495	1,54	13,43	20	560	5	139
Cellular components							
intracellular	$1{,}71\text{x}10^{-7}$	2,01	261,10	302	11023	47	1797
cell-substrate adherens junction	$2{,}25\text{x}10^{-7}$	6,42	2,53	14	107	1	3
cytoplasm	$3{,}04\text{x}10^{-7}$	1,74	186,23	233	7862	142	4683
cell-substrate junction	$3{,}58\text{x}10^{-7}$	6,15	2,63	14	111	1	2
focal adhesion	$8{,}31\text{x}10^{-7}$	6,21	2,42	13	102	13	102
cytoplasmic part	$8{,}75\text{x}10^{-7}$	1,68	133,57	178	5639	0	13
intracellular part	$1{,}94\text{x}10^{-6}$	1,84	254,85	293	10759	0	10
adherens junction	$3{,}85\text{x}10^{-6}$	4,60	3,65	15	154	2	33
intracellular organelle	0,0003	1,49	216,19	248	9127	0	2
cytosol	0,0006	1,61	46,14	68	1948	65	1907
intracellular membrane-bounded organelle	0,0009	1,41	195,56	225	8256	8	198
membrane-bounded organelle	0,0010	1,41	195,80	225	8266	0	2
Cul3-RING ubiquitin ligase complex	0,0014	17,80	0,24	3	10	3	10
basolateral plasma membrane	0,0015	2,66	5,59	14	236	0	114
nuclear chromatin	0,0028	4,01	1,89	7	80	5	36
TAP complex	0,0033	41,44	0,09	2	4	2	4
endoplasmic reticulum	0,0037	1,67	24,16	38	1020	36	905
mitochondrion	0,0039	1,59	29,96	45	1265	44	1229
lysosomal membrane	0,0049	3,25	2,63	8	111	8	111
MHC class I peptide loading complex	0,0053	27,63	0,12	2	5	1	2
organelle membrane	0,0067	1,45	46,40	63	1959	0	7
endoplasmic reticulum membrane	0,0077	1,77	14,83	25	626	24	576
cell part	0,0089	1,84	332,59	344	14041	0	1
cell	0,0090	1,84	332,61	344	14042	1	4
cell junction	0,0100	1,77	13,60	23	574	12	426
nuclear membrane-endoplasmic reticulum network	0,0102	1,72	15,18	25	641	0	2
cullin-RING ubiquitin ligase complex	0,0103	4,08	1,33	5	56	0	8
endomembrane system	0,0211	1,41	34,87	47	1472	6	78
vacuolar membrane	0,0230	2,42	3,46	8	146	0	7
4-aminobutyrate transaminase complex	0,0237	Inf	0,02	1	1	1	1
endoplasmic reticulum quality control compartment	0,0237	Inf	0,02	1	1	1	1
Z disc	0,0248	3,87	1,11	4	47	4	47
nuclear chromosome	0,0259	2,12	4,90	10	207	1	25
cytoplasmic mRNA processing body	0,0334	4,61	0,71	3	30	3	30
mediator complex	0,0363	4,44	0,73	3	31	3	31
postsynaptic density	0,0431	2,74	1,92	5	81	5	81

...continues on next page

Table B.1.: *(...continued)*

					– on chip –	
Go term	**p-value**	**Odds ratio**	**Exp. count**	**Act. count**	**N**	**Act. count**	**N**
I band	0,0458	3,13	1,35	4	57	0	11
nuclear nucleosome	0,0468	41,33	0,05	1	2	1	2
laminin-3 complex	0,0468	41,33	0,05	1	2	1	2
RSF complex	0,0468	41,33	0,05	1	2	1	2
Ku70:Ku80 complex	0,0468	41,33	0,05	1	2	1	2
soluble fraction	0,0492	1,73	7,77	13	328	13	328
	Molecular functions						
histone demethylase activity (H3-dimethyl-K4 specific)	$1{,}46x10^{-5}$	Inf	0,07	3	3	3	3
eukaryotic translation initiation factor 2alpha kinase activity	$5{,}75x10^{-5}$	120,32	0,10	3	4	3	4
histone demethylase activity (H3-K4 specific)	$5{,}75x10^{-5}$	120,32	0,10	3	4	1	2
protein binding	$8{,}00x10^{-5}$	1,52	168,94	204	6886	162	5122
transferase activity. transferring pentosyl groups	0,0007	6,37	1,08	6	44	1	3
ubiquitin-protein ligase activity	0,0010	2,82	5,32	14	217	14	214
small conjugating protein ligase activity	0,0017	2,64	5,64	14	230	0	4
NAD+ ADP-ribosyltransferase activity	0,0018	8,93	0,54	4	22	4	22
acid-amino acid ligase activity	0,0020	2,49	6,40	15	261	7	77
peptide transporter activity	0,0021	15,03	0,27	3	11	1	3
transferase activity. transferring glycosyl groups	0,0023	2,55	5,84	14	238	8	144
catalytic activity	0,0030	1,37	123,06	148	5016	3	111
phospholipid scramblase activity	0,0035	39,99	0,10	2	4	2	4
TAP1 binding	0,0035	39,99	0,10	2	4	2	4
TAP2 binding	0,0035	39,99	0,10	2	4	2	4
histone demethylase activity	0,0035	12,02	0,32	3	13	1	2
3'-5'-exodeoxyribonuclease activity	0,0057	26,66	0,12	2	5	1	4
peptide-transporting ATPase activity	0,0057	26,66	0,12	2	5	0	1
SH3 domain binding	0,0060	3,14	2,72	8	111	8	111
ligase activity	0,0073	1,92	10,97	20	447	13	342
double-stranded RNA binding	0,0074	5,73	0,79	4	32	4	32
demethylase activity	0,0091	8,01	0,44	3	18	0	1
protein domain specific binding	0,0099	1,89	10,55	19	430	5	123
protein N-terminus binding	0,0102	3,50	1,84	6	75	6	74
transcription corepressor activity	0,0104	2,64	3,61	9	147	9	147
O-acyltransferase activity	0,0113	5,02	0,88	4	36	0	2
1-acylglycerol-3-phosphate O-acyltransferase activity	0,0152	13,32	0,20	2	8	2	8
alpha-catenin binding	0,0152	13,32	0,20	2	8	2	8
RNA polymerase II transcription factor activity	0,0180	2,09	6,01	12	245	5	125

...continues on next page

Table B.1.: *(...continued)*

Go term	p-value	Odds ratio	Exp. count	Act. count	N	– on chip – Act. count	N
GTP-Rho binding	0,0193	11,42	0,22	2	9	2	9
transferase activity	0,0202	1,39	40,09	53	1634	26	920
transcription cofactor activity	0,0215	1,83	9,13	16	372	1	40
unfolded protein binding	0,0231	2,61	2,82	7	115	7	115
helicase activity	0,0238	2,41	3,48	8	142	8	111
prenylcysteine oxidase activity	0,0245	Inf	0,02	1	1	1	1
4-hydroxybenzoate decaprenyltransferase activity	0,0245	Inf	0,02	1	1	1	1
4-aminobutyrate transaminase activity	0,0245	Inf	0,02	1	1	1	1
GTP cyclohydrolase I activity	0,0245	Inf	0,02	1	1	1	1
polyribonucleotide nucleotidyltransferase activity	0,0245	Inf	0,02	1	1	1	1
tRNA-specific adenosine deaminase activity	0,0245	Inf	0,02	1	1	1	1
single-stranded DNA specific 3'-5' exodeoxyribonuclease activity	0,0245	Inf	0,02	1	1	1	1
calcium-dependent protein kinase inhibitor activity	0,0245	Inf	0,02	1	1	1	1
chloride-transporting ATPase activity	0,0245	Inf	0,02	1	1	1	1
cholate 7-alpha-dehydrogenase activity	0,0245	Inf	0,02	1	1	1	1
dCTP deaminase activity	0,0245	Inf	0,02	1	1	1	1
exoribonuclease II activity	0,0245	Inf	0,02	1	1	1	1
thymidine phosphorylase activity	0,0245	Inf	0,02	1	1	1	1
mannose transmembrane transporter activity	0,0245	Inf	0,02	1	1	1	1
pyrimidine-nucleoside phosphorylase activity	0,0245	Inf	0,02	1	1	1	1
glycerone-phosphate O-acyltransferase activity	0,0245	Inf	0,02	1	1	1	1
acetoacetyl-CoA reductase activity	0,0245	Inf	0,02	1	1	1	1
receptor signalling protein tyrosine kinase activator activity	0,0245	Inf	0,02	1	1	1	1
acetoacetate-CoA ligase activity	0,0245	Inf	0,02	1	1	1	1
CCR4 chemokine receptor binding	0,0245	Inf	0,02	1	1	1	1
CCR5 chemokine receptor binding	0,0245	Inf	0,02	1	1	1	1
succinate-semialdehyde dehydrogenase binding	0,0245	Inf	0,02	1	1	1	1
DNA 5'-adenosine monophosphate hydrolase activity	0,0245	Inf	0,02	1	1	1	1
UMP kinase activity	0,0245	Inf	0,02	1	1	1	1
histone demethylase activity (H3-trimethyl-K4 specific)	0,0245	Inf	0,02	1	1	1	1
histone demethylase activity (H3-monomethyl-K4 specific)	0,0245	Inf	0,02	1	1	1	1
histone kinase activity (H3-Y41 specific)	0,0245	Inf	0,02	1	1	1	1
interleukin-18 binding	0,0245	Inf	0,02	1	1	1	1
rRNA primary transcript binding	0,0245	Inf	0,02	1	1	1	1

...continues on next page

Table B.1.: *(...continued)*

					– on chip –	
Go term	**p-value**	**Odds ratio**	**Exp. count**	**Act. count**	**N**	**Act. count**	**N**
chemokine receptor antagonist activity	0,0245	Inf	0,02	1	1	1	1
3-hydroxy-2-methylbutyryl-CoA dehydrogenase activity	0,0245	Inf	0,02	1	1	1	1
nicotinamide phosphoribosyltransferase activity	0,0245	Inf	0,02	1	1	1	1
4-hydroxybenzoate nonaprenyltransferase activity	0,0245	Inf	0,02	1	1	1	1
(S)-3-amino-2-methylpropionate transaminase activity	0,0245	Inf	0,02	1	1	1	1
cysteamine dioxygenase activity	0,0245	Inf	0,02	1	1	1	1
fibroblast growth factor 2 binding	0,0245	Inf	0,02	1	1	1	1
UDP-glucuronate 5'-epimerase activity	0,0245	Inf	0,02	1	1	1	1
DNA (cytosine-5-)-methyltransferase activity. acting on CpG substrates	0,0245	Inf	0,02	1	1	1	1
fibrinogen binding	0,0245	Inf	0,02	1	1	1	1
FHA domain binding	0,0245	Inf	0,02	1	1	1	1
syntaxin binding	0,0251	5,22	0,64	3	26	1	13
glycoprotein binding	0,0259	3,82	1,13	4	46	3	31
GTP-dependent protein binding	0,0285	8,88	0,27	2	11	2	11
MHC class I protein binding	0,0285	8,88	0,27	2	11	2	11
bHLH transcription factor binding	0,0285	8,88	0,27	2	11	1	9
RNA polymerase II transcription mediator activity	0,0334	4,62	0,71	3	29	3	29
estradiol 17-beta-dehydrogenase activity	0,0337	7,99	0,29	2	12	2	12
peptide antigen binding	0,0337	7,99	0,29	2	12	2	12
general RNA polymerase II transcription factor activity	0,0339	3,49	1,23	4	50	2	22
3'-5' exonuclease activity	0,0365	4,45	0,74	3	30	1	14
3'-5'-exoribonuclease activity	0,0392	7,27	0,32	2	13	2	11
chloride transmembrane transporter activity	0,0392	7,27	0,32	2	13	0	4
receptor antagonist activity	0,0392	7,27	0,32	2	13	1	6
SNARE binding	0,0396	4,29	0,76	3	31	1	7
galactosyltransferase activity	0,0396	4,29	0,76	3	31	2	23
lipoprotein particle binding	0,0396	4,29	0,76	3	31	0	5
acetyltransferase activity	0,0426	2,75	1,91	5	78	1	12
heat shock protein binding	0,0426	2,75	1,91	5	78	5	60
hydrolase activity. acting on carbon-nitrogen (but not peptide) bonds. in cyclic amidines	0,0430	4,14	0,79	3	32	0	5
tropomyosin binding	0,0450	6,66	0,34	2	14	2	14
tumor necrosis factor receptor superfamily binding	0,0464	4,00	0,81	3	33	0	2
alpha-1.2-mannosyltransferase activity	0,0485	39,87	0,05	1	2	1	2
C-8 sterol isomerase activity	0,0485	39,87	0,05	1	2	1	2

...continues on next page

Table B.1.: *(...continued)*

Go term	p-value	Odds ratio	Exp. count	Act. count	N	– on chip – Act. count	N
beta-dystroglycan binding	0,0485	39,87	0,05	1	2	1	2
RNA polymerase I transcription termination factor activity	0,0485	39,87	0,05	1	2	1	2
protein C-terminal carboxyl O-methyltransferase activity	0,0485	39,87	0,05	1	2	1	2
UDP-glucose:glycoprotein glucosyltransferase activity	0,0485	39,87	0,05	1	2	1	2
branched-chain-amino-acid transaminase activity	0,0485	39,87	0,05	1	2	1	2
coproporphyrinogen oxidase activity	0,0485	39,87	0,05	1	2	1	2
glucose-6-phosphate dehydrogenase activity	0,0485	39,87	0,05	1	2	1	2
glutaminase activity	0,0485	39,87	0,05	1	2	1	2
isocitrate dehydrogenase (NADP+) activity	0,0485	39,87	0,05	1	2	1	2
thymidylate kinase activity	0,0485	39,87	0,05	1	2	1	2
leucine-tRNA ligase activity	0,0485	39,87	0,05	1	2	1	2
bradykinin receptor activity	0,0485	39,87	0,05	1	2	1	2
serum response element binding	0,0485	39,87	0,05	1	2	1	2
peptide antigen-transporting ATPase activity	0,0485	39,87	0,05	1	2	1	2
syntaxin-13 binding	0,0485	39,87	0,05	1	2	1	2
protein tag	0,0485	39,87	0,05	1	2	1	2
CCR1 chemokine receptor binding	0,0485	39,87	0,05	1	2	1	2
CCR2 chemokine receptor binding	0,0485	39,87	0,05	1	2	1	2
sterol response element binding	0,0485	39,87	0,05	1	2	1	2
5'-3' exodeoxyribonuclease activity	0,0485	39,87	0,05	1	2	0	1
cystic fibrosis transmembrane conductance regulator binding	0,0485	39,87	0,05	1	2	1	2
polynucleotide 3'-phosphatase activity	0,0485	39,87	0,05	1	2	1	2
1-alkylglycerophosphocholine O-acetyltransferase activity	0,0485	39,87	0,05	1	2	1	2
cholestenol delta-isomerase activity	0,0485	39,87	0,05	1	2	1	2
procollagen galactosyltransferase activity	0,0485	39,87	0,05	1	2	1	2
5'-deoxyribose-5-phosphate lyase activity	0,0485	39,87	0,05	1	2	1	2
MyoD binding	0,0485	39,87	0,05	1	2	1	2
L-leucine transaminase activity	0,0485	39,87	0,05	1	2	1	2
L-valine transaminase activity	0,0485	39,87	0,05	1	2	1	2
L-isoleucine transaminase activity	0,0485	39,87	0,05	1	2	1	2
KEGG pathway signalling							
cytosolic DNA-sensing pathway	$4{,}38 \times 10^{-5}$	7,28	1,33	8	53	8	53
hepatitis C	0,0016	3,39	3,29	10	131	10	131
valine. leucine and isoleucine degradation	0,0041	5,27	1,08	5	43	5	43
RIG-I-like receptor signalling pathway	0,0079	3,76	1,76	6	70	6	70
valine. leucine and isoleucine biosynthesis	0,0297	8,75	0,28	2	11	2	11

...continues on next page

Table B.1.: *(...continued)*

					– on chip –	
Go term	**p-value**	**Odds ratio**	**Exp. count**	**Act. count**	**N**	**Act. count**	**N**
butanoate metabolism	0,0321	4,74	0,70	3	28	3	28
propanoate metabolism	0,0452	4,09	0,80	3	32	3	32

APPENDIX

C

DIFFERENTIALLY EXPRESSED PROBE SETS DURING MICROARRAY ANALYSIS OF WISP1 DOWN-REGULATED CHONDROCYTES

Table C.1.: *Listed are all 1687 differentially expressed probe sets between shRNA2 transduced chondrocyte samples and their corresponding scrambled control assays (n=5). Probe sets are ordered according to their descending statistical score (logFc) from highest up-regulation to highest down-regulation. Additional information reflects the probe set ID, their corresponding gene symbol and name as well as the adjusted (corrected for multiple comparisons) p-value.*

Probe set ID	Gene symbol	Gene name	logFc	adj.p-val
235258_at	DCP2	DCP2 decapping enzyme homolog (S. cerevisiae)	1,76	$1{,}61 \times 10^{-9}$
232331_at	NA	NA	1,70	$1{,}96 \times 10^{-9}$
204435_at	NUPL1	nucleoporin like 1	1,51	$6{,}59 \times 10^{-9}$
218901_at	PLSCR4	phospholipid scramblase 4	1,41	$1{,}40 \times 10^{-7}$
224296_x_at	NA	NA	1,34	$1{,}86 \times 10^{-6}$
228817_at	ALG9	asparagine-linked glycosylation 9, alpha-1,2-mannosyltransferase homolog (S. cerevisiae)	1,31	$5{,}25 \times 10^{-8}$
213931_at	NA	NA	1,25	$2{,}42 \times 10^{-6}$
243386_at	CASZ1	castor zinc finger 1	1,21	$8{,}13 \times 10^{-7}$
231863_at	ING3	inhibitor of growth family, member 3	1,17	$6{,}64 \times 10^{-7}$
210540_s_at	B4GALT4	UDP-Gal:betaGlcNAc beta 1,4- galactosyltransferase, polypeptide 4	1,15	$1{,}50 \times 10^{-8}$
226293_at	MED19	mediator complex subunit 19	1,12	$5{,}85 \times 10^{-8}$
222763_s_at	WDR33	WD repeat domain 33	1,12	$9{,}78 \times 10^{-8}$
232114_at	MED12L	mediator complex subunit 12-like	1,11	$1{,}45 \times 10^{-6}$
221667_s_at	HSPB8	heat shock 22kDa protein 8	1,07	$2{,}81 \times 10^{-6}$
210674_s_at	NA	NA	1,06	$1{,}26 \times 10^{-7}$
226886_at	GFPT1	glutamine-fructose-6-phosphate transaminase 1	1,05	$1{,}36 \times 10^{-8}$
206002_at	GPR64	G protein-coupled receptor 64	1,04	$5{,}05 \times 10^{-6}$
227713_at	KATNAL1	katanin p60 subunit A-like 1	1,02	$8{,}51 \times 10^{-8}$
201281_at	ADRM1	adhesion regulating molecule 1	1,00	$7{,}56 \times 10^{-8}$

...continues on next page

Table C.1.: *(...continued)*

Probe set ID	Gene symbol	Gene name	logFc	adj.p-val
217917_s_at	DYNLRB1	dynein, light chain, roadblock-type 1	1,00	$4{,}33 \times 10^{-8}$
212919_at	DCP2	DCP2 decapping enzyme homolog (S. cerevisiae)	0,99	$2{,}49 \times 10^{-8}$
217918_at	DYNLRB1	dynein, light chain, roadblock-type 1	0,99	$5{,}62 \times 10^{-8}$
236026_at	GPATCH2	G patch domain containing 2	0,98	$6{,}72 \times 10^{-7}$
236126_at	ACVR2B	activin A receptor, type IIB	0,98	$3{,}08 \times 10^{-7}$
226300_at	MED19	mediator complex subunit 19	0,98	$1{,}26 \times 10^{-7}$
205773_at	CPEB3	cytoplasmic polyadenylation element binding protein 3	0,98	$4{,}70 \times 10^{-7}$
212286_at	ANKRD12	ankyrin repeat domain 12	0,97	$7{,}16 \times 10^{-8}$
1554216_at	CCDC132	coiled-coil domain containing 132	0,96	$2{,}04 \times 10^{-6}$
202817_s_at	SS18	synovial sarcoma translocation, chromosome 18	0,96	$3{,}44 \times 10^{-7}$
1558305_at	GIGYF2	GRB10 interacting GYF protein 2	0,95	$4{,}68 \times 10^{-6}$
211547_s_at	PAFAH1B1	platelet-activating factor acetylhydrolase 1b, regulatory subunit 1 (45kDa)	0,95	$5{,}92 \times 10^{-7}$
235749_at	UGGT2	UDP-glucose glycoprotein glucosyltransferase 2	0,95	$4{,}55 \times 10^{-8}$
1555561_a_at	UGGT2	UDP-glucose glycoprotein glucosyltransferase 2	0,94	$4{,}54 \times 10^{-8}$
244811_at	PHIP	pleckstrin homology domain interacting protein	0,94	$6{,}44 \times 10^{-8}$
218486_at	KLF11	Kruppel-like factor 11	0,94	$1{,}26 \times 10^{-7}$
235760_at	NSD1	nuclear receptor binding SET domain protein 1	0,94	$8{,}33 \times 10^{-7}$
241342_at	TMEM65	transmembrane protein 65	0,93	$4{,}21 \times 10^{-7}$
238174_at	NA	NA	0,92	$1{,}44 \times 10^{-5}$
1560738_at	NA	NA	0,92	$5{,}91 \times 10^{-7}$
228345_at	CHIC1	cysteine-rich hydrophobic domain 1	0,92	$1{,}07 \times 10^{-7}$
1560739_a_at	NA	NA	0,91	$1{,}92 \times 10^{-6}$
227141_at	TYW3	tRNA-yW synthesizing protein 3 homolog (S. cerevisiae)	0,90	$1{,}46 \times 10^{-5}$
201537_s_at	DUSP3	dual specificity phosphatase 3	0,90	$1{,}08 \times 10^{-6}$
212956_at	TBC1D9	TBC1 domain family, member 9 (with GRAM domain)	0,88	$1{,}17 \times 10^{-6}$
229511_at	SMARCE1	SWI/SNF related, matrix associated, actin dependent regulator of chromatin, subfamily e, member 1	0,87	$1{,}78 \times 10^{-5}$
242319_at	DGKG	diacylglycerol kinase, gamma 90kDa	0,86	$1{,}37 \times 10^{-6}$
208078_s_at	NA	NA	0,86	$8{,}03 \times 10^{-8}$
1560485_at	HIVEP1	human immunodeficiency virus type I enhancer binding protein 1	0,85	$7{,}38 \times 10^{-7}$
212876_at	B4GALT4	UDP-Gal:betaGlcNAc beta 1,4- galactosyltransferase, polypeptide 4	0,85	$4{,}44 \times 10^{-7}$
229285_at	RNASEL	ribonuclease L (2',5'-oligoisoadenylate synthetase-dependent)	0,84	$1{,}82 \times 10^{-6}$
227027_at	GFPT1	glutamine-fructose-6-phosphate transaminase 1	0,84	$7{,}16 \times 10^{-8}$
218538_s_at	MRS2	MRS2 magnesium homeostasis factor homolog (S. cerevisiae)	0,84	$1{,}17 \times 10^{-7}$
229526_at	AQP11	aquaporin 11	0,84	$3{,}39 \times 10^{-6}$
206536_s_at	XIAP	X-linked inhibitor of apoptosis	0,84	$4{,}57 \times 10^{-7}$
214553_s_at	ARPP19	cAMP-regulated phosphoprotein, 19kDa	0,84	$1{,}16 \times 10^{-6}$
1554251_at	HP1BP3	heterochromatin protein 1, binding protein 3	0,83	$3{,}48 \times 10^{-6}$

...continues on next page

Table C.1.: *(...continued)*

Probe set ID	Gene symbol	Gene name	logFc	adj.p-val
235471_at	C10orf72	chromosome 10 open reading frame 72	0,83	$9{,}49x10^{-6}$
1559496_at	PPA2	pyrophosphatase (inorganic) 2	0,82	$2{,}56x10^{-7}$
204346_s_at	RASSF1	Ras association (RalGDS/AF-6) domain family member 1	0,82	$5{,}53x10^{-7}$
202282_at	HSD17B10	hydroxysteroid (17-beta) dehydrogenase 10	0,82	$4{,}06x10^{-7}$
218954_s_at	BRF2	BRF2, subunit of RNA polymerase III transcription initiation factor, BRF1-like	0,81	$5{,}31x10^{-7}$
201009_s_at	TXNIP	thioredoxin interacting protein	0,81	$1{,}41x10^{-5}$
211572_s_at	SLC23A2	solute carrier family 23 (nucleobase transporters), member 2	0,81	$6{,}91x10^{-7}$
234986_at	NA	NA	0,80	$1{,}39x10^{-5}$
201010_s_at	TXNIP	thioredoxin interacting protein	0,80	$1{,}35x10^{-5}$
210233_at	IL1RAP	interleukin 1 receptor accessory protein	0,80	$5{,}28x10^{-6}$
241599_at	LSM11	LSM11, U7 small nuclear RNA associated	0,80	$2{,}08x10^{-6}$
203579_s_at	NA	NA	0,78	$2{,}01x10^{-6}$
226268_at	RAB21	RAB21, member RAS oncogene family	0,78	$3{,}21x10^{-6}$
221523_s_at	RRAGD	Ras-related GTP binding D	0,78	$6{,}72x10^{-7}$
1569827_at	ATG7	ATG7 autophagy related 7 homolog (S. cerevisiae)	0,78	$7{,}84x10^{-6}$
244563_at	QSER1	glutamine and serine rich 1	0,78	$4{,}25x10^{-6}$
229551_x_at	ZNF367	zinc finger protein 367	0,78	$7{,}43x10^{-7}$
203634_s_at	CPT1A	carnitine palmitoyltransferase 1A (liver)	0,78	$3{,}08x10^{-6}$
219340_s_at	CLN8	ceroid-lipofuscinosis, neuronal 8 (epilepsy, progressive with mental retardation)	0,78	$1{,}07x10^{-5}$
242062_at	SAMD8	sterile alpha motif domain containing 8	0,78	$1{,}57x10^{-6}$
229908_s_at	UNKL	unkempt homolog (Drosophila)-like	0,77	$9{,}47x10^{-6}$
218955_at	BRF2	BRF2, subunit of RNA polymerase III transcription initiation factor, BRF1-like	0,77	$9{,}35x10^{-7}$
242224_at	GPATCH2	G patch domain containing 2	0,77	$1{,}75x10^{-6}$
1552472_a_at	ACAP2	ArfGAP with coiled-coil, ankyrin repeat and PH domains 2	0,77	$3{,}94x10^{-6}$
202543_s_at	GMFB	glia maturation factor, beta	0,77	$1{,}16x10^{-7}$
229232_at	LRRC57	leucine rich repeat containing 57	0,77	$6{,}74x10^{-7}$
210087_s_at	MPZL1	myelin protein zero-like 1	0,76	$5{,}65x10^{-6}$
227718_at	PURB	purine-rich element binding protein B	0,76	$2{,}09x10^{-6}$
213310_at	EIF2C2	eukaryotic translation initiation factor 2C, 2	0,76	$1{,}48x10^{-5}$
211006_s_at	KCNB1	potassium voltage-gated channel, Shab-related subfamily, member 1	0,75	$1{,}89x10^{-6}$
237571_at	NA	NA	0,75	$1{,}33x10^{-5}$
204565_at	ACOT13	acyl-CoA thioesterase 13	0,75	$1{,}74x10^{-6}$
235579_at	SFRS2IP	splicing factor, arginine/serine-rich 2, interacting protein	0,75	$1{,}42x10^{-5}$
226421_at	AMMECR1	Alport syndrome, mental retardation, midface hypoplasia and elliptocytosis chromosomal region gene 1	0,74	$9{,}16x10^{-7}$
235356_at	NHLRC2	NHL repeat containing 2	0,74	$9{,}33x10^{-6}$
222989_s_at	UBQLN1	ubiquilin 1	0,74	$1{,}67x10^{-5}$

...continues on next page

Table C.1.: *(...continued)*

Probe set ID	Gene symbol	Gene name	logFc	adj.p-val
238738_at	PSMD7	proteasome (prosome, macropain) 26S subunit, non-ATPase, 7	0,74	$1{,}63 \times 10^{-5}$
221193_s_at	ZCCHC10	zinc finger, CCHC domain containing 10	0,74	$2{,}41 \times 10^{-7}$
227724_at	NA	NA	0,74	$3{,}48 \times 10^{-6}$
212800_at	STX6	syntaxin 6	0,74	$7{,}74 \times 10^{-7}$
229711_s_at	MDM2	Mdm2 p53 binding protein homolog (mouse)	0,74	$1{,}49 \times 10^{-6}$
223504_at	DNAJC27	DnaJ (Hsp40) homolog, subfamily C, member 27	0,74	$9{,}46 \times 10^{-7}$
218004_at	BSDC1	BSD domain containing 1	0,73	$7{,}11 \times 10^{-6}$
244841_at	SEC24A	SEC24 family, member A (S. cerevisiae)	0,73	$4{,}78 \times 10^{-6}$
231065_at	PDE6D	phosphodiesterase 6D, cGMP-specific, rod, delta	0,73	$1{,}57 \times 10^{-5}$
239793_at	NA	NA	0,73	$8{,}60 \times 10^{-6}$
223452_s_at	ATL3	atlastin GTPase 3	0,73	$5{,}22 \times 10^{-7}$
223759_s_at	GSG2	germ cell associated 2 (haspin)	0,73	$1{,}18 \times 10^{-6}$
226349_at	C12orf45	chromosome 12 open reading frame 45	0,72	$6{,}94 \times 10^{-6}$
225754_at	AP1G1	adaptor-related protein complex 1, gamma 1 subunit	0,72	$4{,}22 \times 10^{-6}$
209231_s_at	DCTN5	dynactin 5 (p25)	0,72	$1{,}40 \times 10^{-5}$
213154_s_at	BICD2	bicaudal D homolog 2 (Drosophila)	0,72	$1{,}94 \times 10^{-7}$
228092_at	CREM	cAMP responsive element modulator	0,72	$1{,}00 \times 10^{-6}$
214790_at	SENP6	SUMO1/sentrin specific peptidase 6	0,72	$3{,}84 \times 10^{-6}$
1552682_a_at	CASC5	cancer susceptibility candidate 5	0,72	$3{,}41 \times 10^{-7}$
229751_s_at	PUS7L	pseudouridylate synthase 7 homolog (S. cerevisiae)-like	0,72	$9{,}10 \times 10^{-7}$
242112_at	LSM11	LSM11, U7 small nuclear RNA associated	0,71	$7{,}48 \times 10^{-6}$
244664_at	NA	NA	0,71	$1{,}48 \times 10^{-6}$
204204_at	SLC31A2	solute carrier family 31 (copper transporters), member 2	0,71	$5{,}11 \times 10^{-7}$
202816_s_at	SS18	synovial sarcoma translocation, chromosome 18	0,71	$1{,}42 \times 10^{-6}$
208934_s_at	LGALS8	lectin, galactoside-binding, soluble, 8	0,71	$8{,}49 \times 10^{-7}$
203350_at	AP1G1	adaptor-related protein complex 1, gamma 1 subunit	0,71	$2{,}21 \times 10^{-7}$
223505_s_at	DNAJC27	DnaJ (Hsp40) homolog, subfamily C, member 27	0,71	$2{,}40 \times 10^{-6}$
222343_at	BCL2L11	BCL2-like 11 (apoptosis facilitator)	0,71	$4{,}67 \times 10^{-7}$
222808_at	ALG13	asparagine-linked glycosylation 13 homolog (S. cerevisiae)	0,71	$3{,}24 \times 10^{-6}$
231990_at	USP15	ubiquitin specific peptidase 15	0,71	$1{,}60 \times 10^{-5}$
222200_s_at	BSDC1	BSD domain containing 1	0,71	$4{,}76 \times 10^{-6}$
212607_at	AKT3	v-akt murine thymoma viral oncogene homolog 3 (protein kinase B, gamma)	0,71	$3{,}69 \times 10^{-8}$
205415_s_at	ATXN3	ataxin 3	0,71	$1{,}71 \times 10^{-5}$
242321_at	NA	NA	0,70	$1{,}46 \times 10^{-6}$
212702_s_at	BICD2	bicaudal D homolog 2 (Drosophila)	0,70	$8{,}43 \times 10^{-7}$
228357_at	UNK	unkempt homolog (Drosophila)	0,70	$7{,}19 \times 10^{-7}$
219015_s_at	ALG13	asparagine-linked glycosylation 13 homolog (S. cerevisiae)	0,70	$1{,}06 \times 10^{-5}$
209203_s_at	BICD2	bicaudal D homolog 2 (Drosophila)	0,69	$1{,}18 \times 10^{-5}$
204976_s_at	AMMECR1	Alport syndrome, mental retardation, midface hypoplasia and elliptocytosis chromosomal region gene 1	0,69	$6{,}12 \times 10^{-7}$

...continues on next page

Table C.1.: *(...continued)*

Probe set ID	Gene symbol	Gene name	logFc	adj.p-val
227018_at	DPP8	dipeptidyl-peptidase 8	0,69	$1{,}97x10^{-6}$
219720_s_at	C14orf118	chromosome 14 open reading frame 118	0,69	$1{,}01x10^{-5}$
1570038_at	ZNF595	zinc finger protein 595	0,69	$5{,}28x10^{-6}$
210594_x_at	MPZL1	myelin protein zero-like 1	0,69	$1{,}75x10^{-6}$
1556911_at	NA	NA	0,69	$6{,}98x10^{-6}$
201538_s_at	DUSP3	dual specificity phosphatase 3	0,69	$7{,}62x10^{-6}$
224461_s_at	AIFM2	apoptosis-inducing factor, mitochondrion-associated, 2	0,68	$5{,}90x10^{-6}$
221482_s_at	ARPP19	cAMP-regulated phosphoprotein, 19kDa	0,68	$1{,}17x10^{-6}$
224441_s_at	USP45	ubiquitin specific peptidase 45	0,68	$8{,}34x10^{-6}$
220012_at	ERO1LB	ERO1-like beta (S. cerevisiae)	0,68	$1{,}06x10^{-5}$
210405_x_at	TNFRSF10B	tumor necrosis factor receptor superfamily, member 10b	0,68	$7{,}63x10^{-6}$
227859_at	DNAJC27	DnaJ (Hsp40) homolog, subfamily C, member 27	0,68	$5{,}96x10^{-6}$
1554482_a_at	SAR1B	SAR1 homolog B (S. cerevisiae)	0,68	$3{,}69x10^{-7}$
1568733_at	C10orf76	chromosome 10 open reading frame 76	0,68	$4{,}64x10^{-6}$
236223_s_at	RIT1	Ras-like without CAAX 1	0,67	$2{,}37x10^{-6}$
243252_at	NA	NA	0,67	$9{,}23x10^{-6}$
238624_at	NA	NA	0,67	$9{,}26x10^{-7}$
223467_at	RASD1	RAS, dexamethasone-induced 1	0,67	$6{,}55x10^{-7}$
226537_at	HINT3	histidine triad nucleotide binding protein 3	0,67	$2{,}34x10^{-6}$
223651_x_at	CDC23	cell division cycle 23 homolog (S. cerevisiae)	0,67	$1{,}19x10^{-5}$
212099_at	RHOB	ras homolog gene family, member B	0,67	$8{,}12x10^{-7}$
221790_s_at	LDLRAP1	low density lipoprotein receptor adaptor protein 1	0,66	$1{,}80x10^{-6}$
233076_at	JAKMIP3	Janus kinase and microtubule interacting protein 3	0,66	$1{,}34x10^{-5}$
204881_s_at	UGCG	UDP-glucose ceramide glucosyltransferase	0,66	$7{,}38x10^{-7}$
221064_s_at	UNKL	unkempt homolog (Drosophila)-like	0,66	$5{,}47x10^{-6}$
200900_s_at	M6PR	mannose-6-phosphate receptor (cation dependent)	0,66	$1{,}75x10^{-6}$
225659_at	SPOPL	speckle-type POZ protein-like	0,65	$6{,}48x10^{-6}$
226826_at	NA	NA	0,65	$1{,}04x10^{-6}$
228992_at	MED28	mediator complex subunit 28	0,65	$1{,}78x10^{-7}$
205416_s_at	ATXN3	ataxin 3	0,65	$4{,}87x10^{-6}$
219439_at	C1GALT1	core 1 synthase, glycoprotein-N-acetylgalactosamine 3-beta-galactosyltransferase, 1	0,65	$1{,}53x10^{-5}$
212973_at	RPIA	ribose 5-phosphate isomerase A	0,65	$1{,}61x10^{-7}$
202547_s_at	ARHGEF7	Rho guanine nucleotide exchange factor (GEF) 7	0,65	$1{,}06x10^{-5}$
227934_at	KPNA5	karyopherin alpha 5 (importin alpha 6)	0,65	$5{,}55x10^{-6}$
226297_at	NA	NA	0,65	$7{,}28x10^{-7}$
222874_s_at	CLN8	ceroid-lipofuscinosis, neuronal 8 (epilepsy, progressive with mental retardation)	0,65	$8{,}72x10^{-6}$
222402_at	POMP	proteasome maturation protein	0,65	$6{,}80x10^{-6}$
204568_at	KIAA0831	KIAA0831	0,65	$4{,}20x10^{-7}$
1552306_at	ALG10	asparagine-linked glycosylation 10, alpha-1,2-glucosyltransferase homolog (S. pombe)	0,64	$9{,}81x10^{-6}$

...continues on next page

Table C.1.: *(...continued)*

Probe set ID	Gene symbol	Gene name	logFc	adj.p-val
202124_s_at	TRAK2	trafficking protein, kinesin binding 2	0,64	$1{,}48x10^{-6}$
238803_at	HECTD2	HECT domain containing 2	0,64	$6{,}98x10^{-6}$
224931_at	SLC41A3	solute carrier family 41, member 3	0,64	$3{,}22x10^{-6}$
225265_at	RBMS1	RNA binding motif, single stranded interacting protein 1	0,64	$3{,}63x10^{-6}$
212150_at	EFR3A	EFR3 homolog A (S. cerevisiae)	0,64	$7{,}10x10^{-6}$
243463_s_at	RIT1	Ras-like without CAAX 1	0,64	$6{,}90x10^{-6}$
241696_at	CNTLN	centlein, centrosomal protein	0,63	$5{,}11x10^{-7}$
220060_s_at	C12orf48	chromosome 12 open reading frame 48	0,63	$1{,}72x10^{-5}$
224200_s_at	RAD18	RAD18 homolog (S. cerevisiae)	0,63	$8{,}26x10^{-6}$
218254_s_at	SAR1B	SAR1 homolog B (S. cerevisiae)	0,63	$6{,}72x10^{-7}$
228931_at	COQ4	coenzyme Q4 homolog (S. cerevisiae)	0,63	$4{,}30x10^{-6}$
219175_s_at	SLC41A3	solute carrier family 41, member 3	0,62	$6{,}17x10^{-7}$
222105_s_at	NKIRAS2	NFKB inhibitor interacting Ras-like 2	0,62	$4{,}45x10^{-6}$
203658_at	SLC25A20	solute carrier family 25 (carnitine/acylcarnitine translocase), member 20	0,62	$1{,}06x10^{-6}$
200923_at	LGALS3BP	lectin, galactoside-binding, soluble, 3 binding protein	0,62	$5{,}55x10^{-6}$
209301_at	CA2	carbonic anhydrase II	0,62	$9{,}46x10^{-7}$
209100_at	IFRD2	interferon-related developmental regulator 2	0,62	$8{,}21x10^{-6}$
228829_at	ATF7	activating transcription factor 7	0,62	$2{,}88x10^{-6}$
207667_s_at	MAP2K3	mitogen-activated protein kinase kinase 3	0,62	$3{,}76x10^{-6}$
222642_s_at	TMEM33	transmembrane protein 33	0,62	$5{,}81x10^{-6}$
203087_s_at	KIF2A	kinesin heavy chain member 2A	0,62	$1{,}33x10^{-6}$
219557_s_at	NRIP3	nuclear receptor interacting protein 3	0,61	$4{,}98x10^{-6}$
222678_s_at	DCUN1D1	DCN1, defective in cullin neddylation 1, domain containing 1 (S. cerevisiae)	0,61	$1{,}17x10^{-6}$
238506_at	LRRC58	leucine rich repeat containing 58	0,61	$1{,}13x10^{-5}$
222118_at	CENPN	centromere protein N	0,61	$1{,}73x10^{-6}$
224455_s_at	ADPGK	ADP-dependent glucokinase	0,61	$1{,}17x10^{-6}$
222672_at	LYRM4	LYR motif containing 4	0,61	$2{,}44x10^{-7}$
45633_at	GINS3	GINS complex subunit 3 (Psf3 homolog)	0,61	$6{,}42x10^{-7}$
238509_at	CUL1	cullin 1	0,61	$1{,}59x10^{-6}$
209945_s_at	GSK3B	glycogen synthase kinase 3 beta	0,61	$4{,}46x10^{-6}$
229317_at	KPNA5	karyopherin alpha 5 (importin alpha 6)	0,61	$1{,}23x10^{-5}$
1570253_a_at	RHEBL1	Ras homolog enriched in brain like 1	0,61	$1{,}86x10^{-6}$
218596_at	TBC1D13	TBC1 domain family, member 13	0,61	$5{,}63x10^{-6}$
238662_at	ATPBD4	ATP binding domain 4	0,61	$1{,}57x10^{-6}$
212840_at	UBXN7	UBX domain protein 7	0,61	$9{,}59x10^{-7}$
224680_at	TMED4	transmembrane emp24 protein transport domain containing 4	0,60	$4{,}16x10^{-7}$
231102_at	CROT	carnitine O-octanoyltransferase	0,60	$1{,}48x10^{-5}$
222620_s_at	DNAJC1	DnaJ (Hsp40) homolog, subfamily C, member 1	0,60	$6{,}27x10^{-6}$
224962_at	C9orf69	chromosome 9 open reading frame 69	0,60	$3{,}94x10^{-6}$

...continues on next page

Table C.1.: *(...continued)*

Probe set ID	Gene symbol	Gene name	logFc	adj.p-val
204527_at	MYO5A	myosin VA (heavy chain 12, myoxin)	0,60	$4{,}69\text{x}10^{-6}$
226053_at	MAP2K7	mitogen-activated protein kinase kinase 7	0,60	$1{,}01\text{x}10^{-6}$
225424_at	GPAM	glycerol-3-phosphate acyltransferase, mitochondrial	0,60	$1{,}62\text{x}10^{-6}$
227923_at	SHANK3	SH3 and multiple ankyrin repeat domains 3	0,60	$1{,}08\text{x}10^{-5}$
226579_at	NA	NA	0,60	$2{,}18\text{x}10^{-6}$
218719_s_at	GINS3	GINS complex subunit 3 (Psf3 homolog)	0,60	$4{,}34\text{x}10^{-6}$
235119_at	TAF3	TAF3 RNA polymerase II, TATA box binding protein (TBP)-associated factor, 140kDa	0,60	$3{,}26\text{x}10^{-6}$
227932_at	ARIH2	ariadne homolog 2 (Drosophila)	0,60	$5{,}56\text{x}10^{-6}$
226004_at	CABLES2	Cdk5 and Abl enzyme substrate 2	0,60	$3{,}51\text{x}10^{-6}$
1559510_at	BHLHB9	basic helix-loop-helix domain containing, class B, 9	0,60	$1{,}19\text{x}10^{-5}$
206848_at	NA	NA	0,60	$3{,}14\text{x}10^{-6}$
225015_s_at	STK40	serine/threonine kinase 40	0,60	$5{,}52\text{x}10^{-6}$
218581_at	ABHD4	abhydrolase domain containing 4	0,60	$1{,}65\text{x}10^{-5}$
235396_at	C22orf25	chromosome 22 open reading frame 25	0,60	$7{,}45\text{x}10^{-6}$
227133_at	FAM199X	family with sequence similarity 199, X-linked	0,59	$4{,}64\text{x}10^{-6}$
225878_at	KIF1B	kinesin family member 1B	0,59	$7{,}45\text{x}10^{-6}$
244533_at	NA	NA	0,59	$1{,}75\text{x}10^{-6}$
230734_x_at	NA	NA	0,59	$1{,}42\text{x}10^{-6}$
1569024_at	FAM13A	family with sequence similarity 13, member A	0,59	$3{,}48\text{x}10^{-6}$
224613_s_at	DNAJC5	DnaJ (Hsp40) homolog, subfamily C, member 5	0,59	$9{,}52\text{x}10^{-6}$
202533_s_at	DHFR	dihydrofolate reductase	0,59	$3{,}89\text{x}10^{-6}$
243931_at	NA	NA	0,59	$1{,}32\text{x}10^{-5}$
218761_at	RNF111	ring finger protein 111	0,59	$2{,}51\text{x}10^{-6}$
224824_at	FAM36A	family with sequence similarity 36, member A	0,58	$2{,}94\text{x}10^{-6}$
207829_s_at	BNIP1	BCL2/adenovirus E1B 19kDa interacting protein 1	0,58	$1{,}01\text{x}10^{-6}$
1552287_s_at	AFG3L1	AFG3 ATPase family gene 3-like 1 (S. cerevisiae)	0,58	$2{,}97\text{x}10^{-6}$
1554885_a_at	PRIM2	primase, DNA, polypeptide 2 (58kDa)	0,58	$1{,}29\text{x}10^{-5}$
230029_x_at	UBR3	ubiquitin protein ligase E3 component n-recognin 3 (putative)	0,58	$1{,}58\text{x}10^{-5}$
1555274_a_at	SELI	selenoprotein I	0,58	$9{,}25\text{x}10^{-6}$
234311_s_at	GTPBP10	GTP-binding protein 10 (putative)	0,58	$4{,}83\text{x}10^{-6}$
226353_at	SPPL2A	signal peptide peptidase-like 2A	0,58	$1{,}03\text{x}10^{-6}$
37226_at	BNIP1	BCL2/adenovirus E1B 19kDa interacting protein 1	0,58	$1{,}17\text{x}10^{-6}$
223271_s_at	CTDSPL2	CTD (carboxy-terminal domain, RNA polymerase II, polypeptide A) small phosphatase like 2	0,58	$7{,}99\text{x}10^{-7}$
218260_at	DDA1	DET1 and DDB1 associated 1	0,58	$3{,}15\text{x}10^{-6}$
204440_at	CD83	CD83 molecule	0,58	$5{,}46\text{x}10^{-6}$
208936_x_at	LGALS8	lectin, galactoside-binding, soluble, 8	0,58	$1{,}40\text{x}10^{-5}$
217930_s_at	TOLLIP	toll interacting protein	0,58	$4{,}39\text{x}10^{-6}$
229426_at	COX5A	cytochrome c oxidase subunit Va	0,58	$5{,}22\text{x}10^{-6}$
218399_s_at	CDCA4	cell division cycle associated 4	0,58	$2{,}09\text{x}10^{-6}$

...continues on next page

Table C.1.: *(...continued)*

Probe set ID	Gene symbol	Gene name	logFc	adj.p-val
219917_at	ZCCHC4	zinc finger, CCHC domain containing 4	0,58	$9{,}66 \times 10^{-6}$
224164_at	TPM3	tropomyosin 3	0,58	$4{,}64 \times 10^{-6}$
212008_at	UBXN4	UBX domain protein 4	0,58	$3{,}11 \times 10^{-6}$
208103_s_at	ANP32E	acidic (leucine-rich) nuclear phosphoprotein 32 family, member E	0,58	$1{,}16 \times 10^{-5}$
225599_s_at	C8orf83	chromosome 8 open reading frame 83	0,57	$1{,}06 \times 10^{-5}$
214590_s_at	UBE2D1	ubiquitin-conjugating enzyme E2D 1 (UBC4/5 homolog, yeast)	0,57	$1{,}09 \times 10^{-5}$
208908_s_at	CAST	calpastatin	0,57	$2{,}30 \times 10^{-6}$
227822_at	CHFR	checkpoint with forkhead and ring finger domains	0,57	$1{,}07 \times 10^{-5}$
211977_at	GPR107	G protein-coupled receptor 107	0,57	$3{,}31 \times 10^{-6}$
1554010_at	NDST1	N-deacetylase/N-sulfotransferase (heparan glucosaminyl) 1	0,57	$3{,}24 \times 10^{-6}$
1568699_at	C14orf179	chromosome 14 open reading frame 179	0,57	$5{,}90 \times 10^{-6}$
230789_at	ZNF280B	zinc finger protein 280B	0,57	$5{,}60 \times 10^{-6}$
218474_s_at	KCTD5	potassium channel tetramerisation domain containing 5	0,57	$8{,}15 \times 10^{-6}$
222636_at	MED28	mediator complex subunit 28	0,57	$8{,}33 \times 10^{-7}$
232048_at	FAM76B	family with sequence similarity 76, member B	0,57	$1{,}43 \times 10^{-5}$
222621_at	DNAJC1	DnaJ (Hsp40) homolog, subfamily C, member 1	0,57	$6{,}05 \times 10^{-6}$
223749_at	C1QTNF2	C1q and tumor necrosis factor related protein 2	0,56	$2{,}63 \times 10^{-6}$
223005_s_at	C9orf5	chromosome 9 open reading frame 5	0,56	$1{,}47 \times 10^{-5}$
227583_at	POP4	processing of precursor 4, ribonuclease P/MRP subunit (S. cerevisiae)	0,56	$8{,}31 \times 10^{-6}$
215498_s_at	MAP2K3	mitogen-activated protein kinase kinase 3	0,56	$6{,}48 \times 10^{-6}$
208099_x_at	TTLL5	tubulin tyrosine ligase-like family, member 5	0,56	$1{,}43 \times 10^{-5}$
213092_x_at	DNAJC9	DnaJ (Hsp40) homolog, subfamily C, member 9	0,56	$8{,}40 \times 10^{-7}$
57082_at	LDLRAP1	low density lipoprotein receptor adaptor protein 1	0,56	$1{,}04 \times 10^{-6}$
234947_s_at	C10orf84	chromosome 10 open reading frame 84	0,56	$7{,}15 \times 10^{-6}$
1554324_s_at	DYNC2LI1	dynein, cytoplasmic 2, light intermediate chain 1	0,56	$1{,}26 \times 10^{-5}$
227132_at	ZNF706	zinc finger protein 706	0,56	$8{,}43 \times 10^{-6}$
222595_s_at	DIDO1	death inducer-obliterator 1	0,56	$3{,}73 \times 10^{-6}$
218215_s_at	NR1H2	nuclear receptor subfamily 1, group H, member 2	0,56	$6{,}12 \times 10^{-6}$
1553713_a_at	RHEBL1	Ras homolog enriched in brain like 1	0,56	$4{,}02 \times 10^{-6}$
219484_at	HCFC2	host cell factor C2	0,55	$4{,}22 \times 10^{-6}$
234980_at	TMEM56	transmembrane protein 56	0,55	$2{,}88 \times 10^{-6}$
235473_at	MED6	mediator complex subunit 6	0,55	$1{,}17 \times 10^{-5}$
226607_at	C20orf194	chromosome 20 open reading frame 194	0,55	$4{,}52 \times 10^{-6}$
229790_at	TERF2	telomeric repeat binding factor 2	0,55	$6{,}31 \times 10^{-6}$
218409_s_at	DNAJC1	DnaJ (Hsp40) homolog, subfamily C, member 1	0,55	$1{,}97 \times 10^{-6}$
1568678_s_at	FGFR1OP	FGFR1 oncogene partner	0,55	$7{,}98 \times 10^{-6}$
204063_s_at	ULK2	unc-51-like kinase 2 (C. elegans)	0,55	$1{,}22 \times 10^{-6}$
208727_s_at	CDC42	cell division cycle 42 (GTP binding protein, 25kDa)	0,55	$1{,}33 \times 10^{-5}$
218240_at	NKIRAS2	NFKB inhibitor interacting Ras-like 2	0,55	$8{,}96 \times 10^{-6}$

...continues on next page

Table C.1.: *(...continued)*

Probe set ID	Gene symbol	Gene name	logFc	adj.p-val
204716_at	CCDC6	coiled-coil domain containing 6	0,55	$4{,}61 \times 10^{-6}$
244494_at	ZDHHC1	zinc finger, DHHC-type containing 1	0,55	$9{,}47 \times 10^{-6}$
223417_at	RAD18	RAD18 homolog (S. cerevisiae)	0,55	$4{,}96 \times 10^{-6}$
223491_at	COMMD2	COMM domain containing 2	0,54	$1{,}30 \times 10^{-6}$
226282_at	NA	NA	0,54	$1{,}02 \times 10^{-6}$
225089_at	USP40	ubiquitin specific peptidase 40	0,54	$2{,}29 \times 10^{-6}$
215919_s_at	MRPS11	mitochondrial ribosomal protein S11	0,54	$1{,}12 \times 10^{-5}$
225257_at	CCDC97	coiled-coil domain containing 97	0,54	$1{,}22 \times 10^{-6}$
226968_at	KIF1B	kinesin family member 1B	0,54	$8{,}23 \times 10^{-6}$
226233_at	B3GALNT2	beta-1,3-N-acetylgalactosaminyltransferase 2	0,54	$1{,}22 \times 10^{-5}$
223803_s_at	ZCCHC10	zinc finger, CCHC domain containing 10	0,54	$1{,}29 \times 10^{-6}$
213000_at	MORC3	MORC family CW-type zinc finger 3	0,54	$1{,}04 \times 10^{-5}$
225023_at	GOPC	golgi-associated PDZ and coiled-coil motif containing	0,54	$1{,}04 \times 10^{-5}$
221436_s_at	CDCA3	cell division cycle associated 3	0,54	$5{,}22 \times 10^{-6}$
221025_x_at	PUS7L	pseudouridylate synthase 7 homolog (S. cerevisiae)-like	0,54	$2{,}14 \times 10^{-6}$
212812_at	NA	NA	0,54	$1{,}86 \times 10^{-6}$
205474_at	CRLF3	cytokine receptor-like factor 3	0,54	$4{,}46 \times 10^{-6}$
212149_at	EFR3A	EFR3 homolog A (S. cerevisiae)	0,53	$3{,}96 \times 10^{-6}$
221524_s_at	RRAGD	Ras-related GTP binding D	0,53	$8{,}99 \times 10^{-6}$
215499_at	MAP2K3	mitogen-activated protein kinase kinase 3	0,53	$5{,}45 \times 10^{-6}$
208101_s_at	URM1	ubiquitin related modifier 1 homolog (S. cerevisiae)	0,53	$7{,}79 \times 10^{-7}$
222748_s_at	TXNL4B	thioredoxin-like 4B	0,53	$5{,}13 \times 10^{-6}$
236384_at	NA	NA	0,53	$5{,}95 \times 10^{-6}$
226860_at	TMEM19	transmembrane protein 19	0,52	$1{,}16 \times 10^{-6}$
239843_at	RIT1	Ras-like without CAAX 1	0,52	$5{,}54 \times 10^{-6}$
204634_at	NEK4	NIMA (never in mitosis gene a)-related kinase 4	0,52	$2{,}34 \times 10^{-6}$
1552302_at	TMEM106A	transmembrane protein 106A	0,52	$6{,}72 \times 10^{-6}$
223330_s_at	SUGT1	SGT1, suppressor of G2 allele of SKP1 (S. cerevisiae)	0,52	$6{,}90 \times 10^{-6}$
201490_s_at	PPIF	peptidylprolyl isomerase F	0,52	$1{,}01 \times 10^{-5}$
214969_at	MAP3K9	mitogen-activated protein kinase kinase kinase 9	0,52	$1{,}44 \times 10^{-5}$
200787_s_at	PEA15	phosphoprotein enriched in astrocytes 15	0,52	$5{,}32 \times 10^{-6}$
228710_at	NA	NA	0,52	$2{,}33 \times 10^{-6}$
206770_s_at	SLC35A3	solute carrier family 35 (UDP-N-acetylglucosamine (UDP-GlcNAc) transporter), member A3	0,52	$4{,}76 \times 10^{-6}$
204930_s_at	BNIP1	BCL2/adenovirus E1B 19kDa interacting protein 1	0,52	$8{,}52 \times 10^{-6}$
223249_at	CLDN12	claudin 12	0,52	$2{,}92 \times 10^{-6}$
203359_s_at	MYCBP	c-myc binding protein	0,52	$1{,}49 \times 10^{-6}$
202289_s_at	TACC2	transforming, acidic coiled-coil containing protein 2	0,52	$1{,}46 \times 10^{-5}$
221999_at	VRK3	vaccinia related kinase 3	0,52	$5{,}46 \times 10^{-6}$
227658_s_at	PLEKHA3	pleckstrin homology domain containing, family A (phosphoinositide binding specific) member 3	0,52	$1{,}07 \times 10^{-5}$
220058_at	C17orf39	chromosome 17 open reading frame 39	0,52	$2{,}31 \times 10^{-6}$

...continues on next page

Table C.1.: *(...continued)*

Probe set ID	Gene symbol	Gene name	logFc	adj.p-val
1555185_x_at	TERF2	telomeric repeat binding factor 2	0,52	$1{,}14x10^{-6}$
44696_at	TBC1D13	TBC1 domain family, member 13	0,52	$4{,}38x10^{-6}$
226400_at	CDC42	cell division cycle 42 (GTP binding protein, 25kDa)	0,52	$6{,}90x10^{-6}$
218757_s_at	UPF3B	UPF3 regulator of nonsense transcripts homolog B (yeast)	0,52	$4{,}17x10^{-6}$
211744_s_at	CD58	CD58 molecule	0,51	$1{,}13x10^{-5}$
227586_at	TMEM170A	transmembrane protein 170A	0,51	$3{,}05x10^{-6}$
230788_at	GCNT2	glucosaminyl (N-acetyl) transferase 2, I-branching enzyme (I blood group)	0,51	$1{,}25x10^{-5}$
230050_at	NACC2	NACC family member 2, BEN and BTB (POZ) domain containing	0,51	$1{,}23x10^{-5}$
34225_at	WHSC2	Wolf-Hirschhorn syndrome candidate 2	0,51	$5{,}54x10^{-6}$
228951_at	NA	NA	0,51	$8{,}33x10^{-6}$
218743_at	CHMP6	chromatin modifying protein 6	0,51	$4{,}54x10^{-6}$
235384_at	NUDT19	nudix (nucleoside diphosphate linked moiety X)-type motif 19	0,51	$1{,}11x10^{-5}$
222744_s_at	TMLHE	trimethyllysine hydroxylase, epsilon	0,51	$5{,}28x10^{-6}$
220980_s_at	ADPGK	ADP-dependent glucokinase	0,51	$3{,}27x10^{-6}$
228830_s_at	ATF7	activating transcription factor 7	0,51	$5{,}76x10^{-6}$
236388_at	NA	NA	0,51	$7{,}05x10^{-6}$
218038_at	ATP5SL	ATP5S-like	0,51	$3{,}03x10^{-6}$
224416_s_at	MED28	mediator complex subunit 28	0,51	$5{,}79x10^{-6}$
1553096_s_at	BCL2L11	BCL2-like 11 (apoptosis facilitator)	0,51	$1{,}19x10^{-5}$
211849_s_at	RNGTT	RNA guanylyltransferase and 5'-phosphatase	0,51	$7{,}29x10^{-6}$
201700_at	CCND3	cyclin D3	0,51	$3{,}63x10^{-6}$
219473_at	GDAP2	ganglioside induced differentiation associated protein 2	0,51	$6{,}79x10^{-6}$
1555501_s_at	RSRC1	arginine/serine-rich coiled-coil 1	0,51	$9{,}58x10^{-6}$
201710_at	MYBL2	v-myb myeloblastosis viral oncogene homolog (avian)-like 2	0,51	$4{,}84x10^{-6}$
203858_s_at	COX10	COX10 homolog, cytochrome c oxidase assembly protein, heme A: farnesyltransferase (yeast)	0,50	$2{,}63x10^{-6}$
226763_at	SESTD1	SEC14 and spectrin domains 1	0,50	$1{,}46x10^{-5}$
202293_at	STAG1	stromal antigen 1	0,50	$1{,}18x10^{-5}$
225881_at	SLC35B4	solute carrier family 35, member B4	0,50	$3{,}94x10^{-6}$
221829_s_at	TNPO1	transportin 1	0,50	$5{,}79x10^{-6}$
221550_at	COX15	COX15 homolog, cytochrome c oxidase assembly protein (yeast)	0,50	$9{,}24x10^{-6}$
225600_at	C8orf83	chromosome 8 open reading frame 83	0,50	$4{,}09x10^{-6}$
201068_s_at	PSMC2	proteasome (prosome, macropain) 26S subunit, ATPase, 2	0,50	$3{,}89x10^{-6}$
218561_s_at	LYRM4	LYR motif containing 4	0,50	$2{,}82x10^{-6}$
201543_s_at	SAR1A	SAR1 homolog A (S. cerevisiae)	0,50	$9{,}15x10^{-7}$
212809_at	NFATC2IP	nuclear factor of activated T-cells, cytoplasmic, calcineurin-dependent 2 interacting protein	0,50	$1{,}14x10^{-5}$
1555964_at	ARL17A	ADP-ribosylation factor-like 17A	0,50	$2{,}85x10^{-6}$

...continues on next page

Table C.1.: *(...continued)*

Probe set ID	Gene symbol	Gene name	logFc	adj.p-val
223156_at	MRPS23	mitochondrial ribosomal protein S23	0,50	$3{,}96 \times 10^{-6}$
1556579_s_at	IGSF10	immunoglobulin superfamily, member 10	0,50	$9{,}29 \times 10^{-6}$
45828_at	ATP5SL	ATP5S-like	0,50	$1{,}54 \times 10^{-6}$
200813_s_at	PAFAH1B1	platelet-activating factor acetylhydrolase 1b, regulatory subunit 1 (45kDa)	0,50	$7{,}82 \times 10^{-6}$
231906_at	HOXD8	homeobox D8	0,50	$1{,}39 \times 10^{-5}$
212423_at	ZCCHC24	zinc finger, CCHC domain containing 24	0,50	$4{,}39 \times 10^{-6}$
215749_s_at	GORASP1	golgi reassembly stacking protein 1, 65kDa	0,50	$5{,}63 \times 10^{-6}$
212112_s_at	STX12	syntaxin 12	0,49	$2{,}46 \times 10^{-6}$
1553274_a_at	SNRNP48	small nuclear ribonucleoprotein 48kDa (U11/U12)	0,49	$6{,}70 \times 10^{-6}$
227493_s_at	KIAA1143	KIAA1143	0,49	$3{,}66 \times 10^{-6}$
211368_s_at	CASP1	caspase 1, apoptosis-related cysteine peptidase (interleukin 1, beta, convertase)	0,49	$1{,}08 \times 10^{-5}$
229732_at	ZNF823	zinc finger protein 823	0,49	$3{,}16 \times 10^{-6}$
208810_at	NA	NA	0,49	$6{,}96 \times 10^{-6}$
218896_s_at	C17orf85	chromosome 17 open reading frame 85	0,49	$2{,}97 \times 10^{-6}$
210788_s_at	DHRS7	dehydrogenase/reductase (SDR family) member 7	0,49	$6{,}73 \times 10^{-6}$
228008_at	NA	NA	0,49	$8{,}16 \times 10^{-6}$
200815_s_at	PAFAH1B1	platelet-activating factor acetylhydrolase 1b, regulatory subunit 1 (45kDa)	0,49	$3{,}93 \times 10^{-6}$
225331_at	CCDC50	coiled-coil domain containing 50	0,49	$2{,}67 \times 10^{-6}$
218547_at	DHDDS	dehydrodolichyl diphosphate synthase	0,49	$7{,}73 \times 10^{-6}$
225825_at	C20orf194	chromosome 20 open reading frame 194	0,48	$9{,}20 \times 10^{-6}$
204203_at	CEBPG	CCAAT/enhancer binding protein (C/EBP), gamma	0,48	$2{,}83 \times 10^{-6}$
201851_at	SH3GL1	SH3-domain GRB2-like 1	0,48	$6{,}64 \times 10^{-6}$
217870_s_at	CMPK1	cytidine monophosphate (UMP-CMP) kinase 1, cytosolic	0,48	$2{,}93 \times 10^{-6}$
212530_at	NEK7	NIMA (never in mitosis gene a)-related kinase 7	0,48	$4{,}04 \times 10^{-6}$
206555_s_at	THUMPD1	THUMP domain containing 1	0,48	$8{,}86 \times 10^{-6}$
201853_s_at	CDC25B	cell division cycle 25 homolog B (S. pombe)	0,48	$3{,}29 \times 10^{-6}$
206348_s_at	PDK3	pyruvate dehydrogenase kinase, isozyme 3	0,48	$6{,}07 \times 10^{-6}$
222635_s_at	MED28	mediator complex subunit 28	0,48	$1{,}00 \times 10^{-6}$
219129_s_at	SAP30L	SAP30-like	0,48	$1{,}07 \times 10^{-5}$
201471_s_at	SQSTM1	sequestosome 1	0,48	$5{,}96 \times 10^{-6}$
212397_at	RDX	radixin	0,48	$6{,}08 \times 10^{-6}$
219458_s_at	NSUN3	NOP2/Sun domain family, member 3	0,48	$6{,}84 \times 10^{-6}$
209578_s_at	POFUT2	protein O-fucosyltransferase 2	0,48	$1{,}38 \times 10^{-5}$
204336_s_at	RGS19	regulator of G-protein signalling 19	0,48	$2{,}04 \times 10^{-6}$
224987_at	C6orf89	chromosome 6 open reading frame 89	0,48	$5{,}90 \times 10^{-6}$
224967_at	UGCG	UDP-glucose ceramide glucosyltransferase	0,47	$1{,}88 \times 10^{-6}$
226175_at	TTC9C	tetratricopeptide repeat domain 9C	0,47	$6{,}35 \times 10^{-6}$
212194_s_at	TM9SF4	transmembrane 9 superfamily protein member 4	0,47	$4{,}98 \times 10^{-6}$
209954_x_at	SS18	synovial sarcoma translocation, chromosome 18	0,47	$5{,}05 \times 10^{-6}$

...continues on next page

Table C.1.: *(...continued)*

Probe set ID	Gene symbol	Gene name	logFc	adj.p-val
239413_at	CEP152	centrosomal protein 152kDa	0,47	1,73x10^{-6}
212419_at	ZCCHC24	zinc finger, CCHC domain containing 24	0,47	4,88x10^{-6}
223700_at	MND1	meiotic nuclear divisions 1 homolog (S. cerevisiae)	0,47	9,21x10^{-6}
207467_x_at	CAST	calpastatin	0,47	7,18x10^{-6}
224478_s_at	C7orf50	chromosome 7 open reading frame 50	0,47	4,38x10^{-6}
238599_at	IRAK1BP1	interleukin-1 receptor-associated kinase 1 binding protein 1	0,47	9,34x10^{-6}
200901_s_at	M6PR	mannose-6-phosphate receptor (cation dependent)	0,47	1,32x10^{-5}
218579_s_at	DHX35	DEAH (Asp-Glu-Ala-His) box polypeptide 35	0,47	1,30x10^{-5}
219207_at	EDC3	enhancer of mRNA decapping 3 homolog (S. cerevisiae)	0,47	6,90x10^{-6}
205482_x_at	SNX15	sorting nexin 15	0,47	1,31x10^{-5}
202346_at	UBE2K	ubiquitin-conjugating enzyme E2K (UBC1 homolog, yeast)	0,46	2,22x10^{-6}
223336_s_at	RAB18	RAB18, member RAS oncogene family	0,46	6,93x10^{-6}
219531_at	CEP72	centrosomal protein 72kDa	0,46	1,03x10^{-5}
202095_s_at	BIRC5	baculoviral IAP repeat-containing 5	0,46	9,47x10^{-6}
223098_s_at	LONP2	lon peptidase 2, peroxisomal	0,46	1,42x10^{-5}
200803_s_at	TMBIM6	transmembrane BAX inhibitor motif containing 6	0,46	5,43x10^{-6}
203112_s_at	WHSC2	Wolf-Hirschhorn syndrome candidate 2	0,46	7,79x10^{-6}
238974_at	C2orf69	chromosome 2 open reading frame 69	0,46	3,23x10^{-6}
214169_at	NA	NA	0,46	1,19x10^{-5}
226216_at	INSR	insulin receptor	0,46	1,43x10^{-5}
200755_s_at	CALU	calumenin	0,46	4,88x10^{-6}
230532_at	CXorf38	chromosome X open reading frame 38	0,46	1,22x10^{-5}
203519_s_at	UPF2	UPF2 regulator of nonsense transcripts homolog (yeast)	0,46	5,63x10^{-6}
229208_at	HAUS2	HAUS augmin-like complex, subunit 2	0,46	7,00x10^{-6}
223307_at	CDCA3	cell division cycle associated 3	0,46	1,33x10^{-5}
1555041_a_at	NAGA	N-acetylgalactosaminidase, alpha-	0,46	6,93x10^{-6}
1553956_at	ALS2CR4	amyotrophic lateral sclerosis 2 (juvenile) chromosome region, candidate 4	0,45	1,22x10^{-5}
207657_x_at	TNPO1	transportin 1	0,45	1,03x10^{-5}
227818_at	CCDC21	coiled-coil domain containing 21	0,45	7,27x10^{-6}
226946_at	C5orf33	chromosome 5 open reading frame 33	0,45	4,89x10^{-6}
223009_at	C11orf59	chromosome 11 open reading frame 59	0,45	4,60x10^{-6}
217520_x_at	NA	NA	0,45	1,31x10^{-5}
221268_s_at	SGPP1	sphingosine-1-phosphate phosphatase 1	0,45	1,34x10^{-5}
213501_at	ACOX1	acyl-Coenzyme A oxidase 1, palmitoyl	0,45	1,16x10^{-5}
202944_at	NAGA	N-acetylgalactosaminidase, alpha-	0,45	2,78x10^{-6}
222039_at	KIF18B	kinesin family member 18B	0,45	5,07x10^{-6}
200868_s_at	RNF114	ring finger protein 114	0,45	6,93x10^{-6}
210417_s_at	PI4KB	phosphatidylinositol 4-kinase, catalytic, beta	0,45	9,48x10^{-6}
219122_s_at	THG1L	tRNA-histidine guanylyltransferase 1-like (S. cerevisiae)	0,45	1,20x10^{-5}

...continues on next page

Table C.1.: *(...continued)*

Probe set ID	Gene symbol	Gene name	logFc	adj.p-val
222491_at	HGSNAT	heparan-alpha-glucosaminide N-acetyltransferase	0,45	$8{,}97x10^{-6}$
1554806_a_at	FBXO8	F-box protein 8	0,45	$1{,}38x10^{-5}$
208811_s_at	NA	NA	0,44	$6{,}45x10^{-6}$
225313_at	C20orf177	chromosome 20 open reading frame 177	0,44	$6{,}47x10^{-6}$
212305_s_at	MIA3	melanoma inhibitory activity family, member 3	0,44	$4{,}97x10^{-6}$
201039_s_at	RAD23A	RAD23 homolog A (S. cerevisiae)	0,44	$7{,}75x10^{-6}$
223186_at	NA	NA	0,44	$4{,}09x10^{-6}$
226850_at	SUMF1	sulfatase modifying factor 1	0,44	$3{,}02x10^{-6}$
208728_s_at	CDC42	cell division cycle 42 (GTP binding protein, 25kDa)	0,44	$4{,}45x10^{-6}$
210053_at	TAF5	TAF5 RNA polymerase II, TATA box binding protein (TBP)-associated factor, 100kDa	0,44	$8{,}75x10^{-6}$
209967_s_at	CREM	cAMP responsive element modulator	0,44	$6{,}51x10^{-6}$
203336_s_at	ITGB1BP1	integrin beta 1 binding protein 1	0,44	$3{,}86x10^{-6}$
201894_s_at	NA	NA	0,44	$9{,}93x10^{-6}$
1554105_at	TMEM185A	transmembrane protein 185A	0,44	$9{,}33x10^{-6}$
205598_at	TRAIP	TRAF interacting protein	0,44	$5{,}63x10^{-6}$
218648_at	CRTC3	CREB regulated transcription coactivator 3	0,43	$4{,}25x10^{-6}$
207839_s_at	TMEM8B	transmembrane protein 8B	0,43	$9{,}56x10^{-6}$
226177_at	GLTP	glycolipid transfer protein	0,43	$6{,}12x10^{-6}$
223463_at	RAB23	RAB23, member RAS oncogene family	0,43	$1{,}34x10^{-5}$
219988_s_at	RNF220	ring finger protein 220	0,43	$1{,}04x10^{-5}$
201389_at	ITGA5	integrin, alpha 5 (fibronectin receptor, alpha polypeptide)	0,43	$1{,}14x10^{-5}$
208698_s_at	NONO	non-POU domain containing, octamer-binding	0,43	$5{,}86x10^{-6}$
200788_s_at	PEA15	phosphoprotein enriched in astrocytes 15	0,43	$1{,}13x10^{-5}$
227833_s_at	MBD6	methyl-CpG binding domain protein 6	0,42	$1{,}24x10^{-5}$
223024_at	AP1M1	adaptor-related protein complex 1, mu 1 subunit	0,42	$5{,}56x10^{-6}$
223006_s_at	C9orf5	chromosome 9 open reading frame 5	0,42	$1{,}19x10^{-5}$
226750_at	LARP1B	La ribonucleoprotein domain family, member 1B	0,42	$1{,}04x10^{-5}$
213203_at	SNAPC5	small nuclear RNA activating complex, polypeptide 5, 19kDa	0,42	$4{,}61x10^{-6}$
213906_at	MYBL1	v-myb myeloblastosis viral oncogene homolog (avian)-like 1	0,42	$1{,}22x10^{-5}$
201612_at	ALDH9A1	aldehyde dehydrogenase 9 family, member A1	0,41	$4{,}22x10^{-6}$
212204_at	TMEM87A	transmembrane protein 87A	0,41	$5{,}81x10^{-6}$
210470_x_at	NONO	non-POU domain containing, octamer-binding	0,41	$2{,}97x10^{-6}$
1553162_x_at	C19orf55	chromosome 19 open reading frame 55	0,41	$1{,}22x10^{-5}$
205463_s_at	PDGFA	platelet-derived growth factor alpha polypeptide	0,41	$9{,}47x10^{-6}$
218189_s_at	NANS	N-acetylneuraminic acid synthase	0,41	$1{,}01x10^{-5}$
210378_s_at	SSNA1	Sjogren syndrome nuclear autoantigen 1	0,41	$7{,}90x10^{-6}$
212241_at	NA	NA	0,41	$1{,}05x10^{-5}$
224950_at	PTGFRN	prostaglandin F2 receptor negative regulator	0,41	$1{,}19x10^{-5}$
212137_at	LARP1	La ribonucleoprotein domain family, member 1	0,40	$5{,}23x10^{-6}$

...continues on next page

Table C.1.: *(...continued)*

Probe set ID	Gene symbol	Gene name	logFc	adj.p-val
212923_s_at	C6orf145	chromosome 6 open reading frame 145	0,40	$7{,}52 \times 10^{-6}$
223602_at	USP30	ubiquitin specific peptidase 30	0,40	$1{,}07 \times 10^{-5}$
223515_s_at	COQ3	coenzyme Q3 homolog, methyltransferase (S. cerevisiae)	0,40	$1{,}06 \times 10^{-5}$
222217_s_at	SLC27A3	solute carrier family 27 (fatty acid transporter), member 3	0,40	$7{,}51 \times 10^{-6}$
224983_at	SCARB2	scavenger receptor class B, member 2	0,40	$6{,}02 \times 10^{-6}$
219276_x_at	C9orf82	chromosome 9 open reading frame 82	0,39	$1{,}17 \times 10^{-5}$
218702_at	SARS2	seryl-tRNA synthetase 2, mitochondrial	0,39	$4{,}02 \times 10^{-6}$
238606_at	ZNF747	zinc finger protein 747	0,38	$8{,}00 \times 10^{-6}$
210386_s_at	MTX1	metaxin 1	0,38	$6{,}68 \times 10^{-6}$
218351_at	COMMD8	COMM domain containing 8	0,38	$9{,}18 \times 10^{-6}$
204093_at	CCNH	cyclin H	0,38	$1{,}13 \times 10^{-5}$
64899_at	LPPR2	lipid phosphate phosphatase-related protein type 2	0,36	$9{,}75 \times 10^{-6}$
223305_at	TMEM216	transmembrane protein 216	-0,36	$8{,}88 \times 10^{-6}$
224760_at	SP1	Sp1 transcription factor	-0,37	$1{,}16 \times 10^{-5}$
202584_at	NFX1	nuclear transcription factor, X-box binding 1	-0,37	$1{,}11 \times 10^{-5}$
203816_at	DGUOK	deoxyguanosine kinase	-0,38	$7{,}31 \times 10^{-6}$
223068_at	EML4	echinoderm microtubule associated protein like 4	-0,39	$1{,}06 \times 10^{-5}$
226845_s_at	MYEOV2	myeloma overexpressed 2	-0,39	$6{,}31 \times 10^{-6}$
218126_at	FAM82A2	family with sequence similarity 82, member A2	-0,39	$5{,}90 \times 10^{-6}$
209418_s_at	THOC5	THO complex 5	-0,39	$4{,}99 \times 10^{-6}$
222584_at	MSTO1	misato homolog 1 (Drosophila)	-0,40	$1{,}22 \times 10^{-5}$
44040_at	FBXO41	F-box protein 41	-0,40	$8{,}80 \times 10^{-6}$
202961_s_at	ATP5J2	ATP synthase, H+ transporting, mitochondrial F0 complex, subunit F2	-0,40	$5{,}90 \times 10^{-6}$
225522_at	AAK1	AP2 associated kinase 1	-0,41	$1{,}01 \times 10^{-5}$
212320_at	TUBB	tubulin, beta	-0,41	$5{,}35 \times 10^{-6}$
223063_at	C1orf198	chromosome 1 open reading frame 198	-0,41	$4{,}64 \times 10^{-6}$
200783_s_at	STMN1	stathmin 1	-0,41	$1{,}12 \times 10^{-5}$
225750_at	NA	NA	-0,41	$9{,}33 \times 10^{-6}$
201036_s_at	HADH	hydroxyacyl-Coenzyme A dehydrogenase	-0,41	$1{,}18 \times 10^{-5}$
238038_at	NA	NA	-0,41	$9{,}03 \times 10^{-6}$
224919_at	MRPS6	mitochondrial ribosomal protein S6	-0,42	$5{,}05 \times 10^{-6}$
224883_at	PLDN	pallidin homolog (mouse)	-0,42	$6{,}31 \times 10^{-6}$
201462_at	SCRN1	secernin 1	-0,42	$8{,}72 \times 10^{-6}$
212375_at	EP400	E1A binding protein p400	-0,42	$8{,}72 \times 10^{-6}$
202365_at	UNC119B	unc-119 homolog B (C. elegans)	-0,42	$6{,}30 \times 10^{-6}$
202919_at	MOBKL3	MOB1, Mps One Binder kinase activator-like 3 (yeast)	-0,43	$5{,}34 \times 10^{-6}$
219536_s_at	ZFP64	zinc finger protein 64 homolog (mouse)	-0,43	$6{,}26 \times 10^{-6}$
229528_at	SBNO1	strawberry notch homolog 1 (Drosophila)	-0,43	$6{,}21 \times 10^{-6}$
206855_s_at	HYAL2	hyaluronoglucosaminidase 2	-0,43	$8{,}78 \times 10^{-6}$
209472_at	CCBL2	cysteine conjugate-beta lyase 2	-0,43	$1{,}19 \times 10^{-5}$

...continues on next page

Table C.1.: *(...continued)*

Probe set ID	Gene symbol	Gene name	logFc	adj.p-val
202530_at	MAPK14	mitogen-activated protein kinase 14	-0,43	$5{,}22 \times 10^{-6}$
213574_s_at	KPNB1	karyopherin (importin) beta 1	-0,43	$5{,}68 \times 10^{-6}$
33814_at	PAK4	p21 protein (Cdc42/Rac)-activated kinase 4	-0,43	$1{,}27 \times 10^{-5}$
222819_at	CTPS2	CTP synthase II	-0,43	$6{,}29 \times 10^{-6}$
213275_x_at	CTSB	cathepsin B	-0,43	$4{,}84 \times 10^{-6}$
214853_s_at	SHC1	SHC (Src homology 2 domain containing) transforming protein 1	-0,43	$5{,}37 \times 10^{-6}$
201230_s_at	ARIH2	ariadne homolog 2 (Drosophila)	-0,44	$5{,}70 \times 10^{-6}$
204177_s_at	KLHL20	kelch-like 20 (Drosophila)	-0,44	$3{,}17 \times 10^{-6}$
221203_s_at	YEATS2	YEATS domain containing 2	-0,44	$9{,}21 \times 10^{-6}$
205512_s_at	AIFM1	apoptosis-inducing factor, mitochondrion-associated, 1	-0,44	$2{,}40 \times 10^{-6}$
224937_at	PTGFRN	prostaglandin F2 receptor negative regulator	-0,44	$4{,}87 \times 10^{-6}$
200594_x_at	HNRNPU	heterogeneous nuclear ribonucleoprotein U (scaffold attachment factor A)	-0,44	$4{,}65 \times 10^{-6}$
206853_s_at	MAP3K7	mitogen-activated protein kinase kinase kinase 7	-0,44	$8{,}51 \times 10^{-6}$
224892_at	PLDN	pallidin homolog (mouse)	-0,44	$6{,}84 \times 10^{-6}$
235647_at	AP4S1	adaptor-related protein complex 4, sigma 1 subunit	-0,44	$4{,}69 \times 10^{-6}$
203250_at	RBM16	RNA binding motif protein 16	-0,45	$3{,}78 \times 10^{-6}$
1568609_s_at	NA	NA	-0,45	$1{,}27 \times 10^{-5}$
212836_at	POLD3	polymerase (DNA-directed), delta 3, accessory subunit	-0,45	$2{,}26 \times 10^{-6}$
209141_at	UBE2G1	ubiquitin-conjugating enzyme E2G 1 (UBC7 homolog, yeast)	-0,45	$2{,}86 \times 10^{-6}$
219222_at	RBKS	ribokinase	-0,45	$5{,}43 \times 10^{-6}$
227560_at	SFXN2	sideroflexin 2	-0,45	$3{,}14 \times 10^{-6}$
203339_at	SLC25A12	solute carrier family 25 (mitochondrial carrier, Aralar), member 12	-0,45	$1{,}17 \times 10^{-5}$
221493_at	TSPYL1	TSPY-like 1	-0,45	$9{,}03 \times 10^{-6}$
1554918_a_at	ABCC4	ATP-binding cassette, sub-family C (CFTR/MRP), member 4	-0,46	$9{,}75 \times 10^{-6}$
212676_at	NF1	neurofibromin 1	-0,46	$5{,}69 \times 10^{-6}$
228537_at	GLI2	GLI family zinc finger 2	-0,46	$1{,}28 \times 10^{-5}$
44065_at	C12orf52	chromosome 12 open reading frame 52	-0,46	$9{,}97 \times 10^{-6}$
218377_s_at	RWDD2B	RWD domain containing 2B	-0,46	$1{,}25 \times 10^{-5}$
224100_s_at	DPYSL5	dihydropyrimidinase-like 5	-0,46	$7{,}26 \times 10^{-6}$
217943_s_at	MAP7D1	MAP7 domain containing 1	-0,46	$3{,}11 \times 10^{-6}$
242205_at	NA	NA	-0,46	$6{,}68 \times 10^{-6}$
222471_s_at	KCMF1	potassium channel modulatory factor 1	-0,47	$1{,}35 \times 10^{-5}$
1555967_at	NA	NA	-0,47	$9{,}30 \times 10^{-6}$
226589_at	TMEM192	transmembrane protein 192	-0,47	$9{,}40 \times 10^{-6}$
209692_at	EYA2	eyes absent homolog 2 (Drosophila)	-0,47	$5{,}76 \times 10^{-6}$
227374_at	EARS2	glutamyl-tRNA synthetase 2, mitochondrial (putative)	-0,47	$6{,}29 \times 10^{-6}$
221484_at	B4GALT5	UDP-Gal:betaGlcNAc beta 1,4- galactosyltransferase, polypeptide 5	-0,47	$5{,}08 \times 10^{-6}$

...continues on next page

Table C.1.: *(...continued)*

Probe set ID	Gene symbol	Gene name	logFc	adj.p-val
225577_at	HCG18	HLA complex group 18	-0,47	$6{,}54 \times 10^{-6}$
226343_at	NA	NA	-0,47	$1{,}25 \times 10^{-5}$
223471_at	RAB3IP	RAB3A interacting protein (rabin3)	-0,47	$9{,}84 \times 10^{-6}$
212442_s_at	LASS6	LAG1 homolog, ceramide synthase 6	-0,47	$4{,}63 \times 10^{-6}$
224579_at	SLC38A1	solute carrier family 38, member 1	-0,47	$9{,}83 \times 10^{-6}$
212509_s_at	MXRA7	matrix-remodelling associated 7	-0,47	$3{,}94 \times 10^{-6}$
222441_x_at	SLMO2	slowmo homolog 2 (Drosophila)	-0,47	$7{,}43 \times 10^{-6}$
212645_x_at	BRE	brain and reproductive organ-expressed (TNFRSF1A modulator)	-0,47	$5{,}80 \times 10^{-6}$
228347_at	SIX1	SIX homeobox 1	-0,47	$2{,}76 \times 10^{-6}$
203499_at	EPHA2	EPH receptor A2	-0,47	$4{,}64 \times 10^{-6}$
1556082_a_at	NA	NA	-0,47	$1{,}11 \times 10^{-5}$
212234_at	ASXL1	additional sex combs like 1 (Drosophila)	-0,47	$1{,}03 \times 10^{-5}$
208770_s_at	EIF4EBP2	eukaryotic translation initiation factor 4E binding protein 2	-0,48	$1{,}15 \times 10^{-5}$
203514_at	MAP3K3	mitogen-activated protein kinase kinase kinase 3	-0,48	$3{,}48 \times 10^{-6}$
225486_at	ARID2	AT rich interactive domain 2 (ARID, RFX-like)	-0,48	$1{,}10 \times 10^{-5}$
240233_at	NA	NA	-0,48	$6{,}44 \times 10^{-6}$
203097_s_at	RAPGEF2	Rap guanine nucleotide exchange factor (GEF) 2	-0,48	$6{,}37 \times 10^{-6}$
229106_at	DYNLL2	dynein, light chain, LC8-type 2	-0,48	$2{,}04 \times 10^{-6}$
226485_at	VSIG10	V-set and immunoglobulin domain containing 10	-0,48	$7{,}80 \times 10^{-6}$
224711_at	YY1	YY1 transcription factor	-0,48	$6{,}01 \times 10^{-6}$
213405_at	RAB22A	RAB22A, member RAS oncogene family	-0,48	$7{,}24 \times 10^{-6}$
209859_at	TRIM9	tripartite motif-containing 9	-0,48	$1{,}40 \times 10^{-5}$
231764_at	CHRAC1	chromatin accessibility complex 1	-0,48	$7{,}77 \times 10^{-6}$
213020_at	GOSR1	golgi SNAP receptor complex member 1	-0,48	$9{,}45 \times 10^{-6}$
231844_at	MGC27345	hypothetical protein MGC27345	-0,48	$6{,}08 \times 10^{-6}$
201129_at	SFRS7	splicing factor, arginine/serine-rich 7, 35kDa	-0,48	$1{,}18 \times 10^{-5}$
226620_x_at	DAZAP1	DAZ associated protein 1	-0,48	$4{,}64 \times 10^{-6}$
202767_at	ACP2	acid phosphatase 2, lysosomal	-0,48	$1{,}97 \times 10^{-6}$
201219_at	NA	NA	-0,48	$3{,}94 \times 10^{-6}$
226723_at	CCDC23	coiled-coil domain containing 23	-0,48	$3{,}72 \times 10^{-6}$
228967_at	EIF1	eukaryotic translation initiation factor 1	-0,48	$1{,}09 \times 10^{-5}$
222119_s_at	FBXO11	F-box protein 11	-0,48	$1{,}06 \times 10^{-5}$
227421_at	C21orf57	chromosome 21 open reading frame 57	-0,48	$1{,}23 \times 10^{-5}$
225615_at	IFFO2	intermediate filament family orphan 2	-0,48	$3{,}70 \times 10^{-6}$
213029_at	NFIB	nuclear factor I/B	-0,48	$1{,}15 \times 10^{-5}$
226902_at	USP13	ubiquitin specific peptidase 13 (isopeptidase T-3)	-0,48	$3{,}44 \times 10^{-6}$
223073_at	HIATL1	hippocampus abundant transcript-like 1	-0,49	$1{,}38 \times 10^{-5}$
226132_s_at	MANEAL	mannosidase, endo-alpha-like	-0,49	$6{,}99 \times 10^{-6}$
218412_s_at	GTF2IRD1	GTF2I repeat domain containing 1	-0,49	$5{,}90 \times 10^{-6}$
218242_s_at	SUV420H1	suppressor of variegation 4-20 homolog 1 (Drosophila)	-0,49	$9{,}33 \times 10^{-6}$

...continues on next page

Table C.1.: *(...continued)*

Probe set ID	Gene symbol	Gene name	logFc	adj.p-val
217122_s_at	RP11-345P4.4	similar to solute carrier family 35, member E2	-0,49	$1{,}05 \times 10^{-5}$
223041_at	CD99L2	CD99 molecule-like 2	-0,49	$7{,}89 \times 10^{-6}$
223282_at	TSHZ1	teashirt zinc finger homeobox 1	-0,49	$6{,}34 \times 10^{-6}$
227045_at	ZNF614	zinc finger protein 614	-0,49	$8{,}44 \times 10^{-6}$
218108_at	UBR7	ubiquitin protein ligase E3 component n-recognin 7 (putative)	-0,49	$1{,}59 \times 10^{-6}$
202205_at	VASP	vasodilator-stimulated phosphoprotein	-0,49	$4{,}39 \times 10^{-6}$
226317_at	PPP4R2	protein phosphatase 4, regulatory subunit 2	-0,49	$9{,}09 \times 10^{-6}$
202051_s_at	ZMYM4	zinc finger, MYM-type 4	-0,49	$3{,}76 \times 10^{-6}$
217546_at	MT1M	metallothionein 1M	-0,49	$1{,}34 \times 10^{-6}$
229182_at	NA	NA	-0,49	$4{,}04 \times 10^{-6}$
203007_x_at	LYPLA1	lysophospholipase I	-0,49	$7{,}66 \times 10^{-6}$
213233_s_at	KLHL9	kelch-like 9 (Drosophila)	-0,49	$2{,}41 \times 10^{-6}$
224905_at	WDR26	WD repeat domain 26	-0,49	$3{,}37 \times 10^{-6}$
206373_at	ZIC1	Zic family member 1 (odd-paired homolog, Drosophila)	-0,50	$2{,}31 \times 10^{-6}$
217127_at	CTH	cystathionase (cystathionine gamma-lyase)	-0,50	$1{,}19 \times 10^{-5}$
204057_at	IRF8	interferon regulatory factor 8	-0,50	$6{,}72 \times 10^{-6}$
225224_at	C20orf112	chromosome 20 open reading frame 112	-0,50	$1{,}13 \times 10^{-5}$
218125_s_at	CCDC25	coiled-coil domain containing 25	-0,50	$1{,}19 \times 10^{-5}$
201574_at	ETF1	eukaryotic translation termination factor 1	-0,50	$2{,}29 \times 10^{-6}$
226345_at	NA	NA	-0,50	$3{,}51 \times 10^{-6}$
235772_at	NA	NA	-0,50	$4{,}51 \times 10^{-6}$
227169_at	DNAJC18	DnaJ (Hsp40) homolog, subfamily C, member 18	-0,50	$2{,}16 \times 10^{-6}$
221839_s_at	UBAP2	ubiquitin associated protein 2	-0,50	$1{,}40 \times 10^{-6}$
204849_at	TCFL5	transcription factor-like 5 (basic helix-loop-helix)	-0,50	$9{,}24 \times 10^{-6}$
208502_s_at	PITX1	paired-like homeodomain 1	-0,50	$2{,}37 \times 10^{-6}$
224653_at	EIF4EBP2	eukaryotic translation initiation factor 4E binding protein 2	-0,50	$7{,}81 \times 10^{-6}$
205550_s_at	BRE	brain and reproductive organ-expressed (TNFRSF1A modulator)	-0,50	$2{,}41 \times 10^{-6}$
229813_x_at	DAZAP1	DAZ associated protein 1	-0,50	$8{,}46 \times 10^{-6}$
225574_at	RWDD4A	RWD domain containing 4A	-0,50	$5{,}96 \times 10^{-6}$
201532_at	PSMA3	proteasome (prosome, macropain) subunit, alpha type, 3	-0,50	$2{,}69 \times 10^{-6}$
212463_at	CD59	CD59 molecule, complement regulatory protein	-0,50	$9{,}07 \times 10^{-6}$
203196_at	ABCC4	ATP-binding cassette, sub-family C (CFTR/MRP), member 4	-0,50	$6{,}27 \times 10^{-6}$
212378_at	GART	phosphoribosylglycinamide formyltransferase, phosphoribosylglycinamide synthetase, phosphoribosylaminoimidazole synthetase	-0,51	$1{,}40 \times 10^{-5}$
218862_at	ASB13	ankyrin repeat and SOCS box-containing 13	-0,51	$8{,}43 \times 10^{-7}$
225157_at	MLXIP	MLX interacting protein	-0,51	$1{,}60 \times 10^{-6}$
204275_at	SOLH	small optic lobes homolog (Drosophila)	-0,51	$1{,}11 \times 10^{-6}$
209090_s_at	SH3GLB1	SH3-domain GRB2-like endophilin B1	-0,51	$2{,}17 \times 10^{-6}$

...continues on next page

Table C.1.: *(...continued)*

Probe set ID	Gene symbol	Gene name	logFc	adj.p-val
210740_s_at	ITPK1	inositol 1,3,4-triphosphate 5/6 kinase	-0,51	$1{,}57 \times 10^{-6}$
212120_at	RHOQ	ras homolog gene family, member Q	-0,51	$6{,}24 \times 10^{-6}$
226743_at	SLFN11	schlafen family member 11	-0,51	$1{,}14 \times 10^{-5}$
229533_x_at	ZNF680	zinc finger protein 680	-0,51	$8{,}30 \times 10^{-6}$
226774_at	FAM120B	family with sequence similarity 120B	-0,51	$1{,}57 \times 10^{-6}$
203686_at	MPG	N-methylpurine-DNA glycosylase	-0,51	$6{,}54 \times 10^{-6}$
202084_s_at	SEC14L1	SEC14-like 1 (S. cerevisiae)	-0,51	$9{,}47 \times 10^{-6}$
205283_at	FKTN	fukutin	-0,52	$1{,}37 \times 10^{-5}$
213002_at	MARCKS	myristoylated alanine-rich protein kinase C substrate	-0,52	$5{,}90 \times 10^{-6}$
227665_at	NA	NA	-0,52	$3{,}23 \times 10^{-6}$
218774_at	DCPS	decapping enzyme, scavenger	-0,52	$4{,}61 \times 10^{-6}$
228580_at	HTRA3	HtrA serine peptidase 3	-0,52	$1{,}69 \times 10^{-6}$
209786_at	HMGN4	high mobility group nucleosomal binding domain 4	-0,52	$1{,}29 \times 10^{-5}$
37943_at	ZFYVE26	zinc finger, FYVE domain containing 26	-0,52	$1{,}20 \times 10^{-6}$
238576_at	NA	NA	-0,52	$5{,}11 \times 10^{-6}$
206558_at	SIM2	single-minded homolog 2 (Drosophila)	-0,52	$5{,}01 \times 10^{-6}$
242082_at	MMAB	methylmalonic aciduria (cobalamin deficiency) cblB type	-0,52	$1{,}47 \times 10^{-5}$
224718_at	YY1	YY1 transcription factor	-0,52	$6{,}04 \times 10^{-6}$
217892_s_at	LIMA1	LIM domain and actin binding 1	-0,52	$4{,}70 \times 10^{-6}$
212192_at	KCTD12	potassium channel tetramerisation domain containing 12	-0,52	$5{,}00 \times 10^{-6}$
229664_at	MAPK8	mitogen-activated protein kinase 8	-0,52	$4{,}12 \times 10^{-6}$
214126_at	NA	NA	-0,53	$5{,}69 \times 10^{-6}$
207144_s_at	CITED1	Cbp/p300-interacting transactivator, with Glu/Asp-rich carboxy-terminal domain, 1	-0,53	$8{,}05 \times 10^{-6}$
233825_s_at	CD99L2	CD99 molecule-like 2	-0,53	$8{,}86 \times 10^{-6}$
226033_at	USP31	ubiquitin specific peptidase 31	-0,53	$1{,}01 \times 10^{-5}$
220367_s_at	SAP130	Sin3A-associated protein, 130kDa	-0,53	$3{,}05 \times 10^{-6}$
222629_at	REV1	REV1 homolog (S. cerevisiae)	-0,53	$3{,}52 \times 10^{-6}$
204432_at	SOX12	SRY (sex determining region Y)-box 12	-0,53	$7{,}20 \times 10^{-6}$
224704_at	TNRC6A	trinucleotide repeat containing 6A	-0,53	$8{,}99 \times 10^{-6}$
212875_s_at	C2CD2	C2 calcium-dependent domain containing 2	-0,53	$1{,}86 \times 10^{-6}$
236178_at	C6orf162	chromosome 6 open reading frame 162	-0,53	$5{,}53 \times 10^{-6}$
217910_x_at	MLX	MAX-like protein X	-0,53	$1{,}01 \times 10^{-5}$
223302_s_at	ZNF655	zinc finger protein 655	-0,53	$4{,}87 \times 10^{-6}$
223350_x_at	LIN7C	lin-7 homolog C (C. elegans)	-0,53	$2{,}33 \times 10^{-6}$
222001_x_at	LOC728855	hypothetical LOC728855	-0,53	$1{,}58 \times 10^{-5}$
208704_x_at	APLP2	amyloid beta (A4) precursor-like protein 2	-0,53	$2{,}88 \times 10^{-6}$
217555_at	SMC1A	structural maintenance of chromosomes 1A	-0,53	$5{,}87 \times 10^{-6}$
200696_s_at	GSN	gelsolin (amyloidosis, Finnish type)	-0,53	$3{,}21 \times 10^{-6}$
222457_s_at	LIMA1	LIM domain and actin binding 1	-0,54	$4{,}16 \times 10^{-6}$
226030_at	ACADSB	acyl-Coenzyme A dehydrogenase, short/branched chain	-0,54	$2{,}99 \times 10^{-6}$

...continues on next page

Table C.1.: *(...continued)*

Probe set ID	Gene symbol	Gene name	logFc	adj.p-val
235333_at	B4GALT6	UDP-Gal:betaGlcNAc beta 1,4- galactosyltransferase, polypeptide 6	-0,54	$2{,}21 \times 10^{-6}$
208248_x_at	APLP2	amyloid beta (A4) precursor-like protein 2	-0,54	$2{,}47 \times 10^{-6}$
226180_at	WDR36	WD repeat domain 36	-0,54	$1{,}30 \times 10^{-5}$
217961_at	SLC25A38	solute carrier family 25, member 38	-0,54	$5{,}90 \times 10^{-6}$
224645_at	EIF4EBP2	eukaryotic translation initiation factor 4E binding protein 2	-0,54	$4{,}03 \times 10^{-6}$
227980_at	ZNF322A	zinc finger protein 322A	-0,54	$9{,}47 \times 10^{-6}$
221485_at	B4GALT5	UDP-Gal:betaGlcNAc beta 1,4- galactosyltransferase, polypeptide 5	-0,54	$9{,}84 \times 10^{-6}$
1555874_x_at	MGC21881	hypothetical locus MGC21881	-0,54	$2{,}51 \times 10^{-6}$
218421_at	CERK	ceramide kinase	-0,54	$7{,}22 \times 10^{-6}$
203340_s_at	SLC25A12	solute carrier family 25 (mitochondrial carrier, Aralar), member 12	-0,54	$9{,}91 \times 10^{-6}$
228963_at	RSBN1L	round spermatid basic protein 1-like	-0,54	$4{,}78 \times 10^{-6}$
204798_at	MYB	v-myb myeloblastosis viral oncogene homolog (avian)	-0,54	$5{,}53 \times 10^{-6}$
227234_at	LOC100132815	hypothetical protein LOC100132815	-0,54	$9{,}50 \times 10^{-6}$
229267_at	ANAPC1	anaphase promoting complex subunit 1	-0,54	$4{,}91 \times 10^{-6}$
230685_at	FLJ33630	hypothetical LOC644873	-0,54	$1{,}94 \times 10^{-6}$
225390_s_at	KLF13	Kruppel-like factor 13	-0,54	$9{,}10 \times 10^{-6}$
206510_at	SIX2	SIX homeobox 2	-0,54	$4{,}87 \times 10^{-6}$
226275_at	MXD1	MAX dimerization protein 1	-0,54	$1{,}13 \times 10^{-5}$
224756_s_at	BAT5	HLA-B associated transcript 5	-0,54	$6{,}90 \times 10^{-6}$
221777_at	C12orf52	chromosome 12 open reading frame 52	-0,54	$7{,}68 \times 10^{-7}$
211938_at	EIF4B	eukaryotic translation initiation factor 4B	-0,55	$1{,}04 \times 10^{-5}$
201447_at	TIA1	TIA1 cytotoxic granule-associated RNA binding protein	-0,55	$4{,}31 \times 10^{-7}$
231955_s_at	HIBADH	3-hydroxyisobutyrate dehydrogenase	-0,55	$1{,}13 \times 10^{-5}$
227049_at	ZADH2	zinc binding alcohol dehydrogenase domain containing 2	-0,55	$1{,}55 \times 10^{-5}$
227930_at	EIF2C4	eukaryotic translation initiation factor 2C, 4	-0,55	$4{,}22 \times 10^{-6}$
205031_at	EFNB3	ephrin-B3	-0,55	$1{,}25 \times 10^{-5}$
225097_at	HIPK2	homeodomain interacting protein kinase 2	-0,55	$5{,}62 \times 10^{-6}$
1558568_a_at	NA	NA	-0,55	$1{,}08 \times 10^{-5}$
222253_s_at	POM121L9P	POM121 membrane glycoprotein-like 9 (rat) pseudogene	-0,55	$9{,}22 \times 10^{-6}$
222572_at	PDP1	pyruvate dehyrogenase phosphatase catalytic subunit 1	-0,55	$9{,}39 \times 10^{-6}$
217612_at	TIMM50	translocase of inner mitochondrial membrane 50 homolog (S. cerevisiae)	-0,55	$1{,}20 \times 10^{-5}$
228149_at	C7orf60	chromosome 7 open reading frame 60	-0,55	$1{,}19 \times 10^{-5}$
201080_at	PIP4K2B	phosphatidylinositol-5-phosphate 4-kinase, type II, beta	-0,55	$4{,}35 \times 10^{-6}$
223148_at	PIGS	phosphatidylinositol glycan anchor biosynthesis, class S	-0,55	$1{,}77 \times 10^{-6}$
224735_at	CYBASC3	cytochrome b, ascorbate dependent 3	-0,55	$1{,}28 \times 10^{-6}$
242312_x_at	NA	NA	-0,55	$2{,}47 \times 10^{-6}$
212217_at	PREPL	prolyl endopeptidase-like	-0,55	$5{,}91 \times 10^{-7}$
228520_s_at	APLP2	amyloid beta (A4) precursor-like protein 2	-0,55	$4{,}29 \times 10^{-6}$

...continues on next page

Table C.1.: *(...continued)*

Probe set ID	Gene symbol	Gene name	logFc	adj.p-val
223982_s_at	PNPLA8	patatin-like phospholipase domain containing 8	-0,55	$1{,}70\text{x}10^{-6}$
223310_x_at	PNPLA8	patatin-like phospholipase domain containing 8	-0,56	$4{,}26\text{x}10^{-6}$
65585_at	FAM86B1	family with sequence similarity 86, member B1	-0,56	$9{,}54\text{x}10^{-6}$
208966_x_at	IFI16	interferon, gamma-inducible protein 16	-0,56	$9{,}94\text{x}10^{-6}$
1555872_a_at	NA	NA	-0,56	$2{,}82\text{x}10^{-6}$
231809_x_at	PDCD7	programmed cell death 7	-0,56	$1{,}06\text{x}10^{-5}$
202461_at	EIF2B2	eukaryotic translation initiation factor 2B, subunit 2 beta, 39kDa	-0,56	$1{,}65\text{x}10^{-6}$
225558_at	GIT2	G protein-coupled receptor kinase interacting ArfGAP 2	-0,56	$2{,}40\text{x}10^{-6}$
201301_s_at	ANXA4	annexin A4	-0,56	$1{,}80\text{x}10^{-6}$
201813_s_at	TBC1D5	TBC1 domain family, member 5	-0,56	$5{,}92\text{x}10^{-7}$
227117_at	NA	NA	-0,56	$1{,}02\text{x}10^{-6}$
224955_at	TEAD1	TEA domain family member 1 (SV40 transcriptional enhancer factor)	-0,56	$9{,}69\text{x}10^{-7}$
207174_at	GPC5	glypican 5	-0,56	$3{,}98\text{x}10^{-6}$
227423_at	LRRC28	leucine rich repeat containing 28	-0,56	$6{,}15\text{x}10^{-6}$
225633_at	DPY19L3	dpy-19-like 3 (C. elegans)	-0,56	$2{,}50\text{x}10^{-6}$
213047_x_at	SET	SET nuclear oncogene	-0,56	$6{,}38\text{x}10^{-7}$
225875_s_at	NIPAL3	NIPA-like domain containing 3	-0,56	$4{,}22\text{x}10^{-6}$
225576_at	C6orf72	chromosome 6 open reading frame 72	-0,56	$8{,}97\text{x}10^{-7}$
228698_at	SOX7	SRY (sex determining region Y)-box 7	-0,57	$6{,}36\text{x}10^{-6}$
224763_at	RPL37	ribosomal protein L37	-0,57	$9{,}47\text{x}10^{-6}$
201158_at	NMT1	N-myristoyltransferase 1	-0,57	$2{,}09\text{x}10^{-6}$
1558740_s_at	NA	NA	-0,57	$6{,}92\text{x}10^{-6}$
224654_at	DDX21	DEAD (Asp-Glu-Ala-Asp) box polypeptide 21	-0,57	$1{,}12\text{x}10^{-5}$
216392_s_at	SEC23IP	SEC23 interacting protein	-0,57	$3{,}27\text{x}10^{-6}$
226801_s_at	AIDA	axin interactor, dorsalization associated	-0,57	$7{,}76\text{x}10^{-7}$
203154_s_at	PAK4	p21 protein (Cdc42/Rac)-activated kinase 4	-0,57	$5{,}99\text{x}10^{-6}$
239435_x_at	SHROOM1	shroom family member 1	-0,57	$1{,}02\text{x}10^{-6}$
206245_s_at	IVNS1ABP	influenza virus NS1A binding protein	-0,57	$2{,}97\text{x}10^{-6}$
208877_at	PAK2	p21 protein (Cdc42/Rac)-activated kinase 2	-0,57	$1{,}86\text{x}10^{-6}$
244486_at	NA	NA	-0,57	$6{,}77\text{x}10^{-6}$
1553972_a_at	CBS	cystathionine-beta-synthase	-0,57	$9{,}23\text{x}10^{-6}$
226532_at	NA	NA	-0,57	$5{,}12\text{x}10^{-7}$
242086_at	NA	NA	-0,57	$6{,}33\text{x}10^{-6}$
222263_at	SLC35E1	solute carrier family 35, member E1	-0,57	$5{,}91\text{x}10^{-7}$
209187_at	DR1	down-regulator of transcription 1, TBP-binding (negative cofactor 2)	-0,57	$3{,}03\text{x}10^{-6}$
208651_x_at	CD24	CD24 molecule	-0,58	$1{,}89\text{x}10^{-6}$
236133_x_at	ZNF254	zinc finger protein 254	-0,58	$6{,}14\text{x}10^{-6}$
225572_at	CREB1	cAMP responsive element binding protein 1	-0,58	$5{,}05\text{x}10^{-6}$
1564467_at	FAM161A	family with sequence similarity 161, member A	-0,58	$5{,}05\text{x}10^{-6}$

...continues on next page

Table C.1.: *(...continued)*

Probe set ID	Gene symbol	Gene name	logFc	adj.p-val
229393_at	L3MBTL3	l(3)mbt-like 3 (Drosophila)	-0,58	$1{,}12\text{x}10^{-5}$
224320_s_at	MCM8	minichromosome maintenance complex component 8	-0,58	$5{,}58\text{x}10^{-7}$
213675_at	NA	NA	-0,58	$2{,}88\text{x}10^{-6}$
226246_at	KCTD1	potassium channel tetramerisation domain containing 1	-0,58	$1{,}26\text{x}10^{-5}$
242618_at	HCG18	HLA complex group 18	-0,58	$7{,}12\text{x}10^{-6}$
203636_at	MID1	midline 1 (Opitz/BBB syndrome)	-0,58	$8{,}71\text{x}10^{-6}$
241344_at	NA	NA	-0,58	$1{,}60\text{x}10^{-5}$
226080_at	SSH2	slingshot homolog 2 (Drosophila)	-0,58	$8{,}43\text{x}10^{-6}$
202696_at	OXSR1	oxidative-stress responsive 1	-0,58	$9{,}53\text{x}10^{-7}$
231823_s_at	SH3PXD2B	SH3 and PX domains 2B	-0,59	$3{,}03\text{x}10^{-6}$
213500_at	NA	NA	-0,59	$1{,}22\text{x}10^{-5}$
209479_at	CCDC28A	coiled-coil domain containing 28A	-0,59	$1{,}59\text{x}10^{-6}$
230547_at	KCNC1	potassium voltage-gated channel, Shaw-related subfamily, member 1	-0,59	$4{,}57\text{x}10^{-6}$
213035_at	ANKRD28	ankyrin repeat domain 28	-0,59	$7{,}21\text{x}10^{-6}$
228726_at	NA	NA	-0,59	$8{,}62\text{x}10^{-6}$
226855_at	NA	NA	-0,59	$9{,}15\text{x}10^{-6}$
228029_at	NA	NA	-0,59	$4{,}43\text{x}10^{-6}$
209787_s_at	HMGN4	high mobility group nucleosomal binding domain 4	-0,59	$6{,}78\text{x}10^{-6}$
229824_at	NA	NA	-0,59	$3{,}63\text{x}10^{-6}$
221701_s_at	STRA6	stimulated by retinoic acid gene 6 homolog (mouse)	-0,59	$3{,}43\text{x}10^{-7}$
240300_at	TK2	thymidine kinase 2, mitochondrial	-0,59	$1{,}46\text{x}10^{-5}$
231431_s_at	NA	NA	-0,59	$3{,}16\text{x}10^{-6}$
226820_at	ZNF362	zinc finger protein 362	-0,59	$5{,}08\text{x}10^{-6}$
202708_s_at	HIST2H2BE	histone cluster 2, H2be	-0,59	$8{,}74\text{x}10^{-6}$
228040_at	MGC21881	hypothetical locus MGC21881	-0,59	$3{,}21\text{x}10^{-6}$
232089_at	TIGD7	tigger transposable element derived 7	-0,59	$8{,}31\text{x}10^{-6}$
231382_at	FGF18	fibroblast growth factor 18	-0,59	$4{,}88\text{x}10^{-6}$
238420_at	NA	NA	-0,59	$4{,}17\text{x}10^{-7}$
203967_at	CDC6	cell division cycle 6 homolog (S. cerevisiae)	-0,59	$7{,}53\text{x}10^{-6}$
228453_at	KIAA1632	KIAA1632	-0,59	$4{,}49\text{x}10^{-7}$
209771_x_at	CD24	CD24 molecule	-0,59	$3{,}21\text{x}10^{-6}$
227179_at	STAU2	staufen, RNA binding protein, homolog 2 (Drosophila)	-0,59	$3{,}14\text{x}10^{-6}$
223217_s_at	NFKBIZ	nuclear factor of kappa light polypeptide gene enhancer in B-cells inhibitor, zeta	-0,59	$7{,}75\text{x}10^{-6}$
239332_at	NA	NA	-0,60	$5{,}30\text{x}10^{-6}$
208453_s_at	XPNPEP1	X-prolyl aminopeptidase (aminopeptidase P) 1, soluble	-0,60	$1{,}04\text{x}10^{-6}$
207785_s_at	RBPJ	recombination signal binding protein for immunoglobulin kappa J region	-0,60	$1{,}60\text{x}10^{-6}$
57540_at	RBKS	ribokinase	-0,60	$1{,}14\text{x}10^{-6}$
212528_at	NA	NA	-0,60	$1{,}39\text{x}10^{-6}$
40189_at	SET	SET nuclear oncogene	-0,60	$1{,}10\text{x}10^{-6}$

...continues on next page

Table C.1.: *(...continued)*

Probe set ID	Gene symbol	Gene name	logFc	adj.p-val
224629_at	LMAN1	lectin, mannose-binding, 1	-0,60	$2{,}07\text{x}10^{-7}$
229803_s_at	NA	NA	-0,60	$2{,}33\text{x}10^{-6}$
235003_at	UHMK1	U2AF homology motif (UHM) kinase 1	-0,60	$6{,}79\text{x}10^{-6}$
206099_at	PRKCH	protein kinase C, eta	-0,60	$5{,}46\text{x}10^{-6}$
222589_at	NLK	nemo-like kinase	-0,60	$4{,}14\text{x}10^{-6}$
212699_at	SCAMP5	secretory carrier membrane protein 5	-0,60	$4{,}60\text{x}10^{-6}$
213708_s_at	MLX	MAX-like protein X	-0,60	$1{,}05\text{x}10^{-6}$
200631_s_at	SET	SET nuclear oncogene	-0,60	$1{,}04\text{x}10^{-6}$
244519_at	ASXL1	additional sex combs like 1 (Drosophila)	-0,60	$3{,}14\text{x}10^{-6}$
211871_x_at	GNB5	guanine nucleotide binding protein (G protein), beta 5	-0,60	$1{,}26\text{x}10^{-5}$
225289_at	STAT3	signal transducer and activator of transcription 3 (acute-phase response factor)	-0,61	$6{,}34\text{x}10^{-6}$
227904_at	AZI2	5-azacytidine induced 2	-0,61	$6{,}06\text{x}10^{-7}$
235233_s_at	GMEB1	glucocorticoid modulatory element binding protein 1	-0,61	$3{,}23\text{x}10^{-6}$
212549_at	STAT5B	signal transducer and activator of transcription 5B	-0,61	$4{,}83\text{x}10^{-6}$
225074_at	RAB2B	RAB2B, member RAS oncogene family	-0,61	$2{,}44\text{x}10^{-7}$
212287_at	SUZ12	suppressor of zeste 12 homolog (Drosophila)	-0,61	$2{,}51\text{x}10^{-7}$
208382_s_at	DMC1	DMC1 dosage suppressor of mck1 homolog, meiosis-specific homologous recombination (yeast)	-0,61	$1{,}32\text{x}10^{-5}$
216379_x_at	CD24	CD24 molecule	-0,61	$3{,}13\text{x}10^{-6}$
205678_at	AP3B2	adaptor-related protein complex 3, beta 2 subunit	-0,61	$2{,}36\text{x}10^{-6}$
223421_at	CYHR1	cysteine/histidine-rich 1	-0,61	$1{,}42\text{x}10^{-6}$
217492_s_at	NA	NA	-0,61	$8{,}54\text{x}10^{-7}$
202391_at	BASP1	brain abundant, membrane attached signal protein 1	-0,61	$8{,}12\text{x}10^{-7}$
218338_at	PHC1	polyhomeotic homolog 1 (Drosophila)	-0,61	$2{,}63\text{x}10^{-6}$
212446_s_at	LASS6	LAG1 homolog, ceramide synthase 6	-0,61	$5{,}05\text{x}10^{-6}$
217970_s_at	CNOT6	CCR4-NOT transcription complex, subunit 6	-0,61	$3{,}06\text{x}10^{-6}$
202658_at	PEX11B	peroxisomal biogenesis factor 11 beta	-0,61	$7{,}73\text{x}10^{-7}$
227465_at	KIAA0892	KIAA0892	-0,61	$8{,}97\text{x}10^{-7}$
229394_s_at	GRLF1	glucocorticoid receptor DNA binding factor 1	-0,61	$5{,}29\text{x}10^{-7}$
219770_at	GTDC1	glycosyltransferase-like domain containing 1	-0,61	$5{,}81\text{x}10^{-6}$
213073_at	ZFYVE26	zinc finger, FYVE domain containing 26	-0,61	$1{,}35\text{x}10^{-6}$
235268_at	NA	NA	-0,61	$5{,}51\text{x}10^{-6}$
225685_at	NA	NA	-0,61	$7{,}06\text{x}10^{-6}$
201794_s_at	SMG7	Smg-7 homolog, nonsense mediated mRNA decay factor (C. elegans)	-0,62	$1{,}53\text{x}10^{-6}$
211929_at	HNRNPA3	heterogeneous nuclear ribonucleoprotein A3	-0,62	$9{,}69\text{x}10^{-6}$
230407_at	NA	NA	-0,62	$2{,}73\text{x}10^{-7}$
266_s_at	CD24	CD24 molecule	-0,62	$4{,}29\text{x}10^{-7}$
31799_at	NA	NA	-0,62	$8{,}35\text{x}10^{-6}$
1558027_s_at	PRKAB2	protein kinase, AMP-activated, beta 2 non-catalytic subunit	-0,62	$6{,}72\text{x}10^{-6}$
208703_s_at	APLP2	amyloid beta (A4) precursor-like protein 2	-0,62	$4{,}64\text{x}10^{-6}$

...continues on next page

Table C.1.: *(...continued)*

Probe set ID	Gene symbol	Gene name	logFc	adj.p-val
230207_s_at	DOCK5	dedicator of cytokinesis 5	-0,62	$8{,}53\text{x}10^{-6}$
201814_at	TBC1D5	TBC1 domain family, member 5	-0,62	$1{,}97\text{x}10^{-7}$
214577_at	MAP1B	microtubule-associated protein 1B	-0,62	$1{,}12\text{x}10^{-6}$
228013_at	NA	NA	-0,62	$2{,}04\text{x}10^{-6}$
229943_at	TRIM13	tripartite motif-containing 13	-0,62	$3{,}13\text{x}10^{-6}$
227777_at	C10orf18	chromosome 10 open reading frame 18	-0,62	$1{,}18\text{x}10^{-6}$
220199_s_at	AIDA	axin interactor, dorsalization associated	-0,62	$3{,}17\text{x}10^{-6}$
238008_at	PRR18	proline rich 18	-0,62	$1{,}30\text{x}10^{-5}$
204276_at	TK2	thymidine kinase 2, mitochondrial	-0,62	$5{,}05\text{x}10^{-6}$
204735_at	PDE4A	phosphodiesterase 4A, cAMP-specific (phosphodiesterase E2 dunce homolog, Drosophila)	-0,62	$1{,}76\text{x}10^{-7}$
233030_at	PNPLA3	patatin-like phospholipase domain containing 3	-0,63	$1{,}40\text{x}10^{-5}$
236090_at	NA	NA	-0,63	$4{,}59\text{x}10^{-7}$
223218_s_at	NFKBIZ	nuclear factor of kappa light polypeptide gene enhancer in B-cells inhibitor, zeta	-0,63	$4{,}05\text{x}10^{-6}$
228570_at	BTBD11	BTB (POZ) domain containing 11	-0,63	$3{,}96\text{x}10^{-6}$
239790_s_at	NA	NA	-0,63	$1{,}10\text{x}10^{-6}$
244294_at	GTF2H5	general transcription factor IIH, polypeptide 5	-0,63	$1{,}47\text{x}10^{-5}$
222476_at	CNOT6	CCR4-NOT transcription complex, subunit 6	-0,63	$2{,}04\text{x}10^{-6}$
216060_s_at	DAAM1	dishevelled associated activator of morphogenesis 1	-0,63	$9{,}47\text{x}10^{-6}$
222566_at	SUV420H1	suppressor of variegation 4-20 homolog 1 (Drosophila)	-0,63	$7{,}42\text{x}10^{-6}$
200593_s_at	HNRNPU	heterogeneous nuclear ribonucleoprotein U (scaffold attachment factor A)	-0,63	$3{,}17\text{x}10^{-6}$
222273_at	PAPOLG	poly(A) polymerase gamma	-0,63	$4{,}99\text{x}10^{-6}$
204053_x_at	PTEN	phosphatase and tensin homolog	-0,63	$7{,}68\text{x}10^{-7}$
231775_at	TNFRSF10A	tumor necrosis factor receptor superfamily, member 10a	-0,63	$8{,}92\text{x}10^{-6}$
224947_at	RNF26	ring finger protein 26	-0,63	$9{,}60\text{x}10^{-6}$
209463_s_at	TAF12	TAF12 RNA polymerase II, TATA box binding protein (TBP)-associated factor, 20kDa	-0,63	$7{,}47\text{x}10^{-6}$
228170_at	OLIG1	oligodendrocyte transcription factor 1	-0,63	$4{,}65\text{x}10^{-6}$
203090_at	SDF2	stromal cell-derived factor 2	-0,63	$5{,}92\text{x}10^{-7}$
235457_at	MAML2	mastermind-like 2 (Drosophila)	-0,63	$1{,}10\text{x}10^{-5}$
227004_at	NA	NA	-0,63	$1{,}57\text{x}10^{-5}$
229986_at	LOC100287163	similar to Zinc finger protein 717	-0,63	$4{,}90\text{x}10^{-6}$
212474_at	AVL9	AVL9 homolog (S. cerevisiase)	-0,63	$2{,}37\text{x}10^{-6}$
214880_x_at	CALD1	caldesmon 1	-0,63	$7{,}80\text{x}10^{-6}$
225387_at	TSPAN5	tetraspanin 5	-0,63	$4{,}21\text{x}10^{-6}$
231849_at	KRT80	keratin 80	-0,63	$1{,}36\text{x}10^{-6}$
207020_at	HSF2BP	heat shock transcription factor 2 binding protein	-0,64	$4{,}22\text{x}10^{-6}$
204165_at	WASF1	WAS protein family, member 1	-0,64	$2{,}70\text{x}10^{-6}$
211373_s_at	PSEN2	presenilin 2 (Alzheimer disease 4)	-0,64	$2{,}53\text{x}10^{-6}$
212534_at	ZNF24	zinc finger protein 24	-0,64	$3{,}32\text{x}10^{-7}$

...continues on next page

Table C.1.: *(...continued)*

Probe set ID	Gene symbol	Gene name	logFc	adj.p-val
225973_at	TAP2	transporter 2, ATP-binding cassette, sub-family B (MDR/TAP)	-0,64	$6{,}07 \times 10^{-6}$
203074_at	NA	NA	-0,64	$1{,}59 \times 10^{-6}$
224560_at	TIMP2	TIMP metallopeptidase inhibitor 2	-0,64	$9{,}75 \times 10^{-6}$
201670_s_at	MARCKS	myristoylated alanine-rich protein kinase C substrate	-0,64	$1{,}77 \times 10^{-6}$
1553034_at	SDCCAG8	serologically defined colon cancer antigen 8	-0,64	$9{,}25 \times 10^{-7}$
223097_at	ADPRHL2	ADP-ribosylhydrolase like 2	-0,64	$8{,}13 \times 10^{-7}$
229573_at	USP9X	ubiquitin specific peptidase 9, X-linked	-0,64	$6{,}00 \times 10^{-6}$
230859_at	NA	NA	-0,64	$2{,}37 \times 10^{-6}$
218928_s_at	SLC37A1	solute carrier family 37 (glycerol-3-phosphate transporter), member 1	-0,64	$1{,}02 \times 10^{-5}$
225905_s_at	ST3GAL3	ST3 beta-galactoside alpha-2,3-sialyltransferase 3	-0,64	$1{,}00 \times 10^{-6}$
222103_at	ATF1	activating transcription factor 1	-0,64	$6{,}68 \times 10^{-6}$
221264_s_at	TARDBP	TAR DNA binding protein	-0,64	$6{,}28 \times 10^{-6}$
202609_at	EPS8	epidermal growth factor receptor pathway substrate 8	-0,64	$1{,}12 \times 10^{-6}$
226377_at	NA	NA	-0,64	$6{,}08 \times 10^{-7}$
201642_at	IFNGR2	interferon gamma receptor 2 (interferon gamma transducer 1)	-0,64	$5{,}26 \times 10^{-7}$
220947_s_at	TBC1D10B	TBC1 domain family, member 10B	-0,64	$1{,}53 \times 10^{-6}$
225935_at	NA	NA	-0,65	$5{,}23 \times 10^{-7}$
209045_at	XPNPEP1	X-prolyl aminopeptidase (aminopeptidase P) 1, soluble	-0,65	$9{,}59 \times 10^{-7}$
202975_s_at	RHOBTB3	Rho-related BTB domain containing 3	-0,65	$6{,}24 \times 10^{-6}$
200701_at	NPC2	Niemann-Pick disease, type C2	-0,65	$1{,}07 \times 10^{-5}$
225278_at	PRKAB2	protein kinase, AMP-activated, beta 2 non-catalytic subunit	-0,65	$1{,}13 \times 10^{-6}$
238129_s_at	NA	NA	-0,65	$6{,}78 \times 10^{-6}$
216038_x_at	DAXX	death-domain associated protein	-0,65	$6{,}16 \times 10^{-6}$
201142_at	EIF2S1	eukaryotic translation initiation factor 2, subunit 1 alpha, 35kDa	-0,65	$2{,}10 \times 10^{-7}$
203550_s_at	FAM189B	family with sequence similarity 189, member B	-0,65	$4{,}11 \times 10^{-7}$
230179_at	LOC285812	hypothetical protein LOC285812	-0,65	$1{,}31 \times 10^{-5}$
227785_at	SDCCAG8	serologically defined colon cancer antigen 8	-0,65	$1{,}33 \times 10^{-5}$
229699_at	LOC100129550	hypothetical LOC100129550	-0,65	$1{,}40 \times 10^{-5}$
203048_s_at	TTC37	tetratricopeptide repeat domain 37	-0,65	$1{,}14 \times 10^{-6}$
213637_at	NA	NA	-0,65	$1{,}57 \times 10^{-6}$
219342_at	CASD1	CAS1 domain containing 1	-0,65	$1{,}26 \times 10^{-5}$
214733_s_at	YIPF1	Yip1 domain family, member 1	-0,65	$8{,}79 \times 10^{-7}$
228400_at	SHROOM3	shroom family member 3	-0,65	$1{,}50 \times 10^{-5}$
201449_at	TIA1	TIA1 cytotoxic granule-associated RNA binding protein	-0,65	$1{,}51 \times 10^{-5}$
215416_s_at	STOML2	stomatin (EPB72)-like 2	-0,65	$3{,}40 \times 10^{-7}$
238604_at	NA	NA	-0,66	$2{,}44 \times 10^{-6}$
226666_at	DAAM1	dishevelled associated activator of morphogenesis 1	-0,66	$1{,}35 \times 10^{-6}$
224595_at	SLC44A1	solute carrier family 44, member 1	-0,66	$1{,}31 \times 10^{-6}$

...continues on next page

Table C.1.: *(...continued)*

Probe set ID	Gene symbol	Gene name	logFc	adj.p-val
213387_at	ATAD2B	ATPase family, AAA domain containing 2B	-0,66	$3{,}14 \times 10^{-6}$
50965_at	RAB26	RAB26, member RAS oncogene family	-0,66	$1{,}55 \times 10^{-5}$
204278_s_at	EBAG9	estrogen receptor binding site associated, antigen, 9	-0,66	$3{,}33 \times 10^{-7}$
212660_at	PHF15	PHD finger protein 15	-0,66	$1{,}26 \times 10^{-5}$
39582_at	CYLD	cylindromatosis (turban tumor syndrome)	-0,66	$1{,}25 \times 10^{-5}$
227410_at	FAM43A	family with sequence similarity 43, member A	-0,66	$5{,}38 \times 10^{-7}$
202822_at	LPP	LIM domain containing preferred translocation partner in lipoma	-0,66	$9{,}98 \times 10^{-7}$
201143_s_at	EIF2S1	eukaryotic translation initiation factor 2, subunit 1 alpha, 35kDa	-0,66	$3{,}42 \times 10^{-7}$
227961_at	CTSB	cathepsin B	-0,66	$1{,}57 \times 10^{-6}$
217752_s_at	CNDP2	CNDP dipeptidase 2 (metallopeptidase M20 family)	-0,66	$5{,}00 \times 10^{-6}$
218330_s_at	NAV2	neuron navigator 2	-0,66	$1{,}40 \times 10^{-5}$
210817_s_at	CALCOCO2	calcium binding and coiled-coil domain 2	-0,66	$3{,}12 \times 10^{-6}$
203035_s_at	PIAS3	protein inhibitor of activated STAT, 3	-0,67	$4{,}89 \times 10^{-7}$
202011_at	TJP1	tight junction protein 1 (zona occludens 1)	-0,67	$2{,}44 \times 10^{-7}$
229025_s_at	IMMP1L	IMP1 inner mitochondrial membrane peptidase-like (S. cerevisiae)	-0,67	$5{,}28 \times 10^{-6}$
202959_at	MUT	methylmalonyl Coenzyme A mutase	-0,67	$1{,}46 \times 10^{-6}$
1562904_s_at	hCG_1990547	family with sequence similarity 86, member A pseudogene	-0,67	$1{,}74 \times 10^{-5}$
224938_at	NUFIP2	nuclear fragile X mental retardation protein interacting protein 2	-0,67	$1{,}11 \times 10^{-6}$
1554171_at	ZMYM3	zinc finger, MYM-type 3	-0,67	$1{,}54 \times 10^{-6}$
228379_at	NUTF2	nuclear transport factor 2	-0,67	$9{,}73 \times 10^{-6}$
232810_at	AIG1	androgen-induced 1	-0,67	$5{,}02 \times 10^{-6}$
212513_s_at	USP33	ubiquitin specific peptidase 33	-0,67	$5{,}22 \times 10^{-6}$
212061_at	SR140	U2-associated SR140 protein	-0,67	$1{,}75 \times 10^{-6}$
226420_at	MECOM	MDS1 and EVI1 complex locus	-0,67	$1{,}09 \times 10^{-5}$
227770_at	NA	NA	-0,67	$8{,}13 \times 10^{-7}$
202262_x_at	DDAH2	dimethylarginine dimethylaminohydrolase 2	-0,67	$1{,}43 \times 10^{-5}$
229041_s_at	NA	NA	-0,67	$7{,}38 \times 10^{-7}$
211952_at	IPO5	importin 5	-0,67	$3{,}21 \times 10^{-6}$
1553993_s_at	MED25	mediator complex subunit 25	-0,67	$5{,}70 \times 10^{-7}$
201126_s_at	MGAT1	mannosyl (alpha-1,3-)-glycoprotein beta-1,2-N-acetylglucosaminyltransferase	-0,67	$1{,}61 \times 10^{-7}$
227286_at	INO80E	INO80 complex subunit E	-0,67	$9{,}02 \times 10^{-7}$
204252_at	CDK2	cyclin-dependent kinase 2	-0,67	$2{,}01 \times 10^{-7}$
222614_at	RWDD2B	RWD domain containing 2B	-0,67	$1{,}03 \times 10^{-5}$
202386_s_at	KIAA0430	KIAA0430	-0,67	$1{,}48 \times 10^{-6}$
202808_at	C10orf26	chromosome 10 open reading frame 26	-0,68	$3{,}24 \times 10^{-6}$
218069_at	DCTPP1	dCTP pyrophosphatase 1	-0,68	$2{,}37 \times 10^{-7}$
201483_s_at	SUPT4H1	suppressor of Ty 4 homolog 1 (S. cerevisiae)	-0,68	$3{,}67 \times 10^{-6}$
225886_at	DDX5	DEAD (Asp-Glu-Ala-Asp) box polypeptide 5	-0,68	$1{,}23 \times 10^{-6}$

...continues on next page

Table C.1.: *(...continued)*

Probe set ID	Gene symbol	Gene name	logFc	adj.p-val
52651_at	COL8A2	collagen, type VIII, alpha 2	-0,68	$1{,}16 \times 10^{-5}$
202068_s_at	LDLR	low density lipoprotein receptor	-0,68	$1{,}39 \times 10^{-6}$
223349_s_at	BOK	BCL2-related ovarian killer	-0,68	$6{,}08 \times 10^{-7}$
201969_at	NASP	nuclear autoantigenic sperm protein (histone-binding)	-0,68	$6{,}45 \times 10^{-6}$
1555412_at	FBXL21	F-box and leucine-rich repeat protein 21 (gene/pseudogene)	-0,68	$2{,}81 \times 10^{-6}$
225116_at	HIPK2	homeodomain interacting protein kinase 2	-0,68	$1{,}07 \times 10^{-5}$
1555989_at	NA	NA	-0,68	$1{,}02 \times 10^{-5}$
217823_s_at	UBE2J1	ubiquitin-conjugating enzyme E2, J1 (UBC6 homolog, yeast)	-0,68	$8{,}33 \times 10^{-7}$
229176_at	ANKH	ankylosis, progressive homolog (mouse)	-0,68	$4{,}99 \times 10^{-6}$
225921_at	NIN	ninein (GSK3B interacting protein)	-0,68	$8{,}62 \times 10^{-7}$
226245_at	KCTD1	potassium channel tetramerisation domain containing 1	-0,68	$1{,}45 \times 10^{-5}$
226431_at	FAM117B	family with sequence similarity 117, member B	-0,68	$4{,}70 \times 10^{-7}$
214724_at	DIXDC1	DIX domain containing 1	-0,68	$9{,}33 \times 10^{-6}$
212673_at	METAP1	methionyl aminopeptidase 1	-0,68	$7{,}10 \times 10^{-7}$
201729_s_at	KIAA0100	KIAA0100	-0,68	$2{,}02 \times 10^{-7}$
209222_s_at	OSBPL2	oxysterol binding protein-like 2	-0,68	$1{,}18 \times 10^{-7}$
209587_at	PITX1	paired-like homeodomain 1	-0,68	$7{,}71 \times 10^{-6}$
220089_at	L2HGDH	L-2-hydroxyglutarate dehydrogenase	-0,68	$4{,}12 \times 10^{-6}$
238462_at	UBASH3B	ubiquitin associated and SH3 domain containing, B	-0,68	$7{,}97 \times 10^{-6}$
235689_at	MTFMT	mitochondrial methionyl-tRNA formyltransferase	-0,68	$5{,}79 \times 10^{-7}$
229969_at	SEC63	SEC63 homolog (S. cerevisiae)	-0,69	$1{,}33 \times 10^{-5}$
218047_at	OSBPL9	oxysterol binding protein-like 9	-0,69	$1{,}93 \times 10^{-6}$
212608_s_at	NA	NA	-0,69	$1{,}39 \times 10^{-6}$
243063_at	NA	NA	-0,69	$1{,}05 \times 10^{-5}$
226660_at	RPS6KB1	ribosomal protein S6 kinase, 70kDa, polypeptide 1	-0,69	$9{,}11 \times 10^{-6}$
225170_at	WDR5	WD repeat domain 5	-0,69	$5{,}77 \times 10^{-7}$
1552789_at	SEC62	SEC62 homolog (S. cerevisiae)	-0,69	$1{,}30 \times 10^{-5}$
229822_at	NA	NA	-0,69	$8{,}72 \times 10^{-6}$
235232_at	GMEB1	glucocorticoid modulatory element binding protein 1	-0,69	$2{,}78 \times 10^{-6}$
219648_at	MREG	melanoregulin	-0,69	$4{,}04 \times 10^{-6}$
204274_at	EBAG9	estrogen receptor binding site associated, antigen, 9	-0,69	$2{,}16 \times 10^{-7}$
206511_s_at	SIX2	SIX homeobox 2	-0,69	$4{,}23 \times 10^{-6}$
204477_at	RABIF	RAB interacting factor	-0,69	$3{,}09 \times 10^{-6}$
227246_at	PLRG1	pleiotropic regulator 1 (PRL1 homolog, Arabidopsis)	-0,69	$1{,}63 \times 10^{-5}$
226490_at	NHSL1	NHS-like 1	-0,69	$1{,}77 \times 10^{-5}$
213110_s_at	COL4A5	collagen, type IV, alpha 5	-0,70	$5{,}28 \times 10^{-6}$
225407_at	MBP	myelin basic protein	-0,70	$6{,}84 \times 10^{-6}$
222869_s_at	ELAC1	elaC homolog 1 (E. coli)	-0,70	$6{,}15 \times 10^{-7}$
200056_s_at	C1D	C1D nuclear receptor co-repressor	-0,70	$1{,}07 \times 10^{-5}$
225238_at	MSI2	musashi homolog 2 (Drosophila)	-0,70	$3{,}19 \times 10^{-6}$

...continues on next page

Table C.1.: *(...continued)*

Probe set ID	Gene symbol	Gene name	logFc	adj.p-val
241879_at	NA	NA	-0,70	$8{,}97 \times 10^{-7}$
204082_at	PBX3	pre-B-cell leukemia homeobox 3	-0,70	$2{,}07 \times 10^{-7}$
227426_at	SOS1	son of sevenless homolog 1 (Drosophila)	-0,70	$8{,}50 \times 10^{-6}$
214194_at	NA	NA	-0,70	$1{,}26 \times 10^{-7}$
225546_at	EEF2K	eukaryotic elongation factor-2 kinase	-0,70	$5{,}22 \times 10^{-6}$
225202_at	RHOBTB3	Rho-related BTB domain containing 3	-0,70	$1{,}37 \times 10^{-6}$
211804_s_at	CDK2	cyclin-dependent kinase 2	-0,70	$7{,}48 \times 10^{-6}$
212314_at	SEL1L3	sel-1 suppressor of lin-12-like 3 (C. elegans)	-0,70	$4{,}16 \times 10^{-6}$
224596_at	SLC44A1	solute carrier family 44, member 1	-0,70	$5{,}11 \times 10^{-7}$
222630_at	RFX7	regulatory factor X, 7	-0,70	$3{,}37 \times 10^{-6}$
220417_s_at	THAP4	THAP domain containing 4	-0,70	$1{,}91 \times 10^{-7}$
237333_at	RBBP4	retinoblastoma binding protein 4	-0,70	$8{,}03 \times 10^{-6}$
217825_s_at	UBE2J1	ubiquitin-conjugating enzyme E2, J1 (UBC6 homolog, yeast)	-0,70	$6{,}78 \times 10^{-7}$
225876_at	NIPAL3	NIPA-like domain containing 3	-0,70	$1{,}29 \times 10^{-5}$
228843_at	NA	NA	-0,70	$3{,}19 \times 10^{-6}$
217819_at	GOLGA7	golgin A7	-0,71	$1{,}51 \times 10^{-7}$
235585_at	NA	NA	-0,71	$1{,}80 \times 10^{-5}$
202361_at	SEC24C	SEC24 family, member C (S. cerevisiae)	-0,71	$7{,}38 \times 10^{-7}$
228709_at	TPR	translocated promoter region (to activated MET oncogene)	-0,71	$5{,}22 \times 10^{-6}$
225732_at	KLHDC5	kelch domain containing 5	-0,71	$1{,}47 \times 10^{-5}$
1557094_at	LOC728449	hypothetical protein LOC728449	-0,71	$1{,}92 \times 10^{-7}$
238453_at	FGFBP3	fibroblast growth factor binding protein 3	-0,71	$8{,}43 \times 10^{-6}$
201448_at	TIA1	TIA1 cytotoxic granule-associated RNA binding protein	-0,71	$4{,}39 \times 10^{-6}$
222797_at	DPYSL5	dihydropyrimidinase-like 5	-0,71	$1{,}30 \times 10^{-7}$
1552274_at	PXK	PX domain containing serine/threonine kinase	-0,71	$4{,}33 \times 10^{-6}$
224837_at	FOXP1	forkhead box P1	-0,71	$1{,}26 \times 10^{-7}$
202683_s_at	RNMT	RNA (guanine-7-) methyltransferase	-0,71	$1{,}67 \times 10^{-7}$
230241_at	NA	NA	-0,71	$8{,}54 \times 10^{-7}$
214672_at	TTLL5	tubulin tyrosine ligase-like family, member 5	-0,71	$1{,}36 \times 10^{-6}$
235124_at	LOC645212	hypothetical LOC645212	-0,71	$4{,}22 \times 10^{-6}$
200706_s_at	LITAF	lipopolysaccharide-induced TNF factor	-0,71	$5{,}91 \times 10^{-7}$
200704_at	LITAF	lipopolysaccharide-induced TNF factor	-0,71	$7{,}22 \times 10^{-7}$
209341_s_at	IKBKB	inhibitor of kappa light polypeptide gene enhancer in B-cells, kinase beta	-0,71	$2{,}64 \times 10^{-6}$
228603_at	NA	NA	-0,71	$3{,}46 \times 10^{-7}$
223575_at	KIAA1549	KIAA1549	-0,71	$4{,}07 \times 10^{-6}$
226438_at	SNTB1	syntrophin, beta 1 (dystrophin-associated protein A1, 59kDa, basic component 1)	-0,72	$3{,}26 \times 10^{-6}$
203688_at	PKD2	polycystic kidney disease 2 (autosomal dominant)	-0,72	$2{,}58 \times 10^{-7}$
209582_s_at	CD200	CD200 molecule	-0,72	$4{,}06 \times 10^{-7}$
224772_at	NAV1	neuron navigator 1	-0,72	$1{,}58 \times 10^{-6}$

...continues on next page

Table C.1.: *(...continued)*

Probe set ID	Gene symbol	Gene name	logFc	adj.p-val
1557166_at	PDCD4	programmed cell death 4 (neoplastic transformation inhibitor)	-0,72	$1{,}25\text{x}10^{-5}$
202180_s_at	MVP	major vault protein	-0,72	$2{,}99\text{x}10^{-6}$
235045_at	NA	NA	-0,72	$6{,}01\text{x}10^{-6}$
236196_at	NA	NA	-0,72	$1{,}04\text{x}10^{-5}$
1554172_a_at	ZMYM3	zinc finger, MYM-type 3	-0,72	$1{,}24\text{x}10^{-5}$
203020_at	RABGAP1L	RAB GTPase activating protein 1-like	-0,72	$1{,}60\text{x}10^{-6}$
236626_at	ALG1	asparagine-linked glycosylation 1, beta-1,4-mannosyltransferase homolog (S. cerevisiae)	-0,72	$8{,}90\text{x}10^{-6}$
212122_at	RHOQ	ras homolog gene family, member Q	-0,72	$1{,}62\text{x}10^{-5}$
212151_at	PBX1	pre-B-cell leukemia homeobox 1	-0,73	$7{,}42\text{x}10^{-6}$
221969_at	NA	NA	-0,73	$1{,}74\text{x}10^{-5}$
218962_s_at	TMEM168	transmembrane protein 168	-0,73	$2{,}30\text{x}10^{-6}$
221932_s_at	GLRX5	glutaredoxin 5	-0,73	$1{,}03\text{x}10^{-7}$
238043_at	NA	NA	-0,73	$4{,}65\text{x}10^{-6}$
213701_at	C12orf29	chromosome 12 open reading frame 29	-0,73	$2{,}86\text{x}10^{-7}$
211711_s_at	PTEN	phosphatase and tensin homolog	-0,73	$6{,}72\text{x}10^{-7}$
224865_at	FAR1	fatty acyl CoA reductase 1	-0,73	$1{,}15\text{x}10^{-6}$
200597_at	EIF3A	eukaryotic translation initiation factor 3, subunit A	-0,73	$2{,}73\text{x}10^{-7}$
209536_s_at	EHD4	EH-domain containing 4	-0,73	$2{,}58\text{x}10^{-7}$
215189_at	KRT86	keratin 86	-0,73	$7{,}77\text{x}10^{-6}$
240137_at	NA	NA	-0,73	$4{,}80\text{x}10^{-6}$
213977_s_at	CIZ1	CDKN1A interacting zinc finger protein 1	-0,73	$9{,}15\text{x}10^{-7}$
239050_s_at	NA	NA	-0,73	$1{,}47\text{x}10^{-5}$
238992_at	POLI	polymerase (DNA directed) iota	-0,73	$1{,}60\text{x}10^{-5}$
230098_at	PHF20L1	PHD finger protein 20-like 1	-0,73	$1{,}26\text{x}10^{-5}$
204017_at	KDELR3	KDEL (Lys-Asp-Glu-Leu) endoplasmic reticulum protein retention receptor 3	-0,73	$4{,}65\text{x}10^{-6}$
202907_s_at	NBN	nibrin	-0,74	$6{,}28\text{x}10^{-7}$
235980_at	PIK3CA	phosphoinositide-3-kinase, catalytic, alpha polypeptide	-0,74	$1{,}60\text{x}10^{-6}$
226965_at	FAM116A	family with sequence similarity 116, member A	-0,74	$1{,}43\text{x}10^{-6}$
239038_at	C1orf52	chromosome 1 open reading frame 52	-0,74	$1{,}02\text{x}10^{-5}$
224898_at	WDR26	WD repeat domain 26	-0,74	$4{,}18\text{x}10^{-7}$
201800_s_at	OSBP	oxysterol binding protein	-0,74	$9{,}78\text{x}10^{-8}$
201677_at	C3orf37	chromosome 3 open reading frame 37	-0,74	$4{,}29\text{x}10^{-6}$
223316_at	CCDC3	coiled-coil domain containing 3	-0,74	$1{,}89\text{x}10^{-7}$
236016_at	NA	NA	-0,74	$6{,}38\text{x}10^{-7}$
209630_s_at	FBXW2	F-box and WD repeat domain containing 2	-0,74	$3{,}87\text{x}10^{-6}$
229905_at	RAP1GDS1	RAP1, GTP-GDP dissociation stimulator 1	-0,74	$9{,}44\text{x}10^{-6}$
223297_at	AMMECR1L	AMME chromosomal region gene 1-like	-0,74	$3{,}22\text{x}10^{-7}$
219192_at	UBAP2	ubiquitin associated protein 2	-0,74	$1{,}54\text{x}10^{-7}$
242989_at	NA	NA	-0,74	$4{,}64\text{x}10^{-6}$

...continues on next page

Table C.1.: *(...continued)*

Probe set ID	Gene symbol	Gene name	logFc	adj.p-val
204769_s_at	TAP2	transporter 2, ATP-binding cassette, sub-family B (MDR/TAP)	-0,74	$5{,}49 \times 10^{-6}$
203414_at	MMD	monocyte to macrophage differentiation-associated	-0,74	$1{,}17 \times 10^{-7}$
206644_at	NR0B1	nuclear receptor subfamily 0, group B, member 1	-0,74	$4{,}23 \times 10^{-6}$
231399_at	RAB3IP	RAB3A interacting protein (rabin3)	-0,74	$8{,}99 \times 10^{-6}$
228480_at	VAPA	VAMP (vesicle-associated membrane protein)-associated protein A, 33kDa	-0,75	$1{,}12 \times 10^{-5}$
222731_at	ZDHHC2	zinc finger, DHHC-type containing 2	-0,75	$1{,}86 \times 10^{-6}$
1568600_at	CALML4	calmodulin-like 4	-0,75	$7{,}38 \times 10^{-7}$
212361_s_at	ATP2A2	ATPase, Ca++ transporting, cardiac muscle, slow twitch 2	-0,75	$7{,}16 \times 10^{-8}$
235408_x_at	ZNF117	zinc finger protein 117	-0,75	$8{,}13 \times 10^{-6}$
224811_at	NA	NA	-0,75	$5{,}25 \times 10^{-8}$
226126_at	TBCK	TBC1 domain containing kinase	-0,75	$6{,}84 \times 10^{-6}$
201752_s_at	ADD3	adducin 3 (gamma)	-0,75	$7{,}50 \times 10^{-7}$
230832_at	RTF1	Rtf1, Paf1/RNA polymerase II complex component, homolog (S. cerevisiae)	-0,75	$2{,}73 \times 10^{-7}$
202948_at	IL1R1	interleukin 1 receptor, type I	-0,75	$6{,}29 \times 10^{-6}$
224057_s_at	THAP4	THAP domain containing 4	-0,75	$1{,}88 \times 10^{-7}$
224571_at	IRF2BP2	interferon regulatory factor 2 binding protein 2	-0,75	$3{,}63 \times 10^{-6}$
219325_s_at	ELAC1	elaC homolog 1 (E. coli)	-0,75	$2{,}25 \times 10^{-6}$
229735_s_at	NA	NA	-0,75	$1{,}66 \times 10^{-5}$
223197_s_at	SMARCAD1	SWI/SNF-related, matrix-associated actin-dependent regulator of chromatin, subfamily a, containing DEAD/H box 1	-0,75	$7{,}16 \times 10^{-8}$
224688_at	C7orf42	chromosome 7 open reading frame 42	-0,75	$7{,}77 \times 10^{-7}$
228082_at	ASAM	adipocyte-specific adhesion molecule	-0,75	$3{,}97 \times 10^{-6}$
232576_at	NA	NA	-0,75	$1{,}81 \times 10^{-5}$
212173_at	AK2	adenylate kinase 2	-0,75	$8{,}94 \times 10^{-7}$
212888_at	DICER1	dicer 1, ribonuclease type III	-0,75	$3{,}39 \times 10^{-6}$
205969_at	AADAC	arylacetamide deacetylase (esterase)	-0,76	$5{,}47 \times 10^{-6}$
214202_at	NA	NA	-0,76	$3{,}75 \times 10^{-6}$
214985_at	EXT1	exostoses (multiple) 1	-0,76	$3{,}16 \times 10^{-6}$
235843_at	NA	NA	-0,76	$2{,}67 \times 10^{-6}$
228341_at	NA	NA	-0,76	$1{,}80 \times 10^{-5}$
1552727_s_at	ADAMTS17	ADAM metallopeptidase with thrombospondin type 1 motif, 17	-0,76	$5{,}52 \times 10^{-6}$
209175_at	SEC23IP	SEC23 interacting protein	-0,76	$8{,}52 \times 10^{-8}$
212195_at	IL6ST	interleukin 6 signal transducer (gp130, oncostatin M receptor)	-0,76	$7{,}81 \times 10^{-6}$
228217_s_at	PSMG4	proteasome (prosome, macropain) assembly chaperone 4	-0,76	$3{,}63 \times 10^{-6}$
226829_at	AFAP1L2	actin filament associated protein 1-like 2	-0,76	$4{,}23 \times 10^{-6}$
225778_at	RBMS2	RNA binding motif, single stranded interacting protein 2	-0,76	$1{,}04 \times 10^{-6}$
1552790_a_at	SEC62	SEC62 homolog (S. cerevisiae)	-0,76	$1{,}39 \times 10^{-6}$

...continues on next page

Table C.1.: *(...continued)*

Probe set ID	Gene symbol	Gene name	logFc	adj.p-val
228239_at	FAM165B	family with sequence similarity 165, member B	-0,76	$6{,}60 \times 10^{-6}$
218204_s_at	FYCO1	FYVE and coiled-coil domain containing 1	-0,76	$3{,}84 \times 10^{-6}$
212834_at	DDX52	DEAD (Asp-Glu-Ala-Asp) box polypeptide 52	-0,76	$6{,}41 \times 10^{-6}$
228805_at	C5orf25	chromosome 5 open reading frame 25	-0,76	$2{,}73 \times 10^{-7}$
227637_at	TFCP2	transcription factor CP2	-0,77	$2{,}83 \times 10^{-6}$
226325_at	ADSSL1	adenylosuccinate synthase like 1	-0,77	$1{,}44 \times 10^{-6}$
213164_at	NA	NA	-0,77	$2{,}02 \times 10^{-6}$
1554167_a_at	GOLGA7	golgin A7	-0,77	$1{,}58 \times 10^{-6}$
233068_at	NA	NA	-0,77	$2{,}34 \times 10^{-6}$
235428_at	NA	NA	-0,77	$2{,}60 \times 10^{-6}$
238472_at	FBXO9	F-box protein 9	-0,77	$9{,}06 \times 10^{-6}$
225961_at	KLHDC5	kelch domain containing 5	-0,77	$1{,}65 \times 10^{-5}$
208712_at	CCND1	cyclin D1	-0,77	$3{,}78 \times 10^{-6}$
202976_s_at	RHOBTB3	Rho-related BTB domain containing 3	-0,77	$4{,}80 \times 10^{-7}$
228900_at	CYTSB	cytospin B	-0,77	$5{,}68 \times 10^{-6}$
209021_x_at	KIAA0652	KIAA0652	-0,77	$2{,}47 \times 10^{-6}$
224879_at	C9orf123	chromosome 9 open reading frame 123	-0,77	$1{,}75 \times 10^{-7}$
206918_s_at	CPNE1	copine I	-0,77	$5{,}16 \times 10^{-8}$
1558280_s_at	ARHGAP29	Rho GTPase activating protein 29	-0,77	$6{,}89 \times 10^{-6}$
209627_s_at	OSBPL3	oxysterol binding protein-like 3	-0,77	$1{,}69 \times 10^{-5}$
36865_at	ANGEL1	angel homolog 1 (Drosophila)	-0,77	$9{,}15 \times 10^{-7}$
236330_at	NA	NA	-0,77	$2{,}34 \times 10^{-6}$
222482_at	NA	NA	-0,77	$5{,}90 \times 10^{-6}$
202661_at	ITPR2	inositol 1,4,5-triphosphate receptor, type 2	-0,77	$1{,}20 \times 10^{-5}$
238115_at	NA	NA	-0,78	$1{,}07 \times 10^{-5}$
219077_s_at	WWOX	WW domain containing oxidoreductase	-0,78	$9{,}98 \times 10^{-7}$
235521_at	HOXA3	homeobox A3	-0,78	$1{,}33 \times 10^{-5}$
213099_at	ANGEL1	angel homolog 1 (Drosophila)	-0,78	$5{,}63 \times 10^{-7}$
209654_at	KIAA0947	KIAA0947	-0,78	$1{,}63 \times 10^{-7}$
1555973_at	NA	NA	-0,78	$5{,}08 \times 10^{-6}$
230100_x_at	PAK1	p21 protein (Cdc42/Rac)-activated kinase 1	-0,78	$1{,}36 \times 10^{-6}$
211828_s_at	TNIK	TRAF2 and NCK interacting kinase	-0,78	$4{,}97 \times 10^{-6}$
224764_at	ARHGAP21	Rho GTPase activating protein 21	-0,78	$6{,}72 \times 10^{-7}$
202016_at	MEST	mesoderm specific transcript homolog (mouse)	-0,78	$4{,}64 \times 10^{-6}$
209412_at	TRAPPC10	trafficking protein particle complex 10	-0,78	$3{,}35 \times 10^{-7}$
223119_s_at	USP47	ubiquitin specific peptidase 47	-0,78	$9{,}98 \times 10^{-7}$
227131_at	MAP3K3	mitogen-activated protein kinase kinase kinase 3	-0,78	$8{,}32 \times 10^{-8}$
222108_at	AMIGO2	adhesion molecule with Ig-like domain 2	-0,78	$3{,}05 \times 10^{-6}$
229072_at	NA	NA	-0,78	$1{,}63 \times 10^{-5}$
227966_s_at	NA	NA	-0,78	$7{,}75 \times 10^{-6}$
242790_at	SNF8	SNF8, ESCRT-II complex subunit, homolog (S. cerevisiae)	-0,78	$2{,}04 \times 10^{-6}$

...continues on next page

Table C.1.: *(...continued)*

Probe set ID	Gene symbol	Gene name	logFc	adj.p-val
218820_at	C14orf132	chromosome 14 open reading frame 132	-0,78	$8{,}97 \times 10^{-7}$
201484_at	SUPT4H1	suppressor of Ty 4 homolog 1 (S. cerevisiae)	-0,78	$3{,}96 \times 10^{-8}$
201763_s_at	DAXX	death-domain associated protein	-0,78	$2{,}32 \times 10^{-7}$
238623_at	NA	NA	-0,78	$1{,}06 \times 10^{-7}$
205227_at	IL1RAP	interleukin 1 receptor accessory protein	-0,78	$1{,}69 \times 10^{-6}$
230569_at	KIAA1430	KIAA1430	-0,79	$9{,}65 \times 10^{-7}$
203023_at	NOP16	NOP16 nucleolar protein homolog (yeast)	-0,79	$5{,}07 \times 10^{-6}$
212605_s_at	NA	NA	-0,79	$3{,}08 \times 10^{-6}$
1554480_a_at	ARMC10	armadillo repeat containing 10	-0,79	$3{,}99 \times 10^{-6}$
228367_at	ALPK2	alpha-kinase 2	-0,79	$8{,}60 \times 10^{-6}$
201213_at	PPP1R7	protein phosphatase 1, regulatory (inhibitor) subunit 7	-0,79	$5{,}73 \times 10^{-6}$
227454_at	TAOK1	TAO kinase 1	-0,79	$1{,}23 \times 10^{-5}$
226587_at	SNRPN	small nuclear ribonucleoprotein polypeptide N	-0,79	$8{,}74 \times 10^{-6}$
230192_at	TRIM13	tripartite motif-containing 13	-0,79	$7{,}81 \times 10^{-6}$
218684_at	LRRC8D	leucine rich repeat containing 8 family, member D	-0,79	$2{,}55 \times 10^{-7}$
224002_s_at	FKBP7	FK506 binding protein 7	-0,79	$2{,}70 \times 10^{-6}$
228952_at	ENPP1	ectonucleotide pyrophosphatase/phosphodiesterase 1	-0,79	$4{,}97 \times 10^{-6}$
202561_at	TNKS	tankyrase, TRF1-interacting ankyrin-related ADP-ribose polymerase	-0,79	$1{,}32 \times 10^{-6}$
228882_at	TUB	tubby homolog (mouse)	-0,79	$1{,}07 \times 10^{-6}$
213407_at	PHLPP2	PH domain and leucine rich repeat protein phosphatase 2	-0,79	$1{,}89 \times 10^{-7}$
204054_at	PTEN	phosphatase and tensin homolog	-0,79	$5{,}11 \times 10^{-7}$
1560648_s_at	TSPYL1	TSPY-like 1	-0,80	$3{,}70 \times 10^{-7}$
201034_at	ADD3	adducin 3 (gamma)	-0,80	$4{,}70 \times 10^{-7}$
235035_at	SLC35E1	solute carrier family 35, member E1	-0,80	$4{,}49 \times 10^{-8}$
212816_s_at	CBS	cystathionine-beta-synthase	-0,80	$2{,}00 \times 10^{-6}$
217973_at	DCXR	dicarbonyl/L-xylulose reductase	-0,80	$5{,}58 \times 10^{-7}$
1562012_at	NA	NA	-0,80	$7{,}56 \times 10^{-6}$
226762_at	PURB	purine-rich element binding protein B	-0,80	$1{,}17 \times 10^{-5}$
235195_at	FBXW2	F-box and WD repeat domain containing 2	-0,80	$1{,}84 \times 10^{-5}$
226793_at	LOC283267	hypothetical LOC283267	-0,80	$3{,}63 \times 10^{-7}$
223287_s_at	FOXP1	forkhead box P1	-0,80	$2{,}92 \times 10^{-8}$
244040_at	NA	NA	-0,80	$4{,}02 \times 10^{-6}$
225396_at	RBBP4	retinoblastoma binding protein 4	-0,80	$2{,}09 \times 10^{-6}$
214011_s_at	NOP16	NOP16 nucleolar protein homolog (yeast)	-0,80	$2{,}36 \times 10^{-6}$
218974_at	SOBP	sine oculis binding protein homolog (Drosophila)	-0,80	$4{,}87 \times 10^{-6}$
203254_s_at	TLN1	talin 1	-0,80	$1{,}22 \times 10^{-6}$
228650_at	NA	NA	-0,80	$2{,}47 \times 10^{-6}$
229844_at	NA	NA	-0,80	$9{,}24 \times 10^{-8}$
240715_at	TBX5	T-box 5	-0,81	$1{,}94 \times 10^{-7}$
235570_at	NA	NA	-0,81	$1{,}28 \times 10^{-5}$
230782_at	SORD	sorbitol dehydrogenase	-0,81	$5{,}05 \times 10^{-6}$

...continues on next page

Table C.1.: *(...continued)*

Probe set ID	Gene symbol	Gene name	logFc	adj.p-val
225958_at	PHC1	polyhomeotic homolog 1 (Drosophila)	-0,81	$1{,}39 \times 10^{-6}$
202664_at	WIPF1	WAS/WASL interacting protein family, member 1	-0,81	$6{,}93 \times 10^{-6}$
225274_at	PCYOX1	prenylcysteine oxidase 1	-0,81	$4{,}63 \times 10^{-7}$
205902_at	KCNN3	potassium intermediate/small conductance calcium-activated channel, subfamily N, member 3	-0,81	$1{,}54 \times 10^{-5}$
205882_x_at	ADD3	adducin 3 (gamma)	-0,81	$3{,}33 \times 10^{-7}$
231489_x_at	NA	NA	-0,81	$1{,}77 \times 10^{-6}$
225182_at	TMEM50B	transmembrane protein 50B	-0,81	$4{,}10 \times 10^{-8}$
220076_at	ANKH	ankylosis, progressive homolog (mouse)	-0,81	$1{,}80 \times 10^{-5}$
227288_at	SFRS12IP1	SFRS12-interacting protein 1	-0,81	$5{,}92 \times 10^{-7}$
214762_at	ATP6V1G2	ATPase, H+ transporting, lysosomal 13kDa, V1 subunit G2	-0,82	$2{,}56 \times 10^{-7}$
244872_at	RBBP4	retinoblastoma binding protein 4	-0,82	$7{,}76 \times 10^{-6}$
225368_at	HIPK2	homeodomain interacting protein kinase 2	-0,82	$3{,}41 \times 10^{-7}$
221788_at	NA	NA	-0,82	$9{,}92 \times 10^{-6}$
202998_s_at	LOXL2	lysyl oxidase-like 2	-0,82	$3{,}18 \times 10^{-6}$
1552275_s_at	PXK	PX domain containing serine/threonine kinase	-0,82	$1{,}44 \times 10^{-5}$
212248_at	MTDH	metadherin	-0,82	$1{,}40 \times 10^{-6}$
212256_at	GALNT10	UDP-N-acetyl-alpha-D-galactosamine:polypeptide N-acetylgalactosaminyltransferase 10 (GalNAc-T10)	-0,82	$5{,}50 \times 10^{-7}$
202603_at	NA	NA	-0,82	$1{,}06 \times 10^{-7}$
213109_at	TNIK	TRAF2 and NCK interacting kinase	-0,82	$1{,}20 \times 10^{-6}$
202052_s_at	RAI14	retinoic acid induced 14	-0,82	$6{,}35 \times 10^{-7}$
203438_at	STC2	stanniocalcin 2	-0,82	$2{,}77 \times 10^{-6}$
219156_at	SYNJ2BP	synaptojanin 2 binding protein	-0,82	$1{,}80 \times 10^{-7}$
204368_at	SLCO2A1	solute carrier organic anion transporter family, member 2A1	-0,82	$3{,}96 \times 10^{-6}$
229618_at	SNX16	sorting nexin 16	-0,82	$2{,}17 \times 10^{-6}$
239729_at	NA	NA	-0,83	$1{,}45 \times 10^{-6}$
232709_at	NA	NA	-0,83	$4{,}86 \times 10^{-6}$
203242_s_at	PDLIM5	PDZ and LIM domain 5	-0,83	$2{,}81 \times 10^{-6}$
205198_s_at	ATP7A	ATPase, Cu++ transporting, alpha polypeptide	-0,83	$4{,}12 \times 10^{-6}$
222998_at	MAF1	MAF1 homolog (S. cerevisiae)	-0,83	$4{,}37 \times 10^{-8}$
223479_s_at	CHCHD5	coiled-coil-helix-coiled-coil-helix domain containing 5	-0,83	$2{,}25 \times 10^{-6}$
222567_s_at	MEX3C	mex-3 homolog C (C. elegans)	-0,83	$3{,}40 \times 10^{-7}$
218102_at	DERA	2-deoxyribose-5-phosphate aldolase homolog (C. elegans)	-0,83	$4{,}04 \times 10^{-7}$
235531_at	NA	NA	-0,83	$1{,}86 \times 10^{-6}$
224755_at	TM9SF3	transmembrane 9 superfamily member 3	-0,83	$4{,}25 \times 10^{-7}$
213844_at	HOXA5	homeobox A5	-0,83	$4{,}53 \times 10^{-7}$
227836_at	UTP23	UTP23, small subunit (SSU) processome component, homolog (yeast)	-0,83	$3{,}03 \times 10^{-7}$
221249_s_at	FAM117A	family with sequence similarity 117, member A	-0,83	$8{,}54 \times 10^{-7}$
229410_at	SLC35E1	solute carrier family 35, member E1	-0,83	$6{,}08 \times 10^{-8}$

...continues on next page

Table C.1.: *(...continued)*

Probe set ID	Gene symbol	Gene name	logFc	adj.p-val
37590_g_at	NA	NA	-0,83	$1{,}61 \times 10^{-5}$
220646_s_at	KLRF1	killer cell lectin-like receptor subfamily F, member 1	-0,83	$1{,}04 \times 10^{-5}$
235764_at	NA	NA	-0,84	$1{,}56 \times 10^{-5}$
217437_s_at	TACC1	transforming, acidic coiled-coil containing protein 1	-0,84	$7{,}77 \times 10^{-7}$
207124_s_at	GNB5	guanine nucleotide binding protein (G protein), beta 5	-0,84	$4{,}37 \times 10^{-8}$
229674_at	SERTAD4	SERTA domain containing 4	-0,84	$1{,}86 \times 10^{-6}$
227277_at	MTDH	metadherin	-0,84	$7{,}54 \times 10^{-6}$
224691_at	NA	NA	-0,84	$2{,}14 \times 10^{-8}$
228390_at	NA	NA	-0,84	$4{,}25 \times 10^{-6}$
219562_at	RAB26	RAB26, member RAS oncogene family	-0,84	$8{,}36 \times 10^{-6}$
209016_s_at	KRT7	keratin 7	-0,84	$2{,}50 \times 10^{-8}$
223723_at	MFI2	antigen p97 (melanoma associated) identified by monoclonal antibodies 133.2 and 96.5	-0,84	$3{,}43 \times 10^{-6}$
201753_s_at	ADD3	adducin 3 (gamma)	-0,84	$3{,}08 \times 10^{-7}$
228131_at	ERCC1	excision repair cross-complementing rodent repair deficiency, complementation group 1 (includes overlapping antisense sequence)	-0,84	$4{,}05 \times 10^{-6}$
1554690_a_at	TACC1	transforming, acidic coiled-coil containing protein 1	-0,84	$1{,}08 \times 10^{-7}$
244177_at	NA	NA	-0,84	$8{,}51 \times 10^{-6}$
225391_at	LOC93622	hypothetical LOC93622	-0,84	$2{,}01 \times 10^{-6}$
226671_at	LAMP2	lysosomal-associated membrane protein 2	-0,84	$4{,}38 \times 10^{-6}$
226186_at	TMOD2	tropomodulin 2 (neuronal)	-0,84	$1{,}62 \times 10^{-5}$
200911_s_at	TACC1	transforming, acidic coiled-coil containing protein 1	-0,85	$4{,}10 \times 10^{-8}$
230744_at	NA	NA	-0,85	$9{,}42 \times 10^{-6}$
202506_at	SSFA2	sperm specific antigen 2	-0,85	$6{,}24 \times 10^{-7}$
239240_at	NA	NA	-0,85	$1{,}01 \times 10^{-7}$
228075_x_at	TFB1M	transcription factor B1, mitochondrial	-0,85	$2{,}55 \times 10^{-6}$
213970_at	RABL3	RAB, member of RAS oncogene family-like 3	-0,85	$2{,}28 \times 10^{-6}$
1569128_at	C3orf38	chromosome 3 open reading frame 38	-0,85	$3{,}86 \times 10^{-6}$
212403_at	UBE3B	ubiquitin protein ligase E3B	-0,85	$2{,}49 \times 10^{-8}$
217824_at	UBE2J1	ubiquitin-conjugating enzyme E2, J1 (UBC6 homolog, yeast)	-0,85	$8{,}97 \times 10^{-7}$
229572_at	ATP6V0A2	ATPase, H+ transporting, lysosomal V0 subunit a2	-0,85	$5{,}02 \times 10^{-6}$
214769_at	CLCN4	chloride channel 4	-0,86	$3{,}67 \times 10^{-6}$
226657_at	C17orf103	chromosome 17 open reading frame 103	-0,86	$1{,}13 \times 10^{-5}$
213657_s_at	NA	NA	-0,86	$1{,}20 \times 10^{-5}$
235086_at	THBS1	thrombospondin 1	-0,86	$2{,}04 \times 10^{-6}$
206571_s_at	MAP4K4	mitogen-activated protein kinase kinase kinase kinase 4	-0,86	$1{,}77 \times 10^{-6}$
225796_at	PXK	PX domain containing serine/threonine kinase	-0,86	$1{,}77 \times 10^{-7}$
200995_at	IPO7	importin 7	-0,86	$1{,}22 \times 10^{-7}$
200052_s_at	ILF2	interleukin enhancer binding factor 2, 45kDa	-0,86	$2{,}36 \times 10^{-8}$
220112_at	ANKRD55	ankyrin repeat domain 55	-0,86	$3{,}21 \times 10^{-6}$
238512_at	NA	NA	-0,86	$4{,}25 \times 10^{-6}$

...continues on next page

Table C.1.: *(...continued)*

Probe set ID	Gene symbol	Gene name	logFc	adj.p-val
208988_at	KDM2A	lysine (K)-specific demethylase 2A	-0,86	$7{,}83 \times 10^{-7}$
231968_at	UGGT1	UDP-glucose glycoprotein glucosyltransferase 1	-0,86	$3{,}51 \times 10^{-7}$
225567_at	NA	NA	-0,86	$2{,}73 \times 10^{-7}$
244187_at	NA	NA	-0,87	$2{,}35 \times 10^{-7}$
219169_s_at	TFB1M	transcription factor B1, mitochondrial	-0,87	$1{,}51 \times 10^{-7}$
230178_s_at	NA	NA	-0,87	$5{,}38 \times 10^{-7}$
229074_at	NA	NA	-0,87	$6{,}72 \times 10^{-7}$
1560156_at	NA	NA	-0,87	$6{,}97 \times 10^{-7}$
216804_s_at	PDLIM5	PDZ and LIM domain 5	-0,87	$5{,}50 \times 10^{-8}$
229441_at	PRSS23	protease, serine, 23	-0,87	$5{,}75 \times 10^{-7}$
208760_at	UBE2I	ubiquitin-conjugating enzyme E2I (UBC9 homolog, yeast)	-0,88	$2{,}56 \times 10^{-7}$
210754_s_at	LYN	v-yes-1 Yamaguchi sarcoma viral related oncogene homolog	-0,88	$8{,}67 \times 10^{-8}$
226830_x_at	CHD2	chromodomain helicase DNA binding protein 2	-0,88	$1{,}59 \times 10^{-6}$
212148_at	PBX1	pre-B-cell leukemia homeobox 1	-0,88	$1{,}73 \times 10^{-6}$
236217_at	SLC31A1	solute carrier family 31 (copper transporters), member 1	-0,88	$6{,}32 \times 10^{-7}$
238768_at	C2orf68	chromosome 2 open reading frame 68	-0,88	$2{,}79 \times 10^{-6}$
209815_at	PTCH1	patched homolog 1 (Drosophila)	-0,88	$1{,}63 \times 10^{-5}$
205516_x_at	CIZ1	CDKN1A interacting zinc finger protein 1	-0,88	$3{,}16 \times 10^{-8}$
206458_s_at	WNT2B	wingless-type MMTV integration site family, member 2B	-0,88	$4{,}46 \times 10^{-6}$
202840_at	TAF15	TAF15 RNA polymerase II, TATA box binding protein (TBP)-associated factor, 68kDa	-0,89	$1{,}42 \times 10^{-6}$
236313_at	CDKN2B	cyclin-dependent kinase inhibitor 2B (p15, inhibits CDK4)	-0,89	$1{,}23 \times 10^{-5}$
231110_at	NA	NA	-0,89	$1{,}90 \times 10^{-6}$
207826_s_at	ID3	inhibitor of DNA binding 3, dominant negative helix-loop-helix protein	-0,89	$1{,}59 \times 10^{-6}$
1563431_x_at	NA	NA	-0,89	$1{,}64 \times 10^{-5}$
203133_at	SEC61B	Sec61 beta subunit	-0,89	$1{,}36 \times 10^{-8}$
1557900_at	SIM2	single-minded homolog 2 (Drosophila)	-0,89	$5{,}95 \times 10^{-6}$
228168_at	ATP5G3	ATP synthase, H+ transporting, mitochondrial F0 complex, subunit C3 (subunit 9)	-0,89	$7{,}73 \times 10^{-7}$
218309_at	CAMK2N1	calcium/calmodulin-dependent protein kinase II inhibitor 1	-0,89	$3{,}72 \times 10^{-8}$
201302_at	ANXA4	annexin A4	-0,89	$1{,}49 \times 10^{-7}$
1553055_a_at	SLFN5	schlafen family member 5	-0,90	$1{,}23 \times 10^{-5}$
217906_at	KLHDC2	kelch domain containing 2	-0,90	$1{,}64 \times 10^{-8}$
220169_at	TMEM156	transmembrane protein 156	-0,90	$5{,}06 \times 10^{-6}$
201348_at	GPX3	glutathione peroxidase 3 (plasma)	-0,90	$7{,}56 \times 10^{-8}$
1559716_at	INO80C	INO80 complex subunit C	-0,90	$3{,}35 \times 10^{-7}$
235484_at	PTAR1	protein prenyltransferase alpha subunit repeat containing 1	-0,90	$4{,}53 \times 10^{-6}$
204000_at	GNB5	guanine nucleotide binding protein (G protein), beta 5	-0,90	$2{,}45 \times 10^{-7}$
208776_at	PSMD11	proteasome (prosome, macropain) 26S subunit, non-ATPase, 11	-0,90	$9{,}38 \times 10^{-7}$

...continues on next page

Table C.1.: *(...continued)*

Probe set ID	Gene symbol	Gene name	logFc	adj.p-val
224838_at	FOXP1	forkhead box P1	-0,90	$5{,}85 \times 10^{-8}$
222548_s_at	MAP4K4	mitogen-activated protein kinase kinase kinase kinase 4	-0,90	$5{,}96 \times 10^{-6}$
224525_s_at	OLA1	Obg-like ATPase 1	-0,90	$4{,}22 \times 10^{-6}$
222088_s_at	NA	NA	-0,90	$2{,}46 \times 10^{-6}$
230416_at	NA	NA	-0,91	$4{,}10 \times 10^{-8}$
203549_s_at	LPL	lipoprotein lipase	-0,91	$1{,}48 \times 10^{-6}$
219563_at	C14orf139	chromosome 14 open reading frame 139	-0,91	$6{,}64 \times 10^{-7}$
1562013_a_at	NA	NA	-0,91	$1{,}77 \times 10^{-6}$
224859_at	CD276	CD276 molecule	-0,92	$1{,}64 \times 10^{-8}$
203123_s_at	SLC11A2	solute carrier family 11 (proton-coupled divalent metal ion transporters), member 2	-0,92	$1{,}23 \times 10^{-7}$
235076_at	CALCOCO2	calcium binding and coiled-coil domain 2	-0,92	$6{,}64 \times 10^{-7}$
227692_at	GNAI1	guanine nucleotide binding protein (G protein), alpha inhibiting activity polypeptide 1	-0,92	$1{,}10 \times 10^{-6}$
226220_at	METTL9	methyltransferase like 9	-0,92	$1{,}34 \times 10^{-6}$
37152_at	PPARD	peroxisome proliferator-activated receptor delta	-0,92	$5{,}05 \times 10^{-7}$
213852_at	NA	NA	-0,92	$5{,}70 \times 10^{-7}$
208939_at	SEPHS1	selenophosphate synthetase 1	-0,92	$3{,}11 \times 10^{-7}$
226279_at	PRSS23	protease, serine, 23	-0,92	$4{,}10 \times 10^{-6}$
209623_at	MCCC2	methylcrotonoyl-Coenzyme A carboxylase 2 (beta)	-0,92	$3{,}25 \times 10^{-8}$
203159_at	GLS	glutaminase	-0,92	$9{,}07 \times 10^{-6}$
221964_at	TULP3	tubby like protein 3	-0,92	$2{,}25 \times 10^{-7}$
212944_at	SLC5A3	solute carrier family 5 (sodium/myo-inositol cotransporter), member 3	-0,92	$2{,}26 \times 10^{-7}$
219806_s_at	C11orf75	chromosome 11 open reading frame 75	-0,92	$1{,}34 \times 10^{-6}$
225764_at	ETV6	ets variant 6	-0,92	$8{,}18 \times 10^{-7}$
225120_at	PURB	purine-rich element binding protein B	-0,93	$8{,}52 \times 10^{-8}$
200685_at	SFRS11	splicing factor, arginine/serine-rich 11	-0,93	$1{,}72 \times 10^{-7}$
243444_at	SRD5A3	steroid 5 alpha-reductase 3	-0,93	$1{,}48 \times 10^{-6}$
211955_at	IPO5	importin 5	-0,93	$3{,}96 \times 10^{-8}$
1558237_x_at	NA	NA	-0,93	$2{,}91 \times 10^{-7}$
203126_at	IMPA2	inositol(myo)-1(or 4)-monophosphatase 2	-0,93	$6{,}98 \times 10^{-8}$
226406_at	C18orf25	chromosome 18 open reading frame 25	-0,93	$2{,}54 \times 10^{-8}$
202626_s_at	LYN	v-yes-1 Yamaguchi sarcoma viral related oncogene homolog	-0,93	$1{,}46 \times 10^{-8}$
214091_s_at	GPX3	glutathione peroxidase 3 (plasma)	-0,93	$5{,}44 \times 10^{-7}$
202119_s_at	CPNE3	copine III	-0,93	$1{,}28 \times 10^{-8}$
219217_at	NARS2	asparaginyl-tRNA synthetase 2, mitochondrial (putative)	-0,93	$1{,}75 \times 10^{-7}$
223366_at	NA	NA	-0,93	$3{,}04 \times 10^{-6}$
1555974_a_at	NA	NA	-0,93	$1{,}17 \times 10^{-5}$
230031_at	HSPA5	heat shock 70kDa protein 5 (glucose-regulated protein, 78kDa)	-0,94	$3{,}94 \times 10^{-6}$

...continues on next page

Table C.1.: *(...continued)*

Probe set ID	Gene symbol	Gene name	logFc	adj.p-val
202499_s_at	SLC2A3	solute carrier family 2 (facilitated glucose transporter), member 3	-0,94	$7{,}45\text{x}10^{-6}$
225496_s_at	SYTL2	synaptotagmin-like 2	-0,94	$1{,}02\text{x}10^{-6}$
202951_at	STK38	serine/threonine kinase 38	-0,94	$6{,}78\text{x}10^{-7}$
203878_s_at	MMP11	matrix metallopeptidase 11 (stromelysin 3)	-0,94	$2{,}22\text{x}10^{-7}$
226997_at	ADAMTS12	ADAM metallopeptidase with thrombospondin type 1 motif, 12	-0,94	$1{,}50\text{x}10^{-7}$
227274_at	SYNJ2BP	synaptojanin 2 binding protein	-0,94	$8{,}55\text{x}10^{-8}$
227199_at	DIP2A	DIP2 disco-interacting protein 2 homolog A (Drosophila)	-0,94	$1{,}03\text{x}10^{-6}$
244779_at	NA	NA	-0,94	$2{,}08\text{x}10^{-7}$
202254_at	SIPA1L1	signal-induced proliferation-associated 1 like 1	-0,94	$6{,}00\text{x}10^{-6}$
1556138_a_at	NA	NA	-0,95	$1{,}17\text{x}10^{-6}$
225871_at	STEAP2	six transmembrane epithelial antigen of the prostate 2	-0,95	$5{,}71\text{x}10^{-6}$
219357_at	GTPBP1	GTP binding protein 1	-0,95	$1{,}03\text{x}10^{-7}$
242051_at	NA	NA	-0,95	$6{,}26\text{x}10^{-6}$
235337_at	NA	NA	-0,95	$1{,}81\text{x}10^{-6}$
202479_s_at	TRIB2	tribbles homolog 2 (Drosophila)	-0,95	$2{,}86\text{x}10^{-6}$
227116_at	NA	NA	-0,95	$6{,}82\text{x}10^{-6}$
212536_at	ATP11B	ATPase, class VI, type 11B	-0,95	$1{,}65\text{x}10^{-6}$
225543_at	NA	NA	-0,95	$2{,}93\text{x}10^{-7}$
222547_at	MAP4K4	mitogen-activated protein kinase kinase kinase kinase 4	-0,95	$1{,}28\text{x}10^{-5}$
211358_s_at	CIZ1	CDKN1A interacting zinc finger protein 1	-0,96	$2{,}18\text{x}10^{-8}$
224722_at	MIB1	mindbomb homolog 1 (Drosophila)	-0,96	$2{,}56\text{x}10^{-7}$
228310_at	ENAH	enabled homolog (Drosophila)	-0,96	$4{,}04\text{x}10^{-6}$
218181_s_at	MAP4K4	mitogen-activated protein kinase kinase kinase kinase 4	-0,96	$2{,}29\text{x}10^{-6}$
230821_at	ZNF148	zinc finger protein 148	-0,96	$4{,}87\text{x}10^{-6}$
227846_at	GPR176	G protein-coupled receptor 176	-0,96	$1{,}26\text{x}10^{-8}$
1559067_a_at	NA	NA	-0,96	$6{,}72\text{x}10^{-7}$
204682_at	LTBP2	latent transforming growth factor beta binding protein 2	-0,96	$5{,}81\text{x}10^{-7}$
225864_at	FAM84B	family with sequence similarity 84, member B	-0,96	$8{,}33\text{x}10^{-7}$
226834_at	NA	NA	-0,96	$9{,}23\text{x}10^{-6}$
212714_at	LARP4	La ribonucleoprotein domain family, member 4	-0,96	$4{,}53\text{x}10^{-7}$
1555500_s_at	SLC2A4RG	SLC2A4 regulator	-0,96	$1{,}75\text{x}10^{-7}$
201362_at	IVNS1ABP	influenza virus NS1A binding protein	-0,96	$6{,}62\text{x}10^{-7}$
213289_at	APOOL	apolipoprotein O-like	-0,96	$9{,}29\text{x}10^{-8}$
227620_at	SLC44A1	solute carrier family 44, member 1	-0,97	$6{,}20\text{x}10^{-6}$
213790_at	ADAM12	ADAM metallopeptidase domain 12	-0,97	$6{,}04\text{x}10^{-6}$
225953_at	RPRD1A	regulation of nuclear pre-mRNA domain containing 1A	-0,97	$6{,}72\text{x}10^{-6}$
203789_s_at	SEMA3C	sema domain, immunoglobulin domain (Ig), short basic domain, secreted, (semaphorin) 3C	-0,97	$7{,}32\text{x}10^{-7}$
59631_at	TXNRD3	thioredoxin reductase 3	-0,97	$6{,}65\text{x}10^{-8}$
212771_at	FAM171A1	family with sequence similarity 171, member A1	-0,97	$1{,}06\text{x}10^{-7}$

...continues on next page

Table C.1.: *(...continued)*

Probe set ID	Gene symbol	Gene name	logFc	adj.p-val
201124_at	ITGB5	integrin, beta 5	-0,97	$3{,}02 \times 10^{-6}$
217949_s_at	VKORC1	vitamin K epoxide reductase complex, subunit 1	-0,97	$1{,}38 \times 10^{-8}$
235363_at	NA	NA	-0,97	$6{,}96 \times 10^{-7}$
230383_x_at	NA	NA	-0,97	$3{,}08 \times 10^{-7}$
227138_at	CRTAP	cartilage associated protein	-0,97	$5{,}73 \times 10^{-6}$
225363_at	PTEN	phosphatase and tensin homolog	-0,97	$4{,}04 \times 10^{-7}$
238431_at	NA	NA	-0,98	$3{,}43 \times 10^{-7}$
203881_s_at	DMD	dystrophin	-0,98	$4{,}40 \times 10^{-6}$
203044_at	CHSY1	chondroitin sulfate synthase 1	-0,98	$6{,}88 \times 10^{-8}$
201430_s_at	DPYSL3	dihydropyrimidinase-like 3	-0,98	$1{,}45 \times 10^{-5}$
1559007_s_at	NA	NA	-0,98	$4{,}57 \times 10^{-6}$
230154_at	NA	NA	-0,98	$1{,}19 \times 10^{-5}$
224778_s_at	NA	NA	-0,98	$3{,}97 \times 10^{-8}$
218057_x_at	COX4NB	COX4 neighbor	-0,98	$6{,}58 \times 10^{-9}$
201765_s_at	HEXA	hexosaminidase A (alpha polypeptide)	-0,98	$1{,}81 \times 10^{-7}$
208944_at	TGFBR2	transforming growth factor, beta receptor II (70/80kDa)	-0,98	$2{,}49 \times 10^{-8}$
227518_at	SLC35E1	solute carrier family 35, member E1	-0,98	$4{,}53 \times 10^{-7}$
228335_at	CLDN11	claudin 11	-0,99	$1{,}58 \times 10^{-7}$
211953_s_at	IPO5	importin 5	-0,99	$1{,}81 \times 10^{-7}$
218847_at	IGF2BP2	insulin-like growth factor 2 mRNA binding protein 2	-0,99	$6{,}35 \times 10^{-7}$
222559_s_at	RPRD1A	regulation of nuclear pre-mRNA domain containing 1A	-0,99	$2{,}48 \times 10^{-6}$
200931_s_at	VCL	vinculin	-0,99	$3{,}39 \times 10^{-9}$
228482_at	NA	NA	-0,99	$4{,}35 \times 10^{-6}$
235093_at	PEX13	peroxisomal biogenesis factor 13	-0,99	$6{,}98 \times 10^{-8}$
203852_s_at	NA	NA	-0,99	$4{,}04 \times 10^{-6}$
230302_at	NA	NA	-0,99	$4{,}37 \times 10^{-8}$
231233_at	NA	NA	-0,99	$4{,}46 \times 10^{-6}$
213388_at	PDE4DIP	phosphodiesterase 4D interacting protein	-0,99	$3{,}03 \times 10^{-6}$
215128_at	NA	NA	-1,00	$1{,}08 \times 10^{-6}$
225951_s_at	CHD2	chromodomain helicase DNA binding protein 2	-1,00	$1{,}73 \times 10^{-7}$
202498_s_at	SLC2A3	solute carrier family 2 (facilitated glucose transporter), member 3	-1,00	$4{,}84 \times 10^{-6}$
232231_at	RUNX2	runt-related transcription factor 2	-1,00	$8{,}86 \times 10^{-6}$
225865_x_at	TH1L	TH1-like (Drosophila)	-1,00	$4{,}28 \times 10^{-9}$
222558_at	RPRD1A	regulation of nuclear pre-mRNA domain containing 1A	-1,00	$1{,}97 \times 10^{-7}$
211954_s_at	IPO5	importin 5	-1,00	$1{,}48 \times 10^{-8}$
224769_at	NA	NA	-1,00	$1{,}64 \times 10^{-8}$
219283_at	C1GALT1C1	C1GALT1-specific chaperone 1	-1,00	$2{,}58 \times 10^{-7}$
227357_at	TAB3	TGF-beta activated kinase 1/MAP3K7 binding protein 3	-1,00	$1{,}51 \times 10^{-7}$
243999_at	SLFN5	schlafen family member 5	-1,00	$4{,}29 \times 10^{-7}$
232914_s_at	SYTL2	synaptotagmin-like 2	-1,01	$5{,}13 \times 10^{-7}$
224882_at	ACSS1	acyl-CoA synthetase short-chain family member 1	-1,01	$1{,}34 \times 10^{-8}$

...continues on next page

Table C.1.: *(...continued)*

Probe set ID	Gene symbol	Gene name	logFc	adj.p-val
1553117_a_at	STK38	serine/threonine kinase 38	-1,01	$3{,}63 \times 10^{-6}$
217645_at	COX16	COX16 cytochrome c oxidase assembly homolog (S. cerevisiae)	-1,01	$3{,}73 \times 10^{-6}$
200845_s_at	PRDX6	peroxiredoxin 6	-1,01	$1{,}70 \times 10^{-7}$
227123_at	RAB3B	RAB3B, member RAS oncogene family	-1,01	$1{,}54 \times 10^{-5}$
207992_s_at	AMPD3	adenosine monophosphate deaminase 3	-1,02	$2{,}00 \times 10^{-7}$
225276_at	GSPT1	G1 to S phase transition 1	-1,02	$2{,}78 \times 10^{-8}$
225006_x_at	TH1L	TH1-like (Drosophila)	-1,02	$7{,}71 \times 10^{-9}$
222504_s_at	COX4NB	COX4 neighbor	-1,02	$3{,}96 \times 10^{-8}$
227363_s_at	COX4NB	COX4 neighbor	-1,02	$1{,}41 \times 10^{-8}$
218362_s_at	DIS3	DIS3 mitotic control homolog (S. cerevisiae)	-1,02	$1{,}61 \times 10^{-7}$
225261_x_at	TH1L	TH1-like (Drosophila)	-1,02	$5{,}10 \times 10^{-9}$
202213_s_at	CUL4B	cullin 4B	-1,02	$1{,}55 \times 10^{-5}$
226591_at	SNRPN	small nuclear ribonucleoprotein polypeptide N	-1,02	$1{,}48 \times 10^{-5}$
202118_s_at	CPNE3	copine III	-1,02	$5{,}59 \times 10^{-6}$
230183_at	EXT1	exostoses (multiple) 1	-1,02	$1{,}81 \times 10^{-7}$
202625_at	LYN	v-yes-1 Yamaguchi sarcoma viral related oncogene homolog	-1,03	$1{,}17 \times 10^{-8}$
208932_at	PPP4C	protein phosphatase 4 (formerly X), catalytic subunit	-1,03	$9{,}42 \times 10^{-9}$
242263_at	TMED5	transmembrane emp24 protein transport domain containing 5	-1,03	$3{,}40 \times 10^{-6}$
1569129_s_at	C3orf38	chromosome 3 open reading frame 38	-1,03	$1{,}00 \times 10^{-5}$
230238_at	ANKRD43	ankyrin repeat domain 43	-1,03	$7{,}74 \times 10^{-7}$
201150_s_at	TIMP3	TIMP metallopeptidase inhibitor 3	-1,03	$1{,}07 \times 10^{-6}$
203232_s_at	ATXN1	ataxin 1	-1,03	$6{,}97 \times 10^{-7}$
224940_s_at	PAPPA	pregnancy-associated plasma protein A, pappalysin 1	-1,03	$6{,}42 \times 10^{-7}$
202604_x_at	ADAM10	ADAM metallopeptidase domain 10	-1,03	$1{,}45 \times 10^{-7}$
235079_at	NA	NA	-1,03	$2{,}08 \times 10^{-6}$
200713_s_at	MAPRE1	microtubule-associated protein, RP/EB family, member 1	-1,03	$7{,}80 \times 10^{-9}$
225842_at	PHLDA1	pleckstrin homology-like domain, family A, member 1	-1,03	$1{,}10 \times 10^{-5}$
235635_at	ARHGAP5	Rho GTPase activating protein 5	-1,03	$1{,}53 \times 10^{-6}$
200623_s_at	CALM3	calmodulin 3 (phosphorylase kinase, delta)	-1,04	$1{,}93 \times 10^{-8}$
220607_x_at	TH1L	TH1-like (Drosophila)	-1,04	$6{,}59 \times 10^{-9}$
218170_at	ISOC1	isochorismatase domain containing 1	-1,04	$1{,}58 \times 10^{-7}$
218042_at	COPS4	COP9 constitutive photomorphogenic homolog subunit 4 (Arabidopsis)	-1,04	$5{,}68 \times 10^{-8}$
228569_at	PAPOLA	poly(A) polymerase alpha	-1,04	$3{,}93 \times 10^{-6}$
221906_at	TXNRD3	thioredoxin reductase 3	-1,04	$3{,}03 \times 10^{-7}$
226934_at	CPSF6	cleavage and polyadenylation specific factor 6, 68kDa	-1,04	$8{,}29 \times 10^{-7}$
214953_s_at	APP	amyloid beta (A4) precursor protein	-1,04	$4{,}89 \times 10^{-7}$
228555_at	CAMK2D	calcium/calmodulin-dependent protein kinase II delta	-1,04	$2{,}76 \times 10^{-7}$
231894_at	NA	NA	-1,04	$1{,}78 \times 10^{-8}$
225311_at	IVD	isovaleryl Coenzyme A dehydrogenase	-1,04	$1{,}13 \times 10^{-8}$

...continues on next page

Table C.1.: *(...continued)*

Probe set ID	Gene symbol	Gene name	logFc	adj.p-val
209131_s_at	SNAP23	synaptosomal-associated protein, 23kDa	-1,04	$1{,}57 \times 10^{-6}$
235433_at	APOOL	apolipoprotein O-like	-1,04	$5{,}10 \times 10^{-9}$
242289_at	NA	NA	-1,05	$3{,}69 \times 10^{-7}$
209459_s_at	ABAT	4-aminobutyrate aminotransferase	-1,05	$1{,}03 \times 10^{-5}$
226985_at	FGD5	FYVE, RhoGEF and PH domain containing 5	-1,05	$3{,}47 \times 10^{-8}$
220195_at	MBD5	methyl-CpG binding domain protein 5	-1,05	$3{,}26 \times 10^{-7}$
227624_at	TET2	tet oncogene family member 2	-1,05	$2{,}56 \times 10^{-7}$
239919_at	NA	NA	-1,06	$4{,}16 \times 10^{-7}$
222305_at	HK2	hexokinase 2	-1,06	$1{,}25 \times 10^{-5}$
211056_s_at	SRD5A1	steroid-5-alpha-reductase, alpha polypeptide 1 (3-oxo-5 alpha-steroid delta 4-dehydrogenase alpha 1)	-1,06	$2{,}54 \times 10^{-8}$
230156_x_at	CHD2	chromodomain helicase DNA binding protein 2	-1,06	$5{,}79 \times 10^{-6}$
1559006_at	NA	NA	-1,06	$7{,}04 \times 10^{-7}$
203364_s_at	KIAA0652	KIAA0652	-1,06	$6{,}46 \times 10^{-9}$
226974_at	NEDD4L	neural precursor cell expressed, developmentally down-regulated 4-like	-1,06	$8{,}32 \times 10^{-8}$
214895_s_at	ADAM10	ADAM metallopeptidase domain 10	-1,07	$1{,}64 \times 10^{-6}$
201468_s_at	NQO1	NAD(P)H dehydrogenase, quinone 1	-1,07	$7{,}41 \times 10^{-8}$
236600_at	SPG20	spastic paraplegia 20 (Troyer syndrome)	-1,07	$2{,}46 \times 10^{-6}$
226183_at	GSK3B	glycogen synthase kinase 3 beta	-1,07	$7{,}16 \times 10^{-8}$
1556216_s_at	NA	NA	-1,07	$6{,}04 \times 10^{-6}$
239229_at	NA	NA	-1,08	$1{,}75 \times 10^{-6}$
221019_s_at	COLEC12	collectin sub-family member 12	-1,08	$2{,}56 \times 10^{-8}$
203371_s_at	NDUFB3	NADH dehydrogenase (ubiquinone) 1 beta subcomplex, 3, 12kDa	-1,08	$1{,}50 \times 10^{-7}$
209068_at	HNRPDL	heterogeneous nuclear ribonucleoprotein D-like	-1,08	$4{,}55 \times 10^{-7}$
200603_at	PRKAR1A	protein kinase, cAMP-dependent, regulatory, type I, alpha (tissue specific extinguisher 1)	-1,08	$2{,}44 \times 10^{-7}$
208999_at	SEP8	septin 8	-1,08	$1{,}36 \times 10^{-8}$
203603_s_at	ZEB2	zinc finger E-box binding homeobox 2	-1,09	$1{,}73 \times 10^{-5}$
227480_at	SUSD2	sushi domain containing 2	-1,09	$1{,}43 \times 10^{-6}$
235320_at	ARL6	ADP-ribosylation factor-like 6	-1,09	$3{,}94 \times 10^{-6}$
235318_at	FBN1	fibrillin 1	-1,09	$2{,}58 \times 10^{-6}$
218764_at	PRKCH	protein kinase C, eta	-1,09	$2{,}45 \times 10^{-7}$
241902_at	MKX	mohawk homeobox	-1,09	$6{,}00 \times 10^{-6}$
226179_at	SLC25A37	solute carrier family 25, member 37	-1,09	$7{,}16 \times 10^{-8}$
228395_at	NA	NA	-1,09	$4{,}89 \times 10^{-7}$
241443_at	NA	NA	-1,10	$2{,}34 \times 10^{-6}$
232007_at	AGPAT5	1-acylglycerol-3-phosphate O-acyltransferase 5 (lysophosphatidic acid acyltransferase, epsilon)	-1,10	$2{,}97 \times 10^{-6}$
225897_at	MARCKS	myristoylated alanine-rich protein kinase C substrate	-1,10	$3{,}63 \times 10^{-7}$
206214_at	PLA2G7	phospholipase A2, group VII (platelet-activating factor acetylhydrolase, plasma)	-1,11	$3{,}75 \times 10^{-6}$

...continues on next page

Table C.1.: *(...continued)*

Probe set ID	Gene symbol	Gene name	logFc	adj.p-val
228006_at	NA	NA	-1,11	$1{,}12 \times 10^{-5}$
201363_s_at	IVNS1ABP	influenza virus NS1A binding protein	-1,11	$9{,}78 \times 10^{-8}$
227059_at	GPC6	glypican 6	-1,11	$2{,}42 \times 10^{-6}$
203231_s_at	ATXN1	ataxin 1	-1,11	$7{,}68 \times 10^{-7}$
218718_at	PDGFC	platelet derived growth factor C	-1,11	$1{,}63 \times 10^{-7}$
222719_s_at	PDGFC	platelet derived growth factor C	-1,11	$1{,}58 \times 10^{-6}$
1557078_at	SLFN5	schlafen family member 5	-1,11	$3{,}08 \times 10^{-7}$
213567_at	NA	NA	-1,11	$7{,}94 \times 10^{-7}$
222543_at	DERL1	Der1-like domain family, member 1	-1,12	$9{,}78 \times 10^{-8}$
203420_at	FAM8A1	family with sequence similarity 8, member A1	-1,12	$3{,}11 \times 10^{-7}$
240013_at	NA	NA	-1,13	$2{,}19 \times 10^{-7}$
224941_at	PAPPA	pregnancy-associated plasma protein A, pappalysin 1	-1,13	$1{,}63 \times 10^{-6}$
225328_at	NA	NA	-1,13	$8{,}54 \times 10^{-7}$
229011_at	NA	NA	-1,13	$1{,}44 \times 10^{-6}$
212009_s_at	STIP1	stress-induced-phosphoprotein 1	-1,13	$4{,}55 \times 10^{-8}$
223115_at	MED17	mediator complex subunit 17	-1,13	$6{,}59 \times 10^{-9}$
240397_x_at	NA	NA	-1,13	$1{,}07 \times 10^{-6}$
235629_at	NA	NA	-1,13	$9{,}74 \times 10^{-6}$
227536_at	ZC3H13	zinc finger CCCH-type containing 13	-1,14	$3{,}77 \times 10^{-9}$
208940_at	SEPHS1	selenophosphate synthetase 1	-1,14	$8{,}14 \times 10^{-8}$
214848_at	NA	NA	-1,14	$8{,}14 \times 10^{-8}$
206645_s_at	NR0B1	nuclear receptor subfamily 0, group B, member 1	-1,14	$5{,}44 \times 10^{-7}$
225805_at	HNRNPU	heterogeneous nuclear ribonucleoprotein U (scaffold attachment factor A)	-1,14	$3{,}08 \times 10^{-7}$
201691_s_at	TPD52	tumor protein D52	-1,14	$2{,}31 \times 10^{-6}$
209129_at	TRIP6	thyroid hormone receptor interactor 6	-1,15	$9{,}42 \times 10^{-9}$
210959_s_at	SRD5A1	steroid-5-alpha-reductase, alpha polypeptide 1 (3-oxo-5 alpha-steroid delta 4-dehydrogenase alpha 1)	-1,15	$5{,}32 \times 10^{-7}$
236350_at	NA	NA	-1,15	$1{,}14 \times 10^{-6}$
228914_at	NA	NA	-1,15	$2{,}70 \times 10^{-6}$
202765_s_at	FBN1	fibrillin 1	-1,16	$1{,}36 \times 10^{-8}$
212473_s_at	MICAL2	microtubule associated monoxygenase, calponin and LIM domain containing 2	-1,16	$1{,}17 \times 10^{-7}$
233947_s_at	LOC255480	hypothetical protein LOC255480	-1,16	$1{,}06 \times 10^{-6}$
214068_at	BEAN	brain expressed, associated with Nedd4	-1,16	$2{,}81 \times 10^{-6}$
225776_at	RBMS2	RNA binding motif, single stranded interacting protein 2	-1,16	$3{,}26 \times 10^{-7}$
213282_at	APOOL	apolipoprotein O-like	-1,16	$4{,}24 \times 10^{-9}$
200602_at	APP	amyloid beta (A4) precursor protein	-1,16	$4{,}94 \times 10^{-6}$
225601_at	HMGB3	high-mobility group box 3	-1,16	$9{,}46 \times 10^{-8}$
225511_at	GPRC5B	G protein-coupled receptor, family C, group 5, member B	-1,16	$1{,}79 \times 10^{-7}$
222450_at	PMEPA1	prostate transmembrane protein, androgen induced 1	-1,17	$1{,}81 \times 10^{-7}$
223618_at	FMN2	formin 2	-1,17	$1{,}90 \times 10^{-6}$

...continues on next page

Table C.1.: *(...continued)*

Probe set ID	Gene symbol	Gene name	logFc	adj.p-val
228987_at	NA	NA	-1,17	$2{,}45\text{x}10^{-7}$
226777_at	NA	NA	-1,17	$5{,}69\text{x}10^{-7}$
226110_at	PTAR1	protein prenyltransferase alpha subunit repeat containing 1	-1,19	$1{,}15\text{x}10^{-8}$
235747_at	SLC25A16	solute carrier family 25 (mitochondrial carrier; Graves disease autoantigen), member 16	-1,19	$1{,}80\text{x}10^{-7}$
212912_at	RPS6KA2	ribosomal protein S6 kinase, 90kDa, polypeptide 2	-1,19	$3{,}05\text{x}10^{-6}$
226390_at	STARD4	StAR-related lipid transfer (START) domain containing 4	-1,19	$6{,}90\text{x}10^{-6}$
232752_at	LOC100287616	hypothetical protein LOC100287616	-1,20	$1{,}38\text{x}10^{-8}$
218527_at	APTX	aprataxin	-1,20	$3{,}43\text{x}10^{-7}$
225008_at	ASPH	aspartate beta-hydroxylase	-1,20	$6{,}62\text{x}10^{-7}$
225108_at	AGPS	alkylglycerone phosphate synthase	-1,20	$1{,}85\text{x}10^{-7}$
230243_at	RG9MTD2	RNA (guanine-9-) methyltransferase domain containing 2	-1,20	$1{,}23\text{x}10^{-7}$
213330_s_at	STIP1	stress-induced-phosphoprotein 1	-1,20	$3{,}93\text{x}10^{-9}$
203632_s_at	GPRC5B	G protein-coupled receptor, family C, group 5, member B	-1,20	$1{,}81\text{x}10^{-7}$
200712_s_at	MAPRE1	microtubule-associated protein, RP/EB family, member 1	-1,21	$9{,}36\text{x}10^{-9}$
221031_s_at	APOLD1	apolipoprotein L domain containing 1	-1,21	$2{,}22\text{x}10^{-6}$
205756_s_at	F8	coagulation factor VIII, procoagulant component	-1,22	$3{,}97\text{x}10^{-6}$
222750_s_at	SRD5A3	steroid 5 alpha-reductase 3	-1,22	$1{,}65\text{x}10^{-7}$
225786_at	NCRNA00201	non-protein coding RNA 201	-1,22	$9{,}21\text{x}10^{-6}$
218172_s_at	DERL1	Der1-like domain family, member 1	-1,22	$3{,}44\text{x}10^{-8}$
212472_at	MICAL2	microtubule associated monoxygenase, calponin and LIM domain containing 2	-1,22	$2{,}08\text{x}10^{-7}$
230433_at	LOC729970	similar to hCG2028352	-1,22	$5{,}57\text{x}10^{-6}$
213107_at	TNIK	TRAF2 and NCK interacting kinase	-1,22	$7{,}76\text{x}10^{-7}$
232667_at	NA	NA	-1,22	$2{,}56\text{x}10^{-8}$
211984_at	CALM1	calmodulin 1 (phosphorylase kinase, delta)	-1,22	$3{,}37\text{x}10^{-8}$
234975_at	GSPT1	G1 to S phase transition 1	-1,23	$1{,}77\text{x}10^{-5}$
208786_s_at	MAP1LC3B	microtubule-associated protein 1 light chain 3 beta	-1,23	$3{,}77\text{x}10^{-9}$
209503_s_at	PSMC5	proteasome (prosome, macropain) 26S subunit, ATPase, 5	-1,23	$1{,}96\text{x}10^{-9}$
217868_s_at	METTL9	methyltransferase like 9	-1,23	$9{,}24\text{x}10^{-9}$
213865_at	DCBLD2	discoidin, CUB and LCCL domain containing 2	-1,23	$5{,}71\text{x}10^{-6}$
212978_at	LRRC8B	leucine rich repeat containing 8 family, member B	-1,23	$5{,}91\text{x}10^{-7}$
226045_at	FRS2	fibroblast growth factor receptor substrate 2	-1,23	$1{,}75\text{x}10^{-7}$
242442_x_at	RG9MTD2	RNA (guanine-9-) methyltransferase domain containing 2	-1,24	$1{,}02\text{x}10^{-5}$
200749_at	RAN	RAN, member RAS oncogene family	-1,24	$1{,}36\text{x}10^{-8}$
228081_at	CCNG2	cyclin G2	-1,24	$1{,}61\text{x}10^{-6}$
206090_s_at	DISC1	disrupted in schizophrenia 1	-1,24	$8{,}47\text{x}10^{-9}$
228045_at	NA	NA	-1,25	$8{,}03\text{x}10^{-8}$
212815_at	ASCC3	activating signal cointegrator 1 complex subunit 3	-1,25	$1{,}65\text{x}10^{-7}$
214544_s_at	SNAP23	synaptosomal-associated protein, 23kDa	-1,26	$8{,}41\text{x}10^{-6}$
212077_at	CALD1	caldesmon 1	-1,26	$2{,}36\text{x}10^{-8}$

...continues on next page

Table C.1.: *(...continued)*

Probe set ID	Gene symbol	Gene name	logFc	adj.p-val
236723_at	NA	NA	-1,26	$7{,}15\text{x}10^{-7}$
208931_s_at	ILF3	interleukin enhancer binding factor 3, 90kDa	-1,26	$3{,}06\text{x}10^{-9}$
230139_at	NA	NA	-1,26	$2{,}07\text{x}10^{-7}$
202766_s_at	FBN1	fibrillin 1	-1,27	$3{,}39\text{x}10^{-9}$
1555281_x_at	ARMC8	armadillo repeat containing 8	-1,27	$5{,}91\text{x}10^{-7}$
211985_s_at	CALM1	calmodulin 1 (phosphorylase kinase, delta)	-1,27	$5{,}59\text{x}10^{-8}$
213258_at	TFPI	tissue factor pathway inhibitor (lipoprotein-associated coagulation inhibitor)	-1,27	$6{,}01\text{x}10^{-6}$
203548_s_at	LPL	lipoprotein lipase	-1,28	$1{,}07\text{x}10^{-7}$
201431_s_at	DPYSL3	dihydropyrimidinase-like 3	-1,28	$1{,}28\text{x}10^{-8}$
205854_at	TULP3	tubby like protein 3	-1,28	$8{,}14\text{x}10^{-8}$
214803_at	NA	NA	-1,28	$4{,}64\text{x}10^{-6}$
222587_s_at	GALNT7	UDP-N-acetyl-alpha-D-galactosamine:polypeptide N-acetylgalactosaminyltransferase 7 (GalNAc-T7)	-1,28	$1{,}04\text{x}10^{-7}$
1558236_at	NA	NA	-1,28	$6{,}65\text{x}10^{-8}$
208829_at	TAPBP	TAP binding protein (tapasin)	-1,28	$1{,}11\text{x}10^{-6}$
203124_s_at	SLC11A2	solute carrier family 11 (proton-coupled divalent metal ion transporters), member 2	-1,29	$1{,}13\text{x}10^{-8}$
209176_at	SEC23IP	SEC23 interacting protein	-1,29	$2{,}09\text{x}10^{-8}$
212165_at	NA	NA	-1,29	$3{,}93\text{x}10^{-9}$
1555279_at	ARMC8	armadillo repeat containing 8	-1,30	$2{,}56\text{x}10^{-7}$
238868_at	UACA	uveal autoantigen with coiled-coil domains and ankyrin repeats	-1,30	$1{,}62\text{x}10^{-5}$
204675_at	SRD5A1	steroid-5-alpha-reductase, alpha polypeptide 1 (3-oxo-5 alpha-steroid delta 4-dehydrogenase alpha 1)	-1,30	$6{,}59\text{x}10^{-9}$
235346_at	FUNDC1	FUN14 domain containing 1	-1,30	$3{,}72\text{x}10^{-8}$
212327_at	LIMCH1	LIM and calponin homology domains 1	-1,30	$1{,}00\text{x}10^{-5}$
236655_at	TPD52	tumor protein D52	-1,30	$2{,}61\text{x}10^{-7}$
226084_at	MAP1B	microtubule-associated protein 1B	-1,31	$3{,}12\text{x}10^{-8}$
200605_s_at	PRKAR1A	protein kinase, cAMP-dependent, regulatory, type I, alpha (tissue specific extinguisher 1)	-1,31	$9{,}42\text{x}10^{-9}$
224996_at	ASPH	aspartate beta-hydroxylase	-1,31	$3{,}52\text{x}10^{-8}$
209263_x_at	TSPAN4	tetraspanin 4	-1,31	$1{,}26\text{x}10^{-8}$
218541_s_at	C8orf4	chromosome 8 open reading frame 4	-1,32	$8{,}21\text{x}10^{-6}$
229544_at	NA	NA	-1,32	$1{,}91\text{x}10^{-7}$
209598_at	PNMA2	paraneoplastic antigen MA2	-1,33	$7{,}56\text{x}10^{-8}$
239138_at	NA	NA	-1,33	$2{,}27\text{x}10^{-6}$
222846_at	RAB8B	RAB8B, member RAS oncogene family	-1,34	$7{,}23\text{x}10^{-8}$
203818_s_at	SF3A3	splicing factor 3a, subunit 3, 60kDa	-1,34	$2{,}07\text{x}10^{-8}$
1555471_a_at	FMN2	formin 2	-1,34	$2{,}28\text{x}10^{-6}$
228128_x_at	PAPPA	pregnancy-associated plasma protein A, pappalysin 1	-1,34	$6{,}35\text{x}10^{-7}$
238175_at	NA	NA	-1,34	$2{,}44\text{x}10^{-7}$
236363_at	LOC285378	hypothetical protein LOC285378	-1,35	$6{,}62\text{x}10^{-7}$

...continues on next page

Table C.1.: *(...continued)*

Probe set ID	Gene symbol	Gene name	logFc	adj.p-val
201089_at	ATP6V1B2	ATPase, H+ transporting, lysosomal 56/58kDa, V1 subunit B2	-1,35	$3{,}93 \times 10^{-9}$
239425_at	DCUN1D5	DCN1, defective in cullin neddylation 1, domain containing 5 (S. cerevisiae)	-1,36	$7{,}50 \times 10^{-7}$
222447_at	METTL9	methyltransferase like 9	-1,37	$1{,}58 \times 10^{-8}$
230399_at	NA	NA	-1,37	$3{,}27 \times 10^{-7}$
211959_at	IGFBP5	insulin-like growth factor binding protein 5	-1,38	$5{,}32 \times 10^{-7}$
236075_s_at	NA	NA	-1,39	$3{,}72 \times 10^{-8}$
230655_at	NA	NA	-1,40	$2{,}00 \times 10^{-7}$
216326_s_at	HDAC3	histone deacetylase 3	-1,41	$3{,}39 \times 10^{-9}$
218313_s_at	GALNT7	UDP-N-acetyl-alpha-D-galactosamine:polypeptide N-acetylgalactosaminyltransferase 7 (GalNAc-T7)	-1,41	$2{,}94 \times 10^{-9}$
212233_at	MAP1B	microtubule-associated protein 1B	-1,41	$4{,}92 \times 10^{-8}$
224911_s_at	DCBLD2	discoidin, CUB and LCCL domain containing 2	-1,42	$2{,}56 \times 10^{-7}$
202478_at	TRIB2	tribbles homolog 2 (Drosophila)	-1,43	$3{,}03 \times 10^{-7}$
209130_at	SNAP23	synaptosomal-associated protein, 23kDa	-1,43	$1{,}26 \times 10^{-7}$
235192_at	TP53RK	TP53 regulating kinase	-1,43	$9{,}42 \times 10^{-9}$
209409_at	GRB10	growth factor receptor-bound protein 10	-1,43	$1{,}08 \times 10^{-7}$
219181_at	LIPG	lipase, endothelial	-1,45	$5{,}03 \times 10^{-6}$
226633_at	RAB8B	RAB8B, member RAS oncogene family	-1,45	$3{,}78 \times 10^{-9}$
203498_at	RCAN2	regulator of calcineurin 2	-1,46	$5{,}08 \times 10^{-6}$
230135_at	NA	NA	-1,47	$1{,}30 \times 10^{-5}$
218187_s_at	C8orf33	chromosome 8 open reading frame 33	-1,49	$3{,}06 \times 10^{-9}$
225004_at	TMEM101	transmembrane protein 101	-1,50	$5{,}62 \times 10^{-9}$
201287_s_at	SDC1	syndecan 1	-1,50	$4{,}24 \times 10^{-9}$
230175_s_at	NA	NA	-1,50	$7{,}56 \times 10^{-8}$
223641_at	NA	NA	-1,50	$1{,}97 \times 10^{-7}$
224728_at	ATPAF1	ATP synthase mitochondrial F1 complex assembly factor 1	-1,50	$2{,}61 \times 10^{-7}$
227467_at	RDH10	retinol dehydrogenase 10 (all-trans)	-1,51	$9{,}98 \times 10^{-8}$
215506_s_at	DIRAS3	DIRAS family, GTP-binding RAS-like 3	-1,53	$4{,}10 \times 10^{-9}$
200750_s_at	RAN	RAN, member RAS oncogene family	-1,54	$1{,}28 \times 10^{-8}$
1555841_at	C9orf30	chromosome 9 open reading frame 30	-1,55	$3{,}82 \times 10^{-9}$
227547_at	NA	NA	-1,55	$4{,}62 \times 10^{-9}$
237466_s_at	HHIP	hedgehog interacting protein	-1,55	$1{,}14 \times 10^{-5}$
227997_at	IL17RD	interleukin 17 receptor D	-1,56	$9{,}38 \times 10^{-7}$
222400_s_at	ADI1	acireductone dioxygenase 1	-1,56	$3{,}06 \times 10^{-9}$
217761_at	ADI1	acireductone dioxygenase 1	-1,57	$8{,}51 \times 10^{-9}$
209296_at	PPM1B	protein phosphatase 1B (formerly 2C), magnesium-dependent, beta isoform	-1,57	$2{,}24 \times 10^{-8}$
224893_at	ATL3	atlastin GTPase 3	-1,57	$6{,}98 \times 10^{-8}$
232130_at	NA	NA	-1,57	$5{,}18 \times 10^{-9}$
211981_at	COL4A1	collagen, type IV, alpha 1	-1,58	$4{,}70 \times 10^{-7}$

...continues on next page

Table C.1.: *(...continued)*

Probe set ID	Gene symbol	Gene name	logFc	adj.p-val
204114_at	NID2	nidogen 2 (osteonidogen)	-1,58	$7{,}71\text{x}10^{-9}$
1558686_at	NA	NA	-1,59	$3{,}21\text{x}10^{-6}$
221878_at	C2orf68	chromosome 2 open reading frame 68	-1,59	$1{,}60\text{x}10^{-8}$
224702_at	TMEM167A	transmembrane protein 167A	-1,59	3,63E-10
222824_at	NA	NA	-1,60	$1{,}17\text{x}10^{-7}$
201667_at	GJA1	gap junction protein, alpha 1, 43kDa	-1,61	$3{,}08\text{x}10^{-7}$
202214_s_at	CUL4B	cullin 4B	-1,63	$3{,}83\text{x}10^{-9}$
214240_at	GAL	galanin prepropeptide	-1,63	$8{,}51\text{x}10^{-9}$
226776_at	ENY2	enhancer of yellow 2 homolog (Drosophila)	-1,63	$4{,}13\text{x}10^{-7}$
212164_at	TMEM183A	transmembrane protein 183A	-1,64	$2{,}05\text{x}10^{-7}$
226725_at	NA	NA	-1,64	$2{,}16\text{x}10^{-6}$
209264_s_at	TSPAN4	tetraspanin 4	-1,66	$3{,}82\text{x}10^{-9}$
209583_s_at	CD200	CD200 molecule	-1,66	$1{,}26\text{x}10^{-7}$
239468_at	MKX	mohawk homeobox	-1,67	$5{,}63\text{x}10^{-7}$
201058_s_at	MYL9	myosin, light chain 9, regulatory	-1,68	$4{,}50\text{x}10^{-9}$
243880_at	GOSR2	golgi SNAP receptor complex member 2	-1,69	$1{,}58\text{x}10^{-6}$
219094_at	ARMC8	armadillo repeat containing 8	-1,69	$3{,}72\text{x}10^{-8}$
1557487_at	NA	NA	-1,69	$1{,}97\text{x}10^{-7}$
237435_at	NA	NA	-1,73	$2{,}12\text{x}10^{-7}$
202209_at	LSM3	LSM3 homolog, U6 small nuclear RNA associated (S. cerevisiae)	-1,73	6,03E-11
241871_at	CAMK4	calcium/calmodulin-dependent protein kinase IV	-1,74	$3{,}06\text{x}10^{-9}$
216952_s_at	LMNB2	lamin B2	-1,74	6,03E-11
232103_at	BPNT1	3'(2'), 5'-bisphosphate nucleotidase 1	-1,74	$4{,}28\text{x}10^{-9}$
227396_at	PTPRJ	protein tyrosine phosphatase, receptor type, J	-1,74	$7{,}71\text{x}10^{-9}$
231069_at	NA	NA	-1,76	$1{,}39\text{x}10^{-7}$
223775_at	HHIP	hedgehog interacting protein	-1,76	$8{,}90\text{x}10^{-6}$
217923_at	PEF1	penta-EF-hand domain containing 1	-1,77	$1{,}32\text{x}10^{-8}$
229029_at	NA	NA	-1,78	$1{,}63\text{x}10^{-7}$
235603_at	HNRNPU	heterogeneous nuclear ribonucleoprotein U (scaffold attachment factor A)	-1,78	$4{,}19\text{x}10^{-8}$
218247_s_at	MEX3C	mex-3 homolog C (C. elegans)	-1,84	$5{,}18\text{x}10^{-9}$
229744_at	SSFA2	sperm specific antigen 2	-1,84	$4{,}10\text{x}10^{-9}$
65472_at	C2orf68	chromosome 2 open reading frame 68	-1,85	$1{,}79\text{x}10^{-8}$
223001_at	OSTC	oligosaccharyltransferase complex subunit	-1,85	$1{,}83\text{x}10^{-9}$
206290_s_at	RGS7	regulator of G-protein signalling 7	-1,86	$8{,}51\text{x}10^{-9}$
203243_s_at	PDLIM5	PDZ and LIM domain 5	-1,89	$3{,}06\text{x}10^{-9}$
212129_at	NIPA2	non imprinted in Prader-Willi/Angelman syndrome 2	-1,89	$4{,}10\text{x}10^{-9}$
227639_at	PIGK	phosphatidylinositol glycan anchor biosynthesis, class K	-1,96	$3{,}42\text{x}10^{-9}$
219937_at	TRHDE	thyrotropin-releasing hormone degrading enzyme	-1,98	$3{,}00\text{x}10^{-8}$
223690_at	LTBP2	latent transforming growth factor beta binding protein 2	-2,02	$1{,}66\text{x}10^{-7}$

...continues on next page

Table C.1.: *(...continued)*

Probe set ID	Gene symbol	Gene name	logFc	adj.p-val
212133_at	CYFIP1	cytoplasmic FMR1 interacting protein 1	-2,05	$1{,}23 \times 10^{-8}$
201286_at	SDC1	syndecan 1	-2,07	$3{,}93 \times 10^{-9}$
220016_at	AHNAK	AHNAK nucleoprotein	-2,08	$3{,}78 \times 10^{-9}$
205532_s_at	CDH6	cadherin 6, type 2, K-cadherin (fetal kidney)	-2,08	$6{,}57 \times 10^{-7}$
203790_s_at	HRSP12	heat-responsive protein 12	-2,14	$1{,}36 \times 10^{-8}$
225275_at	EDIL3	EGF-like repeats and discoidin I-like domains 3	-2,44	$2{,}56 \times 10^{-7}$
212412_at	PDLIM5	PDZ and LIM domain 5	-2,45	$1{,}83 \times 10^{-9}$
226237_at	NA	NA	-2,48	$2{,}56 \times 10^{-8}$
211980_at	COL4A1	collagen, type IV, alpha 1	-2,81	$3{,}77 \times 10^{-9}$

APPENDIX

D

GENE ONTOLOGY ANALYSIS OF ALL SIGNIFICANTLY REGULATED GENES IN WISP1 DOWN-REGULATED CHONDROCYTES

Table D.1.: *All 1402 significantly regulated genes, detected during the WISP1 array data analysis in chondrocytes, were continuative assigned to GO terms and KEGG-signalling pathways. Illustrated are: the corresponding subclass name, the expected count, actual count and overall number of genes (N) associated to the GO/KEGG-term. These values are related to and corrected by the total number of all and differentially expressed corresponding genes present on the chip. The corresponding odds-ratio of corrected values is provided by the fraction (N/actual count). Corresponding p-values are results of the hyper-geometric tests.*

					– on chip –		
Go term	**p-value**	**Odds ratio**	**Exp. count**	**Act. count**	**N**	**Act. count**	**N**
	Biological processes						
cellular protein metabolic process	$4{,}27 \times 10^{-8}$	1,56	166,08	229	2486	2	9
cellular metabolic process	$1{,}41 \times 10^{-7}$	1,44	466,98	541	6990	1	15
protein modification process	$5{,}88 \times 10^{-7}$	1,60	107,56	156	1610	10	126
cellular macromolecule catabolic process	$3{,}39 \times 10^{-6}$	1,81	49,50	82	741	0	1
metabolic process	$4{,}16 \times 10^{-6}$	1,38	529,11	592	7920	25	440
cellular protein catabolic process	$7{,}01 \times 10^{-6}$	1,86	41,09	70	615	1	1
protein metabolic process	$7{,}30 \times 10^{-6}$	1,42	194,54	248	2912	0	8
post-translational protein modification	$9{,}02 \times 10^{-6}$	1,57	90,32	130	1352	5	27
modification-dependent protein catabolic process	$1{,}10 \times 10^{-5}$	1,87	38,55	66	577	33	364
proteolysis involved in cellular protein catabolic process	$1{,}13 \times 10^{-5}$	1,84	40,89	69	612	1	23
ubiquitin-dependent protein catabolic process	$2{,}08 \times 10^{-5}$	2,38	15,90	34	238	25	132
protein catabolic process	$2{,}67 \times 10^{-5}$	1,78	42,76	70	640	2	21
regulation of protein metabolic process	$6{,}12 \times 10^{-5}$	1,80	36,01	60	539	5	44
smoothened signalling pathway	0,0001	6,04	2,00	9	30	2	11
intracellular transport	0,0001	1,67	46,50	72	696	1	15
catabolic process	0,0002	1,48	85,51	118	1280	0	3
protein kinase cascade	0,0002	1,74	35,27	57	528	10	91

...continues on next page

Table D.1.: *(...continued)*

Go term	p-value	Odds ratio	Exp. count	Act. count	N	– on chip – Act. count	N
protein amino acid phosphorylation	0,0003	1,60	49,50	74	741	39	415
regulation of smoothened signalling pathway	0,0004	8,43	1,07	6	16	4	8
mitotic cell cycle	0,0004	1,76	29,93	49	448	1	8
negative regulation of cellular protein metabolic process	0,0005	2,30	11,49	24	172	0	1
negative regulation of metabolic process	0,0005	1,56	51,17	75	766	0	2
suckling behavior	0,0006	18,70	0,47	4	7	4	7
phosphorylation	0,0006	1,47	69,35	96	1038	1	15
phosphate metabolic process	0,0008	1,43	80,37	108	1203	3	19
negative regulation of biosynthetic process	0,0011	1,61	37,68	57	564	0	1
regulation of fibroblast growth factor receptor signalling pathway	0,0011	14,03	0,53	4	8	2	3
pattern specification process	0,0012	1,95	16,63	30	249	10	44
carbohydrate transport	0,0014	2,78	5,68	14	85	3	30
ER to Golgi vesicle-mediated transport	0,0015	3,84	2,81	9	42	9	41
tube development	0,0018	2,02	13,36	25	200	1	2
response to estrogen stimulus	0,0021	2,55	6,55	15	98	7	45
negative regulation of gene expression	0,0022	1,60	33,07	50	495	2	9
respiratory system development	0,0022	2,63	5,95	14	89	0	1
transmembrane receptor protein tyrosine kinase signalling pathway	0,0023	1,83	18,10	31	271	2	64
regulation of DNA replication	0,0024	3,04	4,14	11	62	2	6
lung development	0,0026	2,70	5,41	13	81	9	57
chondrocyte development	0,0027	21,02	0,33	3	5	3	5
negative regulation of translation involved in gene-silencing by miRNA	0,0027	21,02	0,33	3	5	3	5
nucleocytoplasmic transport	0,0027	1,99	13,03	24	195	6	16
regulation of translation	0,0030	2,23	8,82	18	132	8	57
proteolysis	0,0030	1,39	70,35	93	1053	23	417
embryonic morphogenesis	0,0030	1,78	19,17	32	287	1	3
regulation of glucose import	0,0030	4,28	2,00	7	30	0	2
cell cycle	0,0030	1,42	60,79	82	910	35	439
interspecies interaction between organisms	0,0031	1,76	19,98	33	299	29	272
establishment of localization in cell	0,0031	1,40	66,94	89	1002	0	1
enzyme linked receptor protein signalling pathway	0,0035	1,62	28,13	43	421	0	4
respiratory tube development	0,0036	2,58	5,61	13	84	0	3
protein localization	0,0038	1,40	64,80	86	970	2	52
cell cycle process	0,0041	1,50	40,82	58	611	0	3
negative regulation of transcription	0,0043	1,58	30,06	45	450	13	126
tube formation	0,0044	3,51	2,67	8	40	1	1

...continues on next page

Table D.1.: *(...continued)*

					– on chip –	
Go term	**p-value**	**Odds ratio**	**Exp. count**	**Act. count**	**N**	**Act. count**	**N**
mitochondrial electron transport, cytochrome c to oxygen	0,0045	Inf	0,13	2	2	2	2
heme a biosynthetic process	0,0045	Inf	0,13	2	2	2	2
UDP-N-acetylglucosamine transport	0,0045	Inf	0,13	2	2	2	2
cysteine biosynthetic process	0,0045	Inf	0,13	2	2	1	1
negative regulation of ryanodine-sensitive calcium-release channel activity	0,0045	Inf	0,13	2	2	2	2
hydrogen sulfide biosynthetic process	0,0045	Inf	0,13	2	2	2	2
negative regulation of translation	0,0045	3,93	2,14	7	32	3	16
protein localization in nucleus	0,0046	2,18	8,48	17	127	2	7
Golgi vesicle transport	0,0046	2,18	8,48	17	127	1	4
cellular protein localization	0,0051	1,57	29,53	44	442	0	4
traversing start control point of mitotic cell cycle	0,0051	14,01	0,40	3	6	3	6
Leydig cell differentiation	0,0051	14,01	0,40	3	6	3	6
negative regulation of smoothened signalling pathway	0,0051	14,01	0,40	3	6	2	4
negative regulation of glucose import	0,0051	14,01	0,40	3	6	3	6
regulation of signal transduction	0,0053	1,40	58,59	78	877	0	18
glucose import	0,0054	3,78	2,20	7	33	0	3
carbohydrate metabolic process	0,0057	1,51	35,54	51	532	16	196
cellular carbohydrate metabolic process	0,0063	1,59	26,59	40	398	0	10
regulation of smooth muscle cell migration	0,0063	7,01	0,80	4	12	1	2
triglyceride biosynthetic process	0,0063	7,01	0,80	4	12	3	9
kidney development	0,0065	2,29	6,68	14	100	10	49
mRNA metabolic process	0,0067	1,61	24,25	37	363	1	5
neural tube development	0,0076	2,71	4,14	10	62	1	10
intracellular signalling cascade	0,0077	1,30	96,27	119	1441	16	261
establishment of protein localization	0,0079	1,38	56,92	75	852	1	10
morphogenesis of an epithelium	0,0084	2,22	6,88	14	103	3	8
negative regulation of glucose transport	0,0085	10,51	0,47	3	7	0	1
ephrin receptor signalling pathway	0,0085	10,51	0,47	3	7	3	7
regulation of protein kinase activity	0,0085	1,62	22,18	34	332	0	9
response to ethanol	0,0085	2,65	4,21	10	63	9	59
dorsal/ventral neural tube patterning	0,0087	6,23	0,87	4	13	4	13
negative regulation of proteolysis	0,0088	4,68	1,34	5	20	3	9
G1 phase	0,0088	4,68	1,34	5	20	1	3
spindle organization	0,0091	3,04	3,01	8	45	0	7
neural tube formation	0,0102	3,28	2,47	7	37	3	7
response to metal ion	0,0104	2,03	8,48	16	127	1	6
regulation of JNK cascade	0,0106	2,56	4,34	10	65	0	6

...continues on next page

Table D.1.: *(...continued)*

Go term	p-value	Odds ratio	Exp. count	Act. count	N	– on chip – Act. count	N
regulation of epidermal growth factor receptor signalling pathway	0,0109	4,38	1,40	5	21	0	1
positive regulation of DNA replication	0,0110	3,66	1,94	6	29	5	26
regulation of cellular metabolic process	0,0113	1,20	219,86	249	3291	0	1
response to carbohydrate stimulus	0,0113	2,69	3,74	9	56	2	7
glucose transport	0,0113	2,69	3,74	9	56	2	22
copper ion transport	0,0115	5,61	0,94	4	14	3	11
regulation of epidermal growth factor receptor activity	0,0115	5,61	0,94	4	14	4	6
positive regulation of transforming growth factor beta receptor signalling pathway	0,0115	5,61	0,94	4	14	4	14
organelle organization	0,0116	1,28	91,19	112	1365	0	8
fibroblast growth factor receptor signalling pathway	0,0118	3,17	2,54	7	38	3	30
protein transport	0,0120	1,36	56,18	73	841	39	388
RNA processing	0,0120	1,44	37,01	51	554	6	54
mitosis	0,0124	1,67	17,10	27	256	23	178
positive regulation of DNA metabolic process	0,0126	2,64	3,81	9	57	0	1
leucine catabolic process	0,0128	28,00	0,20	2	3	2	3
embryonic neurocranium morphogenesis	0,0128	28,00	0,20	2	3	2	3
Sertoli cell differentiation	0,0128	28,00	0,20	2	3	1	1
bronchus development	0,0128	28,00	0,20	2	3	0	1
regulation of mitotic cell cycle	0,0129	1,93	9,42	17	141	4	14
nuclear-transcribed mRNA catabolic process, nonsense-mediated decay	0,0130	3,51	2,00	6	30	6	30
DNA replication	0,0134	1,71	14,83	24	222	12	125
macromolecule biosynthetic process	0,0136	1,19	222,67	251	3333	0	2
embryonic epithelial tube formation	0,0136	3,07	2,61	7	39	0	2
embryonic development	0,0139	1,44	34,74	48	520	6	64
polysaccharide biosynthetic process	0,0141	2,58	3,87	9	58	1	1
M phase	0,0148	1,53	24,72	36	370	1	2
mitotic spindle organization	0,0149	5,10	1,00	4	15	4	12
smooth muscle cell migration	0,0149	5,10	1,00	4	15	0	3
response to inorganic substance	0,0160	1,73	13,50	22	202	3	16
thymus development	0,0161	3,90	1,54	5	23	5	23
protein homooligomerization	0,0163	2,16	6,01	12	90	7	58
forebrain development	0,0169	1,91	8,95	16	134	6	50
response to drug	0,0169	1,72	13,56	22	203	21	190
ER-nuclear signalling pathway	0,0177	3,24	2,14	6	32	2	3
cellular membrane organization	0,0180	1,48	27,59	39	413	5	53
spinal cord dorsal/ventral patterning	0,0184	7,00	0,60	3	9	2	4
embryonic camera-type eye development	0,0184	7,00	0,60	3	9	1	1

...continues on next page

Table D.1.: *(...continued)*

					– on chip –	
Go term	**p-value**	**Odds ratio**	**Exp. count**	**Act. count**	**N**	**Act. count**	**N**
apical protein localization	0,0184	7,00	0,60	3	9	3	9
positive regulation of coagulation	0,0184	7,00	0,60	3	9	2	3
lipid transport	0,0194	1,80	10,62	18	159	9	68
urogenital system development	0,0196	1,97	7,62	14	114	1	5
developmental growth	0,0196	1,97	7,62	14	114	1	16
M phase of mitotic cell cycle	0,0196	1,60	17,77	27	266	0	3
regulation of metabolic process	0,0197	1,18	230,28	257	3447	0	4
intracellular protein transport	0,0197	1,47	26,92	38	403	18	175
positive regulation of kinase activity	0,0208	1,66	14,63	23	219	1	4
tube morphogenesis	0,0221	1,89	8,48	15	127	0	4
JNK cascade	0,0223	2,06	6,28	12	94	1	28
skeletal system morphogenesis	0,0225	1,99	7,01	13	105	3	24
anatomical structure formation involved in morphogenesis	0,0232	1,46	26,39	37	395	0	13
cellular response to stress	0,0233	1,37	40,22	53	602	0	1
G1 phase of mitotic cell cycle	0,0234	4,31	1,14	4	17	1	10
cell-cell junction assembly	0,0234	4,31	1,14	4	17	2	9
regulation of receptor activity	0,0234	4,31	1,14	4	17	0	3
virus-host interaction	0,0234	4,31	1,14	4	17	1	5
negative regulation of MAPKKK cascade	0,0234	4,31	1,14	4	17	1	7
protein amino acid lipidation	0,0234	2,50	3,54	8	53	1	4
cellular membrane fusion	0,0234	2,50	3,54	8	53	6	22
response to estradiol stimulus	0,0234	2,50	3,54	8	53	8	53
positive regulation of protein kinase activity	0,0240	1,65	14,03	22	210	1	15
acrosome assembly	0,0244	14,00	0,27	2	4	2	4
mRNA capping	0,0244	14,00	0,27	2	4	2	4
seryl-tRNA aminoacylation	0,0244	14,00	0,27	2	4	2	4
smoothened signalling pathway involved in ventral spinal cord patterning	0,0244	14,00	0,27	2	4	0	1
inositol phosphate dephosphorylation	0,0244	14,00	0,27	2	4	2	4
response to folic acid	0,0244	14,00	0,27	2	4	2	4
JAK-STAT cascade involved in growth hormone signalling pathway	0,0244	14,00	0,27	2	4	2	4
sarcoplasmic reticulum calcium ion transport	0,0244	14,00	0,27	2	4	1	1
cellular copper ion homeostasis	0,0250	6,00	0,67	3	10	3	10
negative regulation of JNK cascade	0,0250	6,00	0,67	3	10	3	10
lipoprotein metabolic process	0,0256	2,09	5,68	11	85	1	19
protein amino acid autophosphorylation	0,0256	2,09	5,68	11	85	9	75
morphogenesis of embryonic epithelium	0,0260	2,44	3,61	8	54	0	11
iron ion transport	0,0268	3,34	1,74	5	26	3	23
neuroblast proliferation	0,0268	3,34	1,74	5	26	3	13

...continues on next page

Table D.1.: *(...continued)*

Go term	p-value	Odds ratio	Exp. count	Act. count	N	– on chip – Act. count	N
protein homotetramerization	0,0268	3,34	1,74	5	26	5	26
regulation of MAPKKK cascade	0,0273	1,88	7,95	14	119	2	7
positive regulation of ubiquitin-protein ligase activity during mitotic cell cycle	0,0280	2,26	4,34	9	65	9	65
vesicle-mediated transport	0,0282	1,35	40,69	53	609	15	162
neural tube patterning	0,0285	4,00	1,20	4	18	0	1
embryonic cranial skeleton morphogenesis	0,0285	4,00	1,20	4	18	1	10
spindle assembly	0,0285	4,00	1,20	4	18	4	17
glycoprotein biosynthetic process	0,0286	1,71	11,09	18	166	0	4
pigmentation	0,0287	2,39	3,67	8	55	4	21
embryonic skeletal system morphogenesis	0,0287	2,39	3,67	8	55	4	37
positive regulation of transferase activity	0,0287	1,60	15,10	23	226	0	3
embryonic skeletal system development	0,0292	2,13	5,08	10	76	2	24
mRNA processing	0,0298	1,51	20,11	29	301	22	216
organ morphogenesis	0,0304	1,37	36,48	48	546	7	113
cellular response to stimulus	0,0309	1,29	57,92	72	867	1	5
regulation of epithelial cell differentiation	0,0311	3,19	1,80	5	27	2	7
microtubule cytoskeleton organization	0,0314	1,72	10,42	17	156	4	32
glucose metabolic process	0,0314	1,72	10,42	17	156	8	41
I-kappaB kinase/NF-kappaB cascade	0,0314	1,72	10,42	17	156	3	25
regulation of phosphorylation	0,0316	1,40	29,60	40	443	1	11
nucleobase, nucleoside, nucleotide and nucleic acid metabolic process	0,0326	1,15	257,27	282	3851	7	61
asymmetric protein localization	0,0327	5,25	0,73	3	11	0	1
spinal cord patterning	0,0327	5,25	0,73	3	11	0	1
adrenal gland development	0,0327	5,25	0,73	3	11	3	11
thyroid gland development	0,0327	5,25	0,73	3	11	3	11
copper ion homeostasis	0,0327	5,25	0,73	3	11	0	1
inositol metabolic process	0,0343	3,74	1,27	4	19	1	4
ossification	0,0349	1,70	10,56	17	158	4	46
embryonic organ development	0,0349	1,70	10,56	17	158	0	4
embryonic organ morphogenesis	0,0349	1,81	8,22	14	123	0	3
MAPKKK cascade	0,0352	1,55	16,23	24	243	5	29
neural tube closure	0,0358	3,05	1,87	5	28	5	27
microtubule-based process	0,0361	1,53	17,10	25	256	2	9
osteoblast differentiation	0,0363	2,14	4,54	9	68	3	20
positive regulation of ubiquitin-protein ligase activity	0,0363	2,14	4,54	9	68	0	2
chordate embryonic development	0,0367	1,49	19,64	28	294	0	1
response to steroid hormone stimulus	0,0369	1,63	12,23	19	183	0	12
response to nutrient	0,0371	1,79	8,28	14	124	5	60

...continues on next page

Table D.1.: *(...continued)*

					– on chip –	
Go term	**p-value**	**Odds ratio**	**Exp. count**	**Act. count**	**N**	**Act. count**	**N**
lipoprotein biosynthetic process	0,0379	2,25	3,87	8	58	0	5
proteasomal ubiquitin-dependent protein catabolic process	0,0382	1,83	7,55	13	113	1	14
cellular lipid metabolic process	0,0382	1,35	35,27	46	528	1	3
protein tetramerization	0,0386	2,63	2,54	6	38	0	9
regulation of cell cycle	0,0386	1,47	20,58	29	308	5	37
regulation of protein amino acid phosphorylation	0,0388	1,65	11,49	18	172	1	15
cellular biosynthetic process	0,0389	1,14	267,09	291	3998	0	1
leucine metabolic process	0,0389	9,33	0,33	2	5	0	1
valine metabolic process	0,0389	9,33	0,33	2	5	2	4
mitotic sister chromatid cohesion	0,0389	9,33	0,33	2	5	1	2
negative regulation of neuroblast proliferation	0,0389	9,33	0,33	2	5	2	5
RNA capping	0,0389	9,33	0,33	2	5	0	1
polyol transport	0,0389	9,33	0,33	2	5	0	1
retrograde protein transport, ER to cytosol	0,0389	9,33	0,33	2	5	2	5
positive regulation of telomere maintenance	0,0389	9,33	0,33	2	5	1	2
glycolipid transport	0,0389	9,33	0,33	2	5	2	5
negative regulation of focal adhesion assembly	0,0389	9,33	0,33	2	5	2	5
positive regulation of cellular component movement	0,0391	1,87	6,81	12	102	2	9
protein import into nucleus	0,0406	1,81	7,62	13	114	5	25
embryonic development ending in birth or egg hatching	0,0410	1,47	19,84	28	297	0	4
regulation of telomere maintenance	0,0415	4,67	0,80	3	12	0	2
brain morphogenesis	0,0415	4,67	0,80	3	12	2	7
cellular component organization	0,0415	1,16	171,63	192	2569	2	14
protein amino acid methylation	0,0429	2,34	3,27	7	49	2	14
interphase	0,0430	1,79	7,68	13	115	1	1
regulation of translational initiation	0,0431	2,55	2,61	6	39	3	22
negative regulation of transcription, DNA-dependent	0,0438	1,42	23,38	32	350	9	72
induction of apoptosis	0,0447	1,44	21,71	30	325	13	157
transforming growth factor beta receptor signalling pathway	0,0454	1,88	6,21	11	93	7	46
positive regulation of ligase activity	0,0460	2,04	4,74	9	71	0	2
neuromuscular process controlling balance	0,0466	2,80	2,00	5	30	5	22
response to acid	0,0476	3,30	1,40	4	21	0	2
peptidyl-threonine phosphorylation	0,0476	3,30	1,40	4	21	4	17
platelet-derived growth factor receptor signalling pathway	0,0476	3,30	1,40	4	21	4	18
peptidyl-serine phosphorylation	0,0480	2,47	2,67	6	40	5	25
nuclear import	0,0484	1,76	7,82	13	117	0	3

...continues on next page

Table D.1.: *(...continued)*

Go term	p-value	Odds ratio	Exp. count	Act. count	N	– on chip – Act. count	N
nitrogen compound metabolic process	0,0492	1,13	282,26	305	4225	0	17
Cellular components							
intracellular	$1{,}32\text{x}10^{-18}$	2,04	686,60	801	10452	112	1784
intracellular part	$3{,}71\text{x}10^{-16}$	1,88	665,05	774	10124	0	8
intracellular organelle	$1{,}87\text{x}10^{-15}$	1,74	559,55	675	8518	0	2
intracellular membrane-bounded organelle	$1{,}64\text{x}10^{-14}$	1,68	503,25	617	7661	2	29
membrane-bounded organelle	$2{,}00\text{x}10^{-14}$	1,67	503,65	617	7667	0	2
cytoplasm	$2{,}69\text{x}10^{-13}$	1,63	468,18	577	7127	362	4296
cytoplasmic part	$1{,}64\text{x}10^{-8}$	1,47	311,50	391	4742	0	5
cell part	$2{,}11\text{x}10^{-8}$	2,36	893,13	934	13596	0	2
cell	$2{,}20\text{x}10^{-8}$	2,36	893,19	934	13597	0	4
nuclear part	$1{,}50\text{x}10^{-7}$	1,61	119,29	173	1816	0	4
nucleus	$3{,}75\text{x}10^{-7}$	1,41	316,63	388	4820	368	4637
nuclear lumen	$4{,}66\text{x}10^{-7}$	1,64	94,27	141	1435	0	1
organelle membrane	$4{,}87\text{x}10^{-7}$	1,58	115,42	166	1757	1	4
nucleoplasm	$2{,}51\text{x}10^{-5}$	1,66	58,60	90	892	49	446
endomembrane system	0,0004	1,44	89,01	120	1355	9	75
mitochondrion	0,0009	1,46	66,74	92	1016	89	984
perinuclear region of cytoplasm	0,0013	1,87	18,92	33	288	33	284
mitochondrial envelope	0,0014	1,71	26,80	43	408	0	15
mitochondrial outer membrane	0,0015	2,75	5,72	14	87	14	79
mitochondrial membrane	0,0017	1,72	25,42	41	387	6	37
Golgi apparatus	0,0017	1,47	56,03	78	853	73	788
protein complex	0,0020	1,28	158,77	192	2417	7	113
motile primary cilium	0,0026	21,40	0,33	3	5	3	5
cell-substrate junction	0,0035	2,39	6,90	15	105	2	4
focal adhesion	0,0039	2,45	6,31	14	96	14	96
micro-ribonucleoprotein complex	0,0043	Inf	0,13	2	2	2	2
platelet dense granule	0,0049	14,26	0,39	3	6	0	1
outer membrane	0,0055	2,27	7,23	15	110	1	3
cell-substrate adherens junction	0,0057	2,33	6,57	14	100	0	2
microtubule cytoskeleton	0,0066	1,50	34,95	50	532	0	17
Golgi membrane	0,0067	1,56	28,31	42	431	31	340
nucleolus	0,0077	1,43	44,60	61	679	61	675
cytoskeleton	0,0077	1,31	83,49	105	1271	60	646
nuclear pore	0,0105	2,56	4,34	10	66	10	56
endoplasmic reticulum membrane	0,0110	1,45	36,79	51	560	44	493
platelet dense granule membrane	0,0124	28,50	0,20	2	3	2	3
interleukin-1 receptor complex	0,0124	28,50	0,20	2	3	2	3
cytosol	0,0129	1,29	84,15	104	1281	102	1239

...continues on next page

Table D.1.: *(...continued)*

					– on chip –	
Go term	**p-value**	**Odds ratio**	**Exp. count**	**Act. count**	**N**	**Act. count**	**N**
microtubule	0,0135	1,65	17,21	27	262	23	226
synaptosome	0,0138	2,32	5,19	11	79	11	79
nuclear replication fork	0,0141	5,19	0,99	4	15	0	1
replication fork	0,0141	3,43	2,04	6	31	2	10
microtubule organizing center	0,0142	1,66	16,49	26	251	10	94
nuclear envelope-endoplasmic reticulum network	0,0174	1,41	37,77	51	575	0	2
cytoplasmic mRNA processing body	0,0181	3,76	1,58	5	24	5	24
lysosomal membrane	0,0188	2,31	4,73	10	72	10	72
transport vesicle	0,0188	2,31	4,73	10	72	2	25
Golgi apparatus part	0,0200	1,42	33,76	46	514	1	2
polysome	0,0221	4,39	1,12	4	17	2	13
integral to endoplasmic reticulum membrane	0,0235	2,70	2,89	7	44	5	37
RNA-induced silencing complex	0,0237	14,25	0,26	2	4	2	4
anchored to external side of plasma membrane	0,0237	14,25	0,26	2	4	2	4
nuclear inclusion body	0,0237	14,25	0,26	2	4	2	4
polysomal ribosome	0,0237	14,25	0,26	2	4	2	4
MHC class I peptide loading complex	0,0237	14,25	0,26	2	4	1	2
basolateral plasma membrane	0,0246	1,64	14,06	22	214	6	95
peroxisome	0,0249	2,02	6,37	12	97	11	92
insoluble fraction	0,0261	1,32	51,11	65	778	5	34
nucleoplasm part	0,0294	1,36	37,25	49	567	0	1
endoplasmic reticulum	0,0301	1,28	61,42	76	935	69	852
adherens junction	0,0320	1,75	9,66	16	147	2	25
ER-Golgi intermediate compartment	0,0325	2,50	3,09	7	47	5	30
late endosome	0,0334	1,99	5,91	11	90	4	29
membrane fraction	0,0353	1,30	49,27	62	750	31	461
cytoskeletal part	0,0355	1,28	56,49	70	860	1	2
nuclear chromosome	0,0356	1,69	10,58	17	161	2	24
pore complex	0,0362	2,04	5,26	10	80	0	6
cytoplasmic vesicle	0,0369	1,32	42,24	54	643	14	216
nucleotide-excision repair complex	0,0377	9,50	0,33	2	5	1	3
plasma membrane enriched fraction	0,0377	9,50	0,33	2	5	2	5
Mre11 complex	0,0377	9,50	0,33	2	5	2	5
GPI-anchor transamidase complex	0,0377	9,50	0,33	2	5	2	5
postsynaptic density	0,0389	2,11	4,60	9	70	9	70
Golgi-associated vesicle	0,0397	2,38	3,22	7	49	1	11
cyclin-dependent protein kinase holoenzyme complex	0,0398	4,75	0,79	3	12	3	8
peroxisomal matrix	0,0398	4,75	0,79	3	12	3	12
proteasome complex	0,0416	2,20	3,94	8	60	7	40

...continues on next page

Table D.1.: *(...continued)*

Go term	p-value	Odds ratio	Exp. count	Act. count	N	– on chip – Act. count	N
intrinsic to endoplasmic reticulum membrane	0,0416	2,20	3,94	8	60	1	16
histone acetyltransferase complex	0,0437	2,32	3,28	7	50	1	8
vacuolar membrane	0,0451	1,83	6,96	12	106	0	8
nuclear chromosome, telomeric region	0,0452	3,36	1,38	4	21	3	10
early endosome	0,0479	1,81	7,03	12	107	8	72
lamellipodium	0,0489	2,01	4,80	9	73	8	66
ER to Golgi transport vesicle membrane	0,0492	4,28	0,85	3	13	1	5
Molecular functions							
catalytic activity	$1{,}57\text{x}10^{-5}$	1,33	330,68	391	4885	5	85
nucleotide binding	$2{,}76\text{x}10^{-5}$	1,43	143,98	189	2127	167	1854
protein binding	$6{,}90\text{x}10^{-5}$	1,30	532,13	589	7861	402	5344
purine nucleotide binding	$8{,}34\text{x}10^{-5}$	1,42	123,47	163	1824	0	7
transferase activity	0,0001	1,44	109,26	146	1614	99	1115
protein serine/threonine/tyrosine kinase activity	0,0003	9,23	1,02	6	15	1	2
copper ion transmembrane transporter activity	0,0003	27,66	0,41	4	6	4	5
platelet-derived growth factor receptor binding	0,0005	11,53	0,74	5	11	5	11
GTP binding	0,0008	1,82	23,02	39	340	39	340
MAP kinase kinase activity	0,0011	8,65	0,88	5	13	5	12
guanyl nucleotide binding	0,0016	1,75	23,83	39	352	1	18
transferase activity, transferring phosphorus-containing groups	0,0019	1,45	58,89	81	870	0	1
phosphotransferase activity, alcohol group as acceptor	0,0020	1,51	46,98	67	694	3	20
protein serine/threonine kinase activity	0,0020	1,66	28,09	44	415	32	301
purine nucleoside binding	0,0023	1,34	104,31	132	1541	0	2
nucleoside binding	0,0029	1,33	104,99	132	1551	0	7
kinase activity	0,0037	1,45	50,84	70	751	7	90
SH2 domain binding	0,0044	4,61	1,62	6	24	6	24
ATP binding	0,0045	1,32	95,45	120	1410	120	1410
ubiquitin thiolesterase activity	0,0045	2,77	4,47	11	66	11	66
UDP-glucose:glycoprotein glucosyltransferase activity	0,0046	Inf	0,14	2	2	2	2
UDP-N-acetylglucosamine transmembrane transporter activity	0,0046	Inf	0,14	2	2	2	2
basal transcription repressor activity	0,0046	Inf	0,14	2	2	2	2
TRAIL binding	0,0046	Inf	0,14	2	2	2	2
MHC class I protein binding	0,0047	7,90	0,74	4	11	4	11
double-stranded DNA binding	0,0055	2,44	5,89	13	87	12	65
hydrolase activity, acting on acid anhydrides	0,0063	1,42	50,23	68	742	0	2
pyrophosphatase activity	0,0072	1,41	49,69	67	734	1	1

...continues on next page

Table D.1.: *(...continued)*

					– on chip –	
Go term	**p-value**	**Odds ratio**	**Exp. count**	**Act. count**	**N**	**Act. count**	**N**
protein kinase activity	0,0073	1,46	39,40	55	582	6	55
hydrolase activity, acting on acid anhydrides, in phosphorus-containing anhydrides	0,0079	1,41	49,89	67	737	1	20
transferase activity, transferring hexosyl groups	0,0080	1,92	11,17	20	165	3	22
enzyme binding	0,0084	1,49	34,59	49	511	7	88
binding	0,0085	1,26	802,63	829	11857	31	467
damaged DNA binding	0,0086	3,08	2,98	8	44	8	44
GTPase activity	0,0088	1,81	13,54	23	200	23	200
nucleoside-triphosphatase activity	0,0096	1,40	47,72	64	705	7	56
ubiquitin protein ligase binding	0,0110	3,23	2,50	7	37	7	37
RNA binding	0,0114	1,39	47,25	63	698	51	534
peptidase activator activity	0,0115	4,32	1,42	5	21	1	4
growth factor binding	0,0120	2,11	7,18	14	106	2	17
nucleoside kinase activity	0,0121	5,53	0,95	4	14	1	7
3-oxo-5-alpha-steroid 4-dehydrogenase activity	0,0131	27,60	0,20	2	3	2	3
lipoprotein lipase activity	0,0131	27,60	0,20	2	3	2	3
peptide antigen-transporting ATPase activity	0,0131	27,60	0,20	2	3	2	3
histone methyltransferase activity (H4-K20 specific)	0,0131	27,60	0,20	2	3	2	3
transcription factor binding	0,0133	1,47	32,09	45	474	17	133
insulin receptor binding	0,0138	3,46	2,03	6	30	6	30
thiolester hydrolase activity	0,0140	2,22	5,89	12	87	0	6
actin binding	0,0146	1,57	21,39	32	316	27	263
manganese ion binding	0,0153	1,85	10,36	18	153	18	153
structure-specific DNA binding	0,0155	1,93	8,87	16	131	0	2
cysteine-type peptidase activity	0,0166	1,91	8,94	16	132	8	60
receptor signalling protein serine/threonine kinase activity	0,0170	2,49	3,99	9	59	0	2
endoribonuclease activity, producing 5'-phosphomonoesters	0,0170	3,84	1,56	5	23	2	4
Ras GTPase activator activity	0,0179	2,13	6,09	12	90	1	9
protein kinase regulator activity	0,0185	2,21	5,42	11	80	0	3
glucosyltransferase activity	0,0191	6,90	0,61	3	9	0	1
MHC protein binding	0,0197	4,61	1,08	4	16	0	2
WW domain binding	0,0197	4,61	1,08	4	16	4	16
protein kinase binding	0,0211	1,82	9,95	17	147	11	100
receptor signalling protein activity	0,0219	1,77	10,76	18	159	3	35
triglyceride lipase activity	0,0244	4,25	1,15	4	17	4	17
apoptotic protease activator activity	0,0244	4,25	1,15	4	17	1	2
serine-tRNA ligase activity	0,0251	13,80	0,27	2	4	2	4

...continues on next page

Table D.1.: *(...continued)*

Go term	p-value	Odds ratio	Exp. count	Act. count	N	– on chip – Act. count	N
transforming growth factor beta receptor activity, type II	0,0251	13,80	0,27	2	4	1	2
protein transporter activity	0,0258	2,09	5,69	11	84	11	71
Ran GTPase binding	0,0259	5,92	0,68	3	10	3	10
kinase binding	0,0294	1,68	11,91	19	176	2	23
caspase regulator activity	0,0327	3,14	1,83	5	27	0	2
hydrolase activity	0,0344	1,18	145,74	166	2153	74	907
ligase activity	0,0369	1,41	26,47	36	391	29	295
transferase activity, transferring glycosyl groups	0,0370	1,54	16,31	24	241	17	147
GPI-anchor transamidase activity	0,0399	9,20	0,34	2	5	2	5
polynucleotide adenylyltransferase activity	0,0399	9,20	0,34	2	5	2	5
iron ion transmembrane transporter activity	0,0399	9,20	0,34	2	5	1	3
profilin binding	0,0399	9,20	0,34	2	5	2	5
nucleoside-triphosphate diphosphatase activity	0,0399	9,20	0,34	2	5	1	3
proteoglycan binding	0,0429	4,60	0,81	3	12	1	2
FAD binding	0,0457	2,04	4,74	9	70	9	70
kinase regulator activity	0,0491	1,86	6,30	11	93	0	1
nuclear hormone receptor binding	0,0493	2,01	4,81	9	71	1	7
signal sequence binding	0,0496	3,25	1,42	4	21	0	4
KEGG pathway signalling							
focal adhesion	0,0012	2,09	13,90	26	196	26	196
valine, leucine and isoleucine degradation	0,0027	3,54	3,05	9	43	9	43
glioma	0,0042	2,83	4,47	11	63	11	63
neurotrophin signalling pathway	0,0056	2,16	8,72	17	123	17	123
RNA degradation	0,0060	2,84	4,04	10	57	10	57
ErbB signalling pathway	0,0070	2,39	6,10	13	86	13	86
epithelial cell signalling in Helicobacter pylori infection	0,0076	2,58	4,82	11	68	11	68
lysosome	0,0100	2,07	8,51	16	120	16	120
MAPK signalling pathway	0,0174	1,62	18,58	28	262	28	262
acute myeloid leukemia	0,0177	2,50	4,04	9	57	9	57
protein export	0,0202	3,68	1,63	5	23	5	23
prostate cancer	0,0221	2,08	6,31	12	89	12	89
ubiquitin mediated proteolysis	0,0249	1,83	9,43	16	133	16	133
NOD-like receptor signalling pathway	0,0292	2,26	4,40	9	62	9	62
chronic myeloid leukemia	0,0346	2,08	5,25	10	74	10	74
phosphatidylinositol signalling system	0,0375	2,05	5,32	10	75	10	75
regulation of actin cytoskeleton	0,0382	1,58	14,82	22	209	22	209
SNARE interactions in vesicular transport	0,0488	2,48	2,69	6	38	6	38

APPENDIX
E

ACRONYMS

Table E.1.: *Acronyms*

%	percent
°C	degree Celsius
APS	ammonium persulfate
bp	base pair(s)
cDNA	complementary deoxyribonucleic acid
Chap.	chapter
cm	centimetre
cm^2	square centimetre
CO_2	carbon dioxide
cRNA	complementary ribonucleic acid
d	day(s)
DAPI	4',6-Diamidino-2-phenylindole
ddATP	2,3-dideoxyadenosine-5-triphosphate
ddCTP	2,3-dideoxycytosine-5-triphosphate
ddGTP	2,3-dideoxyguanine-5-triphosphate
ddNTP	dideoxynucleotide-triphosphates
ddTTP	2,3-dideoxythymidine-5-triphosphate
DMEM	Dulbecco's modified eagle's medium
DMSO	dimethylsulfoxide

...continues on next page

Table E.1.: *(...continued)*

DNA	deoxyribonucleic acid
dNTPs	deoxynucleotide triphosphates
DTT	dithiothreitol
E	extinction unit
ECM	extra cellular matrix
EDTA	ethylendiamintetraacetic acid
et al.	et alia
FCS	calfbovine serum
Fig.	figure
FITC	fluorescein isothiocyanate
g	gram(s)
h	hour(s)
HCl	hydrochloric acid
hMSC	human mesenchymal stem cell
HPLC	high performance liquid chromatography
HSC	heamatopoietic stem cells
inf	infinitely/infinite
kb	kilo bases
l	litre
M	molar
mA	milliampere
mg	milligram(s)
min	minute(s)
ml	microlitre(s)
mM	millimolar (millimol per litre)
mRNA	messenger RNA
MCS	multiple cloning site
MSC	mesenchymal stem cell

...continues on next page

Table E.1.: *(...continued)*

n	quantity
nM	nanomolar=nanomol per litre
OD	optical density
PBS	phosphate buffered saline
pg	picogram(s)
PFA	paraformaldehyde
(r)protein	recombinant protein
RNA	ribonucleic acid
rpm	rounds per minute
RT	room temperatur
RT-PCR	reverse transcriptase polymerase chain reaction
rWISP1	recombinant WNT1-inducible-signalling pathway protein 1
rWISP1-T1	recombinant WNT1-inducible-signalling pathway protein 1 transcript variant 1
rWISP1-T2	recombinant WNT1-inducible-signalling pathway protein 1transcript variant 2
rWISP2	recombinant WNT1-inducible-signalling pathway protein 2
SDS	sodium dodecyl sulfate
SDS-PAGE	sodium dodecyl sulfate polyacrylamide gel electrophoresis
Sec.	section
SR	sulforhodamine
Subsec.	subsection
Tab.	table
Taq Thermus aquaticus TEMED	N,N,N',N'-tetramethyl ethylenediamine
Tris base	tris(hydroxymethyl)aminomethane
U	unit(s)

...continues on next page

Table E.1.: *(...continued)*

UV	ultraviolet
x	times, -fold
μg	microgram(s)
μl	microlitre
μM	micrometre(s)
μM	micromolar=micromol per litre

LIST OF PUBLICATIONS

Journal publications

Schlegelmilch K., A. Keller, V. Zehe, S. Hondke, L. Klein-Hitpass, N. Schütze. (2012, submitted) "Identification of WISP1 as an important survival factor in human mesenchymal stem cells."

Nanda I., **K. Schlegelmilch**, T. Haaf, M. Schartl, M. Schmid (2008). "Synteny conservation of the Z chromosome in 14 avian species (11 families) supports a role for Z dosage in avian sex determination." In: Cytogenet Genome Res 122.2, pp. 150-6.

Oral presentations

Schlegelmilch K., A. Keller A., V. Zehe, R. Schenk, N. Schütze (24.-16.03.2011). "Humane mesenchymale Stammzellen (hMSCs) und Tc28a2 Chondrozyten benötigen WISP1 zum Überleben." Osteology Congress, Fürth, Germany.

Hilpert S., V. Monz, **K. Schlegelmilch**, A. Keller, S. Jatzke, N. Schütze (24.-16.03.2011) "Funktionsaufklärung von WISP3 Protein in humanen Chondrozyten." Osteology Congress 2011, Fürth, Germany.

Schlegelmilch K., A. Keller, V. Zehe, N. Schütze (20.-24.10.2010). "Molecular elucidation of WISP1 functions in hMSCs and chondrocytes." 6th International Workshop on the CC Family of Genes, Newcastle, Northern Ireland.

Poster presentations

Hondke S., S. Hilpert, V. Zehe, **K. Schlegelmilch**, A. Keller, N. Schütze (23.-25.05.2012). "WISP1 and -3 affect cell survival in human mesenchymal stem cells (hMSCs) and Tc28a2 chondrocytes". 3rd International Conference of Strategies in Tissue Engineering, Würzburg, Germany.

Hondke S., S. Hilpert, V. Zehe, **K. Schlegelmilch**, A. Keller, S. Wiesner, N. Schütze (29.-31.03.2012). "Funktionsaufklärung von WISP3 Protein in humanen Chondrozyten und humanen mesenchymalen Stammzellen." Osteology Congress, Basel, Switzerland.

Dotterweich J., J. Schneidereit, **K. Schlegelmilch**, L. Klein-Hitpass, F. Jakob, N. Schütze (23.-24.03.2012). "Molekulare Studien zur Interaktion von mesenchymalen Stammzellen mit Myelomzellen." Osteooncology Congress, Tübingen, Germany.

Laug R., V. Zehe, **K. Schlegelmilch**, S. Kunzmann, A. Keller, F. Jakob, N. Schütze (24.-26.03.2011) Funktion von CTGF in Lungenendothelzellen und mesenchymalen Stammzellen. Osteology Congress 2011, Fürth, Germany.

Schlegelmilch K., V. Monz, F. Jakob, N. Schütze (03.-06.03.2010). "Funktionsaufklärung von WISP-Proteinen in mesenchymalen Stammzellen (MSCs) und Chondrozyten." Osteology Congress, Berlin, Germany.

Schlegelmilch K., V. Monz, M. Kunz, J. Pfeilschifter, N. Schütze (11.-15.09.2009). "Towards elucidation of WISP protein function in mesenchymal stem cells and chondrocytes." ASBMR 31st Annual Meeting, Denver, Colorado, USA.

Schlegelmilch K., S. Hilpert, S. Jatzke, F. Jakob, N. Schütze (04.-07.03.2009). "Rekombinante Proteinherstellung und Expressionsanalysen von WISP-Proteinen." Osteology Congress, Frankfurt, Germany.

Schlegelmilch K., R. Schenk, S. Jatzke, U. Nöth, L. Klein-Hitpass, F. Jakob, N. Schütze (09.-11.10.2008). "Function of WISP proteins in human mesenchymal stem cells." BioStar 3rd Congress on Regenerative Biology and Medicine, Stuttgart, Germany.

ERKLÄRUNG

Hiermit erkläre ich ehrenwörtlich, dass ich die vorliegende Dissertation selbständig angefertigt und keine anderen als die angegebenen Quellen und Hilfsmittel verwendet habe. Die Dissertation wurde bisher weder in gleicher noch ähnlicher Form in einem anderen Prüfungsverfahren vorgelegt. Außer dem Diplom in Biologie von der Universität Würzburg habe ich bisher keine weiteren akademischen Grade erworben oder versucht zu erwerben.

Würzburg, den 26. 4. 2012

Katrin Schlegelmilch